

THE INSTITUTE OF PAPER CHEMISTRY, APPLETON, WISCONSIN

STATUS REPORTS

TO THE

PULPING PROCESSES PROJECT ADVISORY COMMITTEE

October 20-21, 1986

The Institute of Paper Chemistry

Appleton, WI 54912

NOTICE & DISCLAIMER

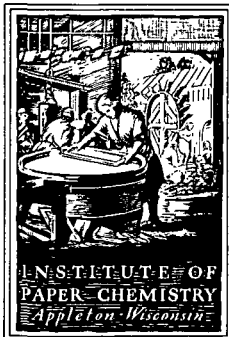
The Institute of Paper Chemistry (IPC) has provided a high standard of professional service and has exerted its best efforts within the time and funds available for this project. The information and conclusions are advisory and are intended only for the internal use by any company who may receive this report. Each company must decide for itself the best approach to solving any problems it may have and how, or whether, this reported information should be considered in its approach.

IPC does not recommend particular products, procedures, materials, or services. These are included only in the interest of completeness within a laboratory context and budgetary constraint. Actual products, procedures, materials, and services used may differ and are peculiar to the operations of each company.

In no event shall IPC or its employees and agents have any obligation or liability for damages, including, but not limited to, consequential damages, arising out of or in connection with any company's use of, or inability to use, the reported information. IPC provides no warranty or guaranty of results.

This information represents a review of on-going research for use by the Project Advisory Committees. The information is not intended to be a definitive progress report on any of the projects and should not be cited or referenced in any paper or correspondence external to your company.

Your advice and suggestions on any of the projects will be most welcome.



THE INSTITUTE OF PAPER CHEMISTRY
Post Office Box 1039
Appleton, Wisconsin 54912
Phone: 414/734-9251
Telex: 469289

September 26, 1986

TO: Members of the Pulping Processes Project Advisory Committee

The next meeting of the Project Advisory Committee for the Pulping Processes area will be held in Appleton on October 20 and 21, 1985. The meeting will convene at 8:00 o'clock Monday morning, October 21, in the Seminar Room of the Continuing Education Center at The Institute of Paper Chemistry. Accommodations are available for Committee Members at the Continuing Education Center. Enclosed is a pink "Security Card" which has instructions for entering the CEC building in the event you find it locked when you arrive. If you have not yet let us know your plans, including lodging, please do so immediately.

You can also stay at the CEC while you are attending other PAC meetings. If you intend to do so, you must inform Barbara Bisby [(414) 738-3328] to ensure your room is kept reserved.

The information enclosed with this letter is for your review prior to the upcoming meeting. The enclosures include:

- (1) the Agenda for this October meeting;
- (2) a list of current Committee Members;
- (3) response to questions raised in Chairman Al Rosen's minutes of the April meeting;
- (4) a list of current M.S. and Ph.D. student work currently in progress at the IPC; and
- (5) the status reports for the individual funded projects.

TO: Members of the PPPAC

September 26, 1986

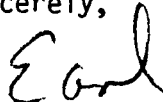
Page 2

The Monday morning and afternoon sessions will cover individual funded projects. The evening session will be in a somewhat lighter vein and include discussions on student research in the general pulping processes area. Please note that the fall sessions for PAC meetings are open to the general membership. Hence you can expect other company representatives besides yourself to be present at this meeting.

The Tuesday session will begin at 8:00 a.m. and end at noon. It will be held in Room K108-109 of the Krannert Building. This session is for Committee business and is not open to the general attendees. Please note that breakfast (7:00 a.m.) and lunch will be served on both days; dinner will be served on Monday evening. These are part of your PAC perks.

I look forward to seeing you in Appleton. If you have any questions, please give me a call.

Sincerely,



Earl W. Malcolm
Director
Chemical Sciences Division

EWM/gmk
Enclosures

AGENDA

PULPING PROCESSES PAC MEETING

THE INSTITUTE OF PAPER CHEMISTRY
APPLETON, WISCONSIN

OCTOBER 20-21, 1986

MONDAY, OCTOBER 20, 1986
CONTINUING EDUCATION CENTER SEMINAR ROOM

7:00	BREAKFAST	
8:15	CONVENE	A. Rosen
8:20	RESEARCH OVERVIEW	E. Malcolm
8:40	PROJECT PRESENTATIONS	
	Fundamentals of Selectivity in Pulping and Bleaching (Project 3475)	D. Dimmel
	Improved Processes for Bleached Pulp (Project 3474)	T. McDonough
10:15	BREAK	
	Development and Application of Analytical Techniques (Project 3477)	D. Easty
	Fine Structure of Wood Pulp Fibers (Projects 3288 and 3521)	R. Atalla
12:00	LUNCH	

1:00 PROJECT PRESENTATIONS (CONTINUED)

KRAFT CHEMICAL RECOVERY

Fundamental Processes in Alkali Recovery Furnaces
(Project 3473-1)

T. Grace
J. Cameron
D. Clay

Black Liquor Combustion
(DOE Project 3473-6)

3:00 BREAK

HIGH-YIELD PULPS

Separation of Strong, Intact Fibers
(Project 3566)

T. McDonough
S. Aziz

Fundamentals of Brightness Stability
(Project 3524)

E. Malcolm
U. Agarwal
S. Lebo

5:30 SOCIAL HOUR
DINNER

7:00 EVENING DISCUSSIONS

Fiber Bonding

Guest Speaker

Student Research

Staff/Students

8:30 END OF THURSDAY SESSION

TUESDAY MORNING - OCTOBER 21, 1986

7:00 BREAKFAST (CEC)

8:00 COMMITTEE MEETING (CEC)

12:00 LUNCH (CEC) END OF TUESDAY SESSION

NEXT MEETING: MARCH 24-25, 1987

PULPING PROCESSES PROJECT ADVISORY COMMITTEE

Mr. Allen Rosen (Chairman) -- 6/87
Section Leader - Products Section
Union Camp Corporation
Technology Center
P. O. Box 3301
Princeton, NJ 08540-0148
(609) 896-1200

Dr. Glendon Brown -- 6/89
Director of Production Technology
Mead Paper
P. O. Box 757
Escanaba, MI 49829
(906) 786-1660

Mr. Dean W. DeCrease -- 6/88
Group Leader, Pulping Research
Hammermill Paper Company
1540 East Lake Road
P. O. Box 10050
Erie, PA 16533
(814) 456-8811

Mr. Wendell B. Hammond -- 6/89
Resident Manager
Willamette Industries, Inc.
Albany Paper Mill
P. O. Box 339
Albany, OR 97321
(503) 926-2281

Mr. Gerald R. Haw -- 6/88
Assistant Pulp Mill Superintendent
Tennessee River Pulp & Paper Company
Packaging Corporation of America
P. O. Box 33
Counce, TN 38326
(901) 689-3111

Dr. Donald C. Johnson -- 6/88
Research Advisor
Weyerhaeuser Company
WTC 2B42
Tacoma, WA 98477
(206) 924-6531

Dr. Thomas C. Kisla -- 6/88
Sr. Product Technology Engineer
Stone Container Corporation
3805 Presidential Parkway, Suite 101
Atlanta, GA 30340
(404) 452-1321

Dr. Samuel McKibbins -- 6/89
Director of Pulping & Bleaching
Champion International
West Nyack Road
West Nyack, NY 10994
(914) 578-7293

Dr. John Rogers -- 6/89
Director, Pulping Processes
James River Corporation
P. O. Box 19090
Green Bay, WI 54307-9090
(414) 498-5997

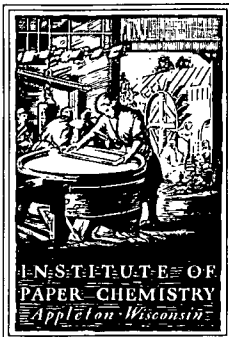
Dr. Ivan Schrodt -- 6/89
Director, Research & Development
Kimberly-Clark Corporation
2100 Winchester Road
Neenah, WI 54956-0056
(414) 721-6136

Mr. Robert W. Snow -- 6/89
Sr. Development Specialist
Owens-Illinois Inc.
1 Seagate 25L-FP
Toledo, OH 43666
(419) 247-7199

Dr. James Turnbull -- 6/89
Group Leader, Brightening Research
MacMillan Bloedel Research
3350 East Broadway
Vancouver, BC
CANADA V5M 4E6
(604) 254-5151

Dr. Benjamin F. Ward -- 6/88
Research Director
Charleston Research
Westvaco Corporation
P. O. Box 5207
North Charleston, SC 29406
(803) 745-3505

EWM/gmk
10/86



THE INSTITUTE OF PAPER CHEMISTRY
Post Office Box 1039
Appleton, Wisconsin 54912
Phone: 414/734-9251
Telex: 469289

September 26, 1986

Mr. Allen Rosen
Section Leader - Products Section
Union Camp Corporation
Technology Center
P. O. Box 3301
Princeton, NJ 08540-0148

Dear Al:

This letter is in response to your report on the April 1986 Pulping Processes Project Advisory Committee meeting. As I have done in the past, I will make this response brief and informal. I expect many of the subjects will be discussed in detail at the October PAC meeting.

General Comments - Staffing

We have had several changes in our staff at the Institute and a brief summary of where we stand and what we intend to do is warranted. Most recently, Werner Lonsky resigned effective September 15 for a position with Kimberly-Clark. This, coupled with the previous departures of Norm Thompson and Leo Schroeder, effectively left us with an organic chemistry staff of one; e.g., Don Dimmel. Clearly this is intolerable and we are taking steps to rectify the situation.

Presently, we are actively searching for an organic chemist. Let me know if you have any suggestions. In addition, we intend to bring two new post-doctoral fellows on board to work with Don Dimmel and Tom McDonough on pulping chemistry and oxygen bleaching respectively. Also, we will make use of a portion of Dr. Umesh Agarwal's time to continue the effort on the photochemistry of brightness reversion. Umesh currently works full time with the DOE project of Rajai Atalla. I anticipate approximately 25% of his time can be made available for the brightness stability project. The turnover in staff undoubtedly will have an adverse effect on progress in both high yield and chemical pulp bleaching. However, we intend to keep a high priority on both of these projects as they are directly relevant to current industry needs.

Projects 3473-1 and 3473-6 - FUNDAMENTAL PROCESSES IN ALKALINE RECOVERY FURNACES

The concerns noted in your letter are being considered by the staff. We are aware of problems with the stability of mill liquors but have not developed any practical alternative to our current method of storage in a cold room. Relative to the interpretation of raw data from our survey of commercial liquors, the current PAC report covers discusses the statistical methods we are currently using for data analysis. This will be discussed at the October PAC meeting. The committee's concern with the relatively long lead time to develop a functional predictive model is appreciated. We are incorporating extensive student effort into this area. Also, we anticipate a postdoctoral fellow will work in the modeling area during 1987. This should help us make rapid progress toward a functional model.

Project 3475 - FUNDAMENTALS OF SELECTIVITY IN PULPING AND BLEACHING

The committee's desire to move to more practical applications of this work is understood. We are attempting to do so. Recent Ph.D. work is centered on ways to promote SET reactions during pulping. We are also looking into the possible uses in bleaching for the SET technology. We are looking for someone with electrochemical experience to help us speed activity in that area. On the carbohydrate side, activity is now under the direction of Don Dimmel. Our current PAC report discusses recent activity on degradation of amorphous cellulose. Concerning the low viscosities, there has been some confusion in past reports as to when a modified TAPPI test was used vs. the standard method. The modified test is run at a reduced concentration and gives viscosities lower than the standard TAPPI test. This will be clarified in the upcoming PAC meeting.

Project 3474 - IMPROVED PROCESSES FOR BLEACHED PULPS

The activity in low lignin pulping, specifically the alkaline sulfite AQ work, has been put on low priority. A Ph.D. thesis is anticipated in this area to help us in our current period of reduced staff. Concerning non-chlorine bleaching with a pretreatment of NO₂ prior to oxygen delignification, the results given in the current PAC report should clarify the question of "impure" dioxide. Suffice it to say that the major impurity was a trace of water which gave small amounts of nitrogen oxides other than NO₂. Regarding the work of Barbara Burns, I anticipate her thesis will be initiated in early October and it will make a significant contribution to the area of medium consistency, high shear mixing with chemical reaction.

Project 3524 - FUNDAMENTALS OF BRIGHTNESS STABILITY

With the departure of Werner Lonsky, the short range goals of this project need to be reevaluated. Specifically, we are considering taking the tech-

niques developed for defining the kinetics of yellowing, the quantification of chromophoric groups, and the identification of radical formation on light exposure and applying them in a study of the effects of standard high yield bleaching techniques. As new professional help becomes available, the more fundamental activity of the project will be reinstated. We expect to carry on one portion of the fundamental studies by bringing Dr. Umesh Agarwal into the project. He will use laser Raman techniques to evaluate the initial photochemical reaction in the yellowing of pulp. This will be discussed at the PAC meeting.

Project 3566 - SEPARATION OF STRONG, INTACT FIBERS

We have come up with a method for the evaluation of fibril angle in fibers, based on a novel dyeing method; this will also be discussed at the upcoming PAC meeting. We continue to pursue methods for bonding strong fibers, both by process variation as well as by externally applied bonding agents. However, the main thrust of this project remains the development of fibers with maximum strength. To alleviate concerns about our high yield pulps made using the Asplund defibrator, we are currently running confirmatory trials at a member company using a Sunds laboratory system.

Project 3288 - FINE STRUCTURE OF WOOD PULP FIBERS

The committee has made it clear that in order to ensure industry support, the fundamental concepts developed in this project area must be related to more practical applications. With the availability of the new equipment funded by DOE, which will make it practical to obtain spectra in reasonable times, we will make a specific effort to do this. Some initial areas are the development of a lignin sensor and in the use of Raman techniques to define the structure of high yield pulps.

Best regards.

Sincerely,



Earl W. Malcolm
Director
Chemical Sciences Division

EWM/gmk
Copy to: Dr. Charles W. Spalding (RAC Chairman)

July 8, 1986

A190

INDEPENDENT STUDY

<u>Student</u>	<u>Advisor</u>	<u>Room</u>	<u>Subject</u>
Beck	Farrington	209	The quantitative determination of stickies in recycled paper.
Boyle	McDonough		Pulping kinetics at low liquor to wood ratio.
Bunker	Conners/ Malcolm	209	Changes in fiber structure during delignification by kraft and alkaline sulfite-AQ.
Cornbower	Johnson/ McDonough	107	The response of white spruce to mechanical pulping after enzymatic degradation of hemicellulose.
Crockett	Easty	Carrel 4	Characterization of paper additives and contaminants by pyrolytic gas chromatography.
Dalgardno	Sprague	Carrel 8	Paper machine modelling: development of linerboard mechanical properties.
Dundore	Lavery	47	Investigation of bonding mechanism during impulse drying.
Fuller	Cameron	So. Res.	Determine the effect of impurities on the sintering and nodulation processes during calcination.
Hayford	Crowe	Annex	A proposal to study the inhibition of stress corrosion cracking in white liquor by tannic acid.
Holton	Dugal	207	The effect of drying on the crystallinity of arabino-4-O-methylglucuronoxylan, glucomannan, and galactoglucomannan.
Kalishek	Crowe	Annex	The effect of white water velocity on the corrosion rate of carbon steel.
Kemps	Waterhouse	Carrel 3	Measurement and analysis of the internal stresses in paper and board.

<u>Student</u>	<u>Advisor</u>	<u>Room</u>	<u>Subject</u>
Leege	Dimmel/ Schroeder	K231	A characterization of the thermodynamic functions of activation for 1,5, anhydromaltitol.
Lewis	Wahren	Carrel 12	Determination of a single characterizing parameter in the screening process.
Luetngen	Stratton	1232	Simulation of paper machine turbulent shear in retention aid systems.
McCarthy, J.	Stratton	1228	A test for carryover impurities.
McKibben	Jones	No lab	The convergence acceleration of MAPPS.
Medvecz	Lonsky	K220	o-quinone formation in hardwood and softwood TMP.
Miller, C.	Dugal	219	Lumen-loading of wood fibers with organic material.
Miller, D.	Yeske	Corro- sion Lab	Electrochemical noise measurements for the detection of pitting of stainless steels.
Plouff	Malcolm	K100	Determination of the lignin distribution in loblolly pine tracheids by scanning-transmission electron microscopy and energy-dispersive spectrometry.
Sands	Dimmel/ Schroeder	K210	The role of the 1,2-hydrate shift mechanism in base-catalyzed aldose-ketose isomerization.
Stoffler	Lonsky	K118	A study aiming at the development of a brightness stabilizing retention aid for high-yield pulps.
Stroh	McDonough		The effect of metal-ion complexes on hydrogen peroxide delignification.
Verrill	Cameron	So. Res.	Sodium fuming during black liquor combustion.
Votsmier	Jones	Carrel 11	Multiple effect black liquor evaporators.

July 8, 1986

THESES IN PROGRESS

<u>Student</u>	<u>Passed to Thesis Candidacy Approval</u>		<u>Subject</u>	<u>Committee</u>	<u>Room</u>
Brigham (Not in residence from July, 1986 on)	6/11/81	8/31/81	The role of particle size and polymer molecular weight on the adsorption and flocculation of pulp fines with a cationic polyelectrolyte.	Stratton, chr. Dugal	
Bovee	6/11/82	8/9/82	The synthesis and evaluation of an alkali insoluble cellulose model.	Dimmel, chr. Schroeder Lonsky	K213
Geddes (Not in residence Sept. & Oct. 1983)	9/2/83	1/10/84	Alkaline degradation of amylose: a kinetic model	Halcomb, chr. Schroeder Johnson Cullinan	K209
Heazel (Not in residence summer 1984)	11/29/83	2/14/84	The influence of sulfonation on sulfite CMP properties.	McDonough, chr. Whitsitt Litvay [adjunct member] Cullinan	K216 K100
Nealey	1/4/84	2/24/84	Isolation and characterization of xyloglucan from suspension cultured loblolly pine cell medium.	Johnson, chr. Easty Cullinan	34
Biasca	1/4/84	2/24/84	Oriented fiber refining: application of individual modes of mechanical action to single pulp fibers.	Baum, chr. Habeger McDonough Michael Jackson (Weyerhaeuser) [adjunct member] Cullinan	71 K27

<u>Student</u>	<u>Passed to Candidacy</u>	<u>Thesis Approval</u>	<u>Subject</u>	<u>Committee</u>	<u>Room</u>
Lebo	6/8/84	6/29/84	The rate and quantum yield of the light induced formation of ortho-quinonoid lignin structure.	Lonsky, chr. McDonough Cullinan	K219
Pugliese	6/8/84	11/7/84	A kinetic analysis of kraft pulp chlorination.	McDonough, chr. Cameron P. Parker Cullinan	K211
Byers	9/4/84	10/4/84	An autoradiographic study of the hemicellulose distribution in the cell walls of <u>Pinus Resinosa</u> tracheids.	Atalla, chr. Johnson	K221
Reed	9/4/84	12/11/84	The role of sulfur species in pulping reactions.	Dimmel, chr. Malcolm Schroeder	K232
Molinarolo, S. (Not in residence Sept. 1984 thru Dec. 1984). (Also July & Aug. 1986).	9/4/84	3/14/85	Sorption of xyloglucan onto cellulose fibers.	Stratton, chr. Johnson	34
Molinarolo, W. (Not in residence Sept. 1984 thru Dec. 1984)	9/4/84	3/14/85	The high temperature alkaline degradation of phenyl- β -D-glucopyranoside.	Dimmel, chr. Schroeder	K210
McCarthy (Not in residence Sept. 1984 thru Dec. 1984)	9/4/84	3/14/85	An investigation of the mechanism of alkaline sizing with alkenyl succinic anhydride.	Stratton, chr. Easty Dugal	K121
Robinson	11/27/84	2/19/85	Characterization of black liquor droplet drying in air, steam, and humid air.	Clay, chr. Grace Lavery	69 SRB

<u>Student</u>	<u>Passed to Candidacy</u>	<u>Thesis Approval</u>	<u>Subject</u>	<u>Committee</u>	<u>Room</u>
Proxmire, P.	11/27/84	2/19/85	The influence of aluminum salts on the retention of titanium dioxide when using cationic polyelectrolyte as a retention aid.	Stratton, chr. Dugal Easty	K121
Berger, Brian	3/28/85	3/14/85	The effects of refining and yield on the z-direction elastic properties of paper.	Baum, chr. Habeger Waterhouse	66
Aiken	6/7/85	6/6/85	The use of a char pile reactor to study char bed processes.	Cameron, chr. Grace Parker, P.	So. Res. Lab.
Berger, Bernard	9/10/85	11/14/85	Transient effects of moisture sorption at various temperatures on the ultrasonically measured elastic moduli of cellulosic materials.	Habeger, chr. Stratton Waterhouse Baum (ex officio)	K27
Bither	9/10/85	1/27/86	Strength development through internal fibrillation and wet pressing.	Waterhouse, chr. Baum Wahren (ex officio)	203A
Barkhau	12/6/85	12/16/85	Anthraquinone inhibited lignin condensation.	Dimmel, chr. Lonsky Malcolm	K232
Wozniak	4/7/86	3/12/86	Preparation and reactions of Diels-Alder adducts of lignin-derived quinones.	Dimmel, chr. Lonsky Malcolm	K205
Kulas	3/25/86	4/16/86	An investigation of the fire-side sulfidization of kraft recovery furnace waterwall tubes.	Grace), co- Yeske), chr. Cameron	

<u>Student</u>	<u>Passed to Thesis Candidacy Approval</u>	<u>Subject</u>	<u>Committee</u>	<u>Room</u>
Triantafill- opoulos (Not in residence summer 1986)	6/13/86			
Crane, K. (Not in residence summer 1986)	6/13/86			
Harper (Not in residence summer 1986)	6/13/86			
Burns, B.	6/27/86			168
Goulet (Not in residence summer 1986)	6/27/86			

STATUS REPORTS
TO THE
PULPING PROCESSES
PROJECT ADVISORY COMMITTEE

OCTOBER 20-21, 1986
THE INSTITUTE OF PAPER CHEMISTRY
APPLETON, WI 54912

TABLE OF CONTENTS

	Page
FINE STRUCTURE OF WOOD PULP FIBERS (Projects 3288 and 3521)	1
SMELT-WATER EXPLOSIONS (Project 3456-2)	49
FUNDAMENTAL PROCESSES IN ALKALI RECOVERY FURNACES (Project 3473-1)	52
Fume Generation	57
Black Liquor Burning	110
Char Burning	178
FUNDAMENTAL STUDIES OF BLACK LIQUOR COMBUSTION (Project 3473-6 [DOE])..	186
IMPROVED PROCESSES FOR BLEACHED PULP (Project 3474)	189
FUNDAMENTALS OF SELECTIVITY IN PULPING AND BLEACHING (Project 3475) ...	198
DEVELOPMENT AND APPLICATION OF ANALYTICAL TECHNIQUES (Project 3477) ...	219
FUNDAMENTALS OF BRIGHTNESS STABILITY (Project 3524)	253
SEPARATION OF STRONG, INTACT FIBERS (Project 3566)	274
COMPUTER MODEL OF RECOVERY FURNACE (Project 3605)	310

THE INSTITUTE OF PAPER CHEMISTRY

Appleton, Wisconsin

Status Report

to the

PULPING PROCESSES

PROJECT ADVISORY COMMITTEE

Project 3288

FINE STRUCTURE OF WOOD PULP FIBERS

Project 3521-2

RAMAN MICROPROBE INVESTIGATION OF MOLECULAR STRUCTURE
AND ORGANIZATION IN THE NATIVE STATE OF WOODY TISSUE

September 9, 1986

PROJECT SUMMARY FORM

DATE: September 11, 1986

PROJECT No. 3288: FINE STRUCTURE OF WOOD PULP FIBERS

PROJECT LEADER: R. H. Atalla

IPC GOAL:

Develop relationships between the critical paper and board property parameters and the way they are achieved as a combination of raw materials selection, principles of sheet design, and processing.

OBJECTIVE:

Define the structure of wood pulp fibers and relate to ultimate web properties.

CURRENT FISCAL YEAR BUDGET: \$75,000

SUMMARY OF RESULTS SINCE LAST REPORT:

SS ^{13}C -NMR studies have shown native celluloses to be composites of two crystalline forms, I_{α} and I_{β} . Their Raman spectra show them to have the same molecular conformation but to have different hydrogen bonding patterns. The distribution between the two forms varies over a wide range among native celluloses. There are indications that variation in the balance between the two forms (I_{α} and I_{β}) may be the key to differences in the response of native celluloses to mercerization or to solvent systems. These results also suggest that the balance between the two forms is an important determinant of mechanical properties.

Our most recent results, based on both proton and ^{13}C spin diffusion studies, confirm our earlier findings that the algal celluloses are composites. The results on native celluloses from higher plants (wood, cotton, ramie); however, suggest that further analyses of the spectra are in order. The spin diffusion studies indicate that the content of I_{α} cellulose in higher plants may indeed be lower than our earlier estimates; of the order of 15 to 20% rather than 35 to 45%. Some questions remain, however, because the spin diffusion studies are complicated by the much smaller fibril diameters in the celluloses from higher plants. We are actively pursuing a critical assessment of the results.

We have continued to use algal celluloses of high crystallinity as system models. We now have a species of Pithophora that in one instance was found to contain 38% cellulose in its walls. Its crystallinity, however, is close to that of the higher plants than other algal celluloses.

The studies on cellulose aggregation have demonstrated that other β -1,4-linked pyranose polymers can coaggregate with cellulose in the cellulose lattice. In particular, we have been able to prepare blends of cellulose and chitosan which give evidence of a mixed lattice. We are now pursuing the possibility of preparing similar blends with mannans and xylans. If we are successful, the x-ray

patterns, Raman spectra, and SS ^{13}C -NMR spectra will be compared with those of celluloses from native woody tissue. If similarities are found, the models of molecular phenomena which determine fiber properties will need to be revised. Furthermore, the usual interpretation of spectral and diffractometric data in terms of a balance between crystalline and amorphous cellulose will need to be reassessed.

We continue to refine our methods for detecting subtle differences between celluloses by combined chemical and spectroscopic techniques.

PLANNED ACTIVITY THROUGH FISCAL YEAR 1987:

1. Use SS ^{13}C -NMR and Raman spectroscopy and x-ray diffractometry to investigate the variability of the I_{α} to I_{β} ratio in native celluloses and its relation to chemical reactivity and to the response to process environments.
2. Investigate the degree to which characteristic spectra and x-ray patterns of wood celluloses are consistent with a model in which linear hemicelluloses are aggregated as part of the crystalline domains.
3. Carry out a preliminary evaluation of the range of variability of wood derived celluloses with respect to the questions outlined above.
4. Assess the properties of coaggregates of cellulose with hemicelluloses and other β -1,4-linked polysaccharides and their potential as a new class of materials.

FUTURE ACTIVITY:

Progress on several projects, including the new areas of high-yield pulping and moisture tolerant webs, will benefit from a better understanding of the relation between fiber and product properties. New information on cellulose and fine fiber structure will be useful in guiding activity. Future work will focus on the structure of native wood fibers and its modification in both conventional chemical and high-yield pulping processes. Particular attention will be given to the factors (yet to be determined) which control fiber properties.

STUDENT RESEARCH:

I. Uhlin, Ph.D.
E. Byers, Ph.D.
Tan Zheng, Special Student

PROJECT SUMMARY FORM

DATE: September 11, 1986

PROJECT No. 3521-2: RAMAN MICROPROBE INVESTIGATION OF MOLECULAR STRUCTURE AND ORGANIZATION IN THE NATIVE STATE OF WOODY TISSUE

PROJECT LEADER: R. H. Atalla

IPC GOAL:

Develop relationships between the critical paper and board property parameters and the way they are achieved as a combination of raw materials selection, principles of sheet design, and processing.

OBJECTIVE:

In conjunction with work sponsored by the DOE, use the Raman Microprobe to develop a better understanding of wood fiber structure. Establish by Raman microprobe spectroscopy the variability of molecular structure and organization in cell walls of native woody tissue. Explore the effects of mechanical and chemical treatments on structure and organization in high-yield pulp fibers.

CURRENT FISCAL YEAR BUDGET: \$45,000*

SUMMARY OF RESULTS SINCE LAST REPORT:

Optimization of the Raman microprobe, together with the new techniques we developed, have permitted acquisition of high quality spectra that clearly indicate a higher level of organization of lignin in the cell walls than heretofore recognized. The spectra show lignin to be oriented with respect to the plane of the cell-wall surface and to vary in amount relative to cellulose, from point to point within the secondary wall.

In the course of our efforts to optimize our methods, we have discovered an unusual interaction between molecular oxygen and native lignin. When samples of native woody tissue are exposed to the laser beam while they are being flushed with a stream of pure oxygen, the level of background fluorescence is substantially reduced. A number of other gases have been tried, but they do not have a similar effect. We conclude that the interaction responsible must be associated with the presence of unpaired electrons in molecular oxygen. We continue to explore this effect because it may provide some insights concerning the processes responsible for color reversion in high yield pulps.

Success of these efforts has led to the award of a grant of \$194,000, under the DOE University Research Instrumentation Program, to enable us to acquire a new multichannel Raman microprobe system which will enable us to continue our studies with far greater efficiency. Delivery of components of the new system should be completed in September.

*This work is also supported by DOE under Project 3521-3 with a Fiscal 1986/87 budget of \$50,000. This is in addition to the DOE grant of \$152,000 toward the acquisition of the new Raman microprobe system.

PLANNED ACTIVITY THROUGH FISCAL YEAR 1987:

A significant part of our effort will be assembly and optimization of the new systems.

Exploration of the spectra of different woods and native fibers will be continued. The effects of chemical treatment on the architecture of the cell walls will also be investigated.

Preliminary assessments will be made of the photophysical processes in lignins. This will include developing a fundamental understanding of the dynamics of electronic transitions in native lignin and the roles they play in color reversion in high-yield pulps. The new spectrometer system allows new experimental techniques that will help in elucidating these reactions. If results warrant, this will become a major use for the new Raman microprobe.

FUTURE ACTIVITY:

Continuation of the program in conjunction with the DOE-supported effort is anticipated through Fiscal 1986/87. The methods developed under this program may be adapted to explore the effects of mechanical and chemical treatments on structure and organization in high-yield pulp fibers.

STUDENT RESEARCH:

J. Bond, Ph.D.

Status Report

FINE STRUCTURE OF WOOD PULP FIBERS

INTRODUCTION

Both Projects 3288 and 3521 are concerned with molecular structure and organization in wood pulp and other cellulosic fibers and the relationships between structure and properties. In pulp based materials, as in all other fiber based composites, the mechanical properties of the composite structures are determined by the properties of the fibers. These in turn are determined by the molecular structure of the dominant components and the manner in which these components are aggregated together in the solid state.

In fibrous polymeric materials the state of aggregation is defined by specification of the degrees of molecular orientation and crystallinity; these are among the most often studied parameters for synthetic fibers. In the case of native fibers the state of aggregation is also defined by native morphology and by the manner in which both morphology and molecular organization are changed in isolation and manufacturing processes such as pulping, bleaching, and papermaking.

Project 3288 has focused on questions of structure in chemical pulps and in related native cellulosic fibers since its inception. It has also been concerned with the mechanisms of aggregation of celluloses in both native and regenerated forms and with their interactions with related cell wall polysaccharides.

Project 3521 was initiated with a focus on the structure of cell walls in wood, with particular emphasis on the organization of lignin in the native

state. It is more logically connected to questions of structure in high-yield pulps, though it is also intended to address questions which are relevant to understanding delignification mechanisms in the manufacture of chemical pulps.

Much of the work under both projects has been based on physical methods for structural investigation. The primary tools have been diffractometry and spectroscopy. Although X-ray diffractometry has been a key tool in much of the work, the primary tool has been Raman spectroscopy. Solid State ^{13}C -NMR has also been used through a collaboration with other laboratories, primarily the National Bureau of Standards.

The application of Raman spectroscopy has been pioneered in the work at the Institute, under Project 3288 and its predecessor, and more recently under 3521. An overview of the effort is presented in a paper, appended as Attachment I, initially prepared for the TAPPI International Conference on Process and Product Quality. In the following sections separate overviews are also provided for more recent studies under each of the projects.

The overview of 3288 begins with an updated summary of our model of polymorphy in cellulose. The results of studies on polymorphy are then outlined, and these are followed with some recent observations on the effects of dehydration of cellulose at the molecular level.

A good overview of the work under 3521 is presented in excerpts from the recent report to the Basic Biology Section at the DOE, which cosponsors the work. In preparation of the excerpt, three of the preprints have been replaced by abstracts. All will be issued in the IPC Technical Paper Series in coming months.

OVERVIEW - PROJECT 3288

The effort under Project 3288 has been primarily in two areas. The first is a continuation of explorations of the nature of polymorphy in native celluloses. The second is an extension of studies on the aggregation of celluloses from nonaqueous solvent systems and from the hydrated state. To place discussion of the recent work in perspective, our current model of cellulose structure will be reviewed briefly.

Model of Structures of Celluloses

As described in somewhat greater detail in Attachment I, the main point of departure for our model of cellulose structure grew out of recognition that the two common polymorphs of cellulose possess distinctly different conformations. Raman spectroscopy, Solid State ^{13}C NMR, and X-ray diffractometry led us to the conclusion that two stable ordered conformations of cellulose coexist with some disordered cellulose in most cellulosic samples. We represent these conformations as K_I , and K_{II} , based on their dominance in celluloses I and II, respectively. The disordered state is represented as k_0 .

The ordered states k_I and k_{II} are thought to approximate twofold helical structures but to depart sufficiently from such structure so that the basic repeat unit of structure is the dimeric anhydrocellobiose unit with nonequivalent anhydroglucose units. The disposition of the individual anhydroglucose units within the anhydrocellobiose unit is thought to be different in the two different ordered conformations. The conformational model has been used as a basis for quantitative resolution of the Raman spectra of many celluloses, as outlined in Attachment I.

The model of cellulose structure was further developed to describe the differences between native celluloses. These differences have been recognized in the past on the basis of diffractometric and infrared spectroscopic studies. However, it was only with the aid of Solid State ^{13}C -NMR spectra that the differences have been interpreted in terms of a composite structure. The model of structure of the native forms is based on the hypothesis that two forms, identified as I_{α} and I_{β} , coexist in all native forms. The I_{α} form appears to be dominant in most algal celluloses and bacterial cellulose, while the I_{β} form appears to be dominant in celluloses from the higher plants. Further Raman spectral studies of the native celluloses have indicated that the two forms have molecules in the same conformation but with different patterns of hydrogen bonding.

Studies on Polymorphy in Native Cellulose

Work in this area continued in collaboration with Dr. D. L. VanderHart at the National Bureau of Standards. The major results are summarized in a paper, the abstract of which is appended as Attachment II. The studies reported in this paper are based on use of spin relaxation and spin diffusion to investigate the morphology of the polymeric solid state. Experiments were carried out in which proton relaxation or ^{13}C relaxation processes were monitored. Such experiments allow enhancement of the signals arising from regions deep in the crystalline domains. Observation of such signals established that the multiplicities in the spectra of native celluloses cannot arise from surface effects but are in fact reflections of inequivalences within the crystalline lattices.

The spin diffusion studies are sensitive to the separation of domains which contribute specific features in the spectra. The spectra acquired in the course of these measurements provide additional evidence that the algal and bacterial celluloses are indeed composites.

These studies have resulted in some revision of the earlier estimates of the proportions of I_{α} and I_{β} celluloses which occur in the native forms. The new estimates of the I_{α} content of algal celluloses are closer to 50%. For the celluloses from the higher plants, the new results raise some question about the presence of the I_{α} component. The results could not demonstrate the presence of the I_{α} component in the higher plant celluloses, but neither do they provide a basis for negating the earlier studies because the procedures are inherently insensitive to levels below 15 to 20%. Thus, the earlier hypothesis concerning the presence of the I_{α} component in higher plant celluloses needs to be revised to indicate an upper limit of 20%, rather than 35% as initially proposed.

Complementing the studies outlined above, the OH region in the Raman spectra of the different native forms has been investigated. It has been possible to resolve the spectra into OH region spectra of the I_{α} and I_{β} forms. These spectra are consistent with the hypothesis that the I_{α} form is the major component in the algal and bacterial celluloses, and a minor component in the higher plant celluloses.

In a separate investigation of polymorphy, samples of cellulose III were prepared by treatment of algal cellulose with anhydrous ammonia. These will be discussed in greater detail in a future report. They are mentioned here because of the observation that when the cellulose III was treated in boiling water and reverted to cellulose I, the I_{α} component appeared to have been substantially converted to the I_{β} form. This is the first instance of conversion of cellulose from one to another of these two forms and provides evidence for a solid state transformation of cellulose from another conformation and lattice to those characteristic of higher plant celluloses.

Studies on Dehydration of Cellulose and Its
Significance in Papermaking

In the course of studies on mercerization and regeneration of different native celluloses, the hydrated state of cellulose immediately preceding freeze drying was examined. The particular concern was to establish whether the drying process resulted in changes that could be detected spectroscopically. This question was posed in connection with Solid State ^{13}C NMR spectra wherein an enhancement of the resolution of the spectra was noted when the samples were moist.

The specific experiments involved acquiring Raman spectra of the samples after the last stage in the washing, while they were still immersed in water, and repeating the measurement after the samples were freeze dried. The spectra were found to change upon drying in a manner that suggested a far greater perturbation of the molecular structure than had generally been recognized. In particular, a number of bands in the low frequency region underwent some changes in relative intensity, and all were broadened to a degree that suggested substantial distortions of the crystalline domains.

To test the relevance of this observation to papermaking operations similar measurements were made on a sample of neverdried bleached pulp before and after it had been freeze dried. Although the changes were not as dramatic as with the mercerized and regenerated celluloses, significant changes in the spectra were observed. A full discussion of these results will be deferred to some future report, but it should be noted that the results indicate significant twisting or distortion at the fibrillar level associated with the drying process. Furthermore, comparison with prior results on effects of refining on the spectra suggest that many of these distortions are irreversible.

Exploratory Studies

In addition to the two major areas outlined above, a number of exploratory studies are continuing. These include the culture of a number of algal species which generate highly crystalline celluloses, and the culture of Acetobacter xylinum, the cellulose producing bacterium. These have been used in our studies of polymorphy and in some of the student research programs.

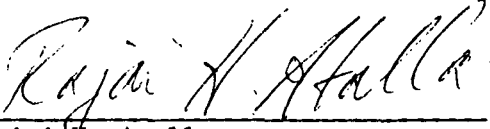
A study of celluloses from biodegraded wood is also currently in progress. The samples are provided by Dr. R. Blanchette of the University of Minnesota department of plant pathology.

OVERVIEW - 3521

Progress under 3521 is outlined in Attachment III which contains excerpts from the report to the Basic Biology Section of the Division of Basic Energy Sciences of the Department of Energy, which has cosponsored the work.

In addition it should be noted that the lasers and the detectors for the new spectrometer systems have been delivered. Delivery of the monochromators is expected by mid-September. Installation should be well underway in early October. It is anticipated that initial emphasis will be on installation of the microprobe system and that it will be operational by mid-October. The ultrafast spectroscopy system will require design and assembly of sampling optics; it will be operational later this year, but its full capabilities will be developed over a longer period.

The Institute of Paper Chemistry


Rajai H. Atalla
Chemical Sciences Division

ATTACHMENT I

**RAMAN SPECTROSCOPY AND THE RAMAN MICROPROBE:
VALUABLE NEW TOOLS FOR CHARACTERIZING
WOOD AND WOOD PULP FIBERS**

R. H. Atalla
The Institute of Paper Chemistry,
Appleton, WI 54912

ABSTRACT

A brief overview of Raman spectroscopy and the photon scattering phenomena which underly it is presented, together with the rationale for applying the methodology to the study of lignocellulosics. The sequence of studies undertaken at The Institute of Paper Chemistry to apply the methods to investigation of celluloses, chemical pulps, wood and high yield fibers are then reviewed.

The program began with studies on cellulose and related model compounds. These early efforts provided a basis for interpretation of the spectra of celluloses and for investigating the effects of various process variables on the aggregation of cellulose in pulp fibers. Among the effects touched upon are the differences between kraft and sulfite pulps, the effects of refining, and the influence of press drying on pulp crystallinity. More recently studies using the Raman microprobe made possible progress in the assignment of the vibrational spectra of cellulose and established the basis for using the microprobe to investigate variability of fibril orientation in native woody tissue.

In addition our extension of the studies to include lignin are noted. These included studies of fiber sections in native wood which show the orientation of lignin in the cell wall and observations of the variability of the ratio of lignin to cellulose.

Finally, the opportunities arising from new instrumental developments are reviewed. The new multichannel detectors will greatly enhance the efficiency of acquisition of spectra and allow more comprehensive explorations of the architecture of fibers. In addition, gated detectors coupled with pulsed laser excitation will allow studies of woody tissue and of high yield pulps that would not be feasible with single channel detection and continuous laser excitation.

INTRODUCTION

Raman scattering was first observed in 1928, and was used to investigate the vibrational states of many molecules in the 1930s. Spectroscopic methods based on the phenomenon have been used in research on the structure of relatively simple molecules since the early days. Over the past twenty years, however, the development of laser sources and new generations of monochromators and detectors have made possible application of Raman spectroscopy to the solution of many problems of technological interest.

In many industrial analytical laboratories Raman spectroscopy is routinely used together with

infrared spectroscopy for acquisition of vibrational spectra from materials under investigation. At least two instrument manufacturers are preparing to market Raman spectrometer systems in the \$25,000 to \$35,000 price range, which places them below the price of FTIR instruments. An important expansion of the potential of the technique has arisen from the use of the Raman microprobe, which permits acquisition of spectra from domains as small as 1 micrometer.

In 1970 the Institute initiated a program with the objective of understanding the states of aggregation of the natural polymers which constitute wood fibers and which determine their influence on properties. The approach is similar to that frequently applied to synthetic polymers within the framework of modern materials science. As part of this broader program an effort was undertaken to develop the application of Raman spectroscopy for characterizing the structure of fibers and in addressing problems arising in pulp and paper technology.

The program has progressed from studies of cellulose and related model compounds to studies of pulps and their response to different process conditions, and more recently to studies of lignins in wood and high yield pulps. This report provides an overview of the progress, the areas currently under active investigation, and the areas opened up by the new generation of systems for Raman spectroscopy.

In the next section primary phenomena and events in Raman scattering are discussed in relation to the parallel processes in infrared absorption. In addition, the section includes a review of the special advantages of Raman spectroscopy in investigating lignocellulosic systems. Next, the key questions in interpretation of the spectra are discussed together with the approach adopted in the Institute's program. Highlights of key results at each stage of the program are reviewed. Finally, the new areas of investigation opened up by the microprobe and by time resolved spectroscopy are outlined. Some results of microprobe studies using single channel detection are presented together with very preliminary results from multichannel systems.

RAMAN SPECTROSCOPY

The phenomena underlying Raman spectroscopy can be described by comparison with infrared spectroscopy as shown schematically in Fig. 1. There it is seen that the primary event in infrared absorption is a transition of a molecule from a ground state (M) to a vibrationally excited state (M^*) by absorption of an infrared photon with energy equal to the difference between the energies of the ground and excited states. The reverse process of infrared emission occurs when a molecule in the excited state (M^*) emits a photon during the transition to the ground state (M). In infrared spectroscopy, one derives information about a sample under investigation by measuring the frequencies of infrared photons it absorbs and interpreting these frequencies in terms of the characteristic vibrational motions of molecules known to absorb at

these frequencies. In the case of more complex samples, some of the frequencies are associated with functional groups that have characteristic localized modes of vibration.

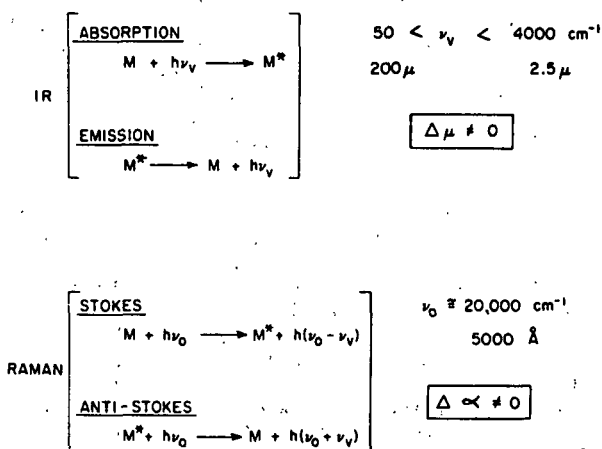


Fig. 1 Schematic representation of infrared and Raman processes. μ = Dipole movement, α = polarizability; ν_v = vibrational frequency, ν_0 = exciting frequency.

As also shown in Fig. 1, the same transitions between molecular vibrational states (M) and (M^*) can result in Raman scattering. The key difference between the Raman and infrared processes are that the photons involved are not absorbed or emitted but rather shifted in frequency by an amount corresponding to the energy of the particular vibrational transition. In the Stokes process, which is the parallel of absorption, the scattered photons are shifted to lower frequencies as the molecules abstract energy from the exciting photons; in the anti-Stokes process, which is parallel to emission, the scattered photons are shifted to higher frequencies as they pick up the energy released by the molecules in the course of transitions to the ground state.

The exciting photons also are typically of much higher energies than those of the fundamental vibrations of most chemical bonds or systems of bonds, usually by a factor ranging from about 6 for OH and CH bonds to about 200 for bonds between very heavy atoms, as for example in I_2 . In our work we most often use the 5145 Å line from Argon ion laser as the exciting frequency.

Measurement of a Raman spectrum requires exposure of the sample to a monochromatic source of exciting photons, and measurement of the frequencies of the scattered photons. Because the intensity of Raman scattering is much lower than that of Rayleigh scattering, a highly selective monochromator is required, and it must be coupled to a very sensitive detector. Rayleigh scattering, which occurs without change in frequency, arises from density variations and optical heterogeneities and is many orders of magnitude more intense than Raman scattering.

Figure 1 also depicts a key difference between Raman scattering and infrared processes. In order

to be active in the infrared spectra, transitions must have a change in the molecular dipole associated with them. For Raman activity, in contrast, the change has to be in the polarizability of the molecule. These two molecular characteristics are qualitatively inversely related. For example, a molecule with a high dipole such as water has a low polarizability. As a consequence, though water absorbs very strongly in the infrared, its Raman scattering is quite weak, and it is almost the ideal solvent for Raman spectroscopy.

The difference between the conditions for activity in the infrared and Raman spectra makes the information from the two forms of spectroscopy complementary in most instances. Symmetric vibrations of highly covalent bond systems result in intense Raman bands and in weak infrared bands. On the other hand, asymmetric vibrations of highly polar bonds result in very strong infrared absorption and weak Raman bands. For example, while the strongest atmospheric bands in infrared absorption are the water bands and the asymmetric bands of CO_2 , the strongest atmospheric bands in Raman spectra are those of the homonuclear N_2 and O_2 , which are transparent to the infrared.

STUDIES OF CELLULOSES AND PULP FIBERS

A number of considerations motivated the selection of Raman spectroscopy as a promising new tool for the study of lignocellulosic materials. The advances in infrared spectroscopy in the 1950s had led to a number of valuable studies of the spectra of cellulosic materials. Applications in the technology of cellulose remained quite limited, however, because of two key difficulties. The first was the problem of optical heterogeneity and the resulting high degree of Rayleigh scattering of infrared photons by cellulosic materials. Because the degree of Rayleigh scattering depends on differences in the refractive indices at optical discontinuities and because the refractive index varies with wavelength in regions of strong absorption, it is difficult to separate extinction due to molecular absorption from extinction due to Rayleigh scattering.

The second problem confronting infrared absorption measurements arose from the hygroscopicity of cellulose. The high extinction due to water in a number of regions in the infrared spectrum made acquisition and interpretation of spectra difficult.

When laser sources and the new generations of monochromators and detectors became available for Raman spectroscopy, it seemed possible that its complementary relationship to infrared absorption might make the technique the better one for investigating the vibrational spectra of cellulosic materials. It became clear early in the assessment that the two primary difficulties in application of infrared spectroscopy will not arise with Raman measurements. The most intense bands in the spectra of cellulose would be associated with skeletal motions involving C-C and C-O bonds, with the hydroxyl groups and adsorbed water contributing only weakly. Furthermore, by the nature of the measurement process, Rayleigh scattered photons, which are at the excitation frequency are rejected

by the monochromator. With these points in mind, a commitment was made to undertake to develop the methodology for acquisition and interpretation of Raman spectra of lignocellulosic materials.

The program envisioned involved a long term effort because the molecular systems of interest are complex, both chemically and vibrationally, and prior work provided very little basis for interpretation of spectra. The plan which guided the work was to begin with the most homogeneous chemical constituent of wood fibers, that is, cellulose. This would be followed by bleached chemical pulps, lignins, wood, and high yield pulps. At every stage, as progress was made in our understanding of the spectra, efforts would be made to use their measurement to characterize the effects of process steps.

The first objective thus was to investigate the Raman spectra of cellulose and the vibrational spectra of a number of sets of model compounds that would provide a basis for interpretation of the spectra of cellulose. The approach to investigating the spectra of cellulose was a semiempirical one based on perturbing the physical structure or state of aggregation of the cellulose and observing the resulting changes in the Raman spectra. The studies of model compounds were based on undertaking normal coordinate analyses of the vibrational motions of sets of related molecules and comparing these to the observed Raman and infrared spectral band of these compounds.

The studies of the model compounds led us to the finding that, with a few exceptions associated with highly localized vibrations involving hydrogen atoms, most of the modes of vibration were very highly coupled and delocalized. Thus the group frequency approach usually used in interpretation of infrared spectra is not applicable to the molecular chain modes of polysaccharides. Group frequencies are usually associated with highly localized modes which are characteristic of particular functional groups; the effect of coupling with adjacent bonds is often a relatively small shift in frequency. In retrospect, the failure of the group frequency method should not have surprised us, because pyranose rings and polymers thereof are made up of systems of C-C and C-O bonds. These bonds have similar reduced masses and bond energies, so their vibrational frequencies are close enough for a high degree of coupling to occur.

The studies of model compounds, though they raised questions about the group frequency approach, nevertheless provided valuable information about the different types of vibrational motions and the regions of the spectra within which they make their greatest contribution. This in turn allowed us to interpret the changes observed in the spectra of celluloses as they were subjected to structural perturbations.

Model Compound Studies

The groups of model compounds studied included the 1,5-anhydro pentitols (1,2), the pentitols and erythritol (3), the pentoses (4), glucose (5), the inositols (6,7), and the cellodextrins (8). In

each instance a number of members of the group was used to develop a force field to describe the molecular vibrations, and the quality of the fit was tested by the ability of the force field to predict the vibrational modes of other members in the group which had not been used in development of the force field. Although there are occasional variations in detail, certain patterns emerge, and these should in most instances be equally valid for cellulose and other related polysaccharides.

The C-H and O-H stretching bands occur in the ranges of 2800 to 3000 cm^{-1} and 3000 to 3600 cm^{-1} , respectively, and are much removed from the frequencies of the other motions which are below 1500 cm^{-1} . The only localized mode below 1500 cm^{-1} is the HCH bending motion at C6 of the anhydroglucose residue; it usually occurs between 1440 and 1500 cm^{-1} . The bands between 1200 and 1440 cm^{-1} are due to modes involving considerable coupling of methine bending, methylene rocking and wagging, and COH in plane bending; these involve angle bending coordinates which include one bond to a hydrogen atom. Significant contributions from ring stretching begin below 1200 cm^{-1} , and these modes together with C-O stretching motions dominate between 950 and 1200 cm^{-1} . Below 950 cm^{-1} , angle bending coordinates involving heavy atoms only (i.e., CCC, COC, OCC) begin to contribute, though ring and C-O stretches and the external modes of the methylene group may be major components. The region between 400 and 700 cm^{-1} is dominated by the heavy atom bending, involving both the C-O bonds and ring motions, although some ring stretching modes still make minor contributions. In some instances, O-H out-of-plane motions may contribute in this region also. Between 300 and 400 cm^{-1} the ring torsions make some contribution, and below 300 cm^{-1} they generally dominate.

In addition to the above generalizations concerning modes which occur in one or another of the classes of model compounds investigated, the spectrum of cellulose can have components due to modes centered at the glycosidic linkages. Computations for cellobiose indicate that these modes are strongly coupled with modes involving similar coordinates in adjacent anhydroglucose rings.

Studies on Cellulose

The perturbations of structure that were the basis of our investigations of the Raman spectra of cellulose were mercerization and regeneration from solution; both were known to result in polymorphic changes and to have significant effects on properties. Our initial studies, which focused on mercerization, led us to the conclusion that celluloses I and II must correspond to different molecular conformations as well as different crystalline lattices (9,10). Our studies of regeneration also supported these findings (11).

In these early studies it was proposed that the two conformations represented small right-handed and left-handed departures, respectively, from the accepted twofold helix structures. In a subsequent study it was noted that adjacent anhydroglucose rings appeared nonequivalent (12), and this was confirmed by Solid State ^{13}C NMR spectra (13, 14). This led to a redefinition of the two stable

conformations in terms of two stable states of anhydro-cellobiose as the repeat unit, with the glycosidic linkages alternating successively between right-handed and left-handed departures from the twofold helix conformation. This new model also permitted development of a method for quantitative analysis of the Raman spectra to establish the conformational distributions of samples of cellulose (15).

More recently, the Raman microprobe has made possible adaptation of some of the methods used in studies of the spectra of single crystals to studies of aggregates of fibrils of cellulose. The fibrils are known to have the molecular chains aligned parallel to their axes. Thus, by recording spectra with the electric vector of the exciting laser beam at different angles to the fibril axes it is possible to identify the vibrational modes of the molecules according to their direction relative to the axes of the molecules. In addition to advancing the assignments of the modes of cellulose, these studies shed new light on the nature of the differences between the highly crystalline algal celluloses and those from the higher plants (16,17).

Studies on Chemical Pulp

Development of the procedure for quantitative resolution of the spectra of cellulosic samples provided the basis for analyses of the spectra of samples of chemical pulps. Although differences between the spectra of celluloses from different plant sources had been noted, most could be interpreted in terms of differences in crystallinity or hemicellulose content or both.

In general, direct comparison of the spectra of pulps of commercial interest revealed few meaningful differences that could be associated with differences in process conditions. This was particularly the case if the samples had been derived from similar wood species by processes involving the higher temperatures associated with most commercial pulping processes.

An important step forward was associated with our recognition of the sensitivity of conformational change to mechanical restraint. While this was well known in connection with mercerization of textile fibers, its relevance to pulp characterization had not been immediately obvious. In two key studies in this area, we discovered that treatment of pulp samples with caustic solutions at the threshold of the mercerizing range could reveal differences in the degree of internal constraint on conversion from cellulose I to cellulose II.

In the first of these studies we detected a difference between kraft and sulfite pulps derived from birch (18,19). We found that the kraft pulp was significantly less converted when treated with 11% NaOH solutions. We interpreted this observation in terms of constraints on the freedom of cellulose molecules to undergo conformational changes. It was speculated that cross links of chemical or mechanical origin were present to a greater extent in the kraft pulp and were responsible for this constraint.

We next examined the effect of mechanical refining on the degree of internal constraint within pulp fibers. It was found that moderate refining of some pulps had little effect on the susceptibility to conformational transformation. However, extensive refining was found to increase the susceptibility to transformation, suggesting that the process does indeed result in reduction of the constraints of morphology (20,21).

In yet another application of Raman spectroscopy to process analysis, the Raman microprobe was used to investigate the effects of press drying on the structure of pulp fibers (22). It was found that the higher heat fluxes associated with press drying result in enhancement of the rate of crystallization in pulp fibers. The crystallization, which was measurable by quantitative analysis of the Raman spectra, appeared to contribute to stiffening of fiber aggregates in press dried sheets.

Lignin and Wood

More recently we have expanded our effort to include the study of lignin in native wood, in groundwoods, and in high yield pulps. In the earliest work spectra were recorded from samples of wood delignified to varying degrees. Spectra of the native lignin were then derived by subtraction. Interpretation of the spectra, however, had to await studies on model compounds.

A study of model compounds was undertaken; it was based on normal coordinate analyses of both infrared and Raman spectra (23). The study included three monosubstituted, three disubstituted, and one trisubstituted model related to the common lignin fragments. Though the study provided a basis for assigning a number of features in the Raman spectra of the native lignins, the result most relevant in the present context was confirmation of the assignments of the aromatic ring stretching band at 1600 cm^{-1} and the alpha carbonyl band at about 1640 cm^{-1} .

The assignments enabled us to move on to one of the most exciting new developments in the area, that is, examination of molecular orientation of lignin in cell walls of native woody tissue. The Raman microprobe allowed acquisition of spectra from domains as small as one micrometer (24,25). It became possible in that context to measure the effect of the polarization of the exciting laser radiation on the intensity of the symmetric aromatic ring stretching band at 1600 cm^{-1} while simultaneously analyzing the polarization of the Raman scattered photons. The results of such observations, illustrated in Fig. 2, can provide information concerning the orientation of the aromatic rings with respect to the electric vector of the incident beam and hence also indicate the orientation relative to the plane of the cell wall. The observations can also provide information about the relative amounts of lignin and cellulose at a particular point in the cell wall.

With the Raman microprobe it was possible for the first time to explore the degree of heterogeneity of structure in the cell walls. While in the first instance such information is important for understanding the molecular architecture of the

cell wall, it has very important implications for the analysis of pulping processes, and studies of fiber properties, particularly in the case of high yield pulps.

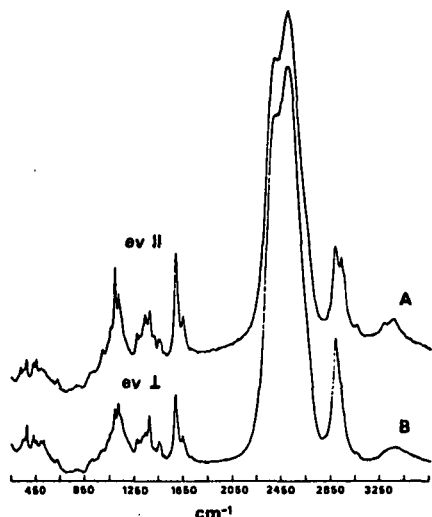


Fig. 2 Raman spectra from a domain approximately 1 μm in diameter in a longitudinal section of the secondary wall. (A) Electric vector parallel to the plane of the cell wall. (B) Electric vector perpendicular to cell wall.

The key findings, reported in greater detail elsewhere (26,27), were that the aromatic rings of the phenylpropane units of lignin are preferentially oriented with respect to the plane of the cell wall. Most often the orientation is in the plane of the cell wall, but in some instances it is perpendicular, while in other instances there is no preferential orientation. Our conclusion has been that lignin is more highly organized than had heretofore been assumed.

Another set of findings concerned the compositional variation within cell walls. It was found that the ratio of lignin to cellulose varied across the cell walls and that the variability is greater between adjacent cells than between different points within the same cell.

Future Studies with Multichannel Detectors

In the work reported so far, the spectra have been acquired with a Raman system that relied on a single channel detection system. That is, the spectra are recorded by scanning the frequency range of interest and observing the intensity of Raman scattered light at each frequency in sequence. In such a system the spectra shown in Fig. 2 required multiple scans over a period of 6 to 8 hours to achieve acceptable signal/noise ratios. Acquisition of data from a number of different locations on the cell wall sufficient to allow statistical analysis would require a prohibitive amount of time, of the order of weeks for a single cell.

To overcome the difficulty we are now assembling a Raman microprobe system equipped with

multichannel detection; the spectral interval of interest can be covered simultaneously by a diode array detector. We have demonstrated that spectra of signal/noise ratio equal to that in Fig. 2, can be acquired in 5 minutes, albeit with some limited sacrifice in spectral resolution.

In addition to facilitating more comprehensive mapping of the variability in cell wall architecture in different types of tissue, the new microprobe will make possible studies of diffusion of chemical reagents through the cell wall. Thus, it will provide data on mass transfer processes in cell walls and shed light on their role in determining key process rates in chemical pulping.

Another application of the Raman system with multichannel gated detection will be analysis of the evolution of excited states in lignin. This will be carried out using pulsed laser excitation, and should contribute to basic understanding of phenomena associated with color degradation in pulps, particularly high yield pulps.

In addition to the applications outlined above, gated multichannel detection and pulsed laser excitation are expected to permit application of Raman spectroscopy to address a number of problems in pulping and papermaking technology that could not be addressed with continuous laser excitation and single channel detection. We look forward to reporting on these in future meetings.

ACKNOWLEDGMENT

The work outlined has been supported by The Institute of Paper Chemistry and by the Biological Energy Research Program of the Department of Energy under Contract No. DE-AC02-82ER12056 and Grant No. DE-FG02-84ER13189. This support is gratefully acknowledged. The author's collaborators in the work are the authors and coauthors of the publications cited below.

REFERENCES

1. Pitzner, L. J., and Atalla, R. H., An investigation of the vibrational spectra of the 1,5-anhydropentitols. *Spectrochimica Acta*, 31A: 911(1975).
2. Pitzner, L. J., Doctoral Dissertation, The Institute of Paper Chemistry, Appleton, WI, 1973.
3. Watson, G. M., Doctoral Dissertation, The Institute of Paper Chemistry, Appleton, WI, 1975.
4. Edwards, S. L., Doctoral Dissertation, The Institute of Paper Chemistry, Appleton, WI, 1976.
5. Wells, H. A., Doctoral Dissertation, The Institute of Paper Chemistry, Appleton, WI, 1977.
6. Williams, R. M., and Atalla, R. H., Vibrational spectra of the inositols. *The Journal of Physical Chemistry* 88: 508(1984).

7. Williams, R. M., Doctoral Dissertation, The Institute of Paper Chemistry, Appleton, WI, 1977.
8. Carlson, K., Doctoral Dissertation, The Institute of Paper Chemistry, Appleton, WI, 1979.
9. Atalla, R. H., and Dimick, B. E., Raman-spectral evidence for differences between the conformations of cellulose I and cellulose II. Carbohydr. Res. 39: C1(1975).
10. Atalla, R. H., Raman spectral studies of polymorphism in cellulose. Part I: celluloses I and II. Proceedings of the Eighth Cellulose Conference, Applied Polymer Symposium No. 28, 659(1976).
11. Atalla, R. H., Dimick, B. E., and Nagel, S. C., Studies of polymorphism in cellulose. Cellulose IV and some effects of temperature. ACS Symposium Series 48: 30-41(1977).
12. Atalla, R. H., Conformational effects in the hydrolysis of cellulose. Adv. Chem. Series 181: 55(1979).
13. Atalla, R. H., Gast, J. C., Sindorf, D. W., Bartuska, V. J., and Maciel, G. E., ^{13}C NMR spectra of cellulose polymorphs. JACS 102: 3249(1980).
14. VanderHart, D. L., and Atalla, R. H., Studies of microstructure in native celluloses using solid state ^{13}C NMR. Macromolecules 17: 1465(1984).
15. Atalla, R. H., The structure of cellulose: quantitative analysis by Raman spectroscopy. J. Appl. Polymer Sci., Appl. Polymer Symp. 37: 295-301(1983).
16. Atalla, R. H., Studies on polymorphism in native cellulose, transactions of the 8th Fundamental Research Symposium, Mechanical Engineering Publications, Ltd, London, 1985, p.59.
17. Wiley, J. H., and Atalla, R. H., Raman spectra of celluloses, in "Solid State Characterization of Cellulose," R. H. Atalla, Ed., ACS Symposium Series, in press.
18. Atalla, R. H., Ranua, J., and Malcolm, E. W., Proc. 1983 Int. Dissolving Pulp Conf., TAPPI Press, 1983, p. 217.
19. Atalla, R. H., Ranua, J., and Malcolm, E. W., Raman spectroscopic studies of the structure of cellulose: a comparison of kraft and sulfite pulps. Tappi J. 67(2): 96-9(Feb., 1984).
20. Woitkovich, C. P., Whitmore, R. E., and Atalla, R. H., The effect of refining on molecular mobility in cellulose. Proc. 1983 International Paper Physics Conference, TAPPI Press, Atlanta, 1983, p. 65.
21. Woitkovich, C. P., Whitmore, R. E., and Atalla, R. H., Effects of refining on molecular mobility of cellulose in loblolly pine fibers. Tappi J., 68(1): 87(1986).
22. Atalla, R. H., Woitkovich, C. P., and Setterholm, V. C., Raman microprobe studies of fiber transformations during dress drying. Tappi J., 7(11): 116(1985).
23. S. M. Ehrhardt, Doctoral Dissertation, The Institute of Paper Chemistry, Appleton, WI, 1983.
24. Atalla, R. H., and Agarwal, U. P., Raman microprobe optimization and sampling technique for studies of plant cell walls. Microbeam Analysis - 1984, (A. D. Romig, Jr., and J. I. Goldstein, eds.) San Francisco Press, San Francisco, 1984, p. 125.
25. Atalla, R. H., and Agarwal, U. P., Recording Raman spectra from plant cell walls, J. Raman Spectroscopy, 17: 229(1986).
26. Atalla, R. H., and Agarwal, U. P., Raman microprobe evidence for lignin orientation in cell walls of native woody tissue. Science 227: 636(1985).
27. Agarwal, U. P., and Atalla, R. H., Studies of molecular orientation and compositional variability within the cell walls of woody tissue. Planta, (in press).

ATTACHMENT II

Further ^{13}C NMR Evidence for the Coexistence
of Two Crystalline Forms in Native Celluloses

D. L. VanderHart

National Bureau of Standards
Polymers Division
Gaithersburg, MD 20899

and

R. H. Atalla

The Institute of Paper Chemistry
Division of Chemical Sciences
Appleton, WI 54911

Abstract

The hypothesis that all native celluloses are composites of two crystalline polymorphs, I_{α} and I_{β} , is further explored using solid state ^{13}C NMR techniques. Spectra of several algal and higher plant celluloses and the effects of acid hydrolysis and mechanical beating are investigated. No significant alteration of the I_{α} and I_{β} ratios is seen upon hydrolysis of a cellulose from cotton linters. However, both beating and hydrolysis are seen to enhance the I_{β} proportion in an algal cellulose obtained from Cladophora.

Methods of enhancing the crystalline core resonances, based on proton rotating frame relaxation and carbon longitudinal relaxation, are used to verify that unit cell inequivalence rather than crystal surface chains determines the crystalline resonance profiles. These studies indicate that the C4 resonance region, from 88-92 ppm in all native celluloses is a faithful monitor of unit cell inequivalences. Also, the higher plant celluloses contain a much smaller fraction of the I_{α} crystalline form than originally proposed. The possibility even exists that the higher plant celluloses represent the pure I_{β} form. If this is true, then it follows from the C4 lineshape that this unit cell contains more than four non-equivalent anhydroglucose residues.

Experiments based on weak ^{13}C - ^{13}C spin exchange were also conducted in order to probe the spatial environment, within a 0.8-1.0nm radius, around individual multiplet components assumed to belong exclusively to the I_{α} or I_{β} forms. It is expected that only those carbons belonging to that form will be able to undergo spin-exchange during a time of 50-70s. The spectrum of such 'nearest neighbors' is isolated for three different multiplet lines in an algal cellulose and two lines in a higher plant cellulose. Results rule

out the possibility that tertiary morphology can give rise to any multiplicity in these spectra. Moreover, the results strongly reinforce the hypothesis of multiple crystalline forms in the algal celluloses; however, no clear evidence for multiple crystalline forms in the higher plant cellulose is found by this method. The spin-exchange results raise a few minor questions about the details of the spectrum belonging to each polymorph. On the basis of all of these results, revised spectra for the I_{α} and I_{β} polymorphs are presented. These represent minor departures from the previously published spectra.

Finally, the spectrum of the Cladophora cellulose which survived the strong acid hydrolysis resembled closely the hydrocellulose spectrum except that the resolution was much better in the former spectrum. A contrast in resolution is consistent with a difference in the average lateral dimensions for the crystallites; this difference is corroborated by electron microscopy. The close similarity of multiplet relative intensities in these two samples, in spite of their different crystallite surface-to-volume ratios verifies that surface resonances are not determining the apparent multiplet intensities, particularly, for the 88-92 ppm region of the C4 resonance.

EXCERPTS FROM

DOE-ER-13189-2

RAMAN MICROPROBE INVESTIGATION OF MOLECULAR STRUCTURE AND
ORGANIZATION IN THE NATIVE STATE OF WOODY TISSUE

Progress Report

for Period July 1, 1985-June 30, 1986

R. H. Atalla

The Institute of Paper Chemistry
Appleton, Wisconsin 54912

NOTICE

This report was prepared as an account of work sponsored by the United States Government. Neither the United States nor the United States Department of Energy, nor any of their employees, nor any of their contractors, subcontractors, or their employees, makes any warranty, express or implied, or assumes any legal liability or responsibility for the accuracy, completeness, or usefulness of any information, apparatus, product or process disclosed or represents that its use would not infringe privately owned rights.

August, 1986

Prepared for

The U.S. DEPARTMENT OF ENERGY

TABLE OF CONTENTS

	Page
SUMMARY	1
PREFACE	2
OVERVIEW OF RESULTS TO DATE	4
Studies on Woody Tissue	5
Studies on Celluloses	6
The Multichannel Spectrometer System	7
Other Studies	8
LITERATURE CITED	10
APPENDIX	
Raman microprobe evidence for lignin orientation in cell walls of native woody tissue R. H. Atalla and U. P. Agarwal. Science 227:636(1985).	
Recording Raman spectra from plant cell walls R. H. Atalla and U. P. Agarwal. J. Raman Spectroscopy 17:229(1986).	
<u>In Situ</u> Raman microprobe studies of plant cell walls: macromolecular organization and compositional variability in the secondary wall of <u>Picea mariana</u> (Mill.) B. S. P. U. P. Agarwal and R. H. Atalla. Planta, in press.	
Band assignments in the Raman spectra of cellulose. Carbohydrate Research, special issue on physical chemical studies on macromolecular carbohydrates J. H. Wiley and R. H. Atalla, in press.	
Raman spectra of celluloses, in "Solid State Characterization of Cellulose," R. H. Atalla, Ed., ACS Symposium Series J. H. Wiley and R. H. Atalla, in press.	
A highly crystalline cellulose from <u>Rhizoclonium Heiroglyphicum</u> R. H. Atalla, R. E. Whitmore, and D. L. VanderHart. Biopolymers 24:421(1985).	
Oxygen sensitive background in the Raman spectra of woody tissue Proc. of 10th Int. Conf. on Raman Spectroscopy, Eugene, Oregon U. P. Agarwal and R. H. Atalla, in press.	

SUMMARY

Raman microprobe spectroscopy has been used to investigate molecular architecture in the cell walls of native woody tissue. At the outset it was demonstrated that spectra can be acquired from cell wall domains as small as 1-3 micrometers in diameter, and that polarized Raman spectra are sensitive to the orientation of the electric vector of the exciting laser beam relative to the plane of the cell wall. Spectra of adjacent points on cell wall sections have been examined and compared with spectra from points in the walls of adjacent cells. The spectra were interpreted in terms of the orientation of molecular species relative to the plane of the cell wall and the compositional variations within the cells and between cells. Both the aromatic components of lignin and the anhydroglucose rings of cellulose appear to be oriented with respect to the plane of the cell wall. The ratio of lignin to cellulose varies from point to point in the cell wall and over an even wider range between points on different cells. Some studies of native celluloses were carried out in order to characterize the spectral features associated with cellulose. In work at another laboratory useful spectra were recorded in less than five minutes with a spectrometer system utilizing multichannel detection. Such a system, funded through DOE-URIP, is currently being assembled in our laboratory; it will be operational in the fall of 1986.

PREFACE

The investigations of the structure of cell walls in woody tissue described in this report are the continuation of a research program initiated under contract No. DE-AC02-82ER12056. The objective of the program is to study the molecular architecture of cell walls in native woody tissue, with particular emphasis on the information that can be developed by application of Raman microprobe spectroscopy.

Under the initial program we demonstrated the feasibility of an approach to investigation of cell wall structure based on Raman microprobe spectroscopy. We showed that it is possible to acquire spectra from cell wall domains as small as 1-3 micrometers in diameter and that polarized Raman spectra acquired from such domains are sensitive to the orientation of the electric vector of the exciting laser beam relative to the plane of the cell wall. Preliminary analysis suggested that the aromatic components of lignin are oriented with respect to the plane of the cell wall, as are also the anhydroglucose rings of the cellulose in the wall. Evidence was also found to support the hypothesis that the ratio of lignin to cellulose varies from point to point in the cell wall and varies over an even wider range between points on different cells.

Under the current program we have developed improved techniques for the acquisition of spectra of the cell walls, and we have carried out some systematic investigations of the spectra of adjacent points on cell wall sections. We have also carried out comparisons between walls of adjacent cells. In these studies we have examined the orientation of molecular species relative to the plane of the cell wall as well as the compositional variations within the cells and between cells. In addition, some studies of native celluloses from algal

sources and from bast fibers were carried out in order to provide insight into the patterns of variations of the spectral features associated with cellulose.

One of the key objectives of our program has been to develop the spectral data base that would allow us to map the variability of molecular orientation from point to point within a cell wall. Only then would it be possible to describe the patterns of variation of molecular organization, and seek to understand their relation to function. The major obstacle we encountered was the time required for the acquisition of each spectrum. The requirement of 4 to 8 hours per spectrum made contemplation of comprehensive mapping studies unreasonable. We, therefore, submitted a proposal to the University Research Instrumentation Program of the Department of Energy (DOE-URIP), to fund the assembly of a spectrometer system utilizing multichannel detection, which would greatly enhance efficiency of data acquisition and make mapping studies quite feasible.

We have received the requisite grant from the DOE-URIP, and we have ordered the components necessary for assembly of the experimental system. In the course of selection of the components we tested a number of candidate systems and demonstrated that useful spectra can indeed be recorded in less than five minutes. We expect the system to be operational in the fall of 1986.

OVERVIEW OF RESULTS TO DATE

The first objective of the program was to demonstrate the use of the Raman microprobe for acquisition of spectra from sections of woody tissue and assess its sensitivity to molecular organization in the cell wall. Once this was established the objective was to carry out investigations on selected samples to provide an indication of the type of information that can become available from this methodology.

The microprobe, which consisted of a specially modified microscope, together with laser beam steering optics, was installed as an attachment to the IPC Raman spectrometer system. The system is based on a single channel high resolution double-monochromator with a continuous Argon ion laser exciting source. The system was then optimized and new sample mounting techniques were developed (1).

Upon completion of the experimental system the primary objective became exploration of both molecular orientation and compositional variations in native woody tissue. A secondary objective was to assess the possibility of assembling a new spectrometer system with a multichannel detector to make possible more comprehensive mapping of the variability of molecular organization.

Pursuit of the primary objective was along two paths. The major one was focused on studies of sections of tissue from black spruce (Picea mariana). Some preliminary studies on loblolly pine (Pinus taeda L.) were also undertaken. The second path, undertaken in part with additional funding from IPC, involved use of the microprobe to investigate native cellulosic fibrillar aggregates from the alga Valonia ventricosa and from ramie, which is a bast fiber; these studies were intended to provide information on the spectral features associated with cellulose.

STUDIES ON WOODY TISSUE

In the studies on woody tissue both transverse and longitudinal sections were investigated. The results to date, which are described in three articles, copies or abstracts of which are attached, showed that it is possible to acquire the desired spectra if appropriate preparation and mounting procedures are used.

The first article (2) entitled "Raman microprobe evidence for lignin orientation in the cell walls of native woody tissue," appeared in SCIENCE, early in 1985. It describes, in concise form, the key findings that the Raman microprobe spectra from the secondary wall of earlywood tissue from black spruce (Picea mariana) reveal evidence of orientation of lignin relative to the plane of the cell wall surface. In most instances the aromatic rings of the phenyl propane structural units are in the plane of the cell wall. In some exceptional cases the units appear perpendicular to the cell wall, suggesting nodes in molecular orientation. An abbreviated report on this work was also included in the Proceedings of the Ninth International Conference on Raman Spectroscopy.

The second article (3) entitled "Recording Raman spectra from plant cell walls", appeared in the Journal of Raman Spectroscopy early in 1986. It describes the experimental procedures used to acquire the spectra, in somewhat greater detail. It also includes some discussion of the spectral features associated with lignin as well as those arising from cellulose.

The third article (4) entitled "In situ Raman microprobe studies of plant cell walls: Macromolecular organization and compositional variability in the secondary wall of Picea mariana (Mill.) B.S.P." is currently "in press" for

publication in PLANTA; it is to appear before the end of 1986. It includes a more detailed account of the studies undertaken to define the range of variability of molecular ordering and composition. It describes the changes in the spectral features associated with cellulose and with lignin, which arise when the electric vector of the exciting radiation is rotated with respect to the plane of the cell wall. In addition to the results noted above concerning the orientation of lignin, the spectra revealed the orientation of cellulose relative to the geometry of the cell wall. The compositional variability was determined by comparing the summed spectra for a particular point. It was found that differences in the relative amounts of cellulose and lignin occurred between adjacent points, as close as 1 to 2 micrometers apart, within the secondary walls of individual cells, but that the differences between points on adjacent cells were in general larger than between different points in the same cell.

The generality of the results concerning woody tissue need to be qualified, of course, by the limited number of samples investigated, and the limited number of spectra acquired from each sample.

STUDIES ON CELLULOSES

The studies on fibrillar aggregates of cellulose had two goals. The first was to characterize more fully than had been done heretofore the Raman spectral features of oriented celluloses. The second was to explore the nature of the native polymorphs of cellulose; recent studies based on solid state ^{13}C NMR spectra had revealed important differences between native celluloses (5,6).

The studies of the Raman spectral features of oriented native celluloses have been described in a preprint (7) entitled "Band assignments in the Raman spectra of celluloses"; it is currently under review for publication in a

special issue of Carbohydrate Research devoted to the physical chemistry of polysaccharides. An abstract of the paper is attached. It presents series of spectra recorded with variation of the polarization of the exciting laser radiation relative to the axes of the fibers. Analysis of the variation of band intensities as a function of polarization revealed new information about the vibrational character of the vibrational displacements. In addition, a limited study of deuterated celluloses was undertaken. The results establish a foundation for assessments of the spectral features of cellulose in the spectra recorded from native tissue.

The studies on polymorphy are described in the preprint of a paper (8), entitled "Raman spectra of celluloses", to be published in the proceedings of the Symposium on Solid State Characterization of Cellulose, edited by the principal investigator for the ACS Symposium Series; an abstract is attached. It discusses comparisons of the spectra of Valonia, ramie, and mercerized ramie celluloses. The spectra indicate that the conformation of the cellulose molecules is the same in Valonia and ramie native celluloses, but that the hydrogen bonding patterns are different. Mercerized ramie and native ramie celluloses differ in both the molecular conformation and the hydrogen bonding patterns.

In the course of our effort to develop spectra of native celluloses, we discovered that a fresh water alga that occurs widely in the fresh waters of Wisconsin lakes and streams, produces cellulose of crystallinity at least equal to that of Valonia celluloses. The finding is described in a paper (9) entitled "A highly crystalline cellulose from Rhizoclonium heiroglyphicum", which is also attached.

THE MULTICHANNEL SPECTROMETER SYSTEM

When we were advised of the DOE-URIP grant, our secondary objective under the present program became the selection, acquisition, and assembly of a

new spectrometer system with multichannel detection. In the course of the selection process we visited both university and manufacturers' laboratories to evaluate the performance of instrument components when used to record spectra from samples of woody tissue.

The finding most relevant in the present context is that it was possible to record spectra of good quality in less than five minutes. Thus, assembly of the new spectrometer system will indeed allow acquisition of spectra within a time frame that is realistic for the mapping studies that we are contemplating.

The new spectrometer system will permit studies using either pulsed or continuous laser excitation. It will also be equipped for detection in both continuous or gated modes. A subsystem will include a microscope interfaced to a triple monochromator, with grating selection available to allow coverage of spectral intervals of varying widths, according to the needs of the particular experiment.

OTHER STUDIES

In addition to the studies outlined above, we have undertaken a number of more limited investigations in support of the primary program, or to explore possible extension of the use of our methodology to other problems in plant biology. Three such efforts are outlined in the following paragraphs.

One of the complex phenomena we have encountered is the laser induced luminescence of woody tissue. We have found it to be particularly sensitive to the presence of oxygen in the atmosphere surrounding the samples under study. A preliminary report (10) on this effort will appear in the Proceedings of the

10th International Conference on Raman Spectroscopy in September, 1986; a preprint is included.

Another group of studies currently underway, supported partially by IPC exploratory research funds, involves adapting some of the organisms we culture for the production of algal and bacterial celluloses to growth in deuterium oxide. Our object is to generate perdeuterated cellulose to be used for the spectral studies.

In another preliminary exploration we have used the Raman microprobe to search for marker aromatic components in the walls of cells generated through plant tissue culture. The spectra were of poor signal to noise ratio, but they did include some weak aromatic bands. If the findings are confirmed with the new spectrometer system, the investigation will be continued in collaboration with colleagues in the Biology Department at the Institute.

LITERATURE CITED

1. R. H. Atalla and U. P. Agarwal, in Microbeam Analysis - 1984, A. D. Romig, Jr. and J. I. Goldstein, Eds., San Francisco Press, 1984, p. 125.
2. R. H. Atalla and U. P. Agarwal. Raman microprobe evidence for lignin orientation in cell walls of native woody tissue. Science 227:636(1985).
3. R. H. Atalla and U. P. Agarwal. Recording Raman spectra from plant cell walls, J. Raman Spectroscopy 17:229(1986).
4. U. P. Agarwal and R. H. Atalla. Studies of molecular orientation and composition variability within the cell walls of woody tissue. Planta, in press.
5. R. H. Atalla and D. L. VanderHart. Native cellulose: a composite of two distinct crystalline forms. Science 223:283-5(Jan. 20, 1984).
6. D. L. VanderHart and R. H. Atalla. Studies of microstructure in native celluloses using solid state ^{13}C NMR. Macromolecules 17:1465(1984).
7. J. H. Wiley and R. H. Atalla. Band assignments in the Raman spectra of cellulose. Carbohydrate Research, special issue on physical chemical studies on macromolecular carbohydrates, in press.
8. J. H. Wiley and R. H. Atalla. Raman spectra of celluloses, in "Solid State Characterization of Cellulose," R. H. Atalla, Ed., ACS Symposium Series, in press.
9. R. H. Atalla, R. E. Whitmore, and D. L. VanderHart. A highly crystalline cellulose from Rhizoclonium Heiroglyphicum, Biopolymers 24:421(1985).
10. U. P. Agarwal and R. H. Atalla, Proc. of 10th Int. Conf. on Raman Spectroscopy, Eugene, Oregon, in press.

Reprint Series
8 February 1985, Volume 227, pp. 636-638

SCIENCE

**Raman Microprobe Evidence for Lignin Orientation in the
Cell Walls of Native Woody Tissue**

Rajai H. Atalla and Umesh P. Agarwal

Raman Microprobe Evidence for Lignin Orientation in the Cell Walls of Native Woody Tissue

Abstract. Raman microprobe spectra from the secondary wall of earlywood tissue from Picea mariana (black spruce) reveal evidence of the orientation of lignin relative to the plane of the cell wall. In most instances, the aromatic rings of the phenyl propane structural units are parallel to the plane of the cell-wall surface.

Among the structural components of plant cell walls, only cellulose has been well characterized with respect to its molecular organization within native tissue (1, 2). In this work we report what we believe to be the first direct evidence for the orientation of components of lignin relative to the morphological features of native woody tissue.

A central problem in studies of plant cell walls is that the methodologies for investigating morphology, namely, electron and optical microscopy, are very limited in their capacity to develop information concerning molecular structure. On the other hand, procedures traditionally used for exploring the molecular structure of cell-wall components require prior isolation of the components by extractive procedures that are frequently destructive of morphological features (3).

The Raman microprobe offers an opportunity to bridge this gap through spectroscopic investigation of individual morphological features in unperturbed plant tissue. The microprobe permits acquisition of Raman spectra from domains as small as 1 μm (4, 5). But its greatest asset in the present context is that molecular orientation within these domains can be established from analysis of the

polarization of Raman scattered light (6, 7).

The particular question that we addressed was the possibility that lignin molecules are oriented with respect to the geometry of the cell walls in native woody tissue. Such information would be helpful for a better understanding of its function. Although some anisotropy in the structure of lignin had been postulated on the basis of measurements of ultraviolet dichroism (8), these measurements were later attributed to form dichroism rather than to molecular orientation (1). The possibility of lignin orientation is suggested by the high degree of organization of cellulose as well as by evidence for orientation of the hemicelluloses in cell walls (9, 10). Our experiments were specifically designed to establish whether the aromatic rings of the phenyl propane units in lignin molecules had preferential orientations with respect to the plane of the cell-wall surface. In the work reported here attention was focused on the secondary wall in earlywood tissue from *Picea mariana* (black spruce).

The microprobe system consisted of a Jobin Yvon Ramanor HG2S equipped by the manufacturer with a Nachet microscope modified for coupling to the spec-

trometer and designed to provide imaging on a glass screen. The microscope serves the dual functions of focusing the exciting laser beam on the domain of interest and of gathering the Raman scattered light and imaging it at the entrance slit of the monochromator. The objective used in the present study was a $\times 100$ (numerical aperture 1.18) liquid-immersion objective corrected for water. The exciting radiation was the 5145- \AA line of an argon ion laser. The system and methodology are described in detail elsewhere (11). Our work and that of others (12) indicate that the spectra arise from domains approximately 1 μm in diameter and 0.5 μm deep.

The woody tissue was sectioned both longitudinally and transversely. The sections, approximately 30 μm thick, were mounted on slides approximately 2 by 3 cm, held in place by cover slips through the centers of which small holes had been drilled. Each slide was then placed in a small flat-bottomed beaker, and D_2O was added to a depth of approximately 1 cm. After the liquid-immersion objective was brought close to the sample, the D_2O was covered with a thin layer of mineral oil to limit both evaporation and exchange with atmospheric moisture. Immersion in D_2O limited laser-induced fluorescence (11), and the D_2O bands provided a convenient internal reference for intensity measurements. The possibility of spectral effects arising from extractives, which constitute less than 1 percent of the secondary wall, was excluded on the basis of comparisons of spectral features from extracted and unextracted tissue.

The central point of the experiments was to compare spectra recorded with the polarization of the incident laser beam parallel and perpendicular to the plane of the cell wall. In order to avoid complications associated with the dichroism inherent in the optics of the microscope and the monochromator, a polarization scrambler was inserted in the path of the Raman-scattered light at the point of coupling of the microscope to the monochromator, and we obtained the different spectra by rotating the sample about the optical axis of the microscope. This was possible because the microscope was equipped with a rotating stage that had been precisely aligned.

We carried out the alignment of the stage by observing a micrometer slide and adjusting the stage so that it could be rotated without translation. At the higher magnifications, small amounts of residual translations could occur but these were readily compensated for by micro-

translation adjustments. The samples were carefully observed during the rotations and remained in sharp focus throughout. Thus any vertical translation is ruled out. The likelihood of vertical translation accompanying the rotation was also excluded by the invariance of the D_2O bands with rotation when they were measured above a micrometer slide, over a period short enough that the drift in laser power output was insignificant.

The intensity difference between the D_2O peaks in spectra recorded in the parallel and perpendicular modes, as in Fig. 1, A and B, reflect the drift of laser power output over the long periods of data acquisition necessary to attain spectra with reasonable signal-to-noise ratios. To avoid distortion of the relative intensities of the spectral features, the spectra were recorded by summation of many spectral scans short enough (40 minutes) that drift in laser power was insignificant within each individual scan.

Figures 1 and 2 show representative spectra obtained from a longitudinal and a transverse section, respectively. The key observations are the relative reductions in the intensity of the 1600-cm^{-1} spectral band recorded with polarization of the exciting radiation perpendicular to the cell wall. The 1600-cm^{-1} band has been shown to be due to a symmetric stretching of the C-C bonds of the aromatic

ring wherein two bonds across the ring from each other vibrate in opposite phase to the other four C-C bonds (13). It has also been demonstrated that in aromatic rings with substitution patterns typical of those in lignin the 1600-cm^{-1} band tends to be the most intense in the spectrum (14).

The decline in relative intensities of the 1600-cm^{-1} bands in the spectra with polarization perpendicular to the cell wall indicates that the aromatic rings are preferentially oriented in the plane of the cell wall. This interpretation is supported by the observation that the 1650-cm^{-1} band follows a pattern similar to that of the 1600-cm^{-1} band. The 1650-cm^{-1} band is due to α carbonyl groups that are coplanar with the adjacent aromatic ring.

The high degree of orientation of cellulose in the cell walls (1, 2, 15) is also reflected in the spectra of Figs. 1 and 2. The 2900-cm^{-1} band due to the methine C-H stretch changes both in shape and in intensity when the polarization of the exciting radiation relative to the plane of the cell wall is altered. The changes in the 1098-cm^{-1} skeletal band of cellulose are also consistent with the high degree of alignment of the cellulose. Finally, the differences in the OH stretching region between 3100 and 3600 cm^{-1} , particularly in Fig. 1, very likely reflect alignment of crystalline cellulosic domains with the chain axes parallel to the cell axis. The

spectrum in Fig. 1A, recorded with the incident beam perpendicular to the chain direction but with the electric vector parallel to the chain direction, includes two peaks superimposed upon the broader band in this region. These peaks are probably due to intramolecularly hydrogen-bonded OH groups that are parallel to the chain. Such peaks are not seen in the other three spectra reported here because, for all three, the electric vector of the exciting radiation is perpendicular to the chain direction. The OH bands associated with other constituents of native woody tissue are usually quite broad because of intermolecular hydrogen bonding.

Although the spectra shown in Figs. 1 and 2 are representative of the spectra most often observed, the spectra recorded in some other locations showed a lower degree of preferential orientation. In one or two exceptional cases the spectra showed more intense 1600-cm^{-1} bands in the perpendicular polarization mode. This suggests the occurrence of nodes in the orientation of lignin not unlike those known to occur for cellulose in some cell walls (16). The suggestion of nodes, however, is speculative at this time, and further investigation is clearly in order.

We have carried out similar although more limited observations on tissue from *Pinus taeda* L. (loblolly pine). The re-

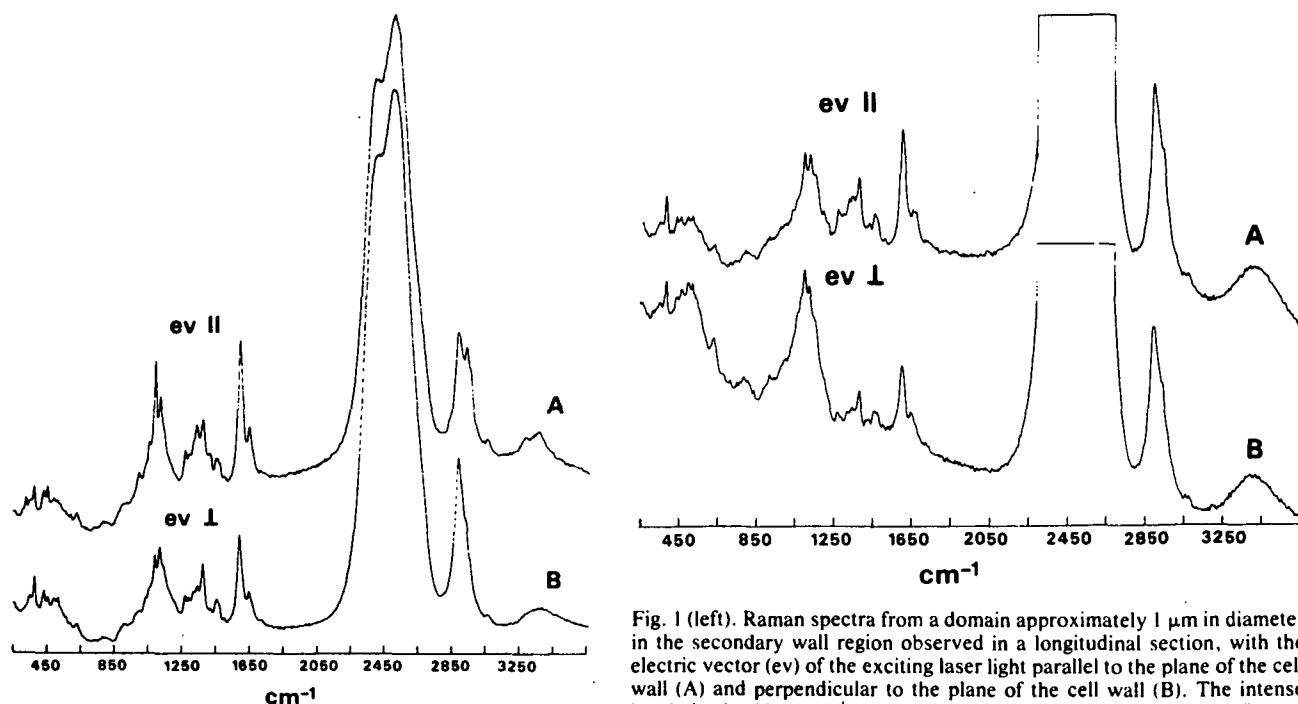


Fig. 1 (left). Raman spectra from a domain approximately $1\ \mu\text{m}$ in diameter in the secondary wall region observed in a longitudinal section, with the electric vector (ev) of the exciting laser light parallel to the plane of the cell wall (A) and perpendicular to the plane of the cell wall (B). The intense bands in the 2500-cm^{-1} region are due to D_2O . Fig. 2 (right). Raman

spectra from a domain approximately $1\ \mu\text{m}$ in diameter in the secondary wall region observed in a cross section, with the electric vector of the exciting laser light parallel to the plane of the cell wall (A) and perpendicular to the plane of the cell wall (B). The D_2O bands are truncated in this plotting of the spectra.

sults fit the pattern outlined for tissue from *Picea mariana*, but it is not possible on this basis to draw conclusions concerning the degree to which our findings are representative of native woody tissue in general.

The most significant of our findings, we believe, is not so much that the orientation of the phenyl ring is most often preferentially in the plane of the cell wall but that the lignin is more highly organized at the molecular level than had heretofore been recognized.

A mapping of variations in molecular orientation throughout an individual cell would make possible detection of nodes in molecular organization and their relation to cell morphology. Such a mapping is not feasible at present, however, because the time needed to acquire spectra such as those in Figs. 1 and 2 is approximately 8 hours. It is anticipated that a new instrumental design incorporating multichannel detection will make it possible to acquire similar spectra in much shorter intervals. More comprehensive studies of the pattern of organization of lignin will then be possible.

RAJAI H. ATALLA

UMESH P. AGARWAL

*Institute of Paper Chemistry,
Appleton, Wisconsin 54912*

References and Notes

1. A. Frey-Wyssling, *The Plant Cell Wall* (Gebrüder Dorntrager, Berlin, 1976).
2. R. D. Preston, *The Physical Biology of Plant Cell Walls* (Chapman and Hall, London, 1974).
3. B. L. Browning, *Methods of Wood Chemistry* (Interscience, New York, 1967).
4. G. J. Rosasco, in *Advances in Infrared and Raman Spectroscopy*, R. J. H. Clark and R. E. Hester, Eds. (Heyden, London, 1980), vol. 7, chap. 4.
5. M. E. Andersen and R. Z. Muggli, *Anal. Chem.* **53**, 1772 (1981).
6. I. W. Shepherd, in *Advances in Infrared and Raman Spectroscopy*, R. J. H. Clark and R. E. Hester, Eds. (Heyden, London, 1977), vol. 3, chap. 4.
7. D. A. Long, *Raman Spectroscopy* (McGraw-Hill, London, 1977).
8. P. W. Lange, *Sven. Papperstidn.* **50**, 150 (1947).
9. R. H. Marchessault and C. Y. Liang, *J. Polym. Sci.* **59**, 357 (1962).
10. D. H. Page, F. El-Hosseniy, M. L. Bidmade, R. Binet, *Appl. Polym. Symp.* **28**, 923 (1976).
11. R. H. Atalla and U. P. Agarwal, in *Microbeam Analysis—1984*, A. D. Romig and J. I. Goldstein, Eds. (San Francisco Press, San Francisco, 1984), p. 125.
12. Lateral resolution of 1 μm is based on our measurements and those of F. Adar (personal communication); depth resolution of 0.5 μm is based on an analysis by G. Turrell [*J. Raman Spectrosc.* **15**, 103 (1984)] and optical heterogeneity of the samples.
13. H. L. Hergert, in *Lignins*, K. V. Sarkanen and C. H. Ludwig, Eds. (Wiley-Interscience, New York, 1971), chap. 7.
14. S. M. Ehrhardt, thesis, Institute of Paper Chemistry (1983).
15. A. K. Kulshreshtha and N. E. Dweltz, in *Cellulose and Other Polysaccharides*, P. C. Mehta and H. C. Srivastava, Eds. (Ahmedabad Textile Industry's Research Association, Ahmedabad, India, 1974), p. 2.
16. This work was supported by institutional research funds of the Institute of Paper Chemistry and the Biological Energy Research program of the Department of Energy under contract DE-AC02-82ER 12056.

21 May 1984; accepted 23 November 1984

Recording Raman Spectra from Plant Cell Walls

R. H. Atalla* and U. P. Agarwal

Division of Chemical Sciences, Institute of Paper Chemistry, Appleton, Wisconsin 54912, USA

A Raman microprobe system has been successfully utilized to obtain luminescence-free spectra from sections of woody tissue. The procedures for optimizing the microprobe and the sample mounting techniques are described. Spectra from the secondary wall of black spruce (*Picea mariana*) indicate that both lignin and cellulose can be studied in their native state.

INTRODUCTION

Procedures traditionally used for exploring molecular structure in plant cell walls require prior isolation of the components by extractive procedures which are frequently destructive of morphology.¹ On the other hand, methodologies for examining morphology, such as optical and electron microscopy, are very limited in their capacity to provide information concerning molecular structure.^{2,3} The Raman microprobe⁴ offers an opportunity to bridge this gap through spectroscopic investigation of individual morphological features in unperturbed plant tissue.^{5,6} In the course of such studies we have developed some new procedures and these and some representative spectra are described in this paper.

The experimental objectives were the acquisition of polarized Raman spectra from microscopic domains in specific morphological features in the cell walls, and observation of changes in the spectra when the polarization of the exciting radiation was rotated relative to the morphological features. The system used is based on an Instruments S.A. Ramanor HG2S equipped with a modified Nachet NS 400 microscope. The 514.5 nm line of a Coherent Radiation 52A laser was used as an excitation source. A Tracor Northern TN1500 data analyser was used to record the spectra. The system could be programmed for multiple scanning when desired. The laser power at the sample was approximately 8 mW.

Two types of procedural development were made. The first is concerned with optimization of the microprobe system and the second concerns sample preparation.

EXPERIMENTAL AND RESULTS

Instrument optimization

Three factors were integrated in optimization of the Raman microprobe system. The first was based on the realization that dichroism in the optics of the microprobe and the monochromator could confound the analysis of spectrum variation as the polarization of incident light was altered relative to the morphological features. The decision was therefore made to keep the plane of incident polarization stationary with respect to the optical system. Rotation of polarization relative to

morphological features was accomplished instead by installation of a rotating stage on the microprobe and rotation of the samples about the optical axis.

The second modification grew out of the observation that the dichroism of the microprobe favored a polarization that is least efficiently transmitted by the monochromator. This problem was dealt with by the installation of a polarization scrambler along the optical axis of the scattered radiation path in the microprobe. A significant increase in throughput was observed after installation of the scrambler.

The third factor was a procedural one for alignment of the overall system. The usual procedures for aligning such systems involve mounting a helium neon laser in place of the photomultiplier tube and aligning the components so as to maintain the beam along the optical axis of the system.

To refine the alignment further we mounted a micrometer slide above a front surface mirror on the stage of the microprobe, illuminated it with the laser exciting line and followed the image of the micrometer through the several optical components in the microprobe and the monochromator. At each stage the components were aligned to obtain a centered image. On completion of the process, an image of the micrometer slide could be observed in the plane of the photocathode of the photomultiplier tube. This procedure resulted in an order-of-magnitude improvement in the quality of the signals.

Sample preparation and mounting

Spectra were obtained on samples from woody tissues of black spruce and loblolly pine. In preliminary studies the samples were sectioned to approximately 20-30 μm thickness, extracted and washed, then dried in air and mounted on slides. The Raman spectra recorded from such samples showed weak Raman peaks superimposed on a strong fluorescent background (Fig. 1(a)). The cell walls frequently decomposed at higher laser powers. Attempts to obtain better spectra involved changing the exciting frequency, drench quenching of sections by laser radiation and sample treatment with various chelating agents. Unfortunately, none of these produced satisfactory results, nor did subtraction of the background produce acceptable spectra. As a final resort, wet mounting of the samples was tested.

In the wet-mounting procedure the samples were placed on a slide, covered with water and sandwiched with a glass cover-slip. A thin layer of silicone grease

* Author to whom correspondence should be addressed.

230

R. H. ATALLA AND U. P. AGARWAL

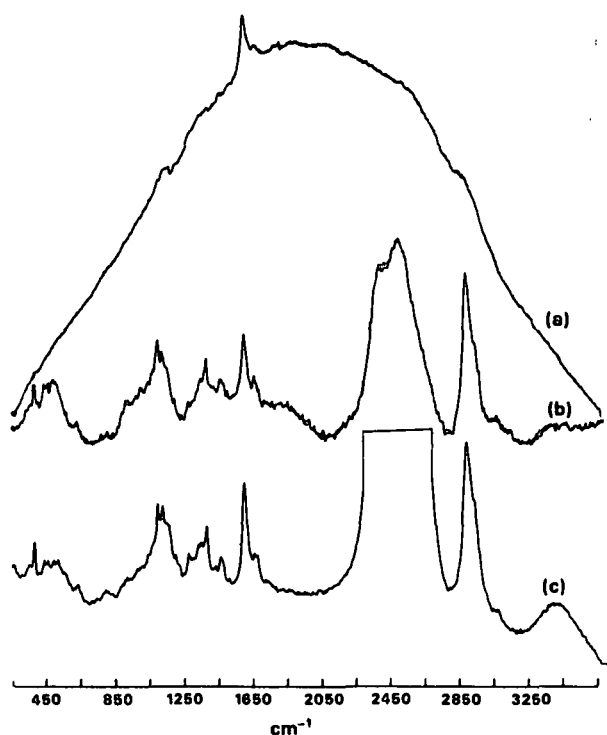


Figure 1. Polarized Raman spectra of plant cell wall cross-sections, electric vector parallel to the plane of the cell wall: (a) air-dried sample; (b) wet sample sandwiched between glass slide and cover-slip; (c) D_2O -immersed sample (cover-slip with a hole used and D_2O peak truncated).

was deposited around the cover-slip to prevent evaporation of water. In this procedure the sample could withstand higher power levels of the incident laser light, and the background fluorescence disappeared completely. In some instances H_2O was replaced with D_2O as the immersion medium in order to minimize overlap between the OH and CH stretching bands. However, the presence of the cover-slips resulted in additional broad spectral features at 500 and 1050 cm^{-1} that could easily be assigned to the silicates in the glass (Fig. 1(b)).⁷ Use of quartz instead of the glass cover-slips improved the situation only marginally. The spectra of the cover-slips might have been accounted for by subtraction, except that the relative intensities of the features varied from one cover-slip to another, and sometimes from point to point within the same cover-slip. This finding is not inconsistent with minor variations in the structure of the glass.

In order to avoid the contributions from the spectra of the cover-slips, a new procedure was developed based on drilling small holes in the center of the cover-slips, immersing them in water or D_2O and using a liquid immersion objective (Fig. 2). With the help of adhesive, a flat-base Pyrex glass beaker was fixed to a slide in a manner that allowed transmitted light to pass through. On the inner side of the bottom yet another portion of a glass slide was attached. The wet sample was sandwiched as before between the cover-slip with a hole at its center and the slide portion so that the cover-slip held the sample immobile on the slide portion. D_2O was slowly added to the beaker until complete immersion of the sample had occurred. The beaker was then mounted on the stage of the microprobe and the water immersion

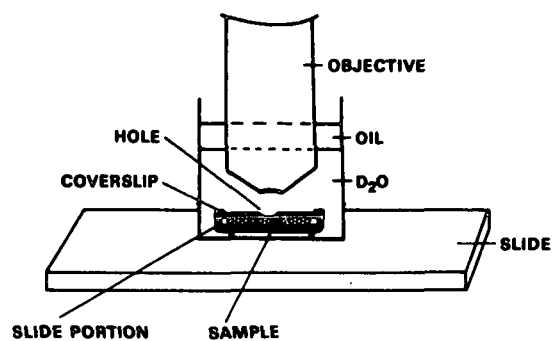


Figure 2. Schematics of the sampling technique.

objective lowered into the D_2O . In order to prevent evaporation of the D_2O , or exchange with atmospheric moisture, a thin layer of mineral oil was placed on the surface of the D_2O after the objective had been submerged in the medium. This procedure resulted in acquisition of the best spectra obtained so far from native woody tissue (Fig. 1(c)).

Immersion in D_2O accomplishes a number of objectives. In addition to providing a heat sink to dissipate energy absorbed by the sample, the D_2O appears to quench the fluorescence of the native samples. Clearly, it prevents dehydration of the samples, and it provides assurance that any spectral features observed in the OH stretching region are primarily associated with the woody tissue rather than absorbed H_2O .

Spectral features

Cell walls of woody tissue consist almost entirely of cellulose, lignin and hemicelluloses.^{2,3} Figure 3(a) shows

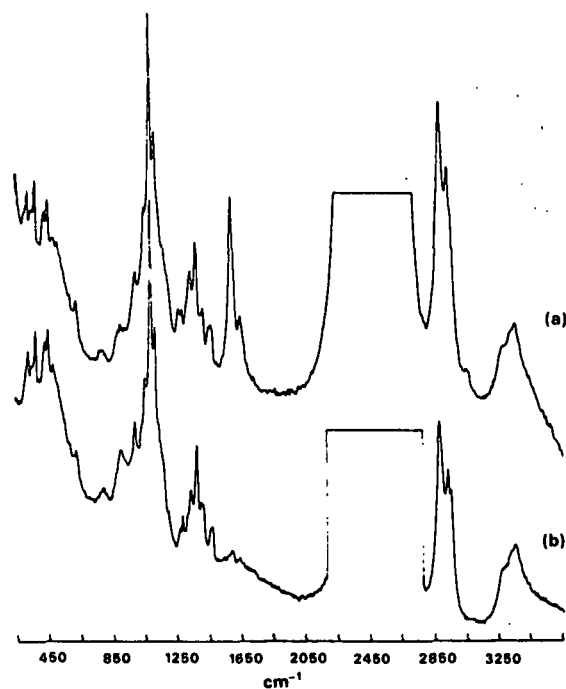


Figure 3. Spectra from the secondary wall of the longitudinal sections, electric vector parallel to the cell wall: (a) native tissue; (b) delignified section.

RECORDING RAMAN SPECTRA FROM PLANT CELL WALLS

231

a Raman spectrum recorded from the secondary wall of a latewood cell in a longitudinal section of black spruce (*Picea mariana*). The electric vector was parallel to the plane of the cell wall surface. On delignification of such a section the spectrum in Fig. 3(b) was obtained. In these spectra most of the sharp features can be associated with cellulose and lignin. The extent to which hemicelluloses affect Raman intensities is not clear at this point, but their contributions are expected to be broad and limited.

Cellulose. Cellulose is a natural polymer of β -1,4-linked anhydroglucose units. Based on previous Raman studies,⁸ features at 330, 380, 1098, 2890 and 2940 cm^{-1} can be easily identified with the cellulose molecule. Additional evidence in this respect is provided by the delignified spectrum in Fig. 3(b) and polarized Raman spectra^{5,6} (not included here). One of the skeletal stretching modes of the cellulose chain has been associated with the 1098 cm^{-1} peak,^{8b} whereas the methine C-H stretches appear around 2890 cm^{-1} .⁸ Other features in the spectra where some overlap with lignin vibrations is expected are detected at 1120, 1150, 1340, 1380 and 1450 cm^{-1} .

Lignin. Cell wall spectra contain regions where no spectral contributions from cellulose and hemicelluloses are expected. In such regions the Raman intensity arises due to lignin molecules. Lignin is considered to be a

polymer of substituted phenyl propane units.⁹ Bands at 1600 and 3075 cm^{-1} (Fig. 3(a)) originate from the aromatic part,¹⁰ whereas the α -carbonyl band occurs at 1650 cm^{-1} . Several other modes are likely to be present in the 800-1450 cm^{-1} region. A comparison of the two spectra in Fig. 3 supports such an expectation. In order to develop a better understanding of cell wall spectra, further studies are currently under way.

CONCLUSION

The developments in the sampling technique, and improvements in efficiently collecting scattered light, have resulted in the acquisition of Raman spectra from sections of plant cell walls. Preliminary studies have shown that most spectral features can be interpreted in terms of the two major components of the woody tissue, cellulose and lignin. The Raman microprobe is clearly a powerful tool capable of generating unique information on the structural aspects of biological tissues.

Acknowledgements

This work was supported by The Institute of Paper Chemistry and the Biological Energy Research Program of the Department of Energy under Contract No. DE-ACO2-82ER 12056. This support is gratefully acknowledged.

REFERENCES

1. B. L. Browning, *Methods of Wood Chemistry*. Interscience, New York (1967).
2. A. Frey-Wyssling, *The Plant Cell Wall*. Gebruder Borntraeger, Berlin (1976).
3. R. D. Preston, *The Physical Biology of Plant Cell Walls*. Chapman and Hall, London (1974).
4. G. J. Rosasco, in *Advances in Infrared and Raman Spectroscopy*, edited by R. J. H. Clark and R. E. Hester, Vol. 7, Chapter 4. Heyden, London (1980).
5. R. H. Atalla and U. P. Agarwal, *Science* **227**, 636 (1985).
6. U. P. Agarwal and R. H. Atalla, unpublished data.
7. J. Etchepare, *Spectrochim. Acta, Part A* **26**, 2147 (1970).
8. (a) R. H. Atalla, *Appl. Polym. Symp.* **28**, 659 (1976); (b) R. H. Atalla, R. E. Whitmore, and C. J. Heimbach, *Macromolecules* **13**, 1717 (1980); (c) J. Wiley, Doctoral Dissertation (in progress), Institute of Paper Chemistry, Appleton, WI.
9. K. V. Sarkanen and C. H. Ludwig (Eds), *Lignins*. Wiley, New York (1971).
10. (a) S. M. Ehrhardt, Doctoral Dissertation, Institute of Paper Chemistry, Appleton, WI (1983); (b) H. L. Hergert, in *Lignins—Occurrence, Formation, Structure and Reactions*, edited by K. V. Sarkanen and C. H. Ludwig, Chapter 7. Wiley, New York (1971).

**IN SITU RAMAN MICROPROBE STUDIES OF PLANT CELL WALLS:
MACROMOLECULAR ORGANIZATION AND COMPOSITIONAL VARIABILITY
IN THE SECONDARY WALL of Picea mariana (Mill.) B. S. P.**

U. P. Agarwal and R. H. Atalla*
Division of Chemical Sciences, Institute of Paper Chemistry,
Appleton, WI 54912 U.S.A.

Abstract. Native-state organization and distribution of cell-wall components in the secondary wall of woody tissue from P. mariana (Black Spruce) have been investigated using polarized Raman microspectroscopy. Evidence for orientation is detected through Raman intensity variations resulting from rotations of the exciting electric vector with respect to cell-wall geometry. Spectral features associated with cellulose and lignin were studied. The changes in cellulose bands indicate that the pyranose rings of the anhydroglucose repeat units are in planes perpendicular to the cross section, while methine C-H bonds are in planes parallel to the cross section. Changes in bands associated with lignin indicate that the aromatic rings of the phenyl-propane units are most often in the plane of the cell-wall surface. However, regions where lignin orientation departs from this pattern also occur. These results represent direct evidence of molecular organization with respect to cellular morphological features in woody tissue, and indicate that cell-wall components are more highly organized than had heretofore been recognized. Studies carried out in order to establish the usefulness and sensitivity of the Raman technique to differences of composition within the cell walls provide evidence of variations in the distribution of cellulose and lignin. Such compositional differences were more prominent between the walls of different cells than within a particular cell wall.

Keywords: Picea mariana, Cell-Wall, Structure, Coniferal, Cellulose, Lignin,
Raman microprobe

*To whom correspondence should be addressed.

BAND ASSIGNMENTS IN THE RAMAN SPECTRA OF CELLULOSES

James H. Wiley, Rajai H. Atalla

The Institute of Paper Chemistry, Appleton, Wisconsin 54912

ABSTRACT

Our investigations of the vibrational spectra of celluloses have been extended by using the Raman microprobe to study the spectra of native celluloses. The microprobe allows spectra to be recorded from domains as small as 1 micron and thereby greatly increases the potential of Raman spectroscopy as a tool for studying the structure of cellulose fibers. Series of spectra in which the polarization of the incident light was varied relative to the fiber axis were recorded from oriented fibers. Analysis of band intensities as a function of polarization revealed new information about the directional character of the vibrational displacements. In addition, a limited study of deuterated celluloses was conducted to identify the modes which involve hydrogen motions. The information from the studies of intensities and deuterated celluloses aided in the interpretation of the vibrational spectrum of cellulose. Although a complete assignment of the spectrum was not possible, this new information provides a more thorough characterization of the bands than has been possible in previous studies and establishes a foundation for future microprobe studies of native tissues.

RAMAN SPECTRA OF CELLULOSES

James H. Wiley and Rajai H. Atalla

ABSTRACT

An investigation to study molecular orientation and polymorphy in cellulose fibers, and to further assign the bands in the vibrational spectrum of cellulose was conducted utilizing the Raman microprobe. The microprobe allows spectra to be recorded from domains as small as 1 micron and thereby greatly increases the potential of Raman spectroscopy as a tool for studying the structure of cellulose fibers. In the band assignment work, spectra were recorded from oriented fibers by varying the polarization of the incident light relative to the fiber axis. Analysis of the band intensities revealed new information about the directional character of the vibrational displacements. This information was used in conjunction with the spectra of deuterated celluloses and normal coordinate analyses of cellulose model compounds to make assignments.

Cellulose polymorphy was studied by comparing the spectra of Valonia, ramie, and mercerized ramie. It appears that the conformation of the cellulose backbone is the same in Valonia and ramie celluloses, but that the hydrogen bonding patterns are different. Mercerized cellulose and native celluloses differ in both their backbone conformations and hydrogen bonding patterns.

Cellulose orientation in the plane perpendicular to the chain axis was studied by recording spectra of ramie cross sections with different polarizations of the incident light relative to the cell wall surface. The intensities are consistent with random cellulose orientation. It appears, however, that the sample preparation techniques can influence the cellulose orientation. Therefore, further studies will be necessary to understand the molecular orientation in cellulose fibers.

A Highly Crystalline Cellulose from *Rhizoclonium Hieroglyphicum*

RAJAI H. ATALLA and REBECCA E. WHITMORE, *The Institute of Paper Chemistry, Appleton, Wisconsin 54912*; and DAVID L. VANDERHART, *Polymers Division, NBS, Washington, DC 20234*

In relation to our studies of crystalline forms in native celluloses,^{1,2} we have recently investigated cellulose from the cell walls of the alga, *Rhizoclonium hieroglyphicum*, which we find to be at least as highly ordered as is commonly recognized for cellulose from *Valonia ventricosa*. Although the occurrence of crystalline celluloses in algae from the chlorophyceae class family (which includes *Valonia*) has been noted by Preston,³ the availability of celluloses comparable to those of *Valonia* from these ubiquitous algae seems to have been overlooked in studies of cellulose structure. We believe the *Rhizoclonium* cellulose provides a suitable substrate for studies of structure, based on both diffractometry and spectrometry. We have carried out preliminary characterization based on x-ray diffraction, solid state ¹³C-nmr, and Raman spectroscopy.

The alga here described came to our attention in the course of assessing benthic deposits exposed during a period of depressed water levels in the High Falls flowage along the Peshtigo River in northeast Wisconsin. The texture of the dried deposits seemed similar to the characteristic texture of aggregates of cellulosic fibers. An x-ray diffractogram revealed the presence of highly crystalline cellulose and led us to pursue identification of the alga and the more detailed characterization.

For the preliminary studies, fresh samples of the alga were gathered in the same general vicinity where the dried deposits were first encountered. Isolation of the cellulose from the cell walls was carried out by procedures generally accepted for the purification of *Valonia* celluloses.³ These procedures include extraction with ethanol and a chloroform/ethanol mixture (2:1) followed by boiling for 6 h in a 1% sodium hydroxide solution under nitrogen. The isolated cellulose was washed and freeze-dried in preparation for instrumental characterization.

The x-ray diffractogram was recorded on a North American Phillips diffractometer, using nickel-filtered copper K_{α} radiation. The solid-state ¹³C-nmr spectra were recorded on a Bruker CXP 200 instrument, operating at frequencies of 50.3 MHz for ¹³C and 200 MHz for protons.²

An x-ray diffractogram recorded from a pressed pellet is shown in Fig. 1. It is quite similar to a diffractogram reported for *Valonia* by Harada and Goto.⁴ The relative intensities of the 101 and 10 $\bar{1}$ peaks suggest some uniplanar orientation of the sample.

In Fig. 2, the solid-state ¹³C-nmr spectrum of the *Rhizoclonium* cellulose (A) is compared with one recorded under similar conditions from *Valonia ventricosa* (C). The figure also includes the spectrum of a sample of *Rhizoclonium*

422

BIOPOLYMERS VOL. 24 (1985)

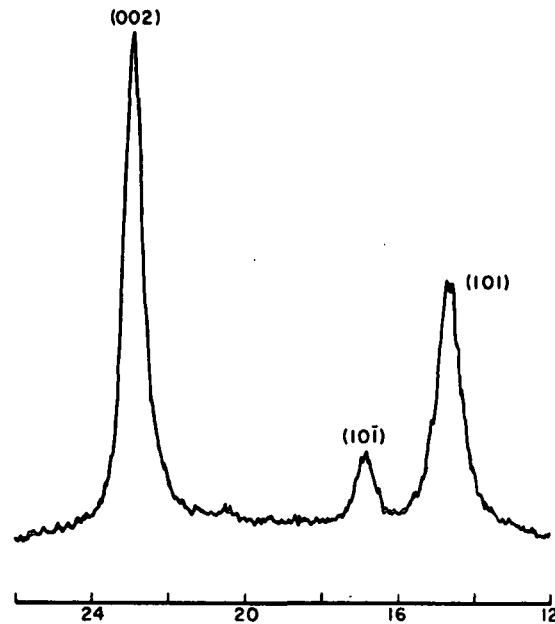


Fig. 1. X-ray diffractogram of cellulose isolated from *Rhizoclonium hieroglyphicum*.

cellulose that had been boiled in 4*N* HCl for 5 h (B). The three spectra are indistinguishable within the limits of detection.

The solid-state ^{13}C -nmr spectra of native celluloses have been resolved into spectra corresponding to two distinct crystalline forms, I_α and I_β , which are believed to coexist in all native celluloses, with I_α dominant in bacterial and algal celluloses, while I_β is dominant in celluloses from higher plants.¹ Within

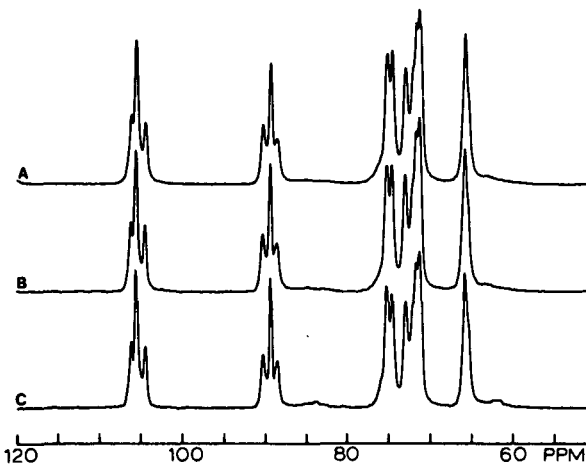


Fig. 2. ^{13}C -nmr spectra of celluloses from (A) alkali extracted *Rhizoclonium hieroglyphicum*, (B) sample A after 5 h hydrolysis in 4 normal HCl, and (C) *Valonia ventricosa*. Spectra were recorded under conditions comparable to those in Ref. 1.

RESEARCH COMMUNICATIONS

423

this framework, spectra A and C in Fig. 2 indicate that the proportions of I_α and I_β in *Rhizoclonium* cellulose are similar to those for *Valonia* cellulose. The similarity of spectra A and B, indicating no measurable change in the relative amounts of I_α and I_β after several hours of exposure to severe hydrolytic conditions, excludes the possibility that either of the two distinct components represents a less ordered phase, which would be more susceptible to hydrolysis. Similar conclusions had previously been derived from experiments based on the hydrolysis of cotton.⁵

In addition to our own studies, samples of *Rhizoclonium* cellulose from the same source have been examined by electron diffraction in other laboratories (H. Chanzy and J. F. Revol, personal communications). They were found to possess crystalline microfibrils larger and somewhat more ordered than those from *Valonia ventricosa*.

Acknowledgment is made of support for this work through the Exploratory Research Fund of The Institute of Paper Chemistry and from the Basic Biology Research Program of the Department of Energy under Grant No. DE-FG02-84ER12189. We thank H. S. Dugal for bringing the benthal deposits to our attention, and M. Mischuk and J. Blum for identification of the alga. T. Early and L. Amos provided preliminary SS ¹³C-nmr spectra.

References

1. Atalla, R. H. & VanderHart, D. L. (1984) *Science* **223**, 281.
2. VanderHart, D. L. & Atalla, R. H. (1984) *Macromolecules* **17**, 1465.
3. Preston, R. D. & Nicolai, E. (1952) *Proc. R. Soc. London* **B140**, 244.
4. Harada, H. & Goto, T. (1982) in *Cellulose and Other Natural Polymer Systems*, Brown, R. M., Ed., Plenum, New York, p. 383.
5. VanderHart, D. L. & Earl, W. L. (1981) *Macromolecules* **14**, 570.

Received July 30, 1984

Accepted September 24, 1984

OXYGEN SENSITIVE BACKGROUND IN THE RAMAN SPECTRA OF WOODY TISSUE

U. P. Agarwal and R. H. Atalla

Chemical Sciences Division
The Institute of Paper Chemistry
Appleton, WI 54912

Efforts to record the Raman spectra of woody tissue are generally frustrated by the high levels of laser induced luminescence. In our previous work using the Raman microprobe we found that mounting the samples in water eliminated most of the luminescence.^{1,2} Because the water immersion method is not readily adapted to macroscopic heterogeneous samples, we sought alternative approaches. An earlier successful microprobe experiment in which the tissue was immersed in mineral oil suggested that the key factor may be either isolation of the sample from atmospheric oxygen, or thermal quenching of the heating effects of the laser, or perhaps a combination of both effects. A series of experiments designed to test these possibilities was undertaken. This involved recording spectra while flushing the samples with a variety of nonreactive gases of different thermal characteristics. These included He, Ar, N₂ and CO₂. The trials with O₂ followed the unexpected initial observations.

The samples were transverse sections of Picea mariana (Black spruce) approximately 30 micrometers thick, which had been allowed to stand overnight exposed to the ambient atmosphere at room temperature. They were loosely mounted between cover slips and inserted in a specially constructed cell designed to allow acquisition of spectra in a 90 degree scattering geometry while flushing the samples with different gases. The cell was mounted in the macrochamber of the spectrometer system described in References 1 and 2. A cylindrical lens was used to focus the laser beam on the samples with the axis of the illuminated sample region parallel to the entrance slit of the spectrometer.

Results and Discussion

The effects of flushing with O₂ and N₂ are shown in Figure 1. Spectrum A was recorded as the sample was flushed with air, spectrum B as it was flushed with N₂, and spectrum C as the N₂ was replaced with O₂. Figure 2 shows spectrum C of Figure 1 on an expanded scale, together with another spectrum recorded about an hour later. Figure 3 shows the final spectrum in Figure 2, together with one recorded after O₂ flushing was discontinued and N₂ flushing resumed. The effects of flushing with all the other gases were similar to those obtained with N₂. The Raman bands superimposed on the luminescence background are typical for woody samples and have been discussed in our previous reports.

The results in Figure 1 suggest that the quenching effects parallel the changes in the partial pressure of O₂ in the gaseous environment.

Figure 2 indicates that continued exposure to O_2 results in enhancement of the quenching effect, suggesting continued adsorption of oxygen within the woody tissue, or further diffusion within the tissue, or perhaps a combination of both effects. Figure 3 indicates that the effect is substantially reversible, suggesting that an interaction involving a physical adsorption process is the dominant effect.

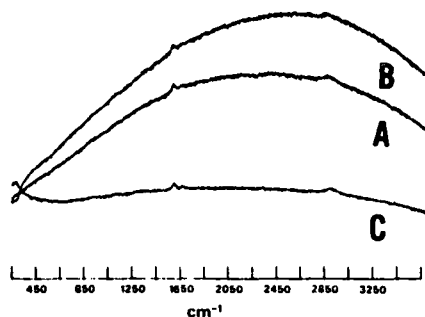


Fig. 1. Woody tissue Raman spectra; (A) Air flushing, (B) N_2 flushing, (C) O_2 flushing; all on the same intensity scale.

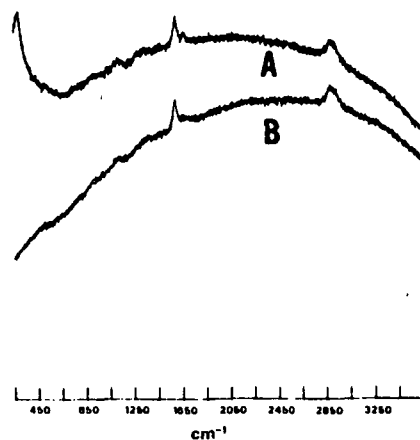


Fig. 2. Raman spectra of the O_2 flushed sample; (A) O_2 flushing just started, (B) one hour later.

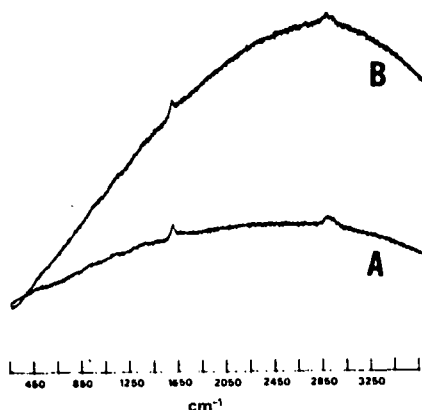


Fig. 3 (Left). Effect of switching over from O_2 flushing (A) to N_2 flushing (B).

Oxygen is known to quench excited states of a number of molecules. However, in most instances the mechanism of its action remains unknown. It appears most likely that the major interaction that we have observed is between O_2 and some of the constituent groups of lignin. Contributions of other minor components of the cell walls cannot be excluded at this time, however.

References

1. R. H. Atalla and U. P. Agarwal, *J. Raman Spectr.*, 17(1986) in press.
2. R. H. Atalla and U. P. Agarwal, *Science*, 227:636(1985).

THE INSTITUTE OF PAPER CHEMISTRY

Appleton, Wisconsin

Status Report

to the

PULPING PROCESSES

PROJECT ADVISORY COMMITTEE

Project 3456-2

SMELT-WATER EXPLOSIONS

August 27, 1986

PROJECT SUMMARY FORM

DATE: August 27, 1986

PROJECT NO. 3456-2: SMELT-WATER EXPLOSIONS

PROJECT LEADERS: T. M. Grace

IPC GOAL:

Increase the capacity potential of processes.

OBJECTIVE:

An increased understanding of the phenomena underlying recovery boiler explosions, and the application of that knowledge to reduce the hazards of operating recovery boilers.

CURRENT FISCAL YEAR BUDGET: \$20,000

SUMMARY OF RESULTS SINCE LAST REPORT:

The experiences of the industry with explosions and other issues related to recovery boiler safety continue to be monitored through active participation with the API Recovery Boiler Committee and BLRBAC. Implementation of findings is done primarily through API.

We continue to review the state of knowledge relevant to smelt-water explosions. Appropriate contacts have been established.

The first part of a separate Nuclear Regulatory Commission-sponsored project on energetics of smelt-water explosions has been completed, and a report will issue through NRC. All recovery boiler explosions show very low thermal to mechanical energy conversion efficiencies (< 0.5%) relative to the heat content in the molten smelt. The remainder of the project will focus on how to scale explosion energetics between different fluid pairs and system sizes.

A graduate student under Prof. M. A. Corradini at UW-Madison has completed a sensitivity study on a one-dimensional vapor explosion model, using parameters specific to the smelt-water system. The most significant parameters affecting the peak pressure and energy conversion ratio were found to be, in order of importance: smelt mass, water mass, inertial constraining mass, final smelt debris size, and fragmentation characteristic time.

A joint proposal, with Prof. Corradini, for a research program to study the triggering, fragmentation and propagation phenomena involved in smelt-water explosions has been prepared and is being submitted to various agencies.

PLANNED ACTIVITY THROUGH FISCAL YEAR 1987:

Continuation of monitoring activities.

Complete remainder of NRC energetics project.

Prepare a report to membership based on the model study at UW-Madison.

Pursue implications of energetics results from NRC study.

FUTURE ACTIVITY:

Continuation of effort until explosions are a thing of the past.

THE INSTITUTE OF PAPER CHEMISTRY

Appleton, Wisconsin

Status Report

to the

PULPING PROCESSES

PROJECT ADVISORY COMMITTEE

Project 3473-1

FUNDAMENTAL PROCESSES IN ALKALI RECOVERY FURNACES

Fume Generation

Black Liquor Burning

Implementation of Black Liquor Combustion Knowledge

August 27, 1986

PROJECT SUMMARY FORM

DATE: August 26, 1986

PROJECT NO. 3473-1: FUNDAMENTAL PROCESSES IN ALKALI RECOVERY FURNACES

PROJECT LEADERS: T. M. Grace, J. H. Cameron, and D. T. Clay

IPC GOAL:

Increase the capacity of existing systems.

OBJECTIVE:

A quantitative description of all key processes in the burning of alkaline process black liquor, encompassing reaction paths and rate equations for drying, pyrolysis, gaseous combustion, char oxidation, sulfide production, and fume formation. The overall goal is a comprehensive understanding of black liquor combustion and application of that knowledge to improve recovery boiler performance.

CURRENT FISCAL YEAR BUDGET: \$230,000

SUMMARY OF RESULTS SINCE LAST REPORT:

Char Burning:

The sulfate-sulfide cycle mode of char burning has been conclusively established. A comprehensive technical report summarizing the char burning work and a separate report on furnace implications have been published. Extra copies of these reports are available and can be obtained on request. Continuing work suggests that direct oxidation of char carbon by O_2 or CO_2 may occur in parallel with the sulfate-sulfide cycle. Some details of the continuing work are provided in the attached report.

Fume Formation:

Considerable progress has been made in understanding fume formation. Previous work had shown that intense fuming occurred when sodium oxide was oxidized to sodium sulfate in a sodium carbonate melt. This phenomenon, which we called oxidative fuming, was unexpected and difficult to interpret in terms of existing concepts of fume formation. We have now shown that oxidative fuming is a manifestation of greatly enhanced fuming rates caused by a marked reduction in the gas-side mass transfer resistance to vaporizing sodium (or potassium). The reduction in mass transfer resistance is due to the creation of a vapor sink (by chemical reaction with oxygen) very close to the gas-melt interface and an attendant reduction in the diffusion boundary-layer thickness. Enhancement of vaporization rates by this mechanism is undoubtedly a general phenomenon inside the recovery furnace and is probably responsible for most, if not all, of the Na_2CO_3 and Na_2SO_4 fume produced in the furnace. We have also shown that $NaCl$ fume production is simply a matter of unenhanced volatilization from a liquid smelt obeying Raoult's law. In addition, we have shown that $NaOH$ vaporization

from melts is very low, so that NaOH vaporization is not a likely source of fume in the furnace. A comprehensive report on the fuming work has been issued, and a paper based on the report is attached. Copies of the report and/or paper are available on request.

Single-Particle Burning:

A phenomenological study of black liquor burning behavior using the single-particle reactor is in progress. This study was intended to provide a data bank on burning behavior by using a large variety of mill liquors and trying to find correlations between properties measurable in the laboratory, behavior in single-particle burning tests, and field performance. The results to date indicate that a random testing program will not provide the desired results. Emphasis is shifting toward controlled experiments in which a single variable is changed and the effects of that change on burning behavior are determined. Results on the work to date are given in the attached report.

We have initiated a collaboration with Dr. Mikko Hupa of Abo Akademi in Finland for research on black liquor combustion. The collaboration agreement is attached.

Paul Miller completed his Ph.D. thesis on swelling and pyrolysis.

Sulfur Release:

Preliminary information on the release of sulfur gases during exposure of black liquor to high temperature oxidizing and reducing conditions has been obtained. Some problems with the system used to get data under reducing conditions have been uncovered. Further work on this subject is needed and is being initiated.

Reactions of Hydrogenous Species:

We have initiated a study of chemical reactions between hydrogen-containing species and smelt. The main hydrogenous species being examined are H_2 , H_2O , and H_2S . The reactions to be studied include those that are related to sulfur release/recapture during pyrolysis and to NaOH formation and stability in smelt. Preliminary data have been obtained but are not yet considered suitable for publication. We are still verifying experimental methods and assessing the phenomena involved.

DOE Project:

There is a very close tie-in between the DOE sponsored work on black liquor combustion and this project. The Phase I/In-Flight Reactor is now operational in upflow mode and generating data on drying rates, pyrolysis, carbon fixation, and particle characteristics as functions of key variables. The equipment necessary to permit operation in downflow mode is on-site and ready to be installed. The design of the Phase II/Char Bed Reactor is being finalized and this reactor should be operational in early 1987. The first Progress Report on the DOE combustion work has been issued and is available. The second Progress Report will be written later this year.

A brief status report on the DOE project is included in the attached material.

PLANNED ACTIVITY THROUGH FISCAL YEAR 1987:

Char Burning:

Greg Aiken will continue his Ph.D. thesis work on CO/CO₂ ratios during pile burning of black liquor char. We will also try to extend the existing sulfate-sulfide cycle model to include parallel burnup of carbon by oxygen.

Fuming:

The main continuing activity on fume formation will be to apply the concept of enhanced mass transfer rates to fume formation from a burning char particle. Chris Verrill will construct an experimental apparatus and obtain some preliminary data in his M.S. research. Extensive work on this problem will be carried out as a Ph.D. thesis.

Ph.D. thesis research will also be initiated by James Cantrell at Ga. Tech. on fume condensation processes and by Kris Goerg on fume deposition.

Single Particle Burning:

The phenomenological study of burning behavior will continue. The breadth of this study will be enhanced by the collaboration with Mikko Hupa. The focus of our phenomenological study will shift to testing of controlled variables. No additional mill liquors are being sought at this time.

Mark Robinson will complete his Ph.D. thesis on the drying of black liquor drops.

Kathy Crane will initiate her Ph.D. thesis on single particle burning in combined convective/radiative heat fields.

Sulfur Release:

Frank Harper will initiate a Ph.D. thesis on sulfur release in black liquor burning.

Hydrogenous Species:

We will continue the fundamental study of reactions between hydrogen-containing species and smelt. The smelt pool reactor is being modified to permit smelt agitation independent of gas flow rates. The initial focus will be on hydrogen reduction of sulfate. Reactions of H₂S and H₂O will also be studied.

DOE Project:

Phase I of the DOE Project, In-Flight Processes, will be completed. The Phase II/Char Bed Reactor will become operational.

Book:

The funded research plan states that we will begin the process of writing a book on the theory of black liquor combustion and its application to recovery operation. The API Recovery Boiler Committee has just initiated a project to have a

series of books on these topics written in the next two years. Accordingly, we do not intend to pursue writing the book at this time.

FUTURE ACTIVITY:

The next two years will involve an intense effort to expand our basic knowledge of black liquor combustion. In a parallel project, a comprehensive mathematical model of the recovery furnace is being developed and should be available in about two years. The model will provide linkages between fundamental information and furnace behavior.

After this two year period, emphasis will shift to application of the results.

STUDENT RESEARCH

Black Liquor Combustion:

M. Robinson	- Convective Drying of B.L. Drops	- Finish Spring 1987
G. Aiken	- Pile Burning of Char	- Finish Summer 1987
K. Crane	- Single Particle Combustion	- Start Fall 1986
F. Harper	- Sulfur Release	- Start Fall 1986

Fuming:

C. Verrill (M.S.)	- Fuming During Char Burning	- Finish March 1987
J. Cantrell (Ga. Tech.)	- Fume Condensation	- Start Fall 1986
K. Goerg	- Fume Deposition	- Start Fall 1986

Other:

G. Kulas	- Lower Furnace Corrosion/Mild Steel	- Finish Spring 1988
K. Mohammadi (pros. Ph.D.)	- Fluid Bed Drying of B.L.	- Start Spring 1987
J. Fuller (M.S.)	- Lime Nodulation	- Finish March 1987

Status Report

FUNDAMENTAL PROCESSES IN ALKALI RECOVERY FURNACES

FUME GENERATION

Our work on fume generation is effectively summarized in the paper, "Fume Generation During Oxidation of Alkali Carbonates/Sulfide Melts," IPC Technical Paper Series Number 195. This paper is attached and constitutes the main part of this report. A membership progress report, "Fume Generation from Alkali Carbonate/Sulfide Melts," Project 3473-1 Report Four, has also been issued and discusses fume generation in more detail.

For now, no further funded research is planned in this area. However, student research on fume generation will continue. As part of his Master's research Christopher Verrill is building an experimental system to study fume generation during black liquor combustion. Chris is planning on pursuing a Ph.D. degree, and his thesis will focus on fume generation during the combustion of a single black liquor droplet.

Kristin Goerg is writing her thesis proposal, which will focus on fume deposition. The knowledge gained during the study of fume generation under oxidizing conditions will allow control of fume composition and generation rates. This ability to manipulate fume will be invaluable for a quantitative study of fume deposition on a cooled surface.

HYDROGEN REACTIONS OCCURRING WITHIN THE KRAFT FURNACE

Funded research is focusing on the reactions involving hydrogen which occur within the kraft furnace. The reactions currently being studied are hydrogen reduction of sodium sulfate and sodium carbonate. These reactions

have been found to be moderately complex, with the reaction rates limited by the interfacial surface area. Since the present understanding of these reactions is incomplete, they will not be discussed in this report.

OTHER STUDENT RESEARCH PROJECTS

Greg Aiken, a Ph.D. candidate, is studying the processing responsible for the carbon dioxide/carbon monoxide ratio observed during the combustion for kraft char. This ratio determines the amount of energy released during char combustion and the amount of oxygen required for combustion.

During her Master's program, Kris Goerg studied carbon dioxide gasification of kraft black liquor char in a sodium carbonate melt. Carbon dioxide gasification of char was found to be considerably slower than char oxidation. This reaction may be significant in determining the carbon dioxide/carbon monoxide ratio from the char bed. A detailed description of this work is contained in "A Kinetic Study of Kraft Char Gasification with Carbon Dioxide," IPC Technical Paper Series Report Number 197, which is attached to this report.

John Fuller, an M.S. candidate, is studying the effect of green liquor dregs on lime sintering during the calcination of lime mud. Once the effect of the dregs is determined, the elements or compounds responsible for the observed effects will be identified.

ATTACHMENT NUMBER 1

FUME GENERATION DURING OXIDATION OF ALKALI CARBONATE/SULFIDE MELTS

J. H. Cameron
The Institute of Paper Chemistry
Appleton, Wisconsin 54912

ABSTRACT

Air oxidation of Na_2S in $\text{Na}_2\text{S}/\text{Na}_2\text{CO}_3$ melts produces copious quantities of Na_2CO_3 fume. This phenomenon was unexpected and very difficult to interpret in terms of previous concepts of fume production by formation and volatilization of elemental Na or NaOH.

Based on the experimental results obtained in this study, the large quantity of fume which can be generated during sulfide oxidation is a result of Na oxidation in the gas phase. Oxidation of Na in the gas phase significantly lowers the partial pressure of Na. Since the driving force for vaporization is the difference between the equilibrium vapor pressure of Na at the gas-melt interface and the partial pressure of Na in the gas phase, this reduction in partial pressure of Na significantly increases Na vaporization rates and allows fuming to proceed with only mild reducing conditions in the melt.

INTRODUCTION

One of the principal steps in the kraft pulping process is the recovery of the pulping chemicals. In the recovery process, the black liquor from the pulping process is burned in a recovery furnace. In the furnace, the combustion of the carbonaceous char produced from the pyrolysis of the black liquor occurs in a molten salt environment consisting principally of Na_2CO_3 and Na_2S . During the burning of the kraft black liquor a large quantity of fume particles are produced from the volatilization and condensation of the inorganic sodium compounds. These particles are typically 0.25 to 1.0 μm in diameter and are composed principally of Na_2CO_3 and Na_2SO_4 .

Fume significantly affects the design and operation of the recovery furnace. These particles form deposits on the heat transfer surfaces, reducing heat transfer rates and increasing the amount of surface area required for a given steam load. The fume particles that do not deposit on the heat transfer surfaces are collected by the electrostatic precipitators and recycled into the black liquor. This increases the inorganic content of the black liquor and reduces its heating value on a unit weight basis.

Not all aspects of fume are detrimental. The beneficial aspect of the fume is that it captures the sulfur gases released during black liquor pyrolysis and combustion. This occurs through the reaction of Na_2CO_3 with SO_2 and O_2 to form Na_2SO_4 . This Na_2SO_4 is then removed by the precipitators and recycled back into the black liquor.

Recent work by Clay *et al.* (1984) and Cameron *et al.* (1985) has shown that air oxidation of Na_2S in a $\text{Na}_2\text{S}/\text{Na}_2\text{CO}_3$ melt can produce large quantities of Na_2CO_3 fume. The rate of fume generation under oxidizing conditions was found to be considerably greater than the rate under strongly reducing conditions. This phenomenon was unexpected and very difficult to interpret in terms of the existing concept of fume formation by elemental Na formation and volatilization at high-temperature reducing conditions. This paper describes the mechanism responsible for fume generation during air oxidation of Na_2S in a $\text{Na}_2\text{S}/\text{Na}_2\text{CO}_3$ melt.

PREVIOUS WORK

Several researchers have used thermodynamic equilibrium calculations to predict the liquid and gaseous species present in the kraft furnace. Bauer and Dorland

(1964) were one of the first to apply this technique to the kraft furnace. Their study predicted that the volatile fuming species in the furnace are Na and Na₂. They considered NaOH as a liquid species but not as a gaseous species. Thus they a priori eliminated it as a potential source of fume.

More recently Warnqvist (1973) also applied equilibrium thermodynamics to the kraft furnace and concluded that in addition to Na and Na₂, NaOH is an important volatile compound. Warnqvist believed that the earlier study by Bauer and Dorland (1954) was flawed for not including NaOH(g) in the equilibrium calculations.

As stated by Warnqvist (1973) a major assumption in these equilibrium treatments is that "the waste liquor/air (oxygen) system as a whole comes to chemical equilibrium." This assumption is recognized to be somewhat unrealistic, but Warnqvist believed that this technique provides an insight into the processes and chemical species present in the furnace.

Equilibrium treatments predict that the major fume producing species are Na, Na₂, and NaOH. The vaporization rate of a chemical species can be significantly affected by the reaction between the volatile species and any gaseous species, as indicated by Turkdogan (1963). Since furnace gases such as O₂ and CO₂ are reactive with Na and Na₂, equilibrium treatments cannot be used to predict the amount of fume generated through Na and Na₂ vaporization. They can, however, be used to predict the melt composition and the vaporization rate of nonreactive species such as KCl, NaCl, and possibly NaOH.

Turkdogan (1980) states that there are two possible mechanisms for enhanced vaporization of a liquid into a reactive gas: (1) the gas may react with the liquid to form a volatile species or (2) the gas may react with the

vapor from the liquid, lowering the partial pressure of the vapor above the liquid and enhancing the vaporization rate.

Turkdogan et al. (1963, 1980, 1982) have shown that the oxidation of many molten metals can produce large amounts of metal oxide fume. Since there are several similarities between these fuming systems and fuming during sulfide oxidation in a carbonate melt, a review of fuming during oxidation of molten metals is included here.

The increase in fuming during oxidation in these molten metals is attributed to the reaction of the metal vapor with oxygen to form a condensed metal oxide fume. This may be considered to be a counterflux transport process. Oxygen diffuses toward the molten metal surface, and metal vapor diffuses away from the surface. At some distance from the surface the metal vapor and oxygen react to form a metal oxide condensed phase (Figure 1).

(Figure 1 here)

This reaction in the gas phase forms a sink for the metal vapor, reducing its partial pressure. Since the driving force for vaporization is the difference between the vapor pressure of the metal and its partial pressure in the gas phase, this reduction in partial pressure can greatly enhance the rate of vaporization.

The maximum rate of the metal vaporization with this mechanism is equal to the vaporization rate in a vacuum. At the maximum vaporization rate, the metal oxide fume is forming directly at the metal surface. If the oxygen partial pressure is increased beyond this value, the flux of oxygen toward the metal surface is greater than the vaporization rate of the metal. Oxidation

then occurs within the molten metal, forming a metal oxide film. Since the concentration of the volatile species is greatly reduced in this metal oxide film, the formation of this film results in a significant decrease in the vaporization rate of the metal.

EXPERIMENTAL APPARATUS

The fume generation experiments were conducted by monitoring the fume produced from alkali carbonate/sulfate/sulfide melts under different atmospheres. The experimental system consisting of an induction heated reactor, gas meters and fume filter is illustrated in Figure 2. The ceramic reactor was normally charged with approximately 85 g of inorganic salts containing 53 to 80 g of Na_2CO_3 , 2.0 to 20 g of Na_2S , and 0 to 40 g of Na_2SO_4 .

(Figure 2 here)

Two configurations for introducing the purge into the reactor were employed during this study. These configurations consisted of either introducing the N_2/O_2 gas mixture directly into the melt or into the reactor above the melt. Figure 2 illustrates the experimental system with the gases introduced below the melt's surface. With the gases introduced into the melt, oxygen was totally consumed by sulfide oxidation. With the gases introduced above the melt, the sulfide content of the melt was oxidized without any significant mixing of the melt. This configuration would tend to produce a melt with an oxidized surface and also resulted in a residual O_2 concentration above the melt. The effect of residual O_2 was studied by adding different amounts of O_2 to the carrier gas.

The fume generation rate was followed by filtering the off-gas and weighing the fume particles. To ensure that this gravimetric method collected

all the fume particles, the Na content of the off-gas after the filter was checked with a flame photometer. Readings from the flame photometer showed that the filter collected essentially all the fume particles.

The fume particles collected during sulfide oxidation were typically white spherical particles approximately 0.25 to 1.0 μm in diameter. Figure 3 is a scanning electron micrograph (SEM) of fume particles collected during sulfide oxidation. Infrared analysis of these fume particles revealed that they are essentially pure Na_2CO_3 .

(Figure 3 here)

FUME GENERATION WITH GAS INTRODUCED BELOW THE MELT'S SURFACE

In this section, the effects of sulfide concentration, sulfate concentration, temperature, inlet oxygen content, and gas flow rate on fume generation with the gas introduced directly into the melt are described.

Typical Experimental Results with Gas Introduced Below the Melt's Surface

In a typical experiment, the fume generation rate was monitored by filtering the off-gas from the reactor for a five-minute period and weighing the fume collected. Experimental results typical of the majority of the experiments conducted using this procedure are illustrated in Table 1.

(Table 1 here)

It can be seen that the fume generation rate remains at a constant level until the sulfide is nearly totally oxidized. Once the sulfide level reaches a concentration of approximately 0.1 mole/L, the fume generation rate rapidly decreases. Although the relative concentrations of sulfide and sulfate

change significantly during this experiment, little change in the fume generation rate is observed until the sulfide is nearly completely oxidized. This indicates that the ratio of sulfide to sulfate has little effect on the fume generation rate.

Effect of Sulfate Concentration

To determine the effect of sulfate concentration on the rate of fume generation, the fume generation rate was measured at two different initial amounts of sulfate in the melt. The rate of fume generation was followed using the previously described gravimetric method. The results of these experiments are presented in Table 2.

(Table 2 here)

It can be seen that sulfate concentration in the melt does not significantly affect the fume generation rate. Although the melt in Run 43 contained a high level of sulfate, the fume generation rate was only slightly different from that in Run 39 with no initial sulfate present.

Effect of Sulfide Concentration

To determine the effect of sulfide concentration on the rate of fume generation, the fume generation rate was measured with different initial amounts of sulfide in the melt. The effect of sulfide on the rate of fume generation is shown in Table 3.

(Table 3 here)

It is obvious that the amount of sulfide has no significant effect on the rate of fume generation.

Effect of Oxygen Partial Pressure on Fume Generation Rate

To determine the effect of inlet oxygen concentration on the rate of fume generation, the oxygen level in the purge was varied. Preliminary studies of sulfide oxidation with O_2/N_2 mixtures introduced below the melt's surface have shown that essentially all the oxygen supplied to the melt is consumed by sulfide oxidation. Therefore, to maintain a constant off-gas flow rate from the melt, the nitrogen flow to the reactor was held constant and the oxygen flow was adjusted. The results of a series of experiments with varying inlet oxygen concentrations are shown in Table 4.

(Table 4 here)

As shown in this table, the increase in oxygen to the reactor tends to increase the rate of fume generation. However, the fume dependence on the oxygen concentration rate is slight. Although the initial concentration of oxygen in Table 4 increased by a factor of eight, the fume rate less than doubled.

Temperature Effect

To determine the temperature dependence, fume generation rates were measured during Na_2S oxidation at temperatures ranging from 927 to 1038°C. By plotting the \ln of the fume generation rate vs. $1/T$, $^{\circ}K^{-1}$ it was found that the fume generation had an Arrhenius type temperature dependence with an activation energy of approximately 20,000 cal/mol, as shown in Figure 4.

(Figure 4 here)

Effect of Nitrogen Flow Rate on Fume Generation

To determine the effect of the volumetric flow rate on the fume generation rate, the nitrogen flow rate was varied while the oxygen flow rate was

held constant. Since the oxidation rate is limited by the amount of oxygen supplied, the oxidation rate remained the same for each experiment. The results of these experiments using the gravimetric method of following fume generation are given in Table 5.

(Table 5 here)

It is evident that the fume generation rate is nearly proportional to the volumetric purge rate.

Surface Area Effect

The objective of these experiments was to determine if a change in the surface area of the bubbles would affect the fume generation rate. To increase the melt-gas interface, the single purge tube (0.475-cm ID) was replaced with two purge tubes (0.158-cm ID).

The fume generation rates from several sulfide oxidation experiments employing the two purge tubes are shown in Table 6. Also shown in this table are the fume generation rates for the single purge tube.

(Table 6 here)

It can be seen that the fume generation rate using the two purge tube system is nearly the same as that for the single purge tube. Therefore, changes in the melt-gas interfacial area have little effect on the fume generation rate.

Effect of Different Inert Carrier Gases

To determine the effect of gas phase processes, fume generation was studied using different carrier gases. The carrier gas is the inert gas with which the oxygen is mixed. If the rate controlling process for fume generation

during sulfide oxidation is a liquid phase process, the type of carrier gas used should not affect the rate of fume generation. However, if the rate controlling process is a gas phase process, the fume generation rate could be dependent on the type of carrier gas used. Fume generation rates using three different carrier gases are shown in Table 7.

(Table 7 here)

With He as the carrier gas, the fume generation rate was significantly lower than the fume generation rates observed with either N₂ or Ar as carrier gas. This indicates that gas phase processes are significant in fume generation during sulfide oxidation.

FUMING WITH OXYGEN-NITROGEN GAS INTRODUCED ABOVE MELT'S SURFACE

To determine the effect of the mode of gas-liquid contact on oxidative fuming, fume generation during sulfide oxidation was studied with the purge tube located above the melt. Typical fume generation rates during sulfide oxidation using this mode of gas-melt contact are illustrated in Figure 5 and 6.

Figure 5 illustrates the fume generation rates for low levels of oxygen in the purge. At these rates of oxidation, there is not much change in the melt composition, and the rate of fume generation remains essentially constant. Figure 6 illustrates the fume generation rates for higher levels of oxygen in the purge. At these rates of oxidation, the rate of fume generation decreases as the sulfide content of the melt is oxidized to sulfate.

(Figure 5 and 6 here)

These figures show that the oxidation of a sulfide in a sulfide-carbonate melt with the oxygen introduced above the melt usually results in a decrease in the fume generation rates compared to that observed under a pure N₂ purge. Only at extremely low levels of oxygen did the fume generation rate increase. This is in distinct contrast to the large level of fume observed when the gas was introduced into the melt.

In Table 8, the fume generation rates during sulfide oxidation with the purge introduced above the melt's surface are compared to the rates with the purge introduced below the melt's surface. Since the fume generation rate fell off with time during sulfide oxidation when the purge was introduced above the melt's surface, the fume generation rates in Table 8 for this configuration are the initial rates. At the same sulfide oxidation rate, the fume generation rates with the purge introduced above the melt's surface are approximately an order of magnitude lower than those with the purge introduced below the melt's surface.

(Table 8 here)

Equal rates of sulfide oxidation can be achieved with both modes of gas-melt contact. Therefore, if fume results from the formation of a volatile species during sulfide oxidation, this species should be formed in both modes of gas-melt contact. Since little fume is generated when the gas is introduced above the melt's surface, it is unlikely that fume generation during sulfide oxidation results from the formation of a new volatile compound.

The second critical experiment in the development of the fume generation mechanism is the effect of the inert carrier gas on fume generation. The fuming rate with He as the carrier gas was significantly lower than that with either N₂ or Ar as the carrier gas. This indicates that fume formation is a

gas-phase controlled process. It is also a further indication that fume is not the result of the formation of new volatile compounds. The formation of such compounds would be controlled by liquid-phase processes, and the fume generation rate would then be independent of the type of carrier gas used.

Mechanism for Fume Generation under Oxidizing Conditions

Based on the experimental results obtained in this study, the following theory is proposed to explain fume generation during sulfide oxidation:

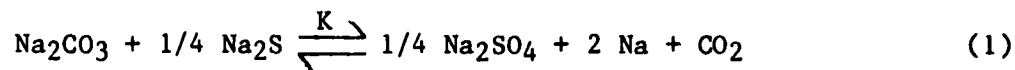
The enhancement of fume generation observed during sulfide oxidation results from the oxidation of Na in the gas phase. This oxidation greatly lowers the partial pressure of Na in the gas phase, increasing Na vaporization from the melt.

Sodium sulfide in the melt is a sufficiently strong reducing agent to produce a significant Na partial pressure. The liquid and gas phase processes occurring during oxidation-enhanced fume generation are illustrated in Figure 7. Sodium and CO₂ are generated in the melt from the equilibrium reaction between Na₂CO₃ and Na₂S, as given by Eq. (1). The Na and CO₂ then evaporate and react with O₂ diffusing toward the melt at some distance δ from the melt. A detailed description of this fume generation mechanism is presented below.

(Figure 7 here)

Liquid Phase Processes

The processes responsible for fume generation during sulfide oxidation can be separated into those processes occurring in the liquid phase and those occurring in the gas phase. In the liquid phase, the concentration of Na in the melt is assumed to be dependent on the equilibrium given by Eq. (1).



Since the melt used for this study consisted primarily of Na_2CO_3 , the activity of Na_2CO_3 is assumed to be approximately 1.0. Then assuming ideal behavior for the Na_2S and Na_2SO_4 , the partial pressure for sodium is described by Eq. (2).

$$P_{\text{Na}} = \frac{K^{1/2} [X_{\text{Na}_2\text{S}}]^{1/8}}{[X_{\text{Na}_2\text{SO}_4}]^{1/8} [P_{\text{CO}_2}]^{1/2}} \quad (2)$$

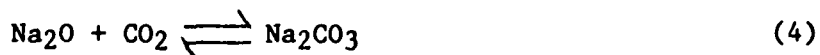
Here, P_M is the partial pressure of component M; X_M is the mole fraction of component M; and K is a constant.

Equation (2) indicates that the equilibrium vapor pressure of Na is only very weakly dependent on the Na_2SO_4 and Na_2S concentrations in the melt. This explains why changes in the Na_2SO_4 and Na_2S concentrations have little effect on the fume generation rate until only a very low concentration of Na_2S remains in the melt.

Gas Phase Processes

The most significant process occurring in the gas phase is the oxidation of Na, which lowers the partial pressure of Na in the gas. Since the rate of Na vaporization depends on the difference between the vapor pressure of Na at the melt-gas interface and the partial pressure in the gas, the reduction in partial pressure increases the Na vaporization rate.

The reactions occurring in the gas phase are represented by Eq. (3) and Eq. (4).



These equations are not intended to represent a mechanism, but are intended to indicate the stoichiometry of the gas phase reactions.

The consumption of CO_2 in the gas also increases the rate of Na vaporization. If only Na was consumed in the gas phase reactions, the CO_2 generated would shift the equilibrium represented by Eq. (1) toward the left and result in a lower vapor pressure for Na.

APPLICATION OF FUME GENERATION THEORY TO THE EXPERIMENTAL RESULTS

Described below is the application of the proposed fume generation theory to the two modes of gas-melt contact used during this study. In one mode of gas-melt contact, the $\text{O}_2\text{-N}_2$ stream was introduced above a relatively quiescent melt. With this mode of oxidation, little fume was observed and the rate of fume generation decreased as the O_2 partial pressure was increased.

In the other mode of gas-melt contact, the $\text{O}_2\text{-N}_2$ stream was introduced below the melt's surface. This mode of oxidation generated a high level of fume. Although the fume generation rate was not highly dependent on the O_2 content of the purge, the fume generation rate increased as the O_2 content of the gas increased.

Interpretation of Fume Generation with Gas Introduced above Melt's Surface

The fume generation behavior observed with the gas introduced above the melt is very similar to that reported in Turkdogan's (1963) study of fuming

during the oxidation of molten metals. At low O_2 partial pressure, the Na evolving from the melt is oxidized above the melt, lowering the partial pressure of Na and increasing the rate of Na vaporization. At higher O_2 partial pressures, the O_2 penetrates to the melt surface. Oxidation of the Na and Na_2S then occurs in the melt and little fume is generated.

The vapor pressure of Na above a $Na_2S-Na_2CO_3$ melt is relatively low compared to the vapor pressure of the metal systems studied by Turkdogan (1963, 1980, 1982). The O_2 partial pressure required to penetrate the boundary layer to the melt surface is also relatively low for Na in the $Na_2S-Na_2CO_3$ melts compared to the metal systems. Therefore, with the gas introduced above the melt, an increase in fume generation is observed only at low O_2 partial pressures. While in the metal systems, an increase in fume generation occurs even at relatively high O_2 partial pressures.

Interpretation of Fume Generation with Gas Introduced below Melt's Surface

The fuming behavior during sulfide oxidation with the gas introduced below the melt's surface was considerably different than that observed with the gas introduced above the melt. The major difference was the relatively high level of fuming during Na_2S oxidation. The effect of O_2 partial pressure was also significantly different in the two modes of gas-melt contact. With the gas stream introduced below the melt's surface, increasing the O_2 partial pressure in the purge resulted in a slight increase in the rate of fume generation. This contrasts to the decrease in fume generation with an increase in O_2 partial pressure when the gas was introduced above the melt. The Na_2S concentration in the melt had different effects on the rate of fuming in the two modes of melt-gas contact. With the gas introduced above the melt, fuming rate

decreased as the Na_2S was oxidized to Na_2SO_4 . With the gas introduced below the melt's surface, the level of Na_2S concentration had no effect on the fuming rate until only low levels of Na_2S remained in the melt.

With the gas introduced below the melt's surface, fume is generated in the bubble as it rises in the melt (Figure 8). The liquid surrounding the bubble is continually renewed, and as a result of the liquid flowing past the bubble the gas in the bubble may undergo toroidal circulation. The basic difference between this mode of oxidation and oxidation with the gas introduced above the melt is the mixing of the liquid at the gas-melt interface.

(Figure 8 here)

In a gas-liquid reaction, the reaction rate may be limited by (A) gas side mass transfer, (B) liquid side mass transfer, (C) the chemical kinetics, or (D) a combination of these processes. Since the oxidation of Na_2S in a carbonate melt is an extremely fast reaction and preliminary experiments showed that it is independent of Na_2S concentration, it is probable that this reaction is mass transfer limited. When the purge tube was located above the melt's surface, only low levels of fume were observed during sulfide oxidation. In this mode of oxidation, the reaction is limited by liquid side mass transfer.

Since large amounts of fume were generated during sulfide oxidation when the gas was introduced below the melt's surface, the melt at the liquid-gas interface is unoxidized in this mode of sulfide oxidation. The sulfide oxidation reaction is then limited by either gas side mass transfer or by chemical kinetics. If kinetics limits the oxidation rate, the majority of the chemical species in the melt at the interface should be oxidized and the fraction of oxidized species should be dependent on the O_2 partial pressure in the purge gas.

This situation would be similar to that with the purge tube introduced above the melt. The fume generation rate should be low and should decrease as the O_2 partial pressure in the gas is increased. Since a high level of fume was present and the fuming rate increases with an increase in O_2 partial pressure, the oxidation rate is not kinetically limited, but is likely gas-phase mass transfer limited.

The effect of different carrier gases on the fume generation rate, shown in Table 7, also indicates that the sulfide oxidation rate is not limited by the chemical kinetics. Helium, the carrier gas in which the diffusivities are the highest, produced the lowest fuming rate. If the Na_2S oxidation reaction was limited by the chemical kinetics, the carrier gas would not affect the reaction rate. The vapor pressure of the volatile species would not be affected by the carrier gas and the only effect the carrier gas would have would be on the rate of flux of the volatile species from the surface. Carrier gases with higher diffusivities such as He would have higher fluxes of the volatile species and would produce higher fuming rates. Since He produced the lowest fuming rate, the reaction rate and fume generation process are not limited by the chemical kinetics.

As the gas bubble rises in the melt, the melt at the interface is constantly mixed. This mixing of the melt and the fast rate of the oxidation reaction results in the reaction being controlled by gas-side mass transfer. Figure 9 illustrates the relative O_2 , Na, and Na_2S concentrations at the interface during Na_2S oxidation.

(Figure 9 here)

The O_2 partial pressure in the gas falls to near zero at the interface. Since the melt is renewed at the interface faster than it is oxidized, the Na and Na_2S concentrations at the interface are nearly identical to those in the bulk melt.

In this situation, Na evolves from the melt and is oxidized near the interface in the gas. This oxidation lowers the partial pressure of Na in the gas and significantly enhances the rate of Na evolution. Since the melt at the interface is constantly renewed, its composition remains constant as the O_2 in the bubble is consumed. The fume generation rate is constant as long as sufficient O_2 remains in the gas to rapidly oxidize the Na evolving from the melt. The fume generation rate observed then depends on the time required for consumption of the O_2 in the bubble.

The rate of O_2 consumption is described by Eq. (5).

$$\frac{d(N_{O_2})}{dt} = S K_g (P_{O_2} - P_{O_2}^*) \quad (5)$$

Here, P_{O_2} is the partial pressure of O_2 in the bulk gas; $P_{O_2}^*$ is the partial pressure at the interface; K_g is the gas phase mass transfer coefficient; N_{O_2} is moles of O_2 ; and S is interfacial surface area.

Since $P_{O_2} \gg P_{O_2}^*$, Eq. (6) can be written as:

$$\frac{d(N_{O_2})}{dt} = S K_g P_{O_2} \quad (6)$$

The partial pressure of O_2 in the gas is shown in Eq. (7):

$$P_{O_2} = \frac{N_{O_2}}{N_{N_2} + N_{O_2}} \times P_t \quad (7)$$

Here, P_t is the total pressure, and N_{N_2} is moles of N_2 .

For the experimental conditions used in this study the O_2 content in the gas during sulfide oxidation is much less than the N_2 content of the gas. The partial pressure of O_2 is then approximated by Eq. (8).

$$P_{O_2} = \frac{N_{O_2}}{N_{N_2}} P_t \quad (8)$$

The rate of O_2 consumption is then given by Eq. (9)

$$\frac{d(N_{O_2})}{dt} = S P_t K_g \frac{N_{O_2}}{N_{N_2}} \quad (9)$$

During sulfide oxidation, the fume generation rate remains constant until the O_2 level in the gas bubble falls below that required to rapidly oxidize the Na being evolved. The weight loss of the melt due to fuming (or fume generated during this period) is then described by Eq. (10).

$$\frac{dF}{dt} = - S K \quad (10)$$

Here, F is the weight of material evolved from the melt during the fuming period, and K is a constant.

Dividing Eq. (10) by Eq. (9) gives the change in fume with the O_2 content of the gas bubble, Eq. (11)

$$\frac{d F}{d (N_{O_2})} = - \frac{K N_{N_2}}{K_g P_t N_{O_2}} \quad (11)$$

Once the O_2 level in the bubble falls to the level where the Na evolved is not oxidized, fume generation essentially stops. Equation (11) can then be integrated between the following boundary conditions.

- 1) For initial moles of O₂ in bubble (N_{O₂I}), fume generation (F) = 0. This boundary condition is simply that no fume is generated until the gas is introduced into the melt and the oxidation process begins.
- 2) For O₂ remaining in bubble when fuming stops (N_{O₂F}), fume generated = measured fume (F_M). This condition is that once the O₂ concentration in the bubble falls below that required to rapidly oxidize the Na evolving from melt, fuming stops and the fume present in the bubble is the measured fume F_M.

$$\int_0^{F_M} dF = - \frac{K N_{N_2}}{kg Pt} \int_{N_{O_2I}}^{N_{O_2F}} \frac{dN_{O_2}}{N_{O_2}} \quad (12)$$

$$F_M = \frac{K N_{N_2}}{Kg Pt} [\ln (N_{O_2I}) - \ln (N_{O_2F})] \quad (13)$$

To test this model of fume generation, the fume generation rates were plotted vs. the ln of the initial O₂ flow rates, Figure (10), for the three different carrier gases in Table 7. From Eq. (13), this plot of the ln of the initial O₂ molar flow rates vs. the fume generation rate should yield a straight line.

(Figure 10 here)

As illustrated in Figure 10, Eq. (13) accurately describes the effect of O₂ on fume generation during sulfide oxidation with the purge introduced below the melt's surface. In Figure 10, fume generation is clearly a logarithmic function of the initial O₂ content of the purge.

The lower fume generation rate in He is due to O₂ having a higher diffusivity in He than it has in either Ar or N₂. This higher diffusivity results in faster consumption of the O₂ and hence a shorter time for fume generation.

The penetration theory first proposed by Higbie (1935) predicts that the mass transfer coefficient should be proportional to the square root of the diffusivity, as given by Eq. (14).

$$K_A \propto D_A^{1/2} \quad (14)$$

Then from Eq. (13), the fume generated as the bubble passes through the melt should be inversely proportional to the square root of the interdiffusivity of O_2 in the carrier gas.

To confirm this, the diffusivities for O_2 in the three inert carrier gases were calculated using the Wilke and Lee (1955) modification of the equation by Hirschfelder, Bird and Spotz (1949).

Table 9 lists the calculated diffusivities of O_2 in the three carrier gases used in this study, the predicted fuming rates relative to the N_2-O_2 system, and the actual fuming rates relative to the N_2-O_2 system. The actual relative fuming rates in this table are the averages of the relative fuming rates for different O_2 levels. The predicted relative fuming rates are based on the change in the gas mass transfer coefficient resulting from changes in the diffusivities of O_2 in the carrier gases. As shown in this table, the actual relative fuming rates are quite close to those predicted on the basis of changes in O_2 diffusivities in the carrier gases.

(Table 9 here)

This mechanism for enhanced fuming under oxidizing conditions accurately explains the effects of the experimental variables on fume generation during sulfide oxidation. The major effects of the experimental variables on fume generation and their relationship to the proposed mechanism are summarized below.

(A) Fume generation during sulfide oxidation with the N_2-O_2 gas system introduced above melt's surface.

1. Fume generation with a N_2-O_2 gas was normally less than that with a pure N_2 . This results from the sulfide oxidation rate being liquid side mass transfer limited in this mode of gas-melt contact. The melt at the gas-melt interface is oxidized and the vapor pressure of Na is low in this oxidized state.
2. Only at very low O_2 partial pressures was the fume generation rate greater than that with a N_2 atmosphere. This results when the low O_2 partial pressures are not sufficient to oxidize the melt's surface. Sodium then vaporizes from the melt and is oxidized in the gas above the melt. This creates a Na sink and increases the rate of Na vaporization.

(B) Fume generation during sulfide oxidation with the N_2-O_2 gas introduced below the melt's surface.

1. Sulfide oxidation in this mode of gas-melt contact produces large quantities of fume. This results from sulfide oxidation being gas-side mass transfer limited. The melt at the gas-melt interface has a relatively high Na vapor pressure. As soon as this Na evolves from the melt it is oxidized in the gas phase. This oxidation drastically lowers the partial pressure of the Na in the gas and increases the vaporization rate.

2. The rate of fuming is nearly proportional to the N_2 purge rate. This results from the rate of oxygen consumption in the gas bubble being inversely proportional to the N_2 flow rate, Eq. (9). Therefore, as the N_2 purge rate increases, the time required for complete consumption of the O_2 in the gas is also increased and more fume is generated.
3. The fume generation rate depends logarithmically on the initial O_2 content of the gas. This results from the rate of consumption of O_2 in the gas bubble being proportional to the O_2 concentration. The rate of O_2 consumption is then a logarithmic function. This logarithmic dependence of the fuming rate is predicted by Eq. (13).
4. The bubble size and hence surface area had no effect on the fume generation rate. This results from the rate of sulfide oxidation, Eq. (9), and the rate of fume generation, Eq. (10), both being directly proportional to the surface area. Since the surface area drops out when these equations are combined, Eq. (11), the surface area of the gas bubble does not affect the fume generation rate.
5. Fume generation during sulfide oxidation is not dependent on the Na_2SO_4 and Na_2S content of the melt. This results from the very weak dependence of Na vapor pressure on the concentration of these compounds, Eq. (2).
6. Carrier gases with higher O_2 interdiffusivities produce lower fume generation rates. This results from higher

interdiffusivities producing faster rates of O₂ consumption. Since the O₂ in the bubble is consumed faster, fuming lasts for a shorter period of time and less fume is produced.

DISCUSSION

The experimental results of this study demonstrate that enhanced fume generation during Na₂S oxidation results from the Na oxidation in the gas phase. Although fume generation was studied in rising gas bubbles, the mechanism for enhanced fume generation can occur anytime an oxidizing atmosphere contacts a reduced melt. All this mechanism requires is that there is enough mixing in the melt that the melt's surface is renewed faster than it is oxidized. This may occur anytime turbulent conditions exist. Therefore, this mechanism likely has a significant effect on the amount of fume generated in the kraft furnace.

Although the vapor pressure of Na in the melts used for this study is relatively low, the reduction in gas-side resistance to Na vaporization resulting from gas phase Na oxidation can result in significant quantities of Na based fume. The maximum rate of Na vaporization under these conditions is the rate in vacuo and is given by the Langmuir equation.

$$J_{\text{Max}} = \frac{P_{\text{Na}}}{\sqrt{2\pi RT M_{\text{Na}}}} \quad (15)$$

Here, J_{max} is the maximum vaporization rate; P_{Na} is the vapor pressure of Na; and M_{Na} is Na's molecular weight.

From estimates of bubble diameter, terminal velocity and melt level, the melt-gas interfacial area present during the fuming experiments is in the

range of a 100 cm². With this surface area, the Langmiur equation predicts that the minimum Na vapor pressure necessary to produce the observed fuming rate is 10⁻⁷ atm at 1200°K. From the free energy, the equilibrium Na vapor pressure for reaction (1) is estimated to be approximately 2 x 10⁻⁴ atm. The vapor pressure of Na is then three orders of magnitude greater than that required to produce the observed fuming rate.

The actual fuming rate is less than the maximum for 3 reasons: 1) fume is generated only as long as O₂ is present in the gas bubble, 2) all Na gas phase oxidation may not occur at the gas-melt interface and 3) the partial oxidation of the melt may produce a Na vapor pressure less than that predicted from the equilibrium calculation. This analysis shows that the Na vapor pressure in the melt is more than sufficient to produce the observed fuming rate.

CONCLUSIONS

The major conclusions reached in this study are summarized below:

1. Fume production is a dynamic process, dependent on mass transfer processes and chemical reactions. This implies that fume in a kraft recovery furnace is more than an equilibrium phenomenon, and that fume production is a potentially manipulatable process.
2. Sodium vaporization can be significant during sulfide oxidation in a Na₂CO₃-Na₂S melt and can result in large quantities of Na₂CO₃ fume. This was an unexpected result, since Na is a reduced species and was previously not thought to be present during an oxidative process.
3. Fume produced during sulfide oxidation results from the oxidation of Na vapor in the gas phase. This oxidation of Na produces a

Na sink in the gas phase, reducing the partial pressure of Na and the mass transfer resistance to vaporization. This vapor sink significantly increases the rate of Na vaporization.

LITERATURE CITED

1. Bauer, T. W.; Dorland, R. M., Can. J. Techn. 32, 91 (1954).
2. Cameron, J. H.; Clay, D. T.; and Grace, T. M. 1985 International Chemical Recovery Conference 11-2, 435; New Orleans, LA.
3. Clay, D. T.; Grace, T. M.; Kapheim, R. J. AIChE Symposium Series 239, 80, 99 (1984).
4. Hirschfelder, J. O.; Bird, R. B.; Spatz, E. L., Trans. Am. Soc. Mech. Engrs. 71, 921 (1949).
5. Turkdogan, E. T.; Grieveson, P.; Darken, L. S., J. Phys. Chem. 67, 1647 (1963).
6. Turkdogan, E. T. Physical chemistry of high temperature technology. Academic Press, New York, 1980.
7. Turkdogan, E. T.; Grieveson, P.; Darken, L. S. Proc. Natl. Hearth Steel Con. 470 (1982).
8. Warnqvist, B., Svensk Papperstid. 76(12), 463-6 (1973).
9. Wilke, C. R.; Lee, C. Y., Ind. Eng. Chem. 47, 1253 (1955).

Table 1. Typical experimental fume generation results with purge introduced below the melt's surface

Run 38

Initial Melt Composition

Na₂CO₃ = 0.77 mole

Na₂S = 0.03 mole

Purge = 1 L/min at 2.1% O₂

Temperature = 927°C

Time, s	Calculated Composition		Fume Generation Rate, g/min	Fume Concentration
	Na ₂ SO ₄ , mole/L	Na ₂ S, mole/L		Moles Na ₂ CO ₃ Mole N ₂
755	0.136	0.549	0.0099	0.00214
1280	0.231	0.455	0.0104	0.00224
1760	0.318	0.368	0.0106	0.00288
2240	0.405	0.281	0.0104	0.00224
2721	0.492	0.195	0.0099	0.00214
3114	0.563	0.124	0.0088	0.00190
3639	0.656	0.029	0.0005	0.00011

Table 2. Effect of sulfate level on fume generation rate.

Purge Rate = 1.0 L/min at 2.1% O ₂ , and	Temperature = 982°C
Run 39	Run 43
Na ₂ CO ₃ = 0.77 mole	Na ₂ CO ₃ = 0.57 mole
Na ₂ S = 0.03 mole	Na ₂ S = 0.03 mole
Na ₂ SO ₄ = 0.00 mole	Na ₂ SO ₄ = 0.30 mole

Time, min	Fume Generation Rate, g/min	Fume Generation Rate, g/min
5	0.0157	0.0125
10	0.0159	0.0127
15	0.0161	0.0121
20	0.0145	0.0149
25	0.0158	0.0103
30		0.0103
35		
Ave.	0.0158 ± 0.0006	0.0130 ± 0.0019

Std. Dev.

Std. Dev.

Table 3. Effect of sulfide level on fume generation rate.

Conditions: Temperature = 954°C

N₂ Flow Rate = 1.0 L/MinO₂ Flow Rate = 0.021 L/min

Na ₂ CO ₃ mole	Na ₂ S mole	Sulfidity, %	Fume Generation Rate g/min ± Std. Dev.
0.77	0.03	3.7	0.0142 ± 0.001
0.60	0.20	25.0	0.0136 ± 0.001
0.55	0.25	31.0	0.0144 ± 0.001

Table 4. Effect of oxygen level in the purge on fume generation rate.

Temperature = 927°C

Run	N ₂ L/min	O ₂ L/min	Fume Generation Rate, g/min
45	1.02	0.0105	0.00892
46	1.02	0.021	0.0105
47	1.02	0.042	0.0121
48	1.01	0.063	0.0145
49	1.02	0.084	0.0146

Table 5. Effect of purge rate on fume generation.

Initial Melt Conditions: $\text{Na}_2\text{CO}_3 = 0.77$ mole
 $\text{Na}_2\text{S} = 0.03$ mole
Temperature = 927°C

Run	N_2 , L/min	Air, L/min	Total N_2 , L/min	Fume Generation Rate \pm Std. Dev., g/min
50	0.04	0.1	0.48	0.00680 ± 0.00032
51	0.6	0.1	0.68	0.00850 ± 0.00076
52	0.8	0.1	0.88	0.01004 ± 0.00042
38	0.9	0.1	0.98	0.01024 ± 0.00032
53	1.06	0.1	1.14	0.01204 ± 0.00042
54	1.23	0.1	1.31	0.01474 ± 0.00198

Table 6. Effect of two purge tubes on fume generation rate.

Run No.	Temp., °C	N ₂ Flow Rate, L/min	O ₂ Flow Rate, L/min	Fuming Rate, g/min ± Std. Dev.	Fuming Rate with Single Purge Tube, g/min
127	953	1.03	0.020	0.0129 ± 0.001	0.0126
128	957	1.03	0.0426	0.0163 ± 0.001	0.0156
129	957	1.01	0.0634	0.0156 ± 0.001	0.0172

Table 7. Effect of carrier gas on fume generation.

Fume Generation Rates Using N₂, Ar, and He

Conditions: N₂, Ar, He = 1.0 L/min He
O₂ = 0.01 to 0.20 L/min
Temperature = 955°C

Gas System	O ₂ Purge Rate, L/min					
	0.01	0.03	0.05	0.10	0.15	0.20
	Fume Generation Rate, g/min					
N ₂ -O ₂	0.0078	0.0128	0.0156	0.0184	0.00232	0.0210
Ar-O ₂	0.0086	0.0126	0.0139	0.0168	0.0182	0.0192
He-O ₂	0.0053	0.0076	0.0083	0.0114	0.0133	0.0142

Table 8. Effect of purge tube location on fume generation during sulfide oxidation.

Initial Conditions
 Na_2CO_3 = 0.77 mole
 Na_2S = 0.03 mole
 Temperature = 955°C

<u>Purge Introduced Below Melt's Surface</u>		<u>Purge Introduced Above Melt's Surface</u>	
Oxidation Rate, mole O_2 consumed/min $\times 10^4$	Fume Rate, g/min	Oxidation Rate, mole O_2 consumed/min $\times 10^4$	Fume Rate, g/min
9.38	0.0106	0.84	0.00146
9.46	0.0134	3.88	0.00100
		7.80	0.00115
		12.00	0.00079
		17.70	0.00044

Table 9. Effect of gas diffusivity of fume generation.

Gas System	Diffusivity \pm Av. Error, cm^2/s	Predicted Relative to $\text{N}_2\text{-O}_2$ Fuming Rates, g/min	Actual Relative to $\text{N}_2\text{-O}_2$ Fuming Rates \pm 1 Std. Dev., g/min
$\text{N}_2\text{-O}_2$	2.44 ± 0.1	1.0	1.0
Ar- O_2	2.38 ± 0.1	1.01	0.93 ± 0.10
He- O_2	8.08 ± 0.3	0.55	0.58 ± 0.07

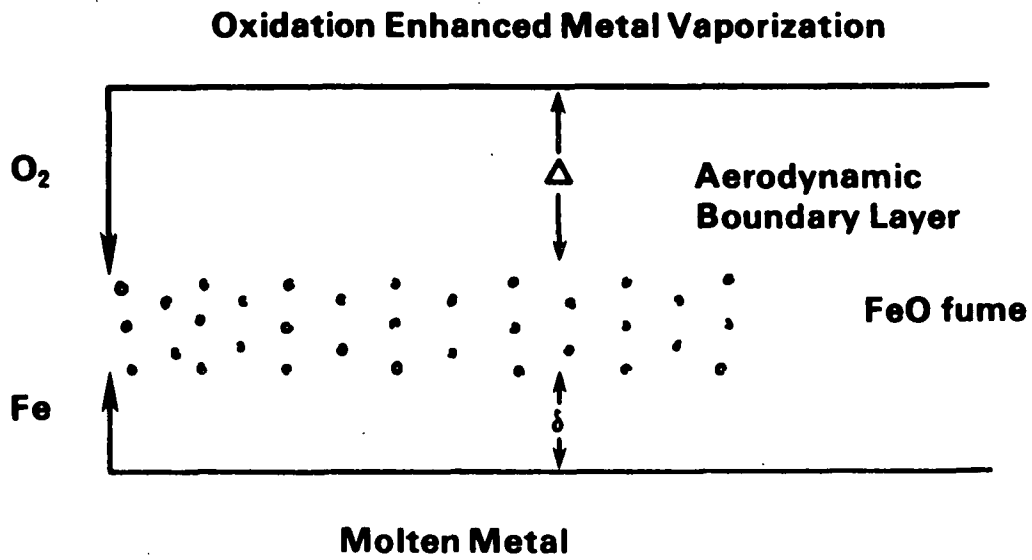


Figure 1. Gas phase oxidation enhanced vaporization.

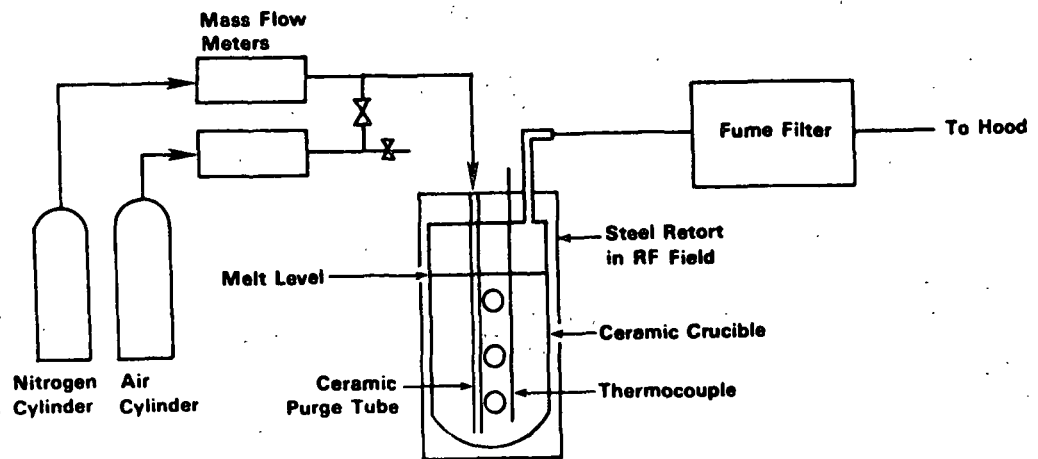


Figure 2. Experimental system.

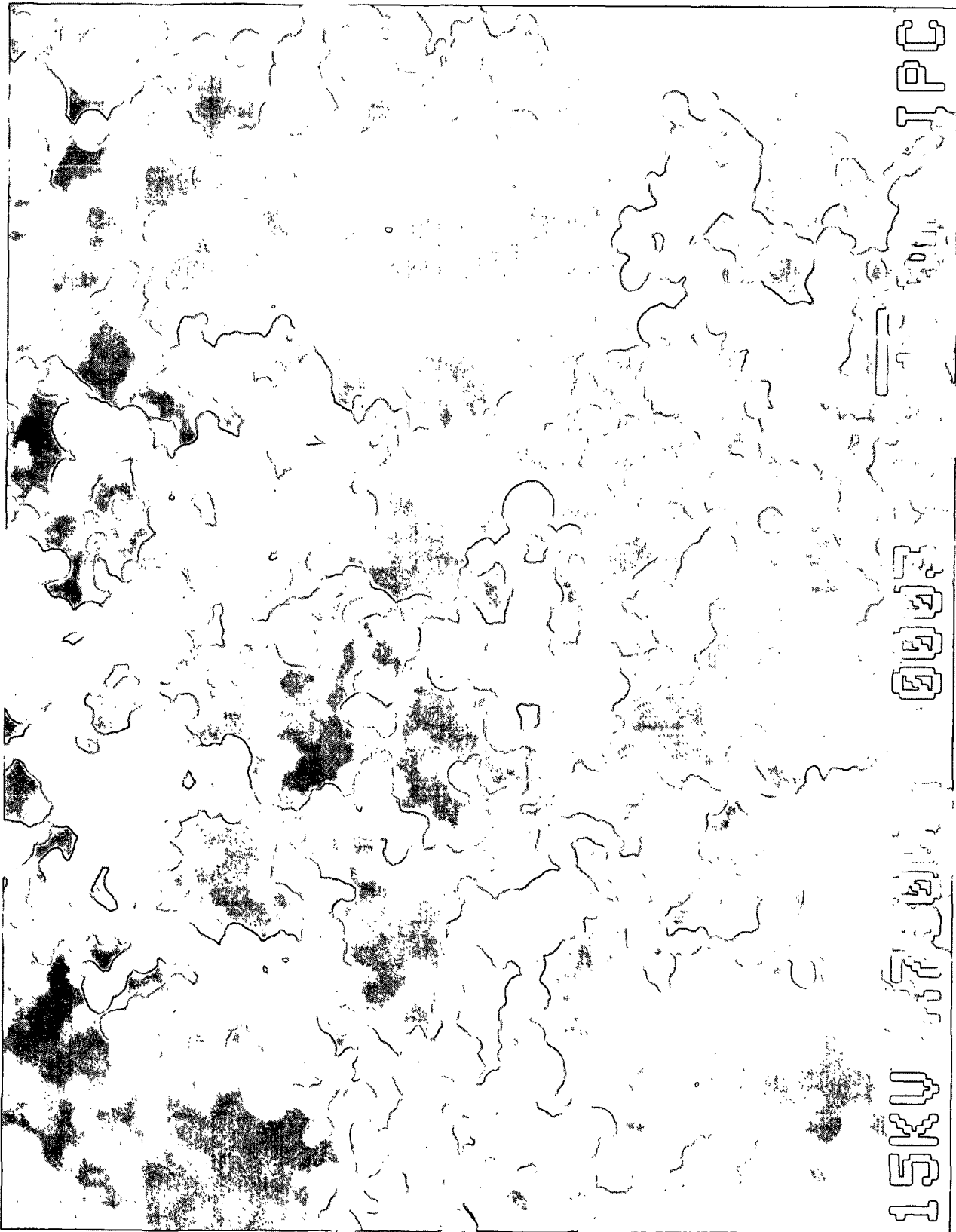


Figure 3. Fume particles collected during sulfide oxidation.

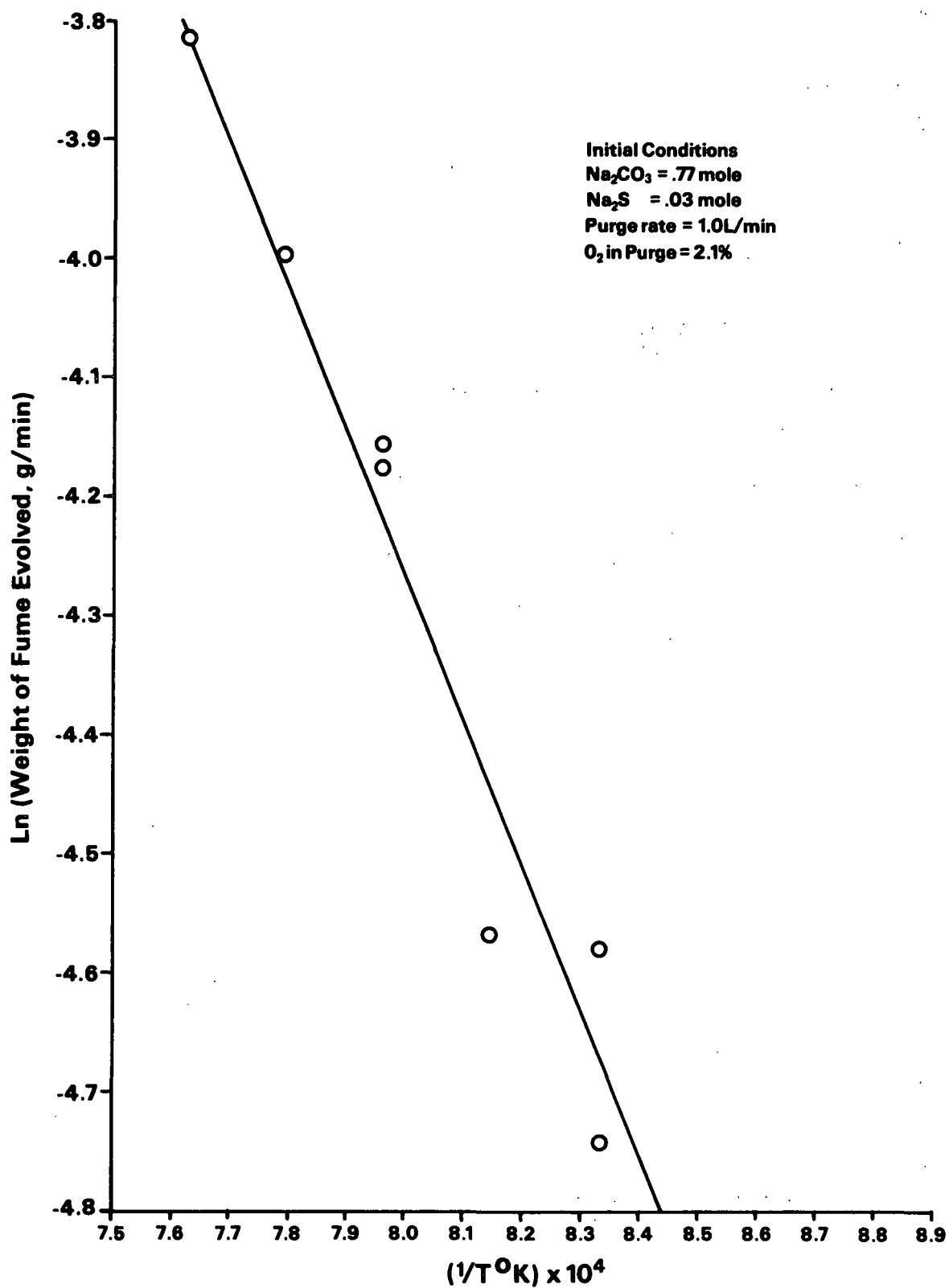


Figure 4. Effect of temperature on fume generation.

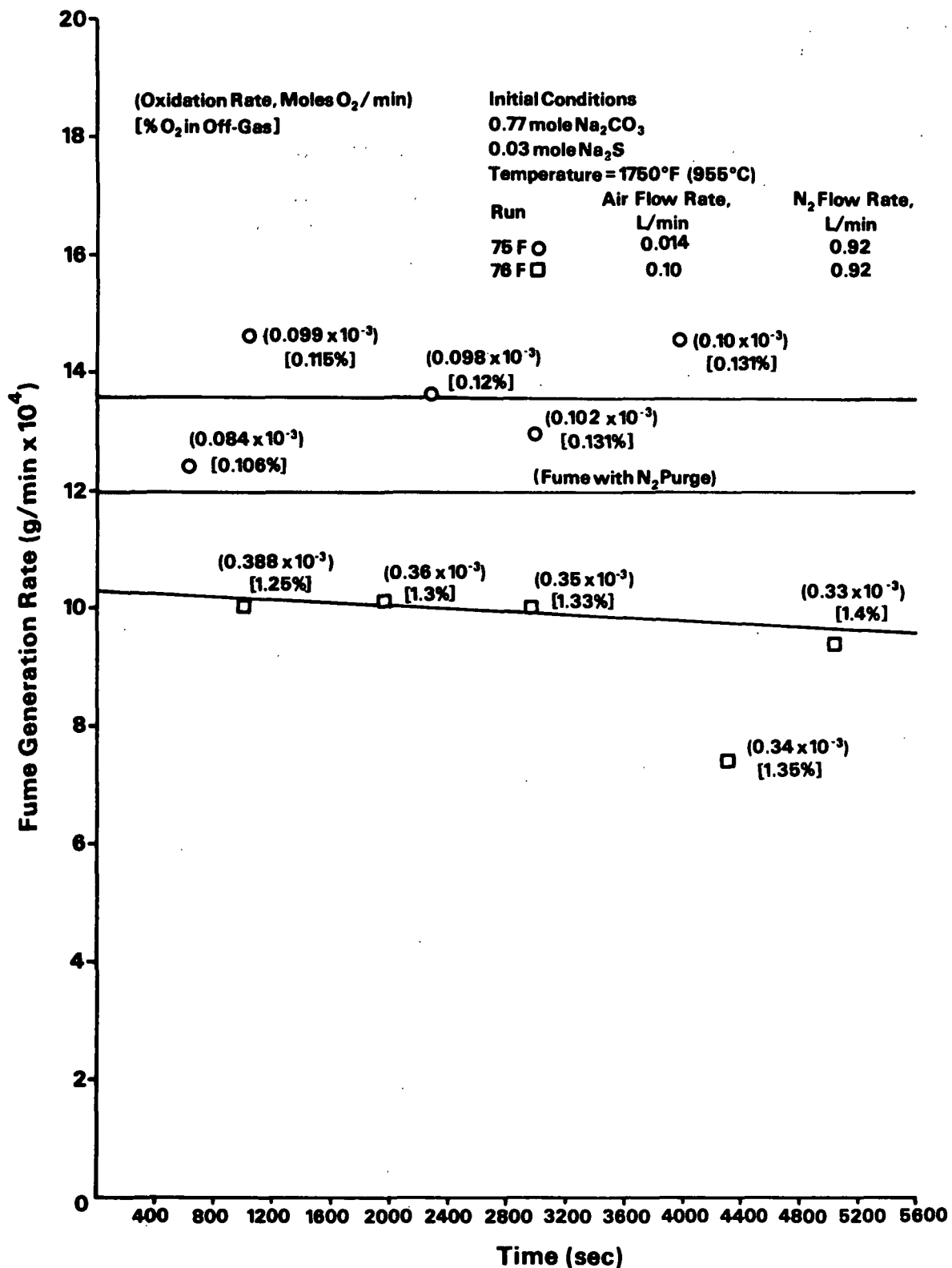


Figure 5. Effect of oxygen on fume generation with purge introduced above melt at low oxygen levels.

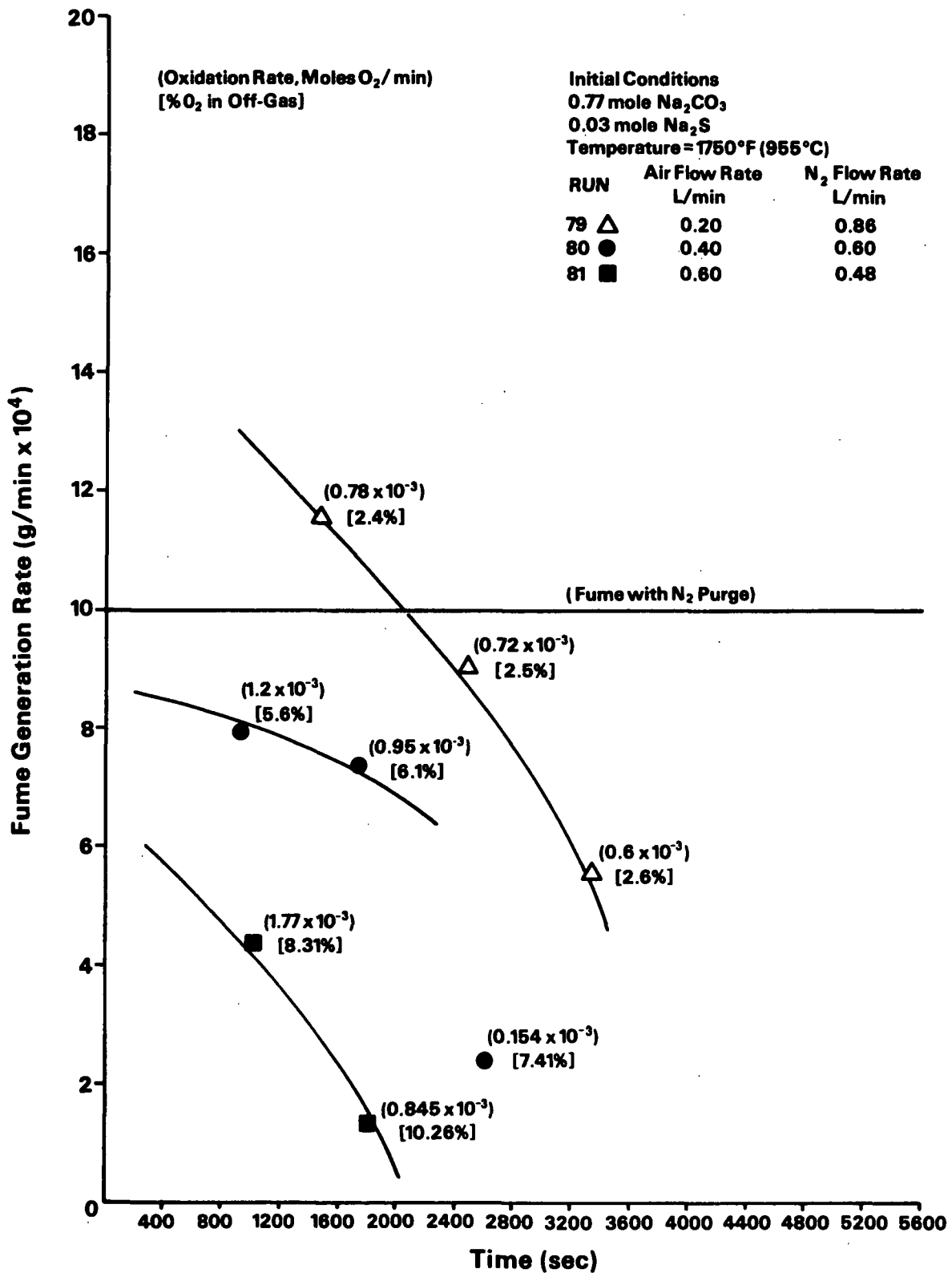


Figure 6. Effect of oxygen on fume generation with purge introduced above melt at high oxygen levels.

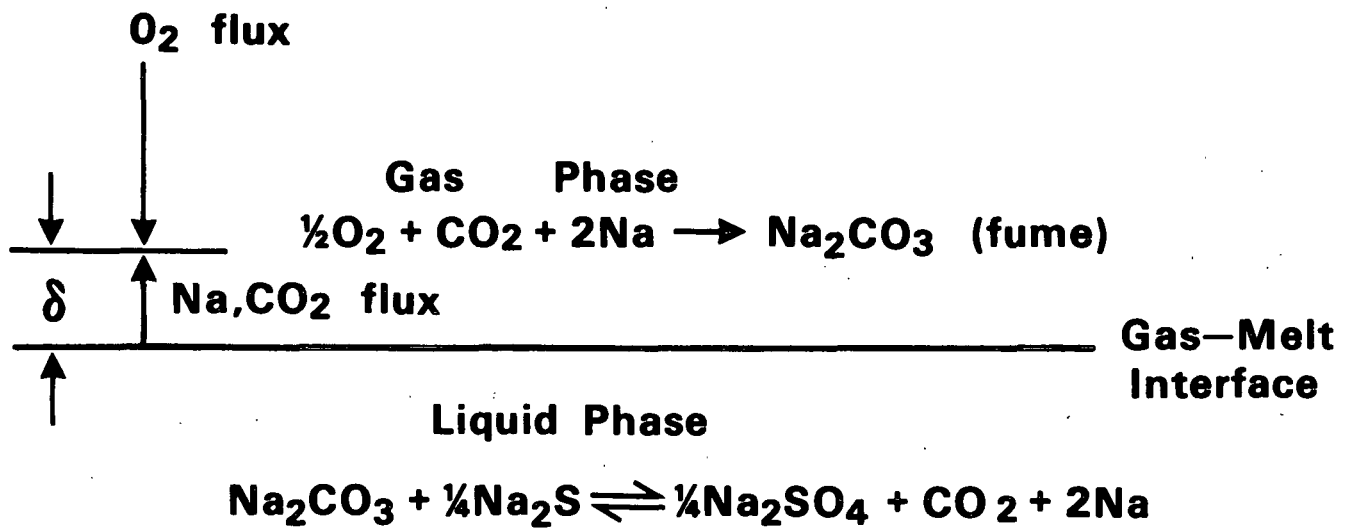


Figure 7. Fume generation under oxidizing conditions.

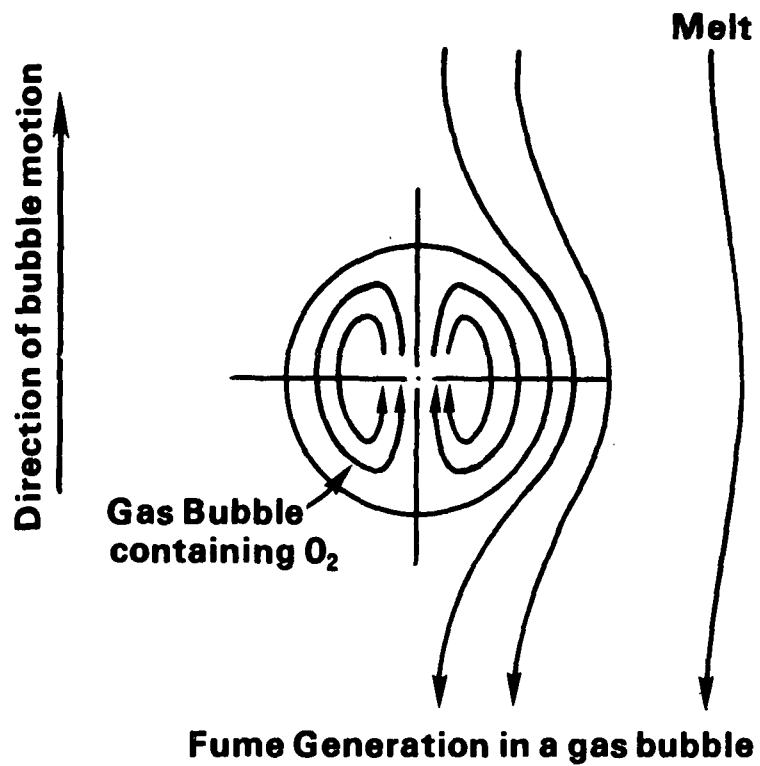


Figure 8. Fume generation in a rising gas bubble.

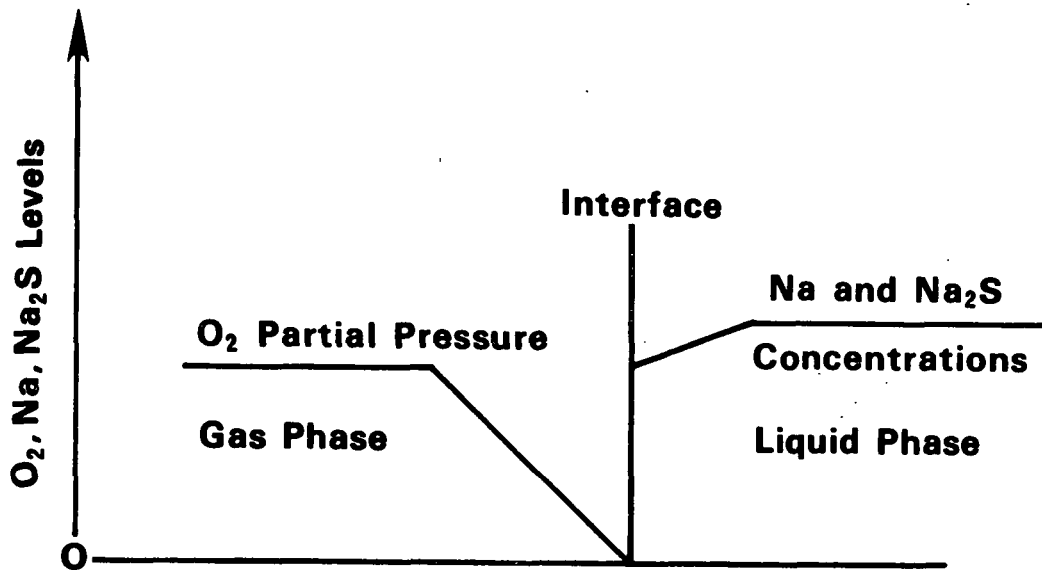


Figure 9. Relative levels of O₂, Na, and Na₂S at bubble interface during sulfide oxidation.

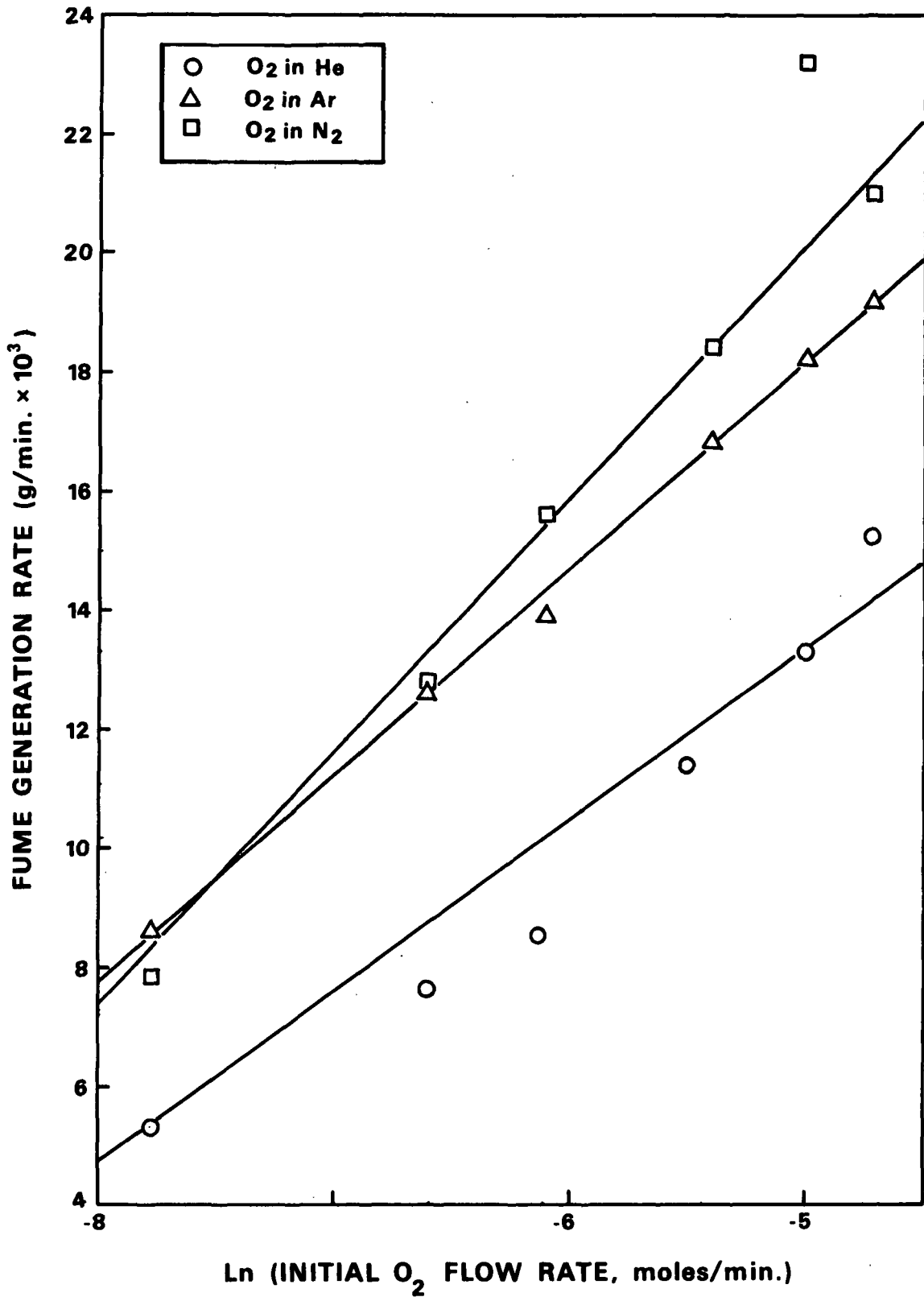


Figure 10. Effect of O₂ on fume generation in N₂, Ar, and He.

ATTACHMENT NUMBER 2

A KINETIC STUDY OF KRAFT CHAR GASIFICATION WITH CO₂

Kristin A. Goerg

Ph.D. Candidate

and

John H. Cameron

Associate Professor

The Institute of Paper Chemistry, Appleton, WI 54912

INTRODUCTION

Part of the burning of kraft black liquor in a recovery furnace is accomplished through a gasification reaction with carbon dioxide. This reaction occurs in a molten salt environment. Due to the high temperature, heterogeneity, and corrosive nature of the material in the char bed, knowledge of the gasification reactions occurring in the kraft recovery furnace is incomplete. Knowledge of the rate of black liquor char gasification will lead to a better understanding of the processes occurring in the char bed.

In this paper, the results of a kinetic study of carbon oxidation with carbon dioxide are presented. The objectives of this study are to determine the controlling parameters for this reaction and develop a rate expression that can be used to determine the relative importance of this reaction.

Although a considerable amount of data has been obtained for this gasification reaction with other forms of carbon, there is little information available for the reaction with kraft char. Because of the high inorganic content of the kraft char, the kinetics of this reaction may be different than the kinetics for other forms of carbon.

PREVIOUS RESEARCH

Many mechanistic studies of the carbon-carbon dioxide reaction have been reported, which

give rise to a variety of rate equations. The simplest mathematical model for a gas-solid reaction was developed by Langmuir. The expression is

$$\text{Rate} = \frac{k_1 C}{1 + k_2 C} \quad (1)$$

C = local gas concentration

Carbon gasification with CO₂ is believed to occur through the adsorption of CO₂ at an active site on the carbon surface, and by desorption of CO. Both adsorption and desorption can occur via a single site or dual site mechanism. This active site theory presumes a surface coverage less than a complete monomolecular layer (1). The Langmuir expression, however, is not adequate for large variations in temperature and pressure.

Ergun *et al.* (1) and Yamouchi and Mukaibo (2) reported a rate equation of

$$\text{Rate} = \frac{k_1 [\text{CO}_2]}{1 + k_2 [\text{CO}_2] + k_3 [\text{CO}]} \quad (2)$$

which is the most widely accepted form. This adequately describes the CO₂ action and the CO inhibition for the overall reaction over ideal carbon surfaces.

Temkin *et al.* (2) claimed that the overall rate of reaction with CO₂ can be expressed by the equation

$$\text{Rate} = k_1 \left[\frac{[\text{CO}_2]}{1 + k_2 [\text{CO}]} \right]^{1/2} \quad (3)$$

In contrast to this equation, Blackwood (2) found that when nuclear-grade graphite was gasified in CO₂ at temperatures between 650 and 870 C and pressures from 1 to 30 atm, the results could be represented by the equation

$$\text{Rate} = \frac{k_1 [\text{CO}_2]}{1 + k_2 [\text{CO}]} \quad (4)$$

Coal chars that were produced at low temperatures, when gasified under similar conditions, give a very high rate of reaction. For these chars, an equation of the type

$$\text{Rate} = \frac{k_1 [\text{CO}_2] + k_4 [\text{CO}_2]^2}{1 + k_2 [\text{CO}] + k_3 [\text{CO}_2]} \quad (5)$$

was suggested by Blackwood and Ingeme (1,2).

Hedden and Lowe (2) gasified nuclear graphite in CO₂ at a partial pressure of 0.1-1.0 atm and found that Eq. (2) held only when the CO/CO₂ ratio was greater than 0.5; otherwise, the results were fitted better by the equation

$$\text{Rate} = \frac{k_1 [\text{CO}_2]}{1 + k_2 [\text{CO}]^{1/2} + k_3 [\text{CO}_2]} \quad (6)$$

Although activation energies for different forms of carbon vary, most authors (1,2) have obtained activation energies between 80 and 90 kcal/mole. Many workers have used carbons of unknown purity and obtained low activation energies because of these impurities. The activation energy for impure carbons is an average of 25 kcal/mole lower than for pure carbons. In kraft char, these impurities are inorganic salts.

The influence of different forms of mass transfer resistance on the gasification of char was studied by Li and van Heiningen (3). A heterogeneous system of black liquor char contained in a reactor vessel was used in their experiments. It was found that external mass transfer resistance is negligible in the gasification of char by carbon dioxide.

The external mass transfer resistance was determined to be only 4-10% of the total mass transfer resistance.

EXPERIMENTAL SYSTEM

The experimental system used to study kraft char gasification with carbon dioxide is shown in Figure 1. To contain the molten sodium carbonate and char, ceramic alumina crucibles (4.13 x 10⁻² m diameter, 1.05 x 10⁻¹ m height) were used. The crucible was contained in a stainless steel retort, which was placed inside the heating coils of an induction furnace. Figure 2 is a schematic of the crucible-retort-coil design.

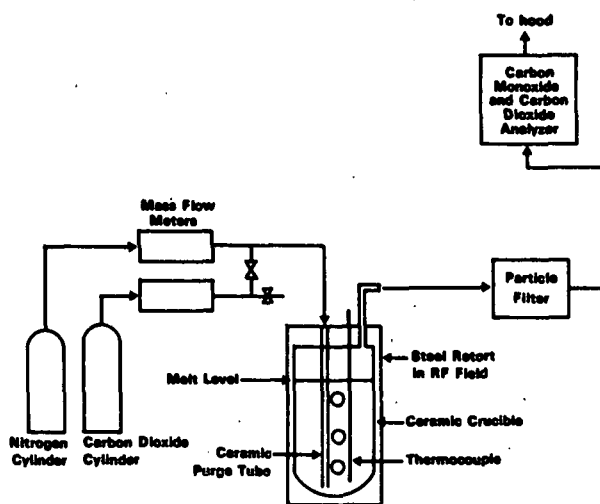


Figure 1. Schematic of experimental system used to study carbon dioxide oxidation of kraft char.

To measure the volumetric flow rate of nitrogen to the reactor, nitrogen was metered from a pressurized gas cylinder through a dry gas meter. A mercury manometer connected to the purge line served as a safety valve. The carbon dioxide was obtained and metered in the same manner. The carbon dioxide entered the nitrogen purge line before reaching the reactor to insure mixing of the two streams. The gases then flowed into the crucible by means of a 4.8 x 10⁻³ m inside diameter ceramic purge tube, which extended into the molten salts and caused mixing of the reactants. The open end of the purge tube was located as close to the bottom of the crucible as possible to try to obtain the most mixing. The temperature was monitored using a nickel-chromium *vs.* nickel-aluminum thermocouple.

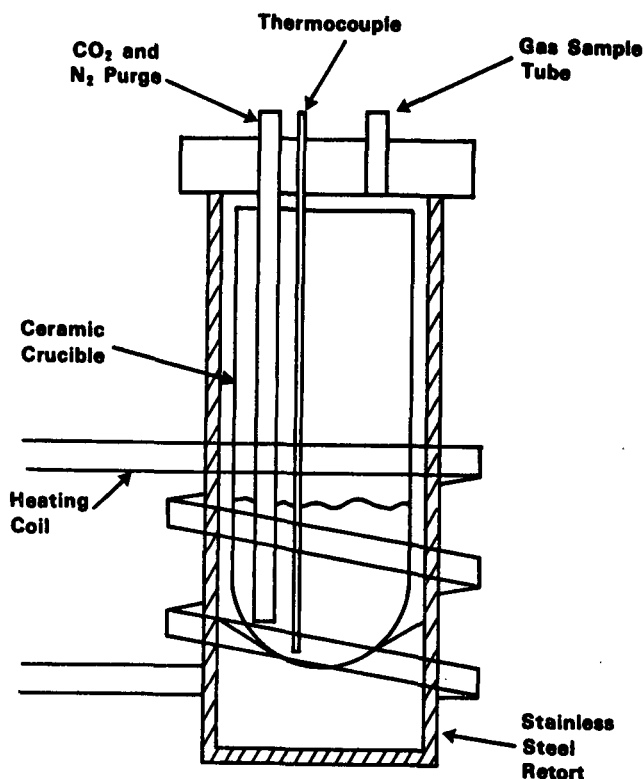


Figure 2. Experimental reactor used to study kraft char oxidation with carbon dioxide.

The gasification rate of reaction was followed by measuring the evolution of CO which was removed from the reactor (along with the N₂ and excess CO₂) through a 4.8 x 10⁻³ m inner diameter steel tube. These gases were passed through an infrared gas analyzer which was capable of simultaneously measuring the carbon dioxide level and carbon monoxide level in the off-gases. The analyzer was calibrated using a standard nitrogen, carbon monoxide, carbon dioxide mixture before each run and checked for drift afterward. The off-gases were vented to the hood after being analyzed for CO and CO₂ composition.

EXPERIMENTAL PROCEDURE

In most gasification runs, 0.77 mole anhydrous granular sodium carbonate and 0.024 mole carbon (1.0 g char at 28.8% carbon) were used. These reactants were mixed before being placed into the crucible.

The crucible, contained in the induction furnace, was slowly brought to the reaction

temperature. During this heat-up period, nitrogen was continually purged through the system. The nitrogen flow rate was kept low enough to prevent the char from flying out of the crucible.

After the crucible temperature was stabilized at the reaction temperature, the nitrogen purge rate was increased. Once the system was stabilized with this new flow rate, the carbon dioxide was introduced into the system. The run was continued until the reaction rate no longer was rapidly decreasing or had leveled off.

EXPERIMENTAL RESULTS

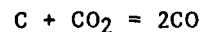
Determination of Char Content

The organic content of the char was determined by reacting one gram of char with air. The organic carbon was defined as the carbon present in the char that is not in the form of carbonate. All the organic carbon was assumed to be converted into CO or CO₂, and the reaction was considered to be complete when the CO and CO₂ content of the off-gas dropped to zero. The carbon content of the char was found to be 28.8 ± 0.9%

Before proceeding to the gasification runs, the char was finely ground. The size distribution of this char was:

Particle Size, μm	% by Weight Greater Than
125	52.7
60	70.6
45	76.6
30	87.9
20	93.1
0	100.0

The stoichiometric equation describing the gasification of kraft char by CO₂ is



Two moles of carbon monoxide are generated for every mole of carbon oxidized.

The char/molten salt mixture was considered to be in equilibrium with the gases above the melt during gasification. Therefore, when analyzing the data with respect to the partial pressure of CO₂ and CO, the concentration of the gases in the product stream was used as the concentration of these gases during reaction.

Effect of Carbon Concentration

To determine the effect of carbon concentration on carbon dioxide oxidation of char, the initial carbon concentration was varied. An increase in the amount of initial carbon produced an increase in the reaction rate. The effect of carbon concentration on the rate of gasification is shown in Figure 3.

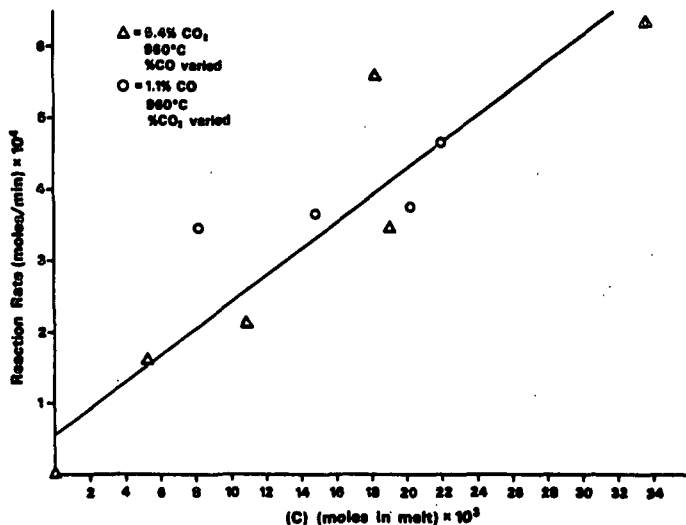


Figure 3. Effect of carbon concentration on reaction rate.

If a plot of $\ln(r)$ vs. $\ln[C]$ is made, the slope of the line is 0.65. This suggests that the rate of reaction is less than first-order in carbon concentration. This may be due to the inhibiting effect of carbon monoxide, since CO concentration increased as the carbon content was increased.

Assuming the rate-limiting step for this reaction occurs on the carbon surface and the reaction is not diffusion limited, the rate of reaction should be first order in carbon concentration. Since the effects of changes in gas concentration within the system could not be separated from the carbon effect, the method of plotting $\ln(r)$ vs $\ln[C]$ does not give an accurate result. It was assumed that the reaction rate is actually first-order in carbon concentration, and this assumption was used for the remainder of this analysis.

Temperature Effects

To determine the effect of temperature on the reaction rate, the char oxidation was studied over the temperature range of 1200-1283 K.

Figure 4 is a plot of reaction rate vs. reaction temperature, showing that the rate of reaction increases as the temperature increases. Since it was not possible to separate the CO and CO₂ effects from the temperature effects, no accurate activation energy could be graphically determined.

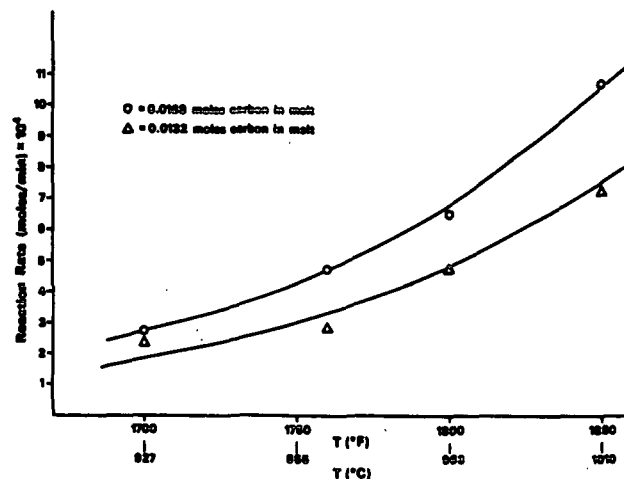


Figure 4. Effect of temperature on reaction rate.

Effect of Carbon Dioxide Partial Pressure

The effect of carbon dioxide concentration on the rate of gasification is illustrated in Figure 5. The carbon dioxide concentration varied from 1-10%. Figure 5 shows that as the concentration of carbon dioxide increases, the rate of reaction also increases. The carbon monoxide concentration could not be held constant as the carbon dioxide concentration was varied - varying one concentration automatically changed the other. The carbon monoxide concentration varied from 0.4-4.1%. It was therefore impossible to graphically determine the order of the gasification reaction with respect to carbon dioxide partial pressure.

Effect of CO Partial Pressure

The effect of carbon monoxide on the rate of reaction is shown in Figure 6. The CO concentration in the system was changed by using standard N₂, CO, CO₂ calibration gases as the reaction gas instead of using only CO₂ and a N₂ purge. The values for this plot were chosen to keep the CO₂ concentration constant at 5%. Figure 6 shows that as the percentage of carbon monoxide is increased, the rate of reaction decreases significantly. With 5% CO in the

system, the reaction rate is approximately four times slower than with 1% CO present. Therefore, the presence of carbon monoxide suppresses the gasification reaction.

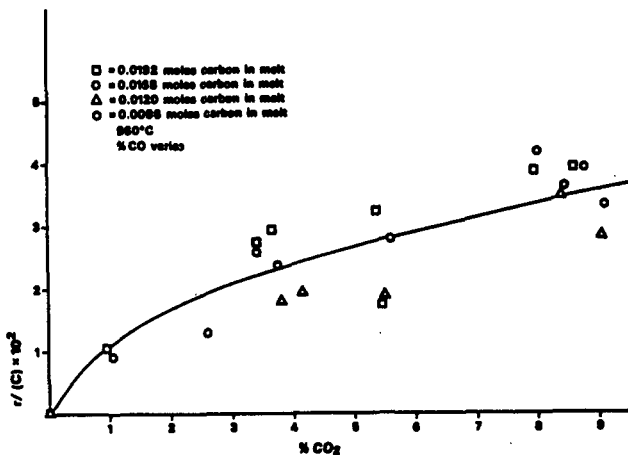


Figure 5. Effect of carbon dioxide concentration on reaction rate.

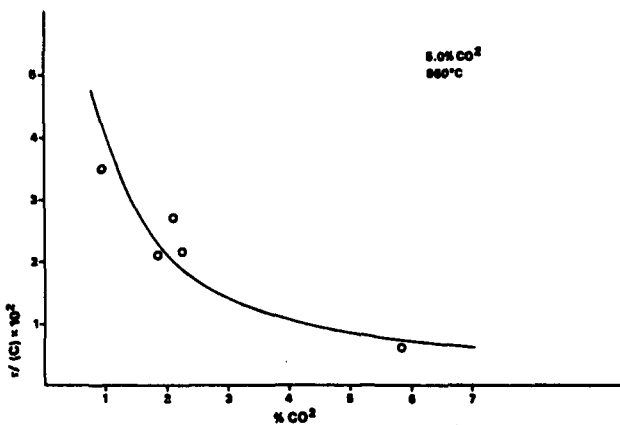


Figure 6. Effect of carbon monoxide concentration on reaction rate.

Mass Transfer Effects

In order to determine if any mass transfer limitations are present during the gasification reaction, the total gas flow rate was changed. The results from these runs were compared to the previous results and are shown in Figure 7. In this plot, the curve is the same curve as in Figure 5. The added values are from the other flow rates.

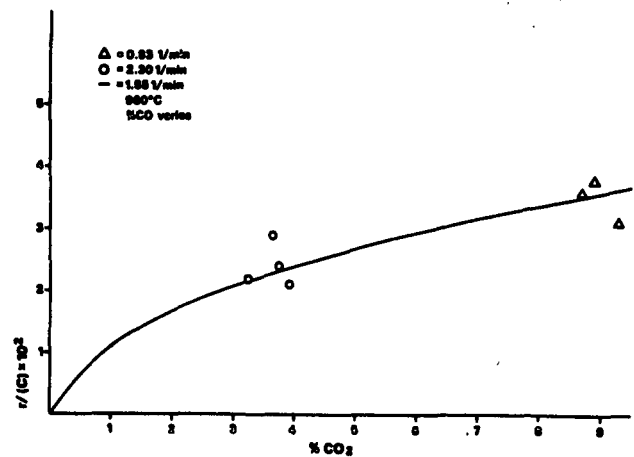


Figure 7. Effect of gas flow rate on reaction rate.

No significant difference in the gasification rate was observed. Therefore, external mass transfer limitations can be considered insignificant during the gasification reaction. The lack of flow rate effects and the high activation energy indicate that oxidation is controlled by kinetic rather than mass transfer effects.

KINETIC MODEL

The gasification reaction of the carbon content of kraft char with CO₂ is believed to occur through the adsorption of CO₂ on an active carbon site. This reaction is first-order in carbon and proportional to the CO₂ level at low CO₂ partial pressure. It is less than first order at higher CO₂ levels and is suppressed by CO. These results indicate that this reaction can be described by the following rate expression

$$\frac{d[C]}{dt} = - \frac{k_1 [PCO_2] [C]}{1 + k_2 [PCO_2] + k_3 [PCO]} e^{-\Delta E/RT} \quad (7)$$

- d[C]/dt is the rate of change of carbon concentration
- [C] is the carbon concentration
- [PCO₂] is the partial pressure of carbon dioxide
- [PCO] is the partial pressure of carbon monoxide
- ΔE is the activation energy
- T is absolute temperature
- R is the gas constant
- k₁, k₂, k₃ are constants

The effect of the four parameters - temperature, carbon concentration, CO₂ partial pressure, and CO partial pressure - was then determined by using a nonlinear regression analysis program (4). This program calculated the four kinetic parameters (k_1 , k_2 , k_3 , and ΔE) found in Eq. (7). The values of these parameters are listed in Table 1.

Table 1. Parameters describing kraft char oxidation with carbon dioxide for Eq. (7).

$$\frac{d[C]}{dt} = - \frac{k_1 [PCO_2] [C]}{1 + k_2 [PCO_2] + k_3 [PCO]} e^{-\Delta E/RT}$$

Parameters	Value	Estimate of Standard Deviation
k_1	6.260×10^9 (atm min) ⁻¹	1.823×10^9 (atm min) ⁻¹
k_2	28.99 atm ⁻¹	8.11 atm ⁻¹
k_3	45.6 atm ⁻¹	13.4 atm ⁻¹
ΔE	54300 cal/mole	2250 cal/mole

The ability of this rate expression to describe the reaction is illustrated in Figure 8. Here, the model is shown by the solid line and the circles indicate the experimental data. Although this is only one data set, all other data sets show similar results.

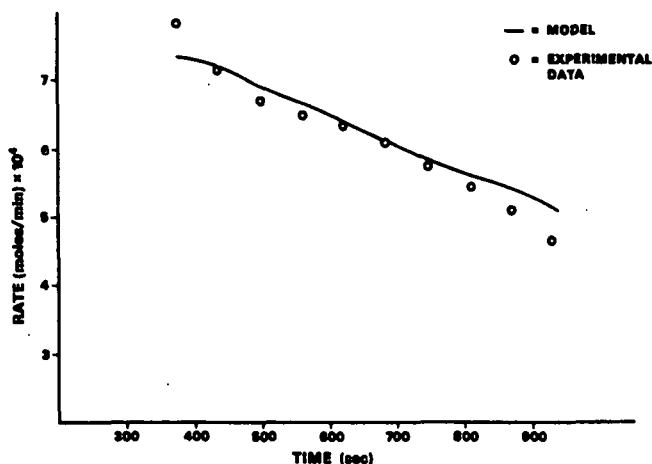


Figure 8. Comparison of kinetic model and experimental data.

This rate expression shows a good correlation with the experimental data. As the CO partial pressure increases, the experimental data indicate that the reaction rate decreases as shown in Figure 6. The data also indicate that the rate of reaction begins to level off as the CO₂ partial pressure increases. This was shown in Figure 5. At low levels of both CO and CO₂ partial pressure, the reaction rate is proportional to the CO₂ partial pressure. This rate expression agrees with the experimental results.

DISCUSSION

Carbon oxidation of kraft char was found to be dependent on carbon concentration, carbon dioxide partial pressure, and carbon monoxide partial pressure, and was found to have a high activation energy. To determine if this reaction is mass transfer or kinetically limited, the effect of different gas flow rates was studied. This was found to have no effect on the oxidation rate. This result, together with the high activation energy, indicates that the reaction is kinetically controlled rather than mass transfer controlled.

LITERATURE CITED

1. Laurendeau, N. M. Heterogeneous kinetics of coal char gasification and combustion. *Prog. Energy Combust. Sci.* (4), 221-268 (1978).
2. Blackman, L. C. F. *Modern aspects of graphite technology*, Academic Press, New York, 1970:158-168.
3. Li, J., van Heiningen, A. R. P. Mass transfer limitations in gasification of black liquor char by CO₂. *TAPPI Proceedings: 1985 International Chemical Recovery*, 459-464.
4. Dye, J. L., Nicely, V. A., *J. Chem. Education* (48), 443 (1971).

Status Report

FUNDAMENTAL PROCESSES IN ALKALI RECOVERY FURNACES

Black Liquor Burning

INTRODUCTION

NEED

There are three main objectives of the kraft chemical recovery cycle. First, to recover and convert spent pulping chemicals into a usable form. Second, to produce the maximum amount of high level energy (steam and electricity) for use throughout the mill. Third, to safely and efficiently process black liquor at solids flow rates at or above equivalent pulping production rates.

The high capital intensity of chemical recovery boilers often results in mill production being limited by the recovery boiler, i.e., the recovery boiler is the pulp mill production bottleneck. Under these circumstances a compromise in objectives must be made. At the present time, situations such as the one above must be made with only limited supporting data on the burning characteristics of black liquor. The present task will document a wide range of black liquor burning phenomena. The resultant data base and supporting interpretation should contribute to improved recovery boiler firing practices. In addition, extreme conditions such as severe blackouts and pluggage of convective gas passages shut the recovery boiler down regardless of other priorities. These emergency situations are influenced by black liquor burning characteristics.

OBJECTIVE

The objective of this task is to characterize black liquor burning. The burning phenomena will be observed and documented. A battery of analytical

and process related tests will be used and/or developed for this purpose. Finally, the black liquors studied will be a wide variety of mill liquors plus a few synthetic liquors.

BACKGROUND

The burning characteristics of black liquor at a particular mill can significantly vary. The ratio of hardwood to softwood or the ratio of semi-chemical liquor to kraft liquor are two variables that reportedly influence burning. The most extensive published burning characteristic study to date has been by Hupa (1985). Hupa divides combustion into four stages: drying, combustion of volatiles, char burning, and inorganic reactions. He has shown that the required time for the first three stages varies significantly with initial droplet diameter, liquor type, and initial gas temperature. The char burning stage was the critical one for distinguishing "good" and "bad" burning liquors. Hupa found that increased liquor swelling during formation of volatiles tended to decrease char burning time, i.e., more "good" burning. Increased levels of Na_2SO_4 , tall oil, and decreasing pH were all shown to negatively influence swelling.

At the beginning of 1984 the IPC chemical recovery group began to study the various stages of black liquor droplet burning. Fundamental studies with synthetic black liquors and characterization work on numerous mill black liquors have been done to date. Sufficient test data and preliminary analyses are available now to form a foundation for quantitative models of black liquor droplet burning. Future test work in this area will require a close intertie with model formulation. The remainder of the report summarizes our progress to date.

FUNDAMENTAL STUDIES

Char burning, the third burning stage, was previously singled out for extensive study (Grace, 1985). There was little known on the influence of the first two stages on char burning. Moreland (1985) studied the influence of water on black liquor combustion. A copy of a paper based on his work is attached. He focused on the influence of initial water content on char reactivity. Lower solids samples (< 75%) bubbled, swelled, and then rapidly burned. Higher solids samples (> 85%) did not bubble, but swelled and burned in a similar manner. The resultant char maximum reactivity declined (\approx 25%) as the initial solids content increased from 75 to 95%. The data also suggest that the decline occurs as a step change at 80% solids rather than as a uniform decrease. A peripheral result, although a very important one, was that regardless of the solids content significant swelling occurred in the volatiles burning stage.

Paul Miller, in an IPC Ph.D. thesis (1986), studied the influence of both physical and chemical variables on black liquor swelling during pyrolysis. The most significant variables affecting swelling were initial liquor solids content, temperature, the ratio of kraft lignin to hydroxy acids, and the extractives content. These variables in some way influence the rheology of pyrolyzing liquor solids so that, as pyrolysis gases escape, chars with different swollen volumes remain. The good swelling chars have a mosaic pattern of paper-thin cells forming an expanded surface. Chemical characteristics consistent with high swelling were low molecular weight lignin in combination with sugar acids, char contents with enriched carboxyl/aromatic ratios, and low initial levels of extractives. Both lignin and sugar acids were essential to maximize swelling. The sugar acid decomposition produces the initial gases. The lignin provides the plasticity to contain the gases as the bubble grows. Miller (1986) found

that 50/50 levels of these two maximized swelling. Copies of two recently released papers are attached which detail this work.

During the volatiles burning stage and particle expansion a significant amount of sulfur is lost. Sulfur release and/or retention is an important burning phenomenon. Brink (1970) showed that sulfur release was dependent on temperature. Sulfur release was lowest in his work for high temperature $> 750^{\circ}\text{C}$ ($> 1380^{\circ}\text{F}$). James Cantrell (1986) recently completed an MS thesis (research work at IPC with degree from Georgia Tech.) in the sulfur release area. The majority of his work was done with a radiant furnace in an air environment at 1090°C (1994°F). Significant sulfur release ($> 60\%$) could be attained with small particle sizes ($< 2\text{ mm}$) and low solids contents ($< 63\%$). Particle sizes above 4 mm and solids contents above 70% showed sulfur release percentages of nominally 10% . Cantrell was not able to observe the burning particles, so sulfur release could not be related to swelling. A summary paper of his work is attached. The sulfur release study is a subject of continuing interest. Frank Harper is preparing a Ph.D. thesis proposal in this area at the present time.

Katherine Crane (1986) studied the volatiles burning rate of black liquor droplets as a function of gas-phase oxygen content, particle size, and gas temperature. Her work in the convective single particle reactor was with a 71.8% solids content black liquor at temperatures from $666\text{--}860^{\circ}\text{C}$ ($1230\text{--}1580^{\circ}\text{F}$). The normalized burning rate only slightly increased over the entire O_2 range ($0\text{--}21\%$) for particles above 3 mm . However for smaller particles, the gas-phase O_2 content did affect the burning rate. The rate continually increased from $0\% \text{ O}_2$ to $10\% \text{ O}_2$. At $10\% \text{ O}_2$ the rate for a 2.5 mm particle was nominally twice that of a 3.1 mm particle. Above $10\% \text{ O}_2$ the rate remained relatively constant for the 2.5 mm particle.

Several insights can be drawn from Crane's work. First, the volatiles burning stage for large (> 3 mm) particles is not strongly dependent on the gas-phase oxygen content. The implication is that gas-phase diffusion of O_2 to the surface and/or straightforward reaction rates proportional to the O_2 content are not the rate limiting step. Second, for all particle sizes the above implication holds true for O_2 levels above 10%. Third, below 10% O_2 and particle sizes below 3 mm there is a significant increase in the normalized volatiles burning rate with an increase in the gas-phase O_2 content. Gas-phase diffusion and/or reaction rates appear to be the rate limiting step. A publication detailing this work will be prepared by the Spring PAC meeting. Crane continued to work in this area last summer. This fall she is preparing a Ph.D. thesis proposal in the area of black liquor droplet burning.

SURVEY STUDIES

Black liquor compositional variations were observed to influence swelling in the IPC fundamental studies. Hupa (1985) showed that composition would also influence burning. A bridge was required between the laboratory and mill liquors. A program was set up to obtain and test mill liquors in the IPC chemical recovery laboratory. The intent of the test data was to

1. Define the range of chemical analyses and burning phenomena of interest
2. Identify significant compositional influences on the burning behavior
3. Suggest the direction for future test and model work.

A tremendous amount of data have been obtained in this effort. Some significant results have been obtained. More will come in the future. The status of this work is described below.

LIQUOR SAMPLES

Black liquor grab samples were collected by mill-operating or technical personnel. The guidelines given to the mills by IPC were

- a. The pulp mill and recovery system should be in a relatively stable operating condition.
- b. The collection point should be either after the concentrator for a low odor design or before the cascade/cyclone evaporator in a direct contact design. In either case it should be before salt cake recycle addition. Note: not all samples met this criteria.
- c. One quart of liquor per sample should be submitted.
- d. A completed questionnaire was to be returned with each sample. This listed general pulp mill conditions and a qualitative assessment of how well the liquor burns.

There were some cases where not all of the guidelines were met.

Several mills sent more than one liquor sample. Many times in these cases the samples represented different ratios of hardwood liquor to softwood liquor. When the samples arrived at IPC they were placed in an 8°C (46°F) cold room. Some liquors required evaporation if their received solids content was less than 65% or droplets of the liquor would not cling to the suspension hook.

ANALYSES

Liquor analyses were divided into three groups. These are listed below.

Process measures

- a. High heating value
- b. Sulfated ash
- c. Residual active alkali

Composition measures

- a. NaOH
- b. Na₂S
- c. Na₂CO₃
- d. Na₂SO₄
- e. Solids content

Elemental analyses

- | | |
|-------|------|
| a. Na | e. C |
| b. K | f. H |
| c. S | g. O |
| d. Cl | |

Tall oil was measured on six samples. An attempt will be made to recover the Na₂S₂O₃ and Na₂SO₃ data for prior ion chromatograph charts. With the exception of the elemental analysis for C, H, and O, all measurements are made by IPC Analytical. The C, H, and O measurements were done only on selected samples. These were determined by Huffman Laboratories, Wheatridge, Colorado. Test procedures and results of screening are listed in Appendix I.

COMBUSTION TESTS

Combustion tests were performed on liquor aliquots which were between 62 and 76% solids content. A summary for the solids method used is given in Appendix I. The combustion tests performed with the liquors were developed at IPC. These are listed below.

- a. Pyrolysis swollen volume
- b. Combustion swollen volume
- c. Pyrolysis normalized rate
- d. Combustion normalized rate
- e. Time to ignition
- f. Time from ignition to maximum swollen volume
- g. Time from ignition to smelt bead

Appendix II contains a description of each one of these tests. All questionnaire and test data are stored in a data base spreadsheet for easy access, analysis, and expansion.

COMBUSTION TEST EQUIPMENT

The IPC single particle reactor (SPR) was used for most of the combustion tests. Figure 1 is a cross section of the SPR.

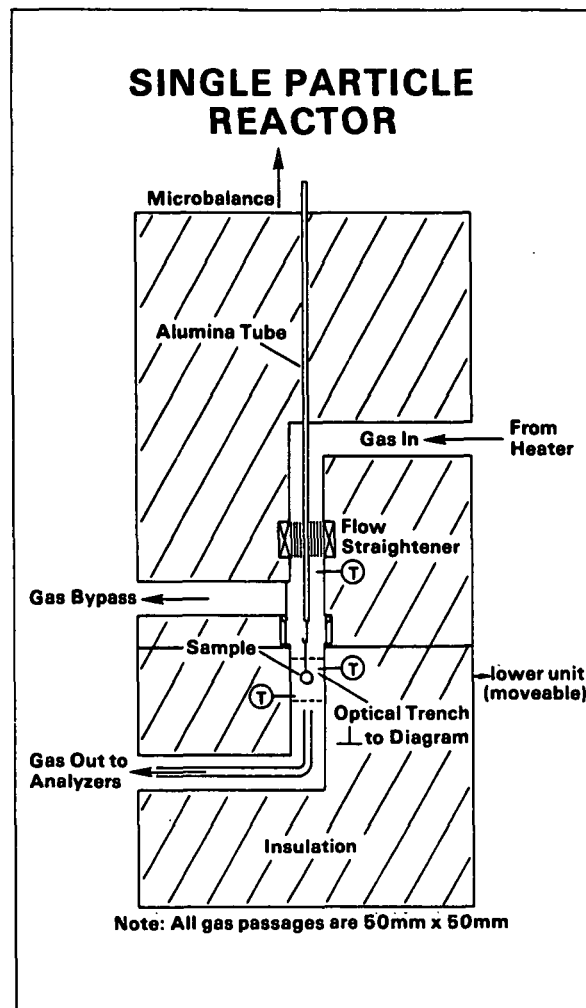


Figure 1. Gravimetric-convective single particle reactor (SPR).

The reactor convectively heats the particles in a hot gas stream. The maximum gas temperature in the particle zone is 900°C (1650°F). Dampening and a pneumatically positioned lower reactor zone enables rapid heating of the particle to the gas temperature. Heat flux measurements during water evaporation show fluxes up to 95 kW/m² (30,000 Btu/h-ft²). These fluxes are comparable to those measured on wall tubes in a recovery furnace. Infrared pyrometer measurement of the burning particle showed a temperature of 1150°C (2100°F). Periodically the holding wire for the liquor also burns through. Its melting point is 1340°C (2450°F). These temperatures are comparable or slightly higher than those in a recovery furnace. Phenomena occurring in the recovery furnace should be observable in the SPR.

The SPR is equipped with a microbalance for real time mass tracking. A 51 x 51-mm (2 x 2-inch) optical trench allows photographic documentation of the burns. Gas analysis equipment is available for CO, CO₂, SO₂, O₂, H₂O, and Na fume measurements.

RESULTS

Liquor Samples

Fifty four (54) samples were studied in detail. Fifty two (52) are mill samples and two are synthetic liquors. The range of collected liquor sources is shown in Table 1. This completes the mill black liquor sample survey.

The two synthetic kraft liquors were produced by Paul Miller and James Cantrell for their research work. Both used 100% loblolly pine and cooked to a kappa number of about 26.

Table 1. Black liquor source characterization.

Number: 52 mill samples
 2 synthetic samples

Mill locations: 21

Country: U.S. (14, all regions), Canada (3), Brazil (2), Sweden (2)

Wood supply: softwood, hardwood, mixture

Type of mill liquor: kraft (46), soda (1), carbonate-nonsulfur (1),
 NSSC (1), GLSC (2), alkaline sulfite (1)

Digester kappa No.: hardwood 10-19.5
 (kraft only) softwood 21-87.5

Oxidized: yes (11), no (43)

Burning assessment: good to poor

The 54 liquors showed a wide range of results in the analytical analyses and combustion tests. Table 2 shows the variable ranges for liquors collected from kraft mills. The nonkraft and synthetic liquors are not included in this tabulation.

The range of analytical characteristics noted in Table 2 indicates that the survey covered a wide spectrum of liquor types. Table 3 lists the burning variability. It is interesting to note that, with only a few exceptions, all liquors were "reported" as good burning.

The process, composition, and elemental analysis measurement ranges are straightforward. The combustion test measurement ranges warrant some discussion. The pyrolysis swollen volume was much larger and had a wider range than did the combustion swollen volume. Char formation during combustion limits the extent of volume growth. The average combustion swollen volume of 26 cc/g initial solids implies a 26 fold increase in the volume of the initial liquor droplet. This

assumes an initial droplet of 70% solids with density 1.43 cc/g. The corresponding diameter increase is by a factor of almost 3. Black liquors clearly can have different degrees of swelling. The pyrolysis and combustion volumetric swelling ranges span multiples of 25 and 5, respectively.

Table 2. Black liquor survey analytical variables range.. (North American kraft mill samples only, 33) [all values based on oven-dried solids at 105°C (221°F)].

Process Measures	Average \pm 95% CL ^a	Range
a. High heating value, Btu/lb	6010 \pm 125	5190-6890
b. Sulfated ash, % as NaOH	36.7 \pm 0.8	41.8-31.9
c. Residual active alkali, % as Na ₂ O	4.6 \pm 1.1	0-13
Composition Measures		
a. NaOH	3.8 \pm 0.9	0-14.5
b. Na ₂ S	2.3 \pm 0.7	0-6.1
c. Na ₂ CO ₃	8.2 \pm 0.6	3.6-12.5
d. Na ₂ SO ₄	4.0 \pm 0.9	0.7-9.5
Elemental Analysis (% ODS) ^b		
a. Na	190.0 \pm 0.4	17.1-21.0
b. K	2.0 \pm 0.2	1.0-3.1
c. S	4.8 \pm 0.9	3.5-6.8
d. Cl	0.9 \pm 0.4	0.21-5.5
e. C	36.6 \pm 1.1	34.0-40.9
f. H	3.4 \pm 0.2	3.1-4.0
g. O	33.4 \pm 1.8	29.7-35.6

^aCL confidence level of the average.

^bC, H, O analysis only on 17 samples.

Table 3. Black liquor survey combustion variable range
(North American kraft mill samples only 33).

Combustion Tests	Average \pm 95% CL ^a	Range
a. Pyrolysis swollen volume, cc/g initial solids	95 \pm 16	7-172
b. Combustion swollen volume, cc/g initial solids	26 \pm 4	11-53
c. Pyrolysis normalized rate x 100, sec ⁻¹	2.4 \pm 0.3	1.5-4.7
d. Combustion normalized rate x 100, sec ⁻¹ ^b	20 \pm 7	8.5-52.1
e. Time to ignition, sec ^c	1.6 \pm 0.2	0.7-2.4
f. Time from ign to max volume, sec	2.3 \pm 0.2	1.4-4.0
g. Time from ign to smelt bead, sec	4.2 \pm 0.2	3.1-6.0

^aSee Table 2.

^bOnly complete on 14 samples.

^cOnly complete on 17 samples.

The pyrolysis and combustion normalized rates indicate the relative change of mass during approximate linear mass loss regions. The pyrolysis rate is mass loss during pyrolysis at 932°F (500°C) in N₂. The combustion rate is mass loss during the volatiles burning period at 1472°F (800°C) in air. The combustion rate is nominally 8 times faster than the pyrolysis rate. Note that there is substantially lower variation in the pyrolysis rate than in the pyrolysis swollen volume. This suggests that heat transfer rather than kinetics may be the rate limiting step.

The time to ignition is essentially the drying stage. The average drying time under test conditions was 1.6 seconds. The time from ignition to maximum volume is called the volatiles burning stage. The char burning stage is the period between the maximum volume and the smelt bead. Note first that there

is a wide range for both of these times. The average of each is approximately 2 seconds. The average total time for droplet burning is then approximately 6 seconds. These combustion test results undoubtedly change with conditions such as gas-phase oxygen content, particle size, and temperature. There is work underway to quantify these different impacts.

VARIABLES INFLUENCING BURNING

One intended function of the liquor survey data base is to identify the significant variables influencing droplet burning characteristics. The initial attempt to find single variables that explained the variations in each one of the combustion measures failed (PAC report Fall 1985). Prior to any next approach being attempted it became apparent that the swelling process was stochastic in nature. This meant that combustion measurements had to be averages of several tests. From 2 to 4 repeats are required to achieve reasonable measures for each combustion test parameter. The second approach to the data analysis is underway. Not all of the necessary repeat tests are complete to date; however, some significant variables have been identified. The second approach has been to attempt multiple linear regression model fitting of the data. The significant variables would be the independent variables identified in the model.

Pyrolysis swollen volume has been the one measurement most thoroughly tested, i.e., the required number of repeats has been made. When this was the dependent variable in the regression fit of liquors for which all data were available (45 liquors), eight significant independent variables were identified. The regression equation formed was

$$\begin{aligned}
 \text{Pyr Sv (cc/gm solid)} &= 146 \\
 &+ 3.96 (\%, \text{Cl}) \\
 &+ 24.5 (\text{sec}^{-1}, \text{pyrolysis rate X100}) \\
 &- 24.4 (\text{sec}, \text{time from ign. to smelt bead}) \\
 &- 3.37 (\%, \text{Na}_2\text{CO}_3 + \text{Na}_2\text{SO}_4) \\
 &+ 7.00 (\%, \text{Na}_2\text{S}) \\
 &- 0.389 (\%, \text{hardwood}) \\
 &+ 0.342 (\text{kappa number}) \\
 &+ 4.17 (\text{pulping process, arbitrary scale})
 \end{aligned}$$

This equation's $r^2 = 0.80$. Figure 2 demonstrates the agreement between the predicted swollen volume and the measured swollen volume. If there were a perfect fit, all calculated data points would fall on the 45° line.

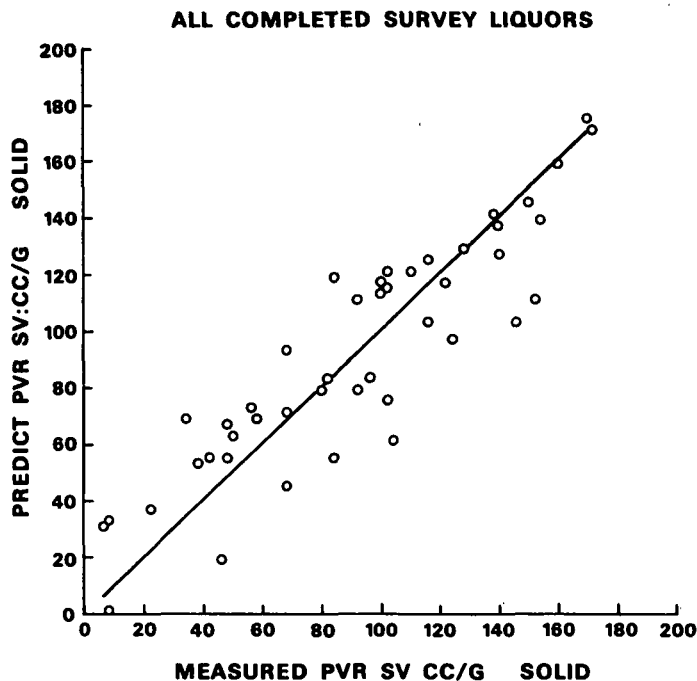


Figure 2. Comparison of eight-variable model prediction with actual data for pyrolysis swollen volume.

A subset of just North American kraft samples was evaluated in a similar manner. In this case five significant independent variables were identified. The regression equation formed was

$$\begin{aligned} \text{Pyr Sv (cc/gm solid)} &= 106 \\ &+ 1.17 (\text{kappa number}) \\ &+ 19.8 (\%, \text{Cl}) \\ &+ 20.0 (\text{sec}^{-1}, \text{pyrolysis rate X100}) \\ &- 4.10 (\%, \text{Na}_2\text{CO}_3 + \text{Na}_2\text{SO}_4) \\ &- 27.3 (\text{sec}, \text{time from ign. to max volume}) \end{aligned}$$

This equation's $r^2 = 0.80$. Figure 3 demonstrates the agreement between the predicted swollen volume and measured swollen volume for these kraft liquors. As one might expect the significant variables for the kraft liquor are a subset of those for all liquors.

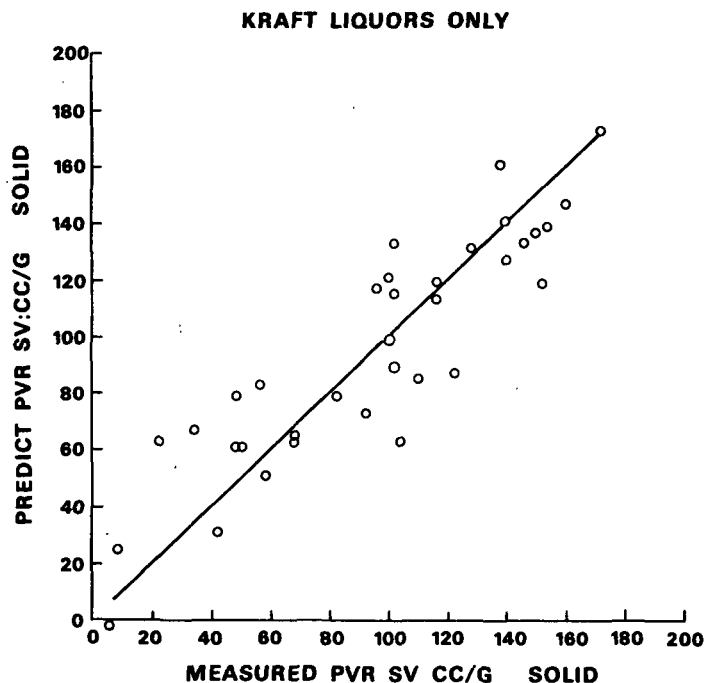


Figure 3. Comparison of five-variable model prediction with actual data for pyrolysis swollen volume.

The most important findings are that pyrolysis swollen volume depends on many compositional variables and it can not be predicted a priori. In both cases two of the variables, pyrolysis rate and a combustion time, were needed in conjunction with analytical measurements to obtain a significant relationship. This supports the contention that the process is stochastic in nature.

Both relationships show that

Pyr Sv increases as - kappa number increases

- liquor Cl content increases

- pyrolysis rate increases

Pyr Sv decreases as - $\text{Na}_2\text{CO}_3 + \text{Na}_2\text{SO}_4$ increases

- burning time increases

For the combined liquor type relationship, hardwood, Na_2S , and the pulping process were also significant variables. It is encouraging to see similarity between some of these variables and the work of Miller (1986). The variation in kappa number effectively changes the ratio of sugar acids to lignin in the black liquor. This had an important impact in Miller's work. The reduction in swollen volume with the addition of sodium salts is also as expected.

Further work in this same direction will be done to identify significant interrelationships with the remaining measurements of the mill survey data set. Now that at least one burning measurement's variation with liquor characteristics has been identified there is hope that others will be identified.

COOPERATIVE STUDY

Dr. Mikko Hupa published the first definitive work on black liquor droplet burning in 1985. He continues to do significant research in this area

with the acquisition of a recent grant from the Finnish government. We have arranged to exchange information, data, and samples for black liquor combustion testing. The letter outlining this agreement is on the next page.

We think that this cooperative work will benefit both parties. Our experimental systems have complementary differences. There are also some differences in test procedure and the definition of the stage transition points that require standardization.

FUTURE DIRECTION

The survey study results, once all the data analysis is complete, at best will identify main combustion variables. In order to advance the fundamental knowledge, more controlled studies are required. These have begun.

Ten kraft cooks have been made by the IPC Pulping Laboratory. Table 4 outlines the conditions. Based on the survey, the primary cooking variables chosen were the kappa number and percent hardwood. The inorganic and extractive components may be added later if necessary. These liquors are presently being evaporated for combustion testing. The test design for this liquor group has not yet been developed.

In-depth studies of droplet drying, sulfur release, and droplet burning rates will be the subject of three Ph.D. theses. Those closely complement the more applied work to date on black liquor droplet burning. Mark Robinson's work on droplet drying should be completed within a year. Frank Harper is just starting on the sulfur release work. Katherine Crane's work on droplet burning rate will expand her MS research project and recent summer work at IPC on a joint IPC/member company project. She is also just starting.

June 12, 1986
Page 2

Dr. Mikko Hupa
Abo Akademi

THE INSTITUTE OF PAPER CHEMISTRY
Post Office Box 1039
Appleton, Wisconsin 54912
Phone: 414/734-9251
Telex: 469289

June 12, 1986

AIR MAIL

Dr. Mikko Hupa
Abo Akademi
Department of Chemical Engineering
SF-20500 Turku
FINLAND

Dear Mikko:

It was a pleasure seeing you again and having you visit IPC for two days. Each time we meet I come away with fresh ideas on experiments to run and ways to look at the problem; I'm sure Dave and John feel the same.

The following is a proposed agreement for formal collaboration between our group and yours for research on black liquor combustion and related areas.

The purpose of the collaboration is to increase the effectiveness of the research on black liquor combustion which each party is currently undertaking.

The collaboration will be mutually beneficial because it will broaden the base of each study and will permit a direct comparison of the differences in burning behavior caused by different experimental techniques.

Specific items which will support this collaboration are as follows.

1. We will exchange liquor samples. Each group will select 6 to 8 liquor samples from their test base and send them to the other. These will be chosen to reflect a wide range of burning behavior and to include any interesting phenomena observed. Along with the samples we will provide:

- a. data on the measured burning characteristics in our own test systems,
 - b. background characterization tests or analyses on each sample,
 - c. as much information as possible on the mill background of the liquor samples.
2. We will exchange selected films of burning tests along with quantitative burning characterizations obtained from these films. The films will be chosen to include the main phenomena each of us has observed.
 3. We will exchange the full data base (quantitative measured burning characteristics and background characterization data) covering all of the other liquors which we are testing. Data on liquor samples obtained from clients for proprietary work would not be included without their express permission.
 4. We will exchange project reports and publications subject to any restrictions of a proprietary nature that might be involved.
 5. We will meet whenever the opportunity presents itself for further exchange of information and ideas.

In any publications which are prepared, we will give full identification and reference to any data or results obtained from the other party. Insofar as possible, publications in the open literature will be jointly authored; joint authorship is the preferred method of publication.

Each group will bear their own costs for any tests performed, samples shipped, etc. No financial exchanges are anticipated during this collaboration.

The formal collaboration will be considered to remain in effect for a two-year period, ending June 30, 1988. A decision on whether to continue a formal collaboration can be made at that time.

I hope you find the above agreement satisfactory. Let me know if there are any problems. Best wishes from all of us.

Very truly yours,



Thomas M. Grace
Group Leader, Recovery
Pulping Sciences
Chemical Sciences Division

1043 East South River Street

Table 4. IPC controlled pulping conditions to generate synthetic black liquors.

Constant Cooking Conditions

16% Effective alkali

25% Sulfidity

12.5% Na₂SO₄ based on Na₂S (as Na₂O)

25% Na₂CO₃ based on NaOH (as Na₂O)

4:1 Liquor:Wood ratio

90 minutes at 173°C (343°F)

Maximum cooking temperature 173°C (343°F)

Ten Liquors Produced

Wood	H-Factor	Kappa Number
Pine	5500	15.0
Pine	1600	32.2
Pine	690	72.7
Birch	1600	16.6
Birch	971	39.0
Birch	160	79.7
P/B 50/50	4000	17.1
P/B 50/50	947	43.5
P/B 50/50	303	96.5
P/B 50/50	971	41.2

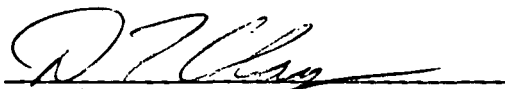
In support of the above research project plus the cooperative project with Hupa a radiant heating section will be added to the single particle reactor. This will decouple gas flow and heat flux.

A clear future need is to assimilate all of this information into a comprehensible model of the burning process. Some of these activities are already underway, running parallel with the experimental effort. More emphasis will be given to the modeling aspect in the future.

REFERENCES

- Brink, D. L.; Thomas, J. F.; Jones, K. A. Malodorous products from the combustion of kraft black liquor. III. A rationale for controlling odors. Tappi 53(5):837(May, 1970).
- Cantrell, J. G. Sulfur gas release during black liquor burning. Georgia Tech./IPC MS thesis (March, 1986).
- Crane, K. A. An empirical model of the volatilization of kraft black liquor droplets during burning. IPC MS, A-190 Research Project (Feb., 1986).
- Grace, T. M.; Cameron, J. H.; Clay, D. T. Char burning Project 3473-1. Summary Technical Report to American Paper Institute Recovery Boiler Committee, The Institute of Paper Chemistry (Feb. 22, 1985).
- Hupa, M.; Solin, P.; Hyöty, P. Combustion behavior of black liquor droplets. 1985 International Chemical Recovery Conference 3:335(April, 1985).
- Miller, P. T. Swelling of kraft black liquor: an understanding of the associated phenomena during pyrolysis. IPC Ph.D. thesis (June, 1986).
- Moreland, B. A.; Clay, D. T. The influence of water on black liquor combustion. IPC MS, A-291 Research Project (March, 1985).

THE INSTITUTE OF PAPER CHEMISTRY



David T. Clay
Associate Professor/Research Associate
Recovery Group
Chemical Sciences Division

APPENDIX I

TEST PROCEDURES

Process Measures

- a. High heating value - essentially TAPPI Test Method T 684 pm-84.
- b. Sulfated ash - TAPPI Test Method T 625 ts-64.
- c. Residual active alkali - TAPPI Test Method T 625 ts-64.

Composition Measures

- a. NaOH - calculated difference between residual active alkali and Na₂S.
- b. Na₂S - NCASI Technical Bulletin No. 68.
- c. Na₂CO₃ - Ion chromatography exclusion.
- d. Na₂SO₄ - TAPPI Test Method T 699 pm-83.
- e. Solids - Surface area extended via ignited sand. Dried at 105°C (221°F) in a forced air convection oven for at least 6 hours, preferably overnight.

Elemental Analyses

- a. Ka - Perchloric acid digestion followed by flame emission.
- b. K - Same as Na.
- c. S - Schoniger flask oxidation followed by TAPPI Test Method T 699 pm-83.
- d. Cl - TAPPI Test Method T 699 pm-83.
- e. C - Measured by Huffmann Laboratories, Wheatridge, Colorado.
- f. H - Same as C.
- g. O - Same as C. Merz modification.

SCREENING OF RESULTS

Process Measures

Tests done in at least duplicate. Values for HHV with standard deviation of 100 or less were accepted. Sulfated ash with standard deviations of less than 1 were accepted. Residual active alkali values have standard deviations of $< \pm 0.2$.

Composition Measures

NaOH was the same as active alkali. Na₂S for the most part was single determination; selected samples were done in duplicate or triplicate. Na₂CO₃ and Na₂SO₄ were single point determinations.

Elemental Analyses

Na and K were single dilutions and at least duplicate aspirations into FE detector. S and Cl were single determinations. C, H, O were duplicate determinations.

APPENDIX II

COMBUSTION TESTS

Pyrolysis Swollen Volume

A black liquor droplet at room temperature and nominally 40 mg (3.8 mm) in total mass is suspended on a wire within a wire spiral. The solids content has been measured. The sample is hung from the Cahn microbalance in the convective SPR (Fig. 1). The reactor is sealed, then 500°C (932°F) N₂ flows over the droplet. Photographs are taken as the droplet swells. The particle maximum volume is determined from the largest area measurement of the photographs. The calculated swollen volume is that of a sphere with the same measured frontal

area. Dividing this volume by the original mass of the droplet solids yields the swollen volume.

Combustion Swollen Volume

A nominal 9 mg (2.3 mm) droplet is burned in air in the convective SPR (Fig. 1). The air temperature is 800°C (1472°F). High speed movies (to be described later) are taken and the frame where the largest volume occurs is blown up. Measurements are then made analogous to the pyrolysis volume measurement.

Pyrolysis Normalized Rate

During the pyrolysis described above the microbalance records the droplet mass loss. The mass loss is approximately linear. The slope of the mass loss vs. time plot divided by the mass of the initial solids is the pyrolysis normalized rate. The wire spiral around the droplet maintains a relatively constant drag despite a changing particle size.

Combustion Normalized Rate

The same procedure described above is done, except in air, with nominally a 9 mg (2.3 mm) droplet and at 800°C (1472°F). The slope of the mass loss vs. time curve is linearized. This is during the volatiles burning stage. The slope divided by the mass of the initial solids is the combustion normalized rate.

Time to Ignition

When the damper opens in the SPR the hot air impinges on the particle. This is time zero. Ignition is the time when the first glow of burning volatiles is seen on the particle. Time to ignition is the difference between these times.

Reaction Time from Ignition to Maximum Volume

During the combustion tests described above medium speed films were taken of the droplet burns. Both color and black/white were used. Speeds were either 32 fps or 64 fps. The time from ignition to the maximum volume was obtained by measuring film length. This was converted to time.

Reaction Time from Ignition to Smelt Bead

This is similar to the previous time. It is the time from the maximum volume until the char mass collapses into a dense smelt bead. The first appearance of the smelt bead is the measurement point. This continued to glow for some time until the inorganics were fully oxidized. The difference between this time and the time to maximum volume is the char burning time.

THE INFLUENCE OF WATER ON BLACK LIQUOR COMBUSTION

B. A. Moreland* and D. T. Clay

The Institute of Paper Chemistry
Appleton, WI 54912

ABSTRACT

Combustion of kraft black liquor droplets showed that the initial moisture content does influence char reactivity. The black liquor samples which ranged in solids content from 68 to 100% were combusted in a 600°C flowing air stream. The 30 to 50 mg samples were suspended in the air stream from an electronic microbalance. Lower solids samples bubbled, swelled, and then rapidly burned. Higher solid samples did not bubble, but swelled and burned in a similar manner. The resultant char maximum reactivity slightly declined as the initial liquor solids content increased. Gas concentration measurements showed that total water evolution was essentially complete near the start of char oxidation. These experimental data suggest that initial liquor moisture levels do affect the reactivity of char even after water has evolved.

BACKGROUND

Present practice in kraft recovery systems is for the spent liquor from the pulping process to be evaporated to about two-thirds solids by weight. The liquor is then sent to the recovery furnace for combustion. Water that enters the furnace with the liquor evaporates and exits the furnace in the flue gas. The latent heat of vaporization of this water is irretrievably lost. This energy loss could be reduced if higher solids contents were produced in liquor concentration systems.

Advanced concentration technologies have been pilot tested (1,2). These are capable of producing liquor solids contents in excess of 80%. However, before a high-solids recovery scheme can be put into practice, the consequences of high-solids combustion should be recognized. Changes in furnace design may be needed to achieve high-solids liquor combustion with good pulping-chemical and energy recovery.

Previous black liquor thermal studies have examined behavior in hot, inert-gas environments (pyrolysis conditions). Pronounced black liquor swelling during pyrolysis has often been found to be a characteristic of liquors that burn well (3-6).

Recently, Hupa (7) has documented the burning of black liquor droplets in an air atmosphere. Many variables were tested, but the influence of higher moisture contents was not reported.

Clay and Ragland (8) examined black liquors of two different moisture contents during combustion as well as pyrolysis. Liquor samples were suspended from an electronic microbalance in an up-flowing, hot gas stream. To evaluate sample reactivity, the

slope of the sample's mass-history curve was ratioed to the initial mass of solids in the sample. Liquor solids content (80 and 100%) was among the variables studied. At 80% solids, the reactivity of samples was higher than that for 100% solids samples, especially when the gas temperature was high (900°C).

The present paper reports the results of the effect of liquor moisture content on black liquor combustibility. Reactivities were determined for liquor samples ranging from 68 to 100% solids content. The combustion experiments were performed in a convective flow reactor similar in design to that used by Clay and Ragland.

Experimental Equipment

The single-particle reactor (SPR) is designed for the study of black liquor combustion or pyrolysis in a flowing-gas environment (see Fig. 1). Pre-weighed samples of liquor are suspended from an electronic microbalance in the reactor. The sample is then subjected to a down-flowing gas stream which has been preheated to a desired temperature. When air is used as the gas medium it is passed through a column of drying agent before being heated.

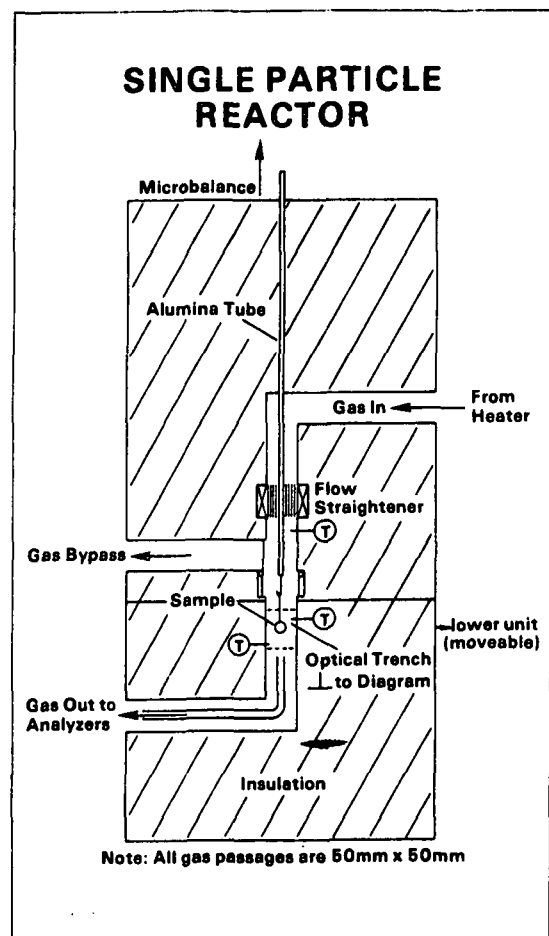


Fig. 1 Schematic diagram of the single-particle reactor.

*Presently employed by Marathon Engineers - Architects - Planners, Inc., Menasha, WI.

While the sample is placed in position, a damper is closed to divert the hot gas. To start a test, the damper is opened. The sample's behavior can be observed through a viewport during the test. Data collection is accomplished with an analog-to-digital converter in conjunction with a microcomputer. Test data are stored on a floppy disk.

Gas analysis equipment can be used to measure concentrations of gaseous components in the exiting stream. For some of the tests in this study, a dew point hygrometer was used to determine the moisture content of the gas leaving the SPR.

APPROACH

Black liquor sample lots of 68, 71, 78, 84, 92, and 100 percent solids by weight were prepared from a common black liquor stock. Liquor samples were concentrated from the base liquor in a vacuum oven. The solids content of a sample lot was determined from the mass of a small portion of "wet" sample and the "dry" mass of the sample after it had been dried in a convection oven for eight hours at 105°C. The sample preparation and solids determination procedures are described in more detail in Appendix 1.

Combustion tests were performed using the liquor samples in the SPR. For all tests, the air stream temperature and flow rate were 600°C and 100 SLPM, respectively. This temperature was used in an effort to slow down and separate the changes a liquor undergoes (drying, pyrolysis and combustion) during the course of an SPR test for closer study.

Black liquor samples were weighed into small bucket-type sample holders, which in turn were hooked to the SPR's microbalance for a test. This bucket-type design shown in Fig. 2 was successful in retaining the sample on the balance as a burn proceeded. This design also caused the drag forces exerted on the sample and holder to be more uniform during the course of a test.

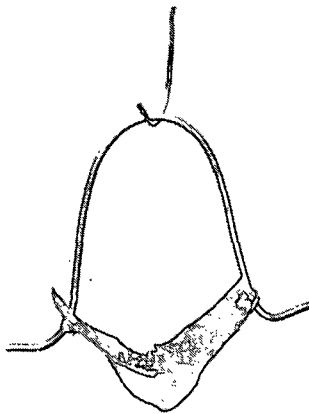


Fig. 2 Photograph of bucket-type sample holder.

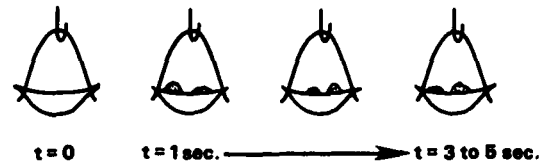
Two series of tests were performed with the SPR. In the first test series, equal sample mass tests, the mass of the samples was approximately 35 mg. In the second set of tests, equal solids mass, the sample mass was such that the mass of solids in a

test sample was about 30 mg. In each test series, four burns were performed with each of the sample lots in a random order.

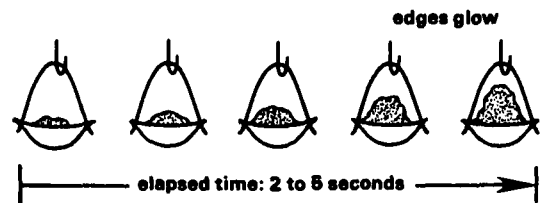
For a test, data collection continued until after data readings became steady and the sample was observed to undergo no further changes. For the last ten seconds of every test the damper was closed to divert the gas flow away from the sample. This allowed balance readings to be obtained without drag on the sample so that an estimate of the total drag force could be made. The computer program for data collection caused data to be gathered every 1.1 seconds throughout the test period.

TEST OBSERVATIONS

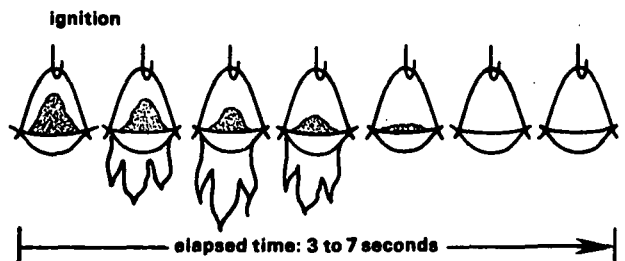
During a burn the behavior of the liquor test sample was observed through the SPR's viewport. Low-solids samples (68 and 71% solids) were observed to pass through three distinct stages which are depicted in the drawings of Fig. 3. Shortly after the hot gas was directed toward the sample, the liquor began to bubble into view. The bubbles, however, would burst and recede to within the sample holder only to be replaced by other bubbles. The behavior exhibited in this liquor bubbling stage is attributed to rapid evaporation and perhaps some pyrolysis gas evolution while the liquor is still in a liquid state.



STAGE 1: Liquor Bubbling



STAGE 2: Swelling



STAGE 3: Char Burning

Fig. 3 General behavior of low-solids samples.

After the bubbling stage there was a perceptible delay as the liquor seemed to gain structural integrity. Stage 2 was typified by the swelling behavior shown in Fig 3. The extent of swelling during this stage appeared to be influenced by the form of the sample holder. Usually the swelling particle did not breach the boundary outlined by the sample holder bucket and handle. As Stage 2 ended, the edges of the swollen particle began to glow bright orange.

As the sample reached its maximum volume, there was also a perceptible delay. Stage 3, the char combustion stage, then followed and was very rapid. The swollen particle ignited and rapidly burned away. After a test, when the sample holder was removed from the reactor, all that remained were traces of ash in the bucket.

The first stage, liquor bubbling, was less apparent for mid-range liquors (78 and 84% solids). For the high-solids samples (92 and 100% solids), first-stage behavior was never observed. No apparent trends were noticed for liquor samples of one solids content to swell more or differently than liquor of another solids content.

The drawings of Fig. 3 and this discussion are descriptive of the behavior seen in most tests. One test in which a 68% solids sample was used was very abnormal and the events of this test deserve description here. Stage 1 appeared to proceed as normal. In Stage 2 though, the sample swelled excessively over the side of the holder. The curious part is that the particle never ignited and burned (i.e., Stage 3 never occurred). The swollen particle was removed from the SPR and inspected (see drawing in Fig. 4). The particle was mostly gray, but had shiny, metallic, bluish-green patches on its surface. Repeatedly the particle was inserted into the reactor, but remained stable to combustion in air at 600°C. Afterward, the particle was broken up and found to be mostly void space within. An explanation of the events of this test may be that pyrolysis gases did not burst from inside the particle as usual. Instead, swelling continued as pyrolysis gases were slowly released. The sudden release of combustible pyrolysis gas may be the trigger that is needed for ignition and combustion of the remaining char material.

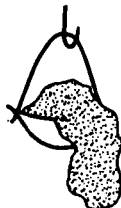


Fig. 4 Stable char particle.

EXPERIMENTAL RESULTS

In Fig. 5 the experimental data obtained in a test using 78% solids sample are shown. The features of the microbalance's response shown in the lower part of Fig. 5 were common to most tests.

The balance's response is initially at a low value, b_1 , but quickly rises to a maximum value, b_{max} , as the drag force of the gas stream develops. The balance reading then decreases. A region of maximum slope was common during the latter part of the balance reading's steady decline. In Fig. 5, the maximum negative slope ($-db/dt_{max}$) in this region is indicated.

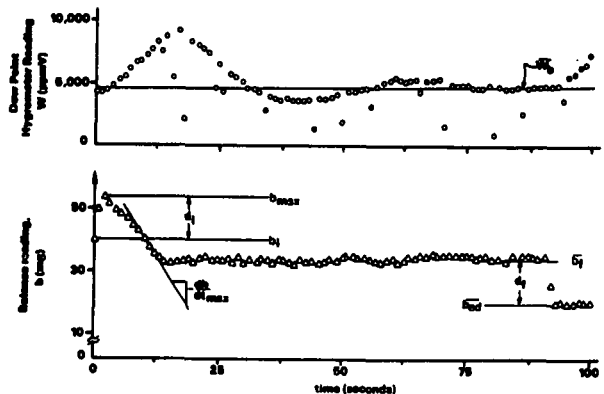


Fig. 5 Experimental data for an SPR combustion test (78% solids liquor in a 600°C air stream 100 SLPM).

In most cases, the end of the maximum rate region was marked by an overall minimum in the balance data. This minimum was then followed by a small rise to a steady value. The end of carbon combustion by the sulfide-sulfate cycle and the oxidation of all residual sulfide to sulfate would explain this behavior (9). At the end of the test, the effect of diverting the gas stream away from the sample can be seen. From the difference between balance readings before and after the damper was closed, b_f and b_{ad} , an estimate of the drag contribution to balance readings was obtained. This difference, d_f , typically ranged from 13 to 16 mg. A less reliable estimate of drag, d_i , was found from the readings with and without drag (b_{max} and b_1) at the start of a test.

It is apparent that the dew point hygrometer (DPH) response (top of Fig. 5) lags far behind the events of a test. The underdamped response of the unit takes a long time to settle down to a final steady value, \bar{W}_b . The water baseline, \bar{W}_b , is the moisture content of the air stream alone without contribution from the liquor sample's moisture. Note that \bar{W}_b does not agree with the initial DPH reading. Ideally it would, but the SPR tests do not start from steady-state condition.

Because of its slow response, the DPH could not be used to directly measure the amount of water evolved over the course of a test. However, a data analysis procedure which used a dynamic response model of the hygrometer unit was used to estimate the time at which water evolution ended during a test (see Appendix 2). The DPH was used in two tests for each level of sample solids content. Using the procedure outlined in Appendix 2, the time at which water evolution stopped was estimated, and then compared to the time at which the balance reading exhibited maximum slope. This

analysis supports the conclusion that water evolution had ended before the maximum balance-reading slope occurred.

A normalized, maximum char reactivity parameter, R_{\max} , was chosen to evaluate the balance responses from SPR tests,

$$R_{\max} = -\frac{1}{m_{1s}} \left(\frac{db}{dt} \right)_{\max} \quad (1)$$

where $(db/dt)_{\max}$ is the maximum negative slope of the balance's output, and m_{1s} is the mass of solids initially in the sample (as determined from the sample's solids content and the predetermined mass of the sample). The symbol "b" was chosen to represent the balance output in order to emphasize that the balance's reading includes contributions from both the mass of the sample and drag forces. The parameter R_{\max} was chosen for several reasons.

1. The only data used to determine R_{\max} was that collected after drag forces had developed and the sample had dried. The parameter is therefore an indication of the rate of carbon degradation rather than sample drying rate, a conclusion supported by DPH analysis.
2. The slope of the balance's output does not depend on the absolute value of the readings. Therefore, uncertainties due to error in the drag force estimates, loss of sample mass before data collection, or inaccuracies in the tare procedure of the balance do not affect the results.
3. The maximum slope of the balance reading was easy to graphically determine.

A summary of the R_{\max} values determined appears in graphical form in Fig. 6. Average values for the equal sample mass and equal solids mass tests are separately presented. Tick lines represent plus and minus one standard deviation.

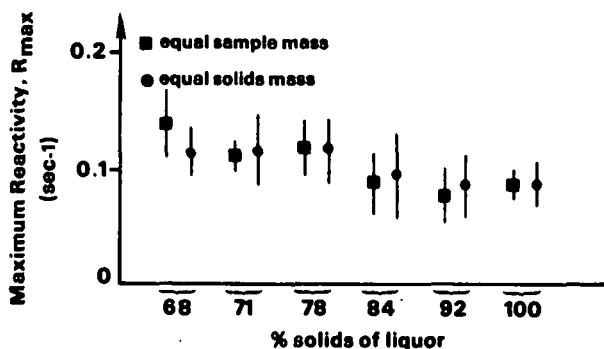


Fig. 6 Maximum reactivity parameter R_{\max} .

Figure 6 suggests that R_{\max} slightly decreases as the solids content of the liquor increases. To

support this, data from both test series were combined and the constants, a_0 and a_1 , of the following relation were determined by linear regression,

$$R_{\max} = a_0 + a_1 \cdot \%S \quad (2)$$

where

$$a_0 = 0.221 \text{ sec}^{-1} \quad (3)$$

$$a_1 = -0.00145 \text{ sec}^{-1} \quad (4)$$

The 99 percent confidence interval of the slope, a_1 , was found to be

$$-0.00233 < a_1 < -0.00056 \quad (5)$$

These results support the conclusion drawn from Fig. 6, i.e., maximum reactivity tends to decrease with increased sample solids content.

DISCUSSION

The tendency for lower-solids samples to burn more rapidly could be explained if the physical and/or chemical makeup of the liquor solids were affected by the initial moisture content. Increased surface area available for heat and mass transfer should lead to higher reaction rates in the SPR. By direct observation alone, no differences were noted in the extent to which liquor samples swelled. Closer examination of the swelling behavior, perhaps using photographic techniques, could perhaps reveal differences in swollen volume. The internal structure of the char particle could also have been affected by the liquor's moisture content. Such differences would be hard to observe during an SPR test. A high amount of internal surface area should cause a particle to be more reactive.

Chemical differences of the samples also cannot be ruled out. A mild evaporation procedure was used in an effort to remove only water from the samples. The harsher conditions required to produce high-solids samples could have caused more volatile, organic components to be driven from the liquor. The presence of moisture in the liquor could also have caused chemical changes during evaporation and initial pyrolysis in the SPR. Moisture in the liquor should keep temperatures within the particle lower for a longer time. This could lead to the formation of condensation products and/or alter the release rates of volatile sulfur species.

CONCLUSIONS

High-solids black liquor combustion was studied in a convective-flow reactor. Liquor samples with solids contents close to the levels of solids burned in state-of-the-art recovery furnaces were observed to exhibit three distinct stages of behavior. When suspended in a 600°C air stream these samples bubbled, then expanded in volume, and finally, burned rapidly. These three stages exemplify a separation of the drying, pyrolysis, and combustion phenomena.

Samples approaching 100 percent solids did not exhibit the bubbling behavior which was observed at lower solids. The swelling and combustion behavior of high-solids samples, however, appeared similar to that shown at lower solids levels.

During tests, samples were attached to a micro-balance. Sample reactivity was determined from the maximum slope of the balance's response. Low-solids samples were slightly more reactive than high-solids samples. The maximum slope of the balance readings occurred after the sample had dried. Apparently, moisture initially in the liquor had an influence on the subsequent combustion of the sample after all the water had been evolved. The cause of this behavior has yet to be identified. It would also be useful to determine whether this effect occurs at higher temperatures.

LITERATURE CITED

1. Clay, D. T. and Karnofski, M. A., Tappi, 64(12): 45-48(1981).
2. Andrews, R. S., Jr. and Roscoe, R. W., Tappi, 64(12): 49-51(1981).
3. Baklien, A., Appita, 14(1): 5-17(1960).
4. Oye, R., Langfors, N. G., Phillips, F. H., and Higgins, H. G., Appita, 31(1): 33-40(1977).
5. Oye, R., Hato, N., and Mizuno, T., Japan TAPPI, 27(1): 71-79(1973).
6. Miller, P. T. and Clay, D. T. Swelling of kraft black liquor during pyrolysis, to be presented at AIChE meeting in Seattle, November, 1985.
7. Hupa, M. and Solin, P., 1985 International Chemical Recovery Conference Proceedings, p. 335 (April, 1985).
8. Clay, D. T. and Ragland, K. W., AIChE Annual Meeting at San Francisco, 1984.
9. Grace, T. M., Cameron, J. H., and Clay, D. T. Role of the sulfate/sulfide cycle in char burning-experimental results and implications. Proceedings of the 1985 International Recovery Conference, New Orleans, 3:371(April, 1985).

ACKNOWLEDGMENTS

Portions of this work were used by one of the authors (BAM) as partial fulfillment of the requirements for the Master of Science degree at The Institute of Paper Chemistry.

APPENDIX 1. Summary of Sample Preparation and Solids Determination Procedures

Black liquor samples were produced from a common base liquor which had been obtained from the Thilmany Pulp and Paper Company in Kaukauna, Wisconsin. The liquor solids analysis is shown in Table 1. A portion of the base liquor was spread evenly in a flat-bottomed dish which was placed in a vacuum oven. Periodically, a sample lot of liquor would be removed and the heating dial of the oven would be incremented. Throughout the procedure, a whispering flow of nitrogen gas was maintained through the oven to prevent Na_2S oxidation.

Table 1. Analysis of black liquor solids.

	Percent of Dried Solids
C	38.6
H	2.7
O	31.7
S	4.2
Na	18.8
K	1.8
Other	2.2

To determine the solids content of a sample lot, a small portion of sample was measured into a preweighed drying dish. Ignited sand was then added to the dish and another weighing was performed. Distilled water was added to cover the contents of the dish. The dish was then placed in a 105°C oven to warm. After a few minutes, the dish was removed from the oven, and its contents were stirred with a glass rod. The glass rod was thoroughly rinsed with distilled water into the dish. The dish was then returned, uncovered, to the oven for eight hours. Afterward, the dish was placed in a desiccator to cool and then weighed once again.

All told, four separate mass measurements are made in the procedure.

- m_1 = mass of the dish
- m_2 = mass of the dish and sample
- m_3 = mass of the dish, sample, and sand
- m_4 = mass of the dish, dried sample, and sand

The sample's wet mass (m_w), dry mass (m_d), and percent solids content (%S) can be determined readily.

$$m_w = m_2 - m_1 \quad (6)$$

$$m_d = m_4 - m_3 + m_w \quad (7)$$

$$\%S = (m_d/m_w) \cdot 100\% \quad (8)$$

The results of these procedures are summarized in Table 2.

Table 2 Summary of sample preparation and solids determination procedures

% Solids ^a	Time ^b (hr:min)	T _{max} (°C) ^c
67.7 ± 2.4	0:00	N/A
71.3 ± 2.0	0:25	< 30
78.3 ± 0.9	1:44	78
84.3 ± 0.7	2:02	78
92.0 ± 0.8	2:22	81
100.0 ± 0.9	6:00	102

^aAverage percent solids ± 95% confidence interval.

^bTotal elapsed time in vacuum oven.

^cMaximum temperature reached in oven.

APPENDIX 2. Analysis of Dew Point Hygrometer Data

The dew point hygrometer (DPH) directly measures the dew point (or frost point) of a gas stream. Handbook data were used to convert the dew point temperature to a moisture concentration in parts per million by volume.

The slow response time of the DPH made it necessary to develop a dynamic response model for the unit. A first-order plus time-delay model was chosen to relate the actual DPH reading obtained, $W(t)$, to the water content of the gas in the SPR, $W_m(t)$. The Laplace transfer function form of this model is:

$$W(s) = \frac{e^{-t_d s}}{\tau s + 1} W_m(s) \quad (9)$$

For the DPH unit, the time constant, τ , and time delay, t_d , were determined to be 5.4 seconds and 2.8 seconds, respectively.

To use this model, the DPH data were first corrected for the water baseline, \bar{W}_b (see Fig. 5). Corrected values, W_c , were obtained by subtracting the baseline from the measured value.

$$W_c = W - \bar{W}_b \quad (10)$$

Negative values for W_c were not accepted and were instead assigned values. Those data points from the oscillatory period at the end of a test were also assigned W_c values of zero even if the calculated value was positive. In Fig. 7, the W_c values found for the example data of Fig. 5 are depicted.

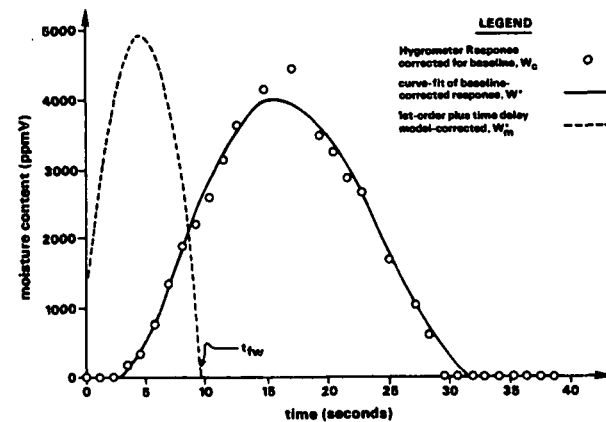


Fig. 7 Relationship between estimated gas-stream moisture content variables.

A linear regression equation, $W^*(t)$, was then used to approximate the W_c data. This equation (a six term polynomial in time, t) was then used with the model to estimate the water evolution from the sample, $W_m^*(t)$.

$$W^*(s) = \frac{e^{-2.8 s}}{5.4 s + 1} W_m^*(s) \quad (11)$$

The estimated time at which water evolution ended, t_{fw} , was then obtained from the $W_m^*(t)$ intercept with zero (Fig. 7).

Values for t_{fw} were compared to two parameters evaluated from the balance response data. Times at which the balance response first and last exhibited a high slope, $t_{i,max}$ and $t_{f,max}$ were determined. These time parameters bounded the time at which $(db/dt)_{max}$ was evaluated. The results of this comparison are summarized in Table 3. These results support the conclusion that water evolution had ended before rapid burning occurred.

Table 3. Comparison of the estimated time at which water evolution ended, t_{fw} , to the time period the balance response exhibited maximum slope, $(t_i \rightarrow t_f)_{max}$

% Solids	t_{fw} (sec)	$t_{i,max}$ (sec)	$t_{f,max}$ (sec)	$t_{fw}/t_{i,max}$	$t_{fw}/t_{f,max}$
68	10.5	11.3	14.8	0.93	0.71
68	9.0	10.2	13.6	0.88	0.66
71	9.7	9.1	12.5	1.07	0.78
71	9.3	7.9	12.7	1.18	0.73
78	9.6	6.8	11.7	1.41	0.82
78	9.0	8.0	12.5	1.13	0.72
84	10.9	11.4	15.9	0.96	0.69
84	7.7	10.6	15.7	0.96	0.49
92	8.7	10.1	16.9	0.86	0.51
92	8.5	10.2	17.0	0.83	0.50
100	13.5	6.6	13.6	2.05	1.01

NOTE: Test data from a second test using 100% solids was disregarded since a significant amount of sample fell from the holder during the test.

SWELLING OF KRAFT BLACK LIQUOR DURING PYROLYSIS

P. T. Miller and D. T. Clay

ABSTRACT

Techniques have been developed to monitor the swollen volume of black liquor particles with time. The key process variables studied were heating rate, temperature, moisture content, and particle size. The results suggest the pyrolysis gases drive the swelling process, with the physical properties of the reacting particle controlling the degree of swelling.

INTRODUCTION

The kraft process is the dominant pulping process today for paper grade pulps. Kraft pulps represent 74% of North American market pulps (1). An advantage of kraft pulping is the efficient recovery of the chemicals and energy value from its spent pulping liquor. This aqueous solution from the process, kraft black liquor, contains dissolved organic and inorganic solids. In the recovery process, kraft black liquor is concentrated to approximately 65% solids content and combusted. The burning of organics contained in kraft black liquor provides a significant amount of energy, which is used to produce steam. The resulting char is then smelted to recover the inorganic solids for reuse in the pulping process. Both steam generation and smelting occur in the same process unit, the recovery boiler.

Kraft recovery boilers typically operate at full solids capacity, leaving little leeway for upsets. Any interruption in the furnace operation can have an immediate detrimental effect on the operation of an entire mill. Steady-state combustion in the recovery furnace is thus of particular importance in maintaining efficient pulp production.

A blackout is defined as the loss of liquor ignition in the recovery boiler and can result in a significant amount of recovery boiler

downtime. Some mills have experienced blackouts which appear to be linked to variations in the properties of black liquor (2). The cause of this poor combustion could not be determined from conventionally measured properties (heat value, solids content, specific gravity and viscosity). Reduced swelling of black liquor has been observed in liquors exhibiting poor combustion characteristics (3,4).

Black liquor swelling is an important process during combustion. Swelling of black liquor particles increases the surface area available for reaction with oxygen and thus improves the combustibility of black liquor. Changes in the swelling of black liquor would alter the flight paths of black liquor particles in a recovery furnace. Excessive swelling of particles can lead to increased entrainment of black liquor char in air. The char becomes deposited on the upper portions of a recovery furnace and leads to increased downtime. These factors indicate that the potential exists for an optimum amount of black liquor swelling during combustion to maintain efficient recovery furnace operation.

Unfortunately, there are limited data on black liquor swelling during pyrolysis (3-6). Studies performed to date have been limited either by empirical analysis, low temperatures or the inability to monitor the swelling process as a function of time.

The present study was undertaken to investigate the swelling characteristics of

kraft black liquor during pyrolysis. The objectives were to quantify the swelling rate and to determine the factors which contribute to swelling. The variables thought to be of importance in swelling were the heating rate, gas temperature, moisture content of the particle, particle size and the black liquor composition. This paper discusses the effect of the process variables. The effect of black liquor composition on swelling will be covered in a subsequent paper.

APPROACH

The reactor used for this study allowed one to view the swelling of black liquor particles during evaporation and pyrolysis. It is shown in Figure 1. Details of the experimental apparatus, experimental procedures, and material preparation can be found in the appendix. Black liquor particles were suspended from a microbalance in a flowing nitrogen gas stream. The particle was primarily heated by convection, with some radiation from the surrounding walls. Heat fluxes in the reactor were experimentally determined. Heat fluxes which were comparable to those found in commercial recovery furnaces could be attained at 900°C.

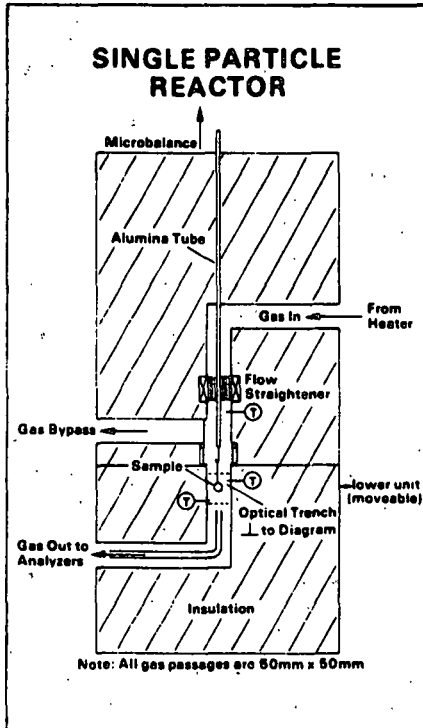


Figure 1. Schematic of single particle reactor.

An optical port was available for viewing and taking photographs of the black liquor particles. The volume of the particles could be inferred from the area of the particle measured from photographs. A gas sampling line below the particle allowed for the analysis of CO and CO₂. Data acquisition was performed by a computer with an analog/digital interface.

The variables studied have been the gas temperature, the heating rate, the solids content of the particle and the particle size. The gas temperature has been varied from 300-900°C. The heating rate was varied by changing the flow rate of the gas stream and keeping the gas temperature constant. The solids content of black liquor was studied at three levels: 65, 80, and 100%. The particle weight was studied from 2-100 mg.

RESULTS

The two process variables with the largest influence on the maximum swollen volume were the gas temperature and the solids content. The influence of these variables is shown in Figure 2. Figure 3 shows photographs of an original and four swollen black liquor particles. The changes in particle volume with time are shown in Figures 4 and 5. Figure 4 shows this change as a function of solids content, while Figure 5 shows the influence of gas temperature.

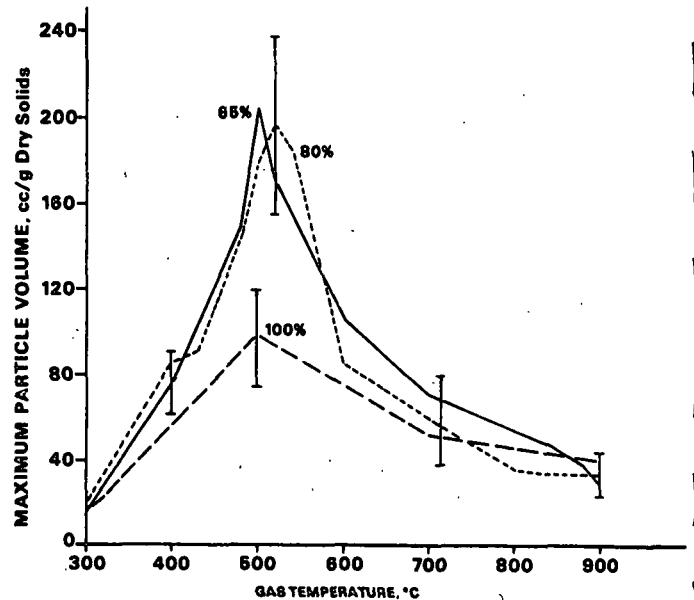


Figure 2. Maximum particle volume vs. gas temperature for 65, 80 and 100% solids black liquors. Brackets indicate ± 1 std. deviation.

Moisture had a large influence on the swollen volume at 500°C. Steam was added to the nitrogen gas stream to determine if the steam could promote swelling for 100% dry black liquor solids at 500°C. The steam/nitrogen mixture was approximately in a 1:1 ratio. The particles pyrolyzed in nitrogen gave a mean maximum particle volume of 46 ± 14 cc/g and the steam/nitrogen mixture gave a maximum particle volume of 53 ± 8 cc/g (± 2 std. dev.). The steam did not have a significant effect on the maximum volume attained. Apparently, moisture must be present initially to influence the swollen volume and was not absorbed from the surrounding gas stream.

Tables 1 and 2 show the results of a 2³ factorial experiment with gas flow rate, gas temperature and black liquor % solids as the independent variables, with the maximum particle volume and the time required to reach maximum volume as dependent variables. The data represent an average of two replicates. The purpose of the analysis was to determine the effect of heating rate on swollen volume. A Yates algorithm was used to calculate the main and interaction effects.

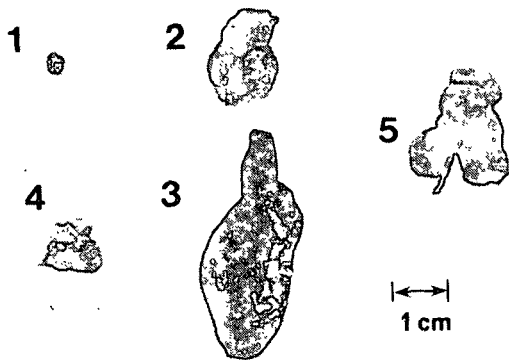


Figure 3. Photographs of black liquor particles. 1. Original particle. 2. 100% solids, 500°C, 40 mg. 3. 65% solids, 500°C, 40 mg. 4. 65% solids, 900°C, 40 mg. 5. 65% solids, 850°C, 80 mg.

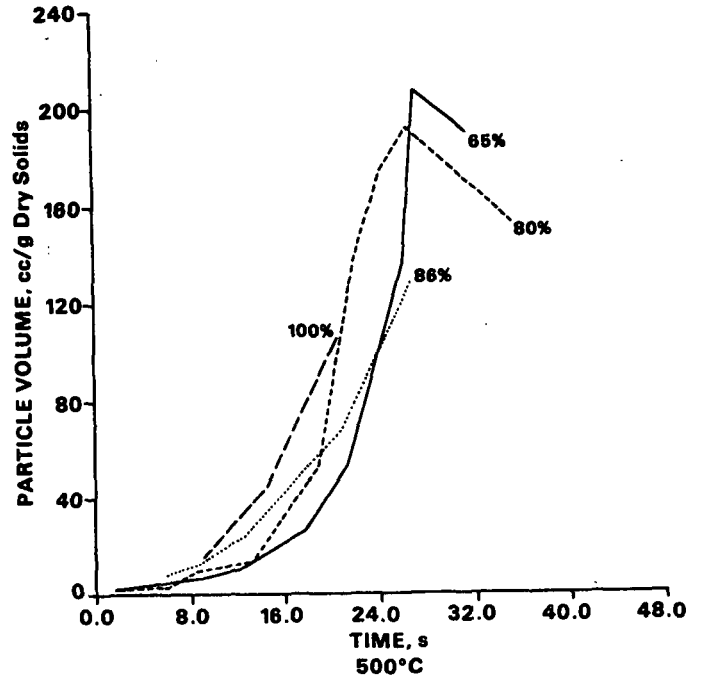


Figure 4. Particle volume vs. time for black liquor particles differing in original solid content (500°C, 30-40 mg). Shrinking also occurred with the 86 and 100% initial solid black liquors but was not documented.

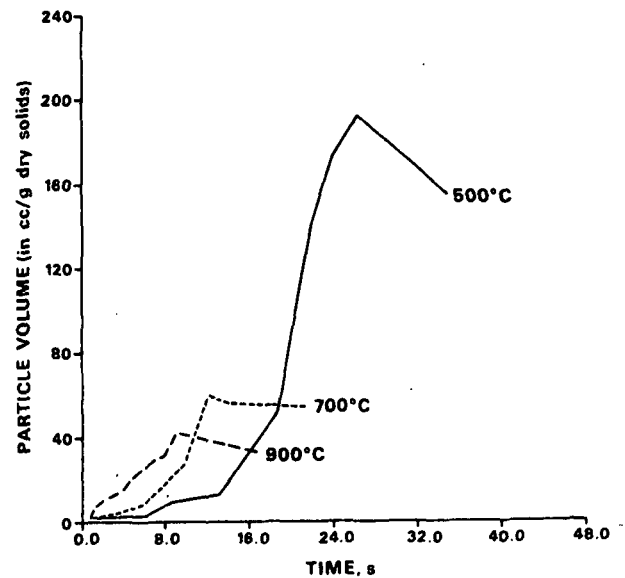


Figure 5. Particle volume vs. time at different temperatures (80% solids, 40 mg).

Table 1. Effect of gas flow rate on volume.

Gas Flow Rate % Solids	Volume (cc/g initial solids)			
	50 Lpm		150 Lpm	
	65%	100%	65%	100%
400°C	71	46	78	38
500°C	200	56	194	52

- Swollen volume \pm 10 cc/g (\pm 2 std. dev.)

Table 2. Effect of gas flow rate on time to maximum volume.

Gas Flow Rate % Solids	Time (s)			
	50 Lpm		150 Lpm	
	65%	100%	65%	100%
400°C	65	48	43	32
500°C	38	29	28	22

- Time \pm 2 s (\pm 2 std. dev.)

Temperature, moisture content and the interaction of these two variables had a significant effect on the final swollen volume attained. All three variables significantly affected the time to reach the maximum swollen volume. Thus, gas flow rate had the effect of changing swelling rate but not the maximum volume attained. The effect of gas flow rate on the heat flux to a particle is shown in Table 3. The heating rate, under the conditions tested, did not influence the maximum swollen volume.

Table 3. Heat flux at various reactor conditions.

Gas Flow Rate	Heat Flux (W/m ²)	
	50 Lpm	150 Lpm
500°C	18,000	33,800
700°C	41,600	68,500
900°C	67,300	106,000

The effect of particle size on the normalized swollen volume (vol./solids) is shown in Table 4. The mean and standard deviation of 9 tests performed at a standard size of 40 mg are also given. The 40 mg particles represented a compromise between the small particles found in a recovery furnace and the relatively large amount of black liquor required to obtain accurate data. The particle size did not appear to have a major influence on the particle swollen volume.

Table 4. Effect of particle size on the normalized swollen volume.

Black Liquor Weight (mg)	Time to Max.	Vol. Norm.
	Vol. (s)	(cc/g)
2	2.5	92
2	3.0	61
4	4.5	88
5	4.0	64
8	6.5	69
11	6.5	85
13	-	71
20	8.0	48
21	8.0	63
48	14.5	61
40	13.0 \pm 2.6	68 \pm 40

(av. \pm 2 std. dev.)

Conditions: 65%, 700°C, 100 Lpm

DISCUSSION

The swelling of kraft black liquor may be viewed as a process with up to three stages. The evaporation stage could be represented as evaporation of water in the absence of pyrolysis gases. This stage was characterized by low swelling rates. This stage was followed by a second of high swelling rates and the evolution of pyrolysis gases. The last stage was particle shrinking.

Pyrolysis gases were monitored by measuring the CO and CO₂ release. CO and CO₂ are significant components of the pyrolysis gases. The CO₂ gas evolution curves of pyrolyzing black liquor particles are shown in Figure 6; the shaded portion indicates the region of significant swelling. The curves were corrected for dead time and a first order time constant. The swelling nearly always ended after the CO₂ evolution peak. The CO profile parallels the CO₂ profile.

Figure 6 indicates that at 900°C pyrolysis began immediately after the test commenced. At high heat fluxes the pyrolysis of black liquor and evaporation of water were occurring simultaneously from the beginning of the test, with the result of a fairly uniform swelling rate until the maximum volume was reached. This contrasted with the swelling behavior at lower temperatures, which could be divided into two regions of differing swelling rates.

The high degree of variability for a given set of conditions could not be explained by the duration of the pyrolysis or the

area under the significant swelling portion of the CO₂ curve. Figure 7 shows the variability of the measured volume for six replicate tests. The variability occurs near the end of the swelling process, which can be explained by thinning of a nonhomogeneous outer char layer, thus exposing weaknesses at different points in the pyrolysis. The structure of a pyrolyzed black liquor char is shown in Fig. 8.

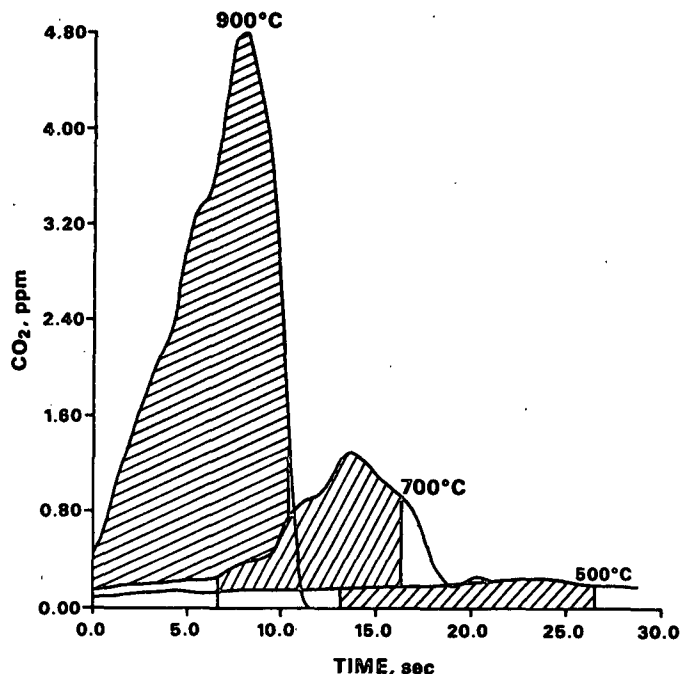


Figure 6. Carbon dioxide concentration of gas stream below the particle as a function of time (80% solids, 40 mg). The shaded portion indicates swelling rates greater than $1 \text{ cm}^3/\text{g-s}$.

Particle shrinkage occurred to the greatest extent at 500°C. At 500°C the particle structure actually deformed and partially collapsed. During shrinking this char appeared to be plastic and deformable. The chars at 700°C and 900°C shrank to a relatively small extent. The structural integrity of the particles was retained, since there was no visible deformation or change of shape. This indicated the chars at higher temperatures were somewhat fixed relative to the chars at lower temperatures and a greater force would be required to deform the higher temperature char particles than those at lower temperatures. The particles at 900°C began to decompose. Beckwith et al., (7) attributed this decomposition to be the vaporization of sodium salts.

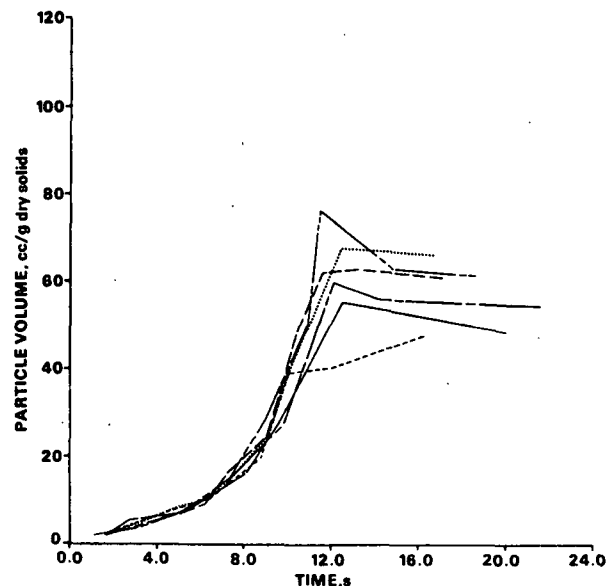


Figure 7. Particle volume vs. time (80% solids, 700°C, 40 mg).

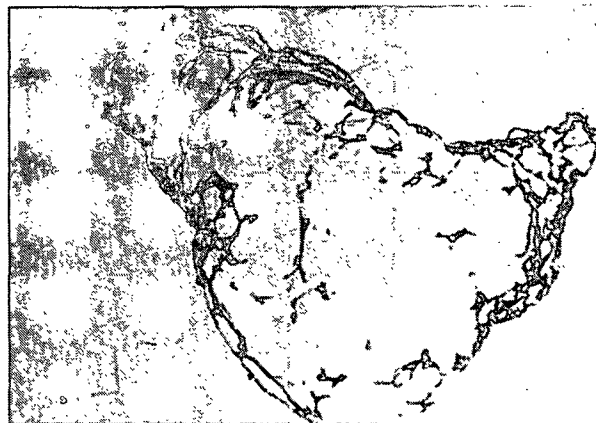


Figure 8. Photograph showing a cross section of a black liquor particle (700°C, 100% solids).

The total volume of gases evolved during pyrolysis of black liquor increased with increasing temperature but the swelling decreased as temperature rose past 500°C. The CO₂/CO profiles could not explain the high degree of variability of tests performed

under identical conditions. The results tended to show that the pyrolysis gases were the driving force of the swelling process, but these gases appeared not to control the extent of swelling.

Physical or plastic properties of the pyrolyzing particle may be the controlling factor in swelling for a given black liquor. Maximum swelling occurred at approximately 500°C. At lower temperatures the material was viscous and did not expand easily. As the temperature increased the fluidity apparently increased with a lowering of viscosity. The fluidity appeared to reach a maximum around 500°C.

As higher temperatures were reached char formation seemed to influence swelling to a greater extent. The char layer appeared to form to a greater extent, and the increased thickness of the outer crust impeded swelling. This was evidenced by swelling that was characterized by surges as weaknesses in the crust were broken through. This contrasted with the relatively uniform swelling that was characteristic of swelling at lower temperatures.

There was some evidence showing the outer shell could play an important role in swelling. Most of the variability in the data occurred near the end of the swelling process. Particle 5 in Figure 3 shows a particle in which the swelling appeared to be complete, when suddenly fluid black liquor was pushed out of the particle interior at a weak point in the outer shell. This behavior occurred primarily at the higher temperatures, where the outside of the particle formed a rigid char, whereas the inside was apparently still fluid and volatile. Weaknesses in the outer crust could result in appendages on the particles and in particle shapes that were less spherical than those pyrolyzed at lower temperatures.

The essential combination of conditions appeared to be a viscous yet deformable droplet expanded via the internal pressure of pyrolysis gases. Moisture enhanced this expansion between 400-700°C. The significant swelling began after most of the water appeared to have been evaporated. This explained why the 80 and 65% solids liquor behaved similarly. The fluidity was too low for significant swelling to take place at lower temperatures. Char formation limited expansion, becoming more important at higher temperatures. The 500°C temperature (maximum swelling) appeared to give the optimum physical properties for swelling.

CONCLUSION

Swollen volumes reached a maximum near 500°C within the 300-900°C temperature range tested. Moisture increased the swelling of black liquor, the effect being greatest near 500°C. This effect was not additive as 65 and 80% liquors behaved similarly. If steam was added to the nitrogen stream, in a 1:1 volume ratio, no significant increase in swelling was noted. The heating rate could influence the swelling rate but was found not to influence the maximum swollen volume attained. The particle size had no influence on the normalized maximum swollen volumes under the conditions tested.

The physical (plastic) properties of black liquor seemed to play an important role in swelling. The pyrolysis gases drove the swelling process but did not appear to control the extent of swelling. Future work with the main components of kraft black liquor should reveal more information as to what factors control swelling. The components to be studied will be the alkali lignin, hydroxy acid, inorganic and extractive fractions of kraft black liquor.

ACKNOWLEDGMENT

Portions of this work were used by one of the authors, P. T. M., as partial fulfillment of the requirements for the Ph.D. degree at The Institute of Paper Chemistry.

LITERATURE CITED

1. Mies, W. E., D. R. Allen, S. Pollitzer, D. Adams, and C. Espe, Pulp and Paper '84, '85 North American Fact Book, Miller Freeman Publications, San Francisco, CA, 1985:237.
2. Kubes, G. J., B. I. Fleming, J. M. MacLeod, and H. Bolker, J. Wood Chem. Technol. 2 (3), 279 (1982).
3. Baklien, A., Appita 14 (1), 5 (1960).
4. Oye, R., N. Hato, and T. Mizuno, Jap. Tappi 27, (2), 71 (1973).
5. Kubes, G. J., Trend (PPRIC) (32), 8 (Winter 1982/1983).
6. Oye, R., N. G. Langfors, F. H. Phillips, and H. G. Higgins, Appita 31, (1), 33 (1977).

7. Beckwith, W. F., D. L. Kasbohn, and J. C. Hassler, AIChE Symp. Series 77, (207), 68 (1981).
8. Ranz, W. E., and W. R. Marshall, Jr., Chem. Eng. Prog. 48, (4), 173 (1952).

APPENDIX

APPARATUS

A schematic of the single particle reactor is shown in Figure 1. The particles were heated by a gas stream in a 50 mm x 50 mm channel. The reactor consisted of a movable lower unit and a stationary upper unit. The hot gas flowed from a heater around two bends, past a flow straightener and down to the particle. The gas flow could be diverted ahead of the particle. The temperature was controlled by a thermocouple (SP) which was located above the damper. Two thermocouples (BD) and (BS), which were located above and below the sample, were used to determine the gas temperature at the particle location.

The particle was attached to a Cahn 2000 microbalance via a wire enclosed in an alumina tube. There was a gas sampling line right below the particle, which was used to monitor the evolution of CO₂ and CO. The gases were detected by infrared instrumentation. The system for CO₂ and CO detection had a 4-second delay time and a time constant of 3.6 seconds. An optical trench allowed the particle to be viewed and photographed. A camera with an autowinder was used to take photographs.

The analog signals from the instruments were converted to digital signals and stored on disk by a data acquisition system. Computer programs were written that stored the following information: reaction time, particle mass, gas temperature, CO and CO₂ concentration and camera switch reading. The data could be collected about seven times a second. The camera switch reading was simply an on-off switch connected to the camera switch; in this way one could determine the times at which photographs were taken.

A test consisted of the following sequence of events: 1) switching the gas stream from air to nitrogen, 2) switching the gas stream to the gas bypass duct, 3) lowering the lower compartment, 4) starting the data acquisition program, 5) attaching the particle to the microbalance, 6) raising the lower compartment

and 7) switching the flow to the particle. Zero time was defined as the time at which the temperature measured at thermocouple (BD) began to rise.

PREPARATION OF THE BLACK LIQUOR SAMPLES

The black liquor was obtained from a kraft laboratory cook of loblolly pine chips. The cooking conditions are shown in Table 5.

Table 5. Kraft cooking conditions.

Sulfidity	25%	Time to temp.	90 min.
Eff. alkali	16%	Time at temp.	94 min.
Liquor/wood	4	Cooking temp.	173°C
Yield	45.7%	H - Factor	2000
Kappa no.	25.7	BL Solids	16.5%

The black liquor was then evaporated in a rotovap under a 95 kPa vacuum in a water bath at 80°C. Initial attempts at evaporation proved unsuccessful due to excessive foaming. This problem was alleviated by evaporating the black liquor to approximately 25% solids on a hot plate and skimming the soap residue off. The liquor was then evaporated in the rotovap to 65% solids.

A second sample was evaporated on a hot plate to about 50% solids. Any soap formed during evaporation was skimmed off as before. The black liquor was then placed in an oven at 140°C under nitrogen and a 95 kPa vacuum. A sample (86% solids) was taken out before evaporation had been completed. This sample was then placed in a desiccator and used for tests requiring dry solids. An 80% solids liquor was made by mixing the 65% solids liquor and the dry solids liquor.

MEASUREMENT OF BLACK LIQUOR CHAR VOLUME

The method described in the literature to determine the volume of pyrolyzed black liquor particles is to measure the amount of fine silica or dried pulp balls which the char displaced (5,6). Details of these procedures were not given; therefore, a suitable procedure was devised. The procedure devised used a relatively coarse sand and varied the container size according to the particle size. A coarser sand was found to give more reproducible results than a finer sand. The accuracy of the method was determined measuring the known volumes of ball bearings. The

standard error (95%) of this procedure was ± 0.05 cc for ball bearings with a volume range of 0.13-3.64 cc.

The particles described in the literature were pyrolyzed at relatively low temperatures (400°C). These particles were more dense, yielding particles with a relatively high char matrix strength. At higher temperatures the char particles were too fragile to be measured by the displacement of sand. Also at these temperatures the particle could not be removed from the reactor without some oxidation taking place.

To gain a better understanding of the kraft black liquor swelling, the measurement of the particle volume during pyrolysis would be desirable. An indirect measurement of particle volume was sought. The analysis of photographs with a planimeter was used initially and found to be acceptable.

A planimeter was used to measure the projected area of the particle. The area measured was then transformed to a volume assuming that the area represented a circle. To increase the sensitivity of the procedure the negatives were put in an enlarger and the projections were enlarged to the desired size and were then traced on paper. A picture of a ball bearing in the reactor was used for calibration purposes. This method was compared to the displacement of sand method for a number of char particles varying in size and shape. The standard error (95%) between the two test methods was found to be ± 0.09 cc for a range of particle volumes from 0.39-1.90 cc.

MEASUREMENT OF THE HEAT FLUX TO THE PARTICLE

The heat flux to the particle was determined by measuring the rate of evaporation of water

from small metal cups. The metal cups were formed in the shape of half spheres. The surface area of the cup was determined by weighing the cup and knowing the weight per unit area of the metal. The evaporation rate was determined by a linear regression of the constant evaporation zone from a mass vs. time plot.

The heat flux can also be determined from a relationship for the forced convection heat transfer to a single sphere by Ranz and Marshall (8). The heat transfer coefficient can be determined from Equation (1). The heat flux can then be determined from Equation (2).

$$Nu = \frac{hD}{k} = 2.0 + 0.60 Re^{1/2} Pr^{1/3} \quad (1)$$

$$Q = h(T_{\infty} - T_o) \quad (2)$$

where: Nu - Nusselt no., h - heat transfer coefficient, D - diameter of the particle, Re - Reynolds no., Pr - Prandtl no., T_{∞} - gas temp., T_o - particle temp. Q - convective heat flux.

The calculated and measured values of heat flux compared well for the range of reactor conditions from 600-900°C and 50-150 Lpm. A laminar velocity profile was assumed in the calculations. The measured values were corrected for radiation by comparing the evaporation rates with the surrounding walls preheated and at room temperature. The radiation component of heat transfer was about 15% of the total heat transferred at 800°C. The correlation coefficient for measured vs. calculated values of heat flux was 0.98 with a slope of 1.0.

THE INFLUENCE OF COMPOSITION ON THE SWELLING OF KRAFT BLACK LIQUOR DURING PYROLYSIS.

P. T. Miller, D. T. Clay, and W. F. W. Lonsky
The Institute of Paper Chemistry
Appleton, WI 54912

ABSTRACT

During the drying and pyrolysis phases of kraft black liquor combustion, significant swelling of individual liquor particles occurs. Swollen volumes can reach 20 to 30 times the original volume during combustion. The swelling process can conceivably affect the combustibility of black liquor and the amount of carryover in a recovery furnace.

The composition of black liquor was found to have a large influence on swelling. A combination of sugar acids and kraft lignin swelled to a larger extent than when either component was pyrolyzed separately. A 1:1 ratio of these two components resulted in maximum swelling for the various ratios tested. The molecular weight of kraft lignin had an effect on swollen volume with higher molecular weight fractions producing lower swelling chars.

Other components were found to reduce the swelling of black liquors. Extractives interfered with the swelling by appearing to change the deformable properties of the pyrolyzing material. Inorganic salts acted as a diluent.

Analysis of the surface characteristics of chars revealed that good swelling chars were composed of small bubbles 50 to 150 microns in diameter. Poor swelling liquors did not exhibit this phenomenon. The formation of bubbles was found to be initiated at 240°C, which closely corresponded to the thermal decomposition temperature of a sugar acid. Kraft lignin appeared to have a major influence on the viscous properties of the pyrolyzing particle. The composition of black liquor determines to a large extent the surface active and viscous forces present in black liquor; these forces are believed to be responsible for the extent to which kraft black liquors deform and swell during pyrolysis.

INTRODUCTION

The kraft process is the dominant pulping process today for paper grade pulps. Kraft pulp represents 74% of North American market pulps (1). An advantage of kraft pulping is the efficient recovery of the chemicals and the energy value from its spent pulping liquor. This aqueous solution from the process, kraft black liquor, contains dissolved organic and inorganic solids. In the recovery process, kraft black liquor is concentrated to approximately 65% solids content and combusted. The burning of organics contained in kraft black liquor provides a significant amount of energy, which is used to produce steam. The resulting char is then smelted to recover the inorganic chemicals for reuse in the pulping process. Both steam generation and smelting occur in the same process unit, the recovery boiler.

Kraft recovery boilers typically operate at full solids capacity, leaving little leeway for

upsets. Any interruption in the furnace operation can have an immediate detrimental effect on the operation of an entire mill. Steady-state combustion in the recovery furnace is thus of particular importance in maintaining efficient pulp production.

A blackout is defined as the loss of liquor ignition in the recovery boiler and can result in a significant amount of recovery boiler downtime. Some mills have experienced blackouts which appear to be linked to variations in the properties of black liquor (2). The cause of this poor combustion could not be determined from conventionally measured properties (heat value, solids content, specific gravity, and viscosity). Reduced swelling of black liquor has been observed in liquors exhibiting poor combustion characteristics (3,4).

Black liquor swelling is an important process during combustion. Swelling of black liquor particles increases the surface area available for reaction with oxygen and thus improves the combustibility of black liquor. Changes in the swelling of black liquor would alter the flight paths of black liquor particles in a recovery furnace. Excessive swelling of particles can lead to increased entrainment of black liquor char in air. The char becomes deposited on the upper portions of a recovery furnace and leads to increased downtime. These factors indicate that the potential exists for an optimum amount of black liquor swelling during combustion to maintain efficient recovery furnace operation.

Unfortunately, there are limited data on black liquor swelling during pyrolysis (3-6). Studies performed to date have been limited either by empirical analysis, low temperatures or the inability to monitor the swelling process as a function of time.

The present study was undertaken to investigate the swelling characteristics of kraft black liquor during pyrolysis. The objectives were to quantify the swelling and to determine the factors which contribute to swelling. The variables thought to be of importance in swelling were the heating rate, gas temperature, moisture content of the particle, particle size, and the black liquor composition.

An earlier paper discussed the effect of heating rate, particle size, pyrolysis temperature, and moisture content on the swelling of kraft black liquors during pyrolysis (7). The present paper discusses the effect of black liquor composition on the swelling of kraft black liquor. The components studied were kraft lignin, sugar acids, extractives, and the inorganic salts. Additional work involving the effect of initial black liquor solid content on swelling will also be discussed.

APPROACH

The reactor used for this study allowed one to view the swelling of black liquor particles during evaporation and pyrolysis. It is shown in Fig. 1. Details of the experimental apparatus, the experimental procedures, and the material preparation can

be found in the appendix. Black liquor particles were placed on a wire which was connected to a microbalance. The particles were heated by flowing a hot nitrogen gas stream past the particle. Heat transfer occurred primarily by convection, with some radiative heat transmitted to the particle from the surrounding reactor walls. Heat fluxes in the reactor were calculated from experimentally determined evaporation rates of water from small metal cups. Heat fluxes which were comparable to those found in commercial recovery furnaces (100 kW/m^2) could be attained at 900°C (7).

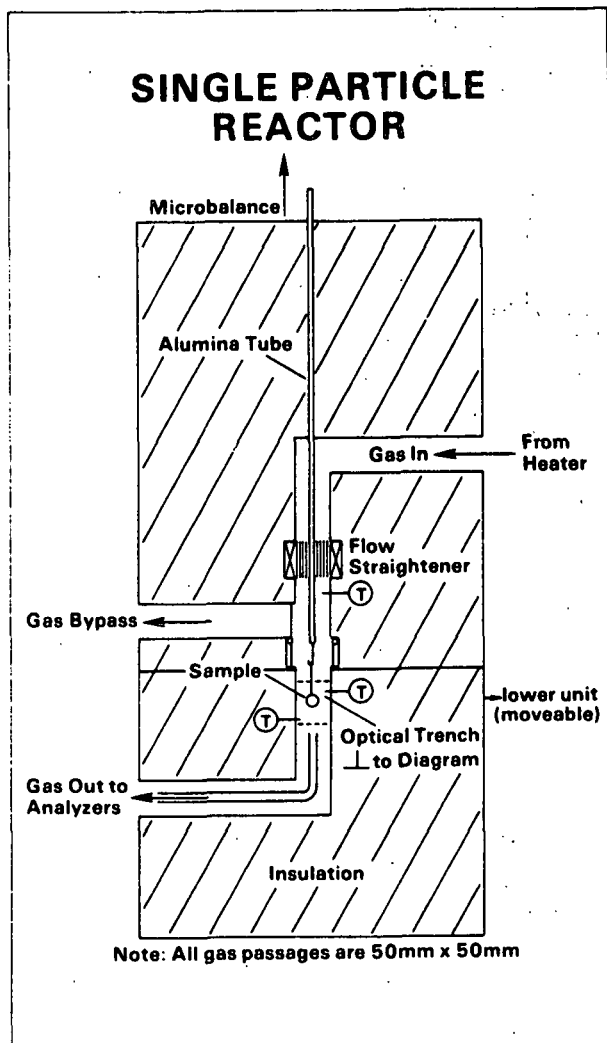


Fig. 1 Schematic of single particle reactor.

An optical port was available for viewing and taking photographs of the black liquor particles. The volume of the particles could be inferred from the projected area of the particle measured from photographs. The volume measurements given in the text were divided by the original dry solids weight of the particle; this way, particles differing in particle size and moisture content and that were pyrolyzed at different temperatures are compared on initial dry solid weight basis. A gas sampling

line below the particle allowed for the analysis of CO , CO_2 and H_2O . Data acquisition was performed by a microcomputer with an analog/digital interface.

The process variables were studied in an earlier paper (7). The particle size (1-4 mm in diam.) had no effect on the maximum particle volume. The heating rate could be changed qualitatively by changing the gas flow rate in the reactor. An increase in the heat flux shortened the time of pyrolysis but had no effect on the maximum volume attained; thus, the heating rate effectively changed the rate of swelling.

The effects of the gas temperature and of the moisture content are shown in Fig. 2. The swollen volume of black liquor particles attained a maximum at 500°C . Moisture present in black liquor increased swelling during pyrolysis between 400 to 600°C . The effect of moisture on swelling was not additive, as 65 and 80% solids black liquor behaved similarly. The swelling was found to occur during the evolution of pyrolysis gases; however, there was no correlation found between the amount of pyrolysis gas evolved and the amount of swelling.

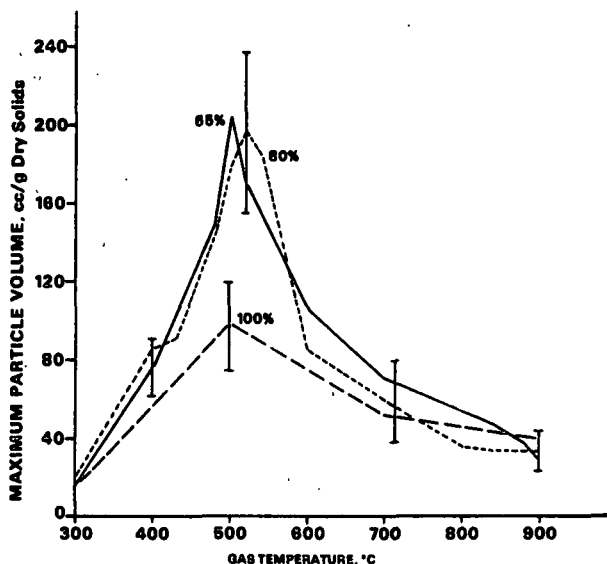


Fig. 2 Maximum particle volume vs. gas temperature for 65, 80 and 100% solids black liquors. Brackets indicate ± 1 std. deviation.

The compositional variables studied were kraft lignin (KL), sugar acids (SA), inorganic salts, and extractives. Kraft lignin was precipitated from the black liquor by acidification to pH 2.5 with $1\text{N H}_2\text{SO}_4$. After removal of kraft lignin and some of the inorganics, the solution contained the sugar acids from black liquor. The isolated kraft lignin and sugar acid solutions were in their acidic form. To simulate the alkaline conditions of kraft black liquors the pH was raised to 12 by using 1N NaOH . A 20% by weight solution of sodium sulfate was used to simulate the inorganic salts found in black liquor. The effect of extractives on the swelling of black liquor was studied in two ways: 1) the

extractives were isolated and added back to black liquor and 2) the black liquor from cooks of extractive-free wood were compared to black liquor derived from wood containing extractives.

The pyrolysis of black liquor could be tested by placing black liquor on a small wire. The sugar acids were not viscous enough to remain attached to the wire during pyrolysis. Small metal cups were used to hold the material during pyrolysis. The metal cups were found to reduce swelling but influenced the various samples in the same manner.

RESULTS

Preliminary tests revealed that a combination of kraft lignin and sugar acids swelled to a greater extent than either component tested separately. The extractives and inorganics were found to reduce swelling. Figure 3 shows the influence of pH and sugar acid/kraft lignin ratio on swelling at 500°C. Table 1 shows that the synergistic effect of KL and SA on swelling also occurred at 900°C.

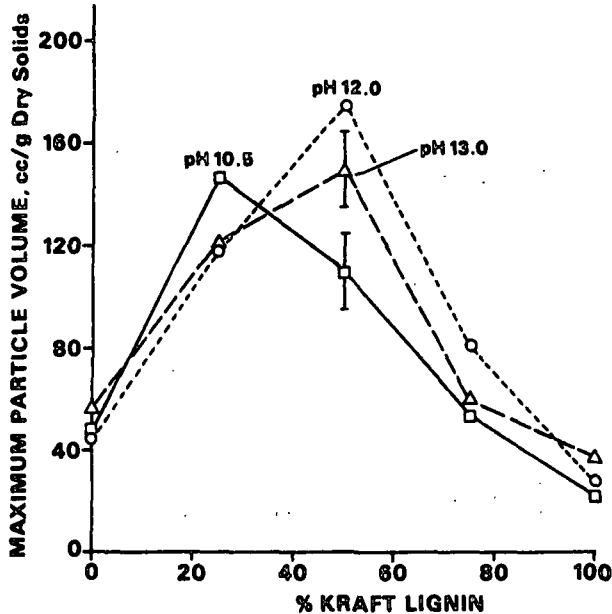


Fig. 3 Maximum particle volume of kraft lignin/sugar acid mixtures at different pH, pyrolyzed at 500°C. Brackets indicate ± 1 std. deviation.

Table 1 Swelling of sugar acids (SA), kraft lignin (KL) and a KL:SA mixture (900°C, pH 12), pyrolysis occurred in small metal cups

Component	SA	KL	SA:KL 1:1
Volume (cm ³ /g)	19	15	76
	24	27	84
	22	21	59
	23	29	53
Mean	22	23	68

LSD - 15 cm³/g, least significant difference (LSD), 95% confidence

The data in the figures represent at least three replications; variability in the figures is represented by plus or minus one standard deviation. The least significant difference (LSD) statistic was the criterion used to determine whether the means of the experimental data presented in the tables were significantly different from one another. The LSD represented the difference required between two means to be able to detect a difference at the 95% confidence level.

Figures 4-6 show the release of carbon dioxide during the pyrolysis of SA, KL, and a 1:1 mixture of the two components. The dashed lines represent the time at which photographs had been taken. The volume of the particle is given above the dashed line. The solid line in Fig. 4 indicates the point at which the lignin solidified. The solid line in Fig. 6 indicates the point at which significant swelling started for the SA/KL mixture.

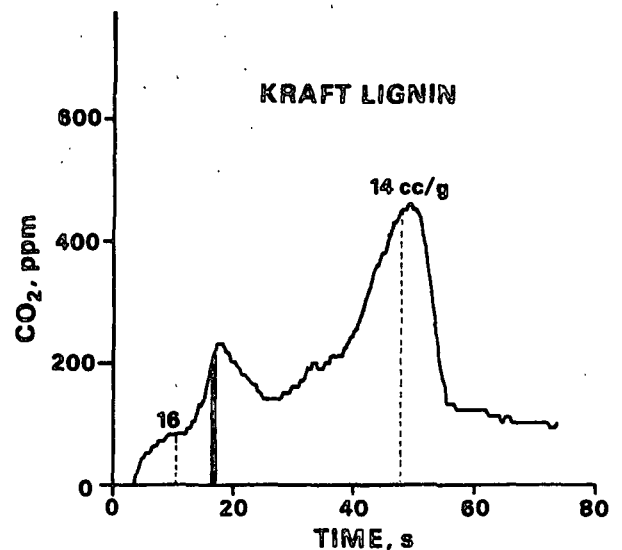


Fig. 4 Carbon dioxide vs. time for kraft lignin pyrolyzed at 500°C (99 mg, 46% solids). Photographs are indicated by dashed lines. Solid line indicates point at which material became a rigid structure.

A solution of kraft lignin was separated into three fractions by ultrafiltration. These lignin fractions were mixed with sugar acids in a 1:1 ratio (dry weight basis) and pyrolyzed at 500°C. The results are shown in Table 2.

Inorganic salts and extractives were added to black liquor. The effect of inorganic salts was determined by adding a 20% by weight solution of sodium sulfate to black liquor. The results are shown in Fig. 7. The solid line indicates the volume expected if the sodium sulfate acted as a diluent.

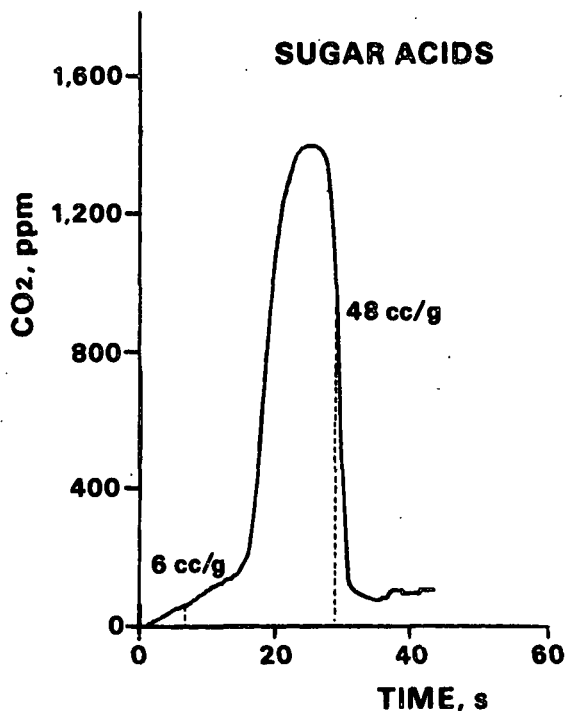


Fig. 5 Carbon dioxide vs. time for sugar acids pyrolyzed at 500°C (88 mg, 51%). Photographs are indicated by dashed lines.

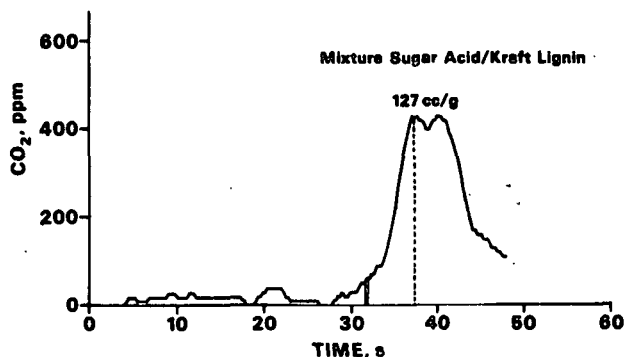


Fig. 6 Carbon dioxide vs. time for a 1:1 mixture of kraft lignin and sugar acids pyrolyzed at 500°C (123 mg, 48% solids). The solid line indicates point at which significant swelling began. The dashed line indicates the time at which a photograph was taken.

The extractives were isolated by TAPPI Standard T264 om-82 with approximately 7% of the wood removed as extractives. Three black liquors differing in extractive content are shown in Table 3. The normal liquor represents a black liquor with no extractives removed. The extractive-free liquor represents black liquor obtained from extractive-free wood. A sample of extractive-free black liquor was mixed with the isolated extractives (7% by weight). Figure 8 shows the effect of extractives added to extractive-free black liquor over a

range of addition levels. The solid line indicates the volume expected if the extractives acted as a diluent.

Table 2 Effect of kraft lignin molecular weight on the swelling of a 1:1 KL:SA mixture; pyrolysis occurred in small metal cups

MW of Kraft Lignin	High	Med.	Low
Volume (cm ³ /g)	44	78	123
	68	88	109
	33	97	106
	--	96	127
Mean	48	90	116
LSD - 21 cm ³ /g			

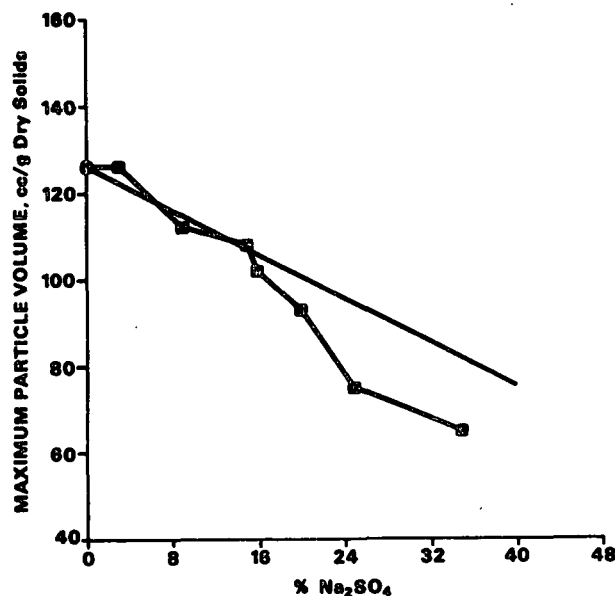


Fig. 7 Effect of Na₂SO₄ concentration on the maximum particle volume at 500°C. The solid line corresponds to Na₂SO₄ acting as a diluent to the swelling process.

Table 3 The effect of extractives on maximum particle swollen volume; pyrolysis occurred in small metal cups

Type	Normal	Ext. Free	Ext. Free + 7% Ext.
Volume (cm ³ /g)	48	109	26
	47	60	19
	44	95	31
		64	
Mean	46	82	25
LSD - 26 cm ³ /g			

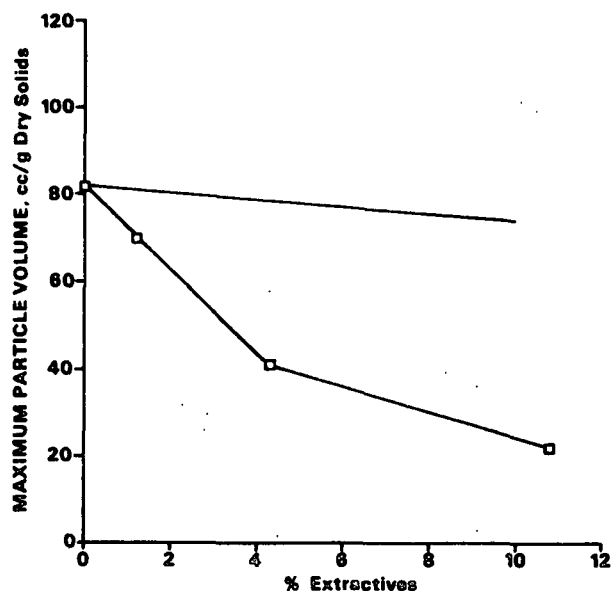


Fig. 8 Effect of extractive concentration on the maximum particle volume at 500°C. Solid line indicates relationship if the extractives were to act as a diluent and not participate in the swelling process.

Black liquors at a range of solids contents (65, 73, 86, 96 and 100%) were prepared for further study. The results are shown in Table 4. Three liquor samples (65, 86, and 100%) with distinctly different rheological properties were chosen for further study. The 65% black liquor was a viscous liquid, the 86% sample a tarry substance and the 100% sample a porous solid. The evolution of carbon dioxide and water vapor during pyrolysis of these black liquors is shown in Fig. 9.

Table 4 The effect of solids content on the maximum particle volume; pyrolysis occurred in small metal cups

% Solids	100%	96%	86%	73%	65%
Volume (cm ³ /g)	97	106	69	105	125
	79	91	63	101	115
	84	89	72	132	124
	--	83	87	136	--
Mean	87	95	68	113	121
LSD - 17 cm ³ /g					

DISCUSSION

The study of the process variables in an earlier paper (7) revealed that the evolution of the pyrolysis gases drove the swelling process. There was no correlation found between the amount of pyrolysis gases evolved and the change in volume for particles at a given temperature. The deformable properties of the black liquor during pyrolysis was hypothesized to determine the extent of swelling. The study of the compositional variables was initiated to further investigate this hypothesis.

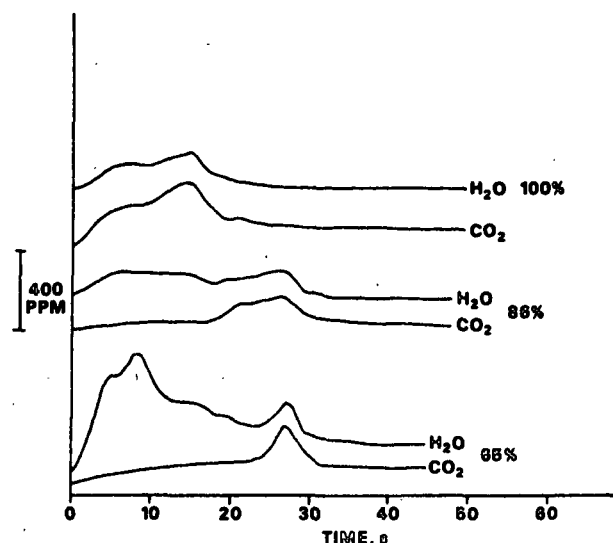


Fig. 9 The water vapor and carbon dioxide evolution curves of black liquor at 65, 86 and 100% solids (30-35 mg, 500°C).

An interaction between equal amounts (dry weight basis) of sugar acids and kraft lignin resulted in the highest swelling of black liquor regardless of the pyrolysis temperature (Fig. 3, Table 1). Figures 4-6 provide some evidence to explain the swelling behavior. Figure 4 shows that when a kraft lignin solution was pyrolyzed, it formed a rigid structure before a significant portion of the pyrolysis gases were evolved. The lignin solutions, when pyrolyzed showed some swelling during evaporation, but once the evaporation was complete no more swelling was observed.

Sugar acids evolved much more gas than kraft lignin as shown in Fig. 5. Expansion of the pyrolyzing sugar acids occurred throughout the pyrolysis process, similarly to black liquor. However, the sugar acids during pyrolysis were more fluid than black liquor and appeared to allow more of the gases to escape. The chars of sugar acids were spherical and composed of a very thin, fragile outside layer.

The combination of KL and SA in a 1:1 ratio (dry weight basis) produced the highest swollen volumes despite evolving a lower amount of pyrolysis gases than the sugar acids for an equivalent amount of starting material. The KL/SA mixtures appeared to have a higher viscosity than sugar acids during pyrolysis, which resulted in higher swollen volumes. The behavior and appearance of the chars from the KL/SA mixture were similar to those derived from black liquor.

The ionization of kraft lignin appears to be important for swelling. The highest swelling occurred when the lignin was fully ionized at pH 12. At pH 10.5 some of the higher molecular weight lignin precipitated out, which adversely affected the swelling at a 1:1 KL:SA ratio. Increasing the pH to 13 did not significantly influence the

swelling, indicating the sodium hydroxide was not directly involved in the swelling mechanism. The effects of pH above 10.5 on swelling were relatively small and were not studied further.

Polydispersity of kraft lignins has been repeatedly reported (8). The kraft lignin was separated into three fractions by ultrafiltration. The single fractions were then mixed with sugar acid solution to simulate black liquors. Liquor containing the higher molecular weight (HMW) fraction of kraft lignin was found to swell significantly less than liquors containing the lower molecular weight (LMW) fractions. A possible explanation for this occurrence was that the low molecular weight lignins increased the surface area available for association with the sugar acids.

Figure 7 shows that sodium sulfate acted as a diluent in the swelling of black liquor up to a 20% by weight addition level. The 25 and 35% data points are significantly different (95% confidence) from the diluent line, which indicated the sodium sulfate interfered with the swelling mechanism at these concentrations. An explanation for this occurrence is not obvious. The results suggest that under the conditions found in a recovery boiler [8-20%, $\text{Na}_2\text{SO}_4 + \text{Na}_2\text{CO}_3$ (9)] the inorganic salts act as a diluent and are not directly involved in the swelling mechanism.

The extractives significantly reduced the swelling behavior of black liquor. The evolution of carbon dioxide from pyrolyzing black liquor particles with and without extractives is shown in Fig. 10 and 11. The dashed lines indicate when photographs were taken, with the volumes indicated above the lines.

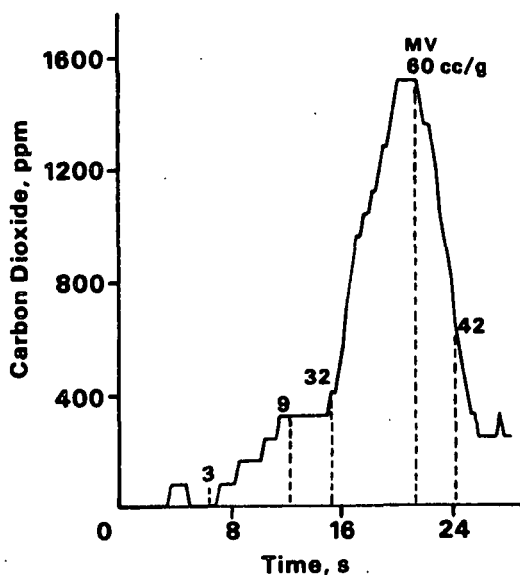


Fig. 10 Carbon dioxide evolution profile for an extractive-free black liquor particle (500°C 63%, 38.4 mg). Photographs indicated by dashed lines, with swollen volumes above them. MV indicates maximum volume.

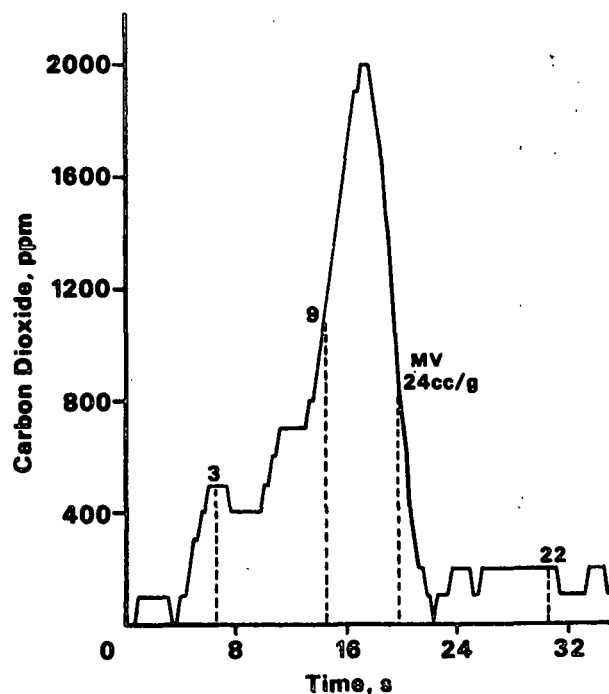


Fig. 11 Carbon dioxide evolution profile for an extractive free black liquor with 8% extractives added (63%, 30.0 mg, 500°C). Photographs indicated by dashed lines, with volumes above them. MV indicates maximum volume.

The particles in Fig. 10 and 11 swelled significantly through the pyrolysis reactions. An indication of the deformability of the char was the shrinking behavior of particles during the decrease in pyrolysis activity. The extractive-free liquor shrank about 30% after reaching maximum volume. The black liquor containing 8% extractives shrank less than 10% after reaching maximum volume. No difference existed in the amount of carbon dioxide given off by particles differing only in extractive content. This indicated the extractives influenced the swelling by changing the deformable characteristics of black liquor and did not influence the extent of volatilization reactions during pyrolysis.

Since the viscous properties of pyrolyzing materials could not be measured, the surface features of high and low swelling chars were analyzed with a scanning electron microscope (SEM). The objective of this effort was to determine any differences in char structure which might help explain the swelling phenomenon. The highly swollen chars were obtained from extractive-free black liquor and LMW KL:SA (1:1). The low swollen volume chars analyzed were black liquor with 8% extractives and HMW KL:SA (1:1). Figures 12-14 show three SEM photographs of chars from black liquor.

Figure 12 shows the formation of bubbles in an extractive-free black liquor particle that was quenched midway through pyrolysis. Figure 13 shows the collapsed bubbles of a char from the same black

liquor after pyrolysis was completed. The bubbles were approximately 50-100 microns in diameter. Analysis of LMW KL:SA systems showed the same type of bubble formation. The black liquor with extractives did not exhibit this feature as shown in Fig. 14. The HMW KL:SA also did not exhibit the formation of bubbles. The results indicated the formation of small bubbles could be necessary to produce highly swollen chars of kraft black liquor. Work with light microscopes confirmed that the structures observed in the SEM were bubbles. The formation of bubbles indicated surface tension could be playing an important role in swelling.

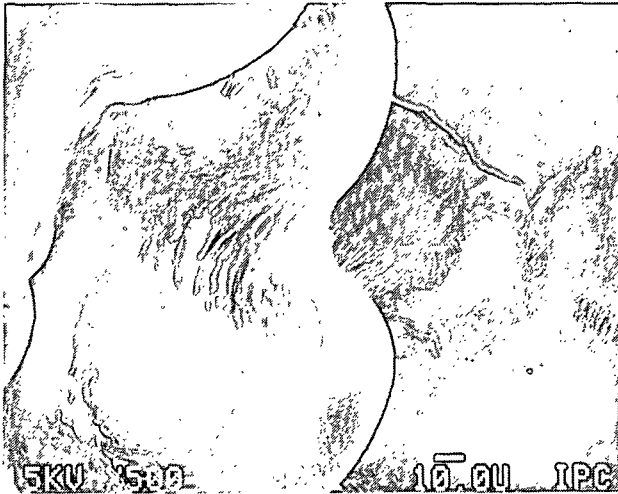


Fig. 12 SEM photograph of an extractive free black liquor quenched midway through pyrolysis.



Fig. 13 SEM photographs of char resulting from the pyrolysis are of an extractive-free black liquor.

The analysis of black liquors differing only in solids content was further investigated. Black liquor above 85% solids swelled to a lesser extent than black liquors below 80% solids for black

liquors pyrolyzed between 400 to 600°C. Figure 15 shows the swelling during pyrolysis of four particles each at a different solids content. For the discussion 86C will be used to designate a char particle pyrolyzed from an 86% black liquor sample.



Fig. 14 SEM photograph of char resulting from the pyrolysis of black liquor containing 8% extractives.

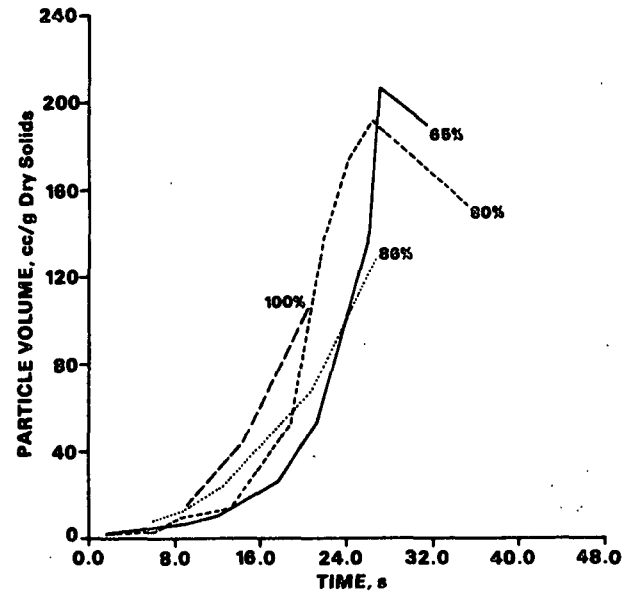


Fig. 15 Particle volume vs. time for black liquor particles differing in original solid content (500°C, 30-40 mg).

The higher swollen chars (65C and 80C) went through an evaporation stage which produced rapid expansions and contractions that were followed by rapid swelling rates. The black liquor with higher solid contents swelled to a larger extent early in the pyrolytic process but never attained the high swelling rates achieved by the lower solid content liquors. This resulted in higher swollen volumes

for the particles that went through a rapid evaporation phase relatively free from pyrolysis.

The carbon dioxide and water vapor release profiles of particles differing in solid contents are shown in Fig. 9. Evaporation and pyrolysis occur as separate processes when subjected to the heat fluxes found at 500°C. The solids content of the black liquors influenced not only the evaporation rate of black liquor but could also influence the subsequent pyrolysis and swelling processes. This was indicated by the broad water vapor (evaporation) and carbon dioxide (pyrolysis) peaks of the 86% solids black liquor (Fig. 9).

Analysis of the surface features of chars differing in solid contents revealed the formation of small bubbles. Thus, the differences in swelling behavior due to the original solids content of black liquor cause a more subtle difference in the pyrolysis of the material. Char particles were analyzed by CP/MAS ¹³C NMR to try and determine major chemical differences which might reflect the swelling behavior. The results of the NMR analysis are shown in Table 5.

Table 5 The swelling and structural characteristic of chars differing in original solids contents. Corrected structural intensities from CP/MAS ¹³C NMR. Pyrolysis at 500°C.

% Solids	65%	73%	86%	100%
Vol. cm ³ /g	121	113	68	87
Corrected Int.				
Carboxyl (165-220 ppm)	10.2	11.3	8.2	8.6
Aromatic (90-165 ppm)	61.4	60.0	65.2	61.1
Aliphatic (90- -30 ppm)	30.6	30.3	29.2	32.31

The aliphatic content did not vary significantly between the chars. The aromatic content was higher for the 86C than the other chars (65C, 73C, 100C). The pyrolysis process was significantly slower for the 86C sample than the others, which may have led to the higher aromatic content. The slower pyrolysis of the 86C was evidenced by the broad pyrolysis peak in Fig. 9 relative to the other chars (65C, 100C).

The carboxyl content of the chars correlated well with the swelling characteristics of the chars. The higher swelling chars (65C and 73C) had a higher carboxyl content than the lower swelling chars (86C and 100C). The chars with similar swelling characteristics also had similar carboxyl contents (65C and 73C, 86C and 100C). The carboxyl content can be attributed to the sugar acid fraction of black liquor.

The ultrafiltration process separates lignin by size. The differences in size of the lignin are not true molecular weight differences but differences in the size of the aggregates of lignin molecules. Fractions of lignin isolated by ultrafiltration can have different physical and chemical

properties. In view of the possible importance of surface active functional group concentration per volume, these differences may influence the swelling behavior observed for the different "molecular weight" fractions of kraft lignin mixed with sugar acids. More work is required to clarify the effect of kraft lignin molecular weight on the swelling behavior of kraft black liquor during pyrolysis.

A hot stage microscope was used to study the swelling behavior of black liquor up to 300°C. The formation of small bubbles occurred at approximately 240°C for both black liquor and a solution of sugar acids. Decomposition of a sugar acid at 250°C was found to occur by Shafizadeh *et al.* (10).

Kraft lignin appeared to control swelling by having a major influence on the viscous properties of KL:SA mixtures. The formation of bubbles occurred at low temperatures and was associated with the decomposition of sugar acids. Higher temperatures resulted in higher swollen volumes which appeared to be related to a more deformable material.

As the pyrolysis temperature was increased past 500°C the swollen volume of chars decreased. This was most likely due to an increase in the rate of char formation. Particles subjected to a nitrogen gas stream at 900°C for a few seconds were taken out and examined. The inside of the particles were still a viscous fluid surrounded by char. The particle size was approximately 3 mm in diameter (comparable to what may be found in a commercial recovery furnace). This indicated that phenomena occurring at lower temperatures (< 500°C) were responsible for the swelling behavior at higher temperatures.

SUMMARY OF FINDINGS

Kraft lignin and sugar acid mixtures swelled more during pyrolysis than either component tested separately. A 1:1 mixture of these two components resulted in the highest swollen volumes of black liquor chars for a given temperature. The addition of extractives interfered with the swelling mechanism. The addition of sodium sulfate, which represented inorganic salts, acted as a diluent up to a 20% by weight addition level.

The formation of bubbles (50-100 microns in diameter) appeared to distinguish highly swollen chars (extractive-free black liquor, LMW KL:SA) from low swollen chars (black liquor with extractives, HMW KL:SA). A correlation was found between the swelling behavior and the carboxyl contents of chars pyrolyzed from black liquors differing only in moisture content. The formation of bubbles was found to initiate at 240°C for black liquor and a sugar acid solution. These observations indicated surface active forces play an important role in the swelling of black liquor during pyrolysis. The analysis of extractive content, kraft lignin molecular weight, and the pyrolysis temperature indicated viscous forces also play an important role in black liquor swelling.

CONCLUSIONS

The rheological properties, although not measured directly, appeared to determine the extent of

swelling during black liquor pyrolysis. An interaction between the sugar acids and kraft lignin in black liquor was responsible for the swelling behavior during pyrolysis. The decomposition of saccharinic acids below 300°C resulted in the formation of bubbles (50-150 microns in diam.); this process appeared to be necessary for highly swollen chars. Kraft lignin appeared to influence swelling by affecting the viscous properties of black liquor during pyrolysis. Pyrolytic decomposition of organic materials at relatively low temperatures (230-500°C) was responsible for the swelling behavior of black liquor at higher temperatures (500-900°C).

ACKNOWLEDGMENT

Portions of this work were used by one of the authors, P. T. M., as partial fulfillment of the requirements for the Ph.D. degree at The Institute of Paper Chemistry. The authors also want to thank the Department of Energy, the Weyerhaeuser Paper Company, and the University of Maine at Orono for their assistance on selected aspects of this study.

LITERATURE CITED

1. Mies, W. E., Allen, D. R., Pollitzer, S., Adams, D., and Espe, C., *Pulp and Paper '84, '85 North American Fact Book*, Miller Freeman Publications, San Francisco, CA, 1985:237.
2. Kubes, G. J., Fleming, B. I., MacLeod, J. M., and Bolker, H., *J. Wood Chem. Technol.*, 2(3): 279(1982).
3. Baklien, A., *Appita*, 14(1): 5(1960).
4. Oye, R., Hato, N., and Mizuno, T., *Jap. Tappi*, 27(2): 71(1973).
5. Kubes, G. J., *Trend (PPRIC)* (32), 8(Winter 1982/1983).
6. Oye, R., Langfors, N. G., Phillips, F. H., and Higgins, H. G., *Appita*, 31(1): 33(1977).
7. Miller, P. T., and Clay, D. T., Presentation at AIChE Mtg. Seattle WA, Aug. 26-28, 1985.
8. Sarkanen, K. V., and Ludwig, C. H., *Lignins - Occurrence, Formation, Structure and Reactions*. Wiley Interscience, 1971:695.
9. Passinen, K. *Proc. Symp. Rec. Pulp. Chem. IUPAC-EUCEPA, Helsinki, Finland, 1968 Eng. Translation:188-209*.
10. Shafizadeh, F., Lai, Y. Z., *Carbohy. Res.*, (42): 39-53(1975).
11. Alen, R., Sjoström, E., *Paperi Puu*, 62(5): 328-30(1980).
12. Alen, R., Sjoström, E., *Paperi Puu*, 62(8): 469-71(1980).

APPENDIX

Apparatus

A schematic of the single particle reactor is shown in Fig. 1. The particles were heated by a gas stream in a 50 mm x 50 mm channel. The reactor consisted of a movable lower unit and a stationary upper unit. The hot gas flowed from an electric heater through two bends, past a flow straightener and down to the particle. The gas flow could be diverted by a damper ahead of the particle. The temperature was controlled by the setpoint of the thermocouple (SP) which was located above the damper. Two thermocouples (BD) and (BS), which were located above and below the sample, were used to determine the gas temperature at the particle location.

The particle was attached to a Cahn 2000 microbalance via a wire enclosed in an alumina tube. A gas sampling line located right below the particle was used to withdraw gas samples at a constant flow rate. An Infrared Industries Inc. Model 702 gas analyzer was used to monitor the evolution of CO₂ and CO. The system had a 4.0 second delay time and a first order time constant of 3.6 seconds. A Beckman Industries Model 865 infrared H₂O analyzer monitored the water vapor content of the gas stream. When the H₂O unit was installed, there was a 2.7-second delay time between units. The water vapor meter had a first order time constant of 3.0 seconds. An optical trench allowed the particle to be viewed and photographed. A 35-mm camera equipped with a zoom lense and an autowinder was used to take photographs.

The analog signals from the instruments were converted to digital signals and stored on disk by a data acquisition system. Computer programs were written that stored the following information: time, particle mass, gas temperature, CO, CO₂, and H₂O concentration and a camera switch reading. The data could be collected about seven times a second. The camera switch reading recorded by the computer was simply an on-off switch connected to the camera switch; in this way one could automatically record the times at which photographs were taken.

A test consisted of the following sequence of events: 1) switching the gas stream from air to nitrogen, 2) diverting the gas stream to the gas by-pass duct, 3) lowering the lower compartment, 4) starting the data acquisition program, 5) attaching the particle to the microbalance, 6) raising the lower compartment and 7) switching the gas flow to the particle. Zero time was defined as the time at which the temperature measured at thermocouple (BD) began to rise.

Preparation of the Black Liquor Samples

Black liquors were obtained from kraft laboratory cooks of loblolly pine chips. The cooking conditions are given in Table 7. The black liquor was concentrated to approximately 25% solids on a hot plate, and the soap residues were skimmed off

before evaporation in a rotary vacuum evaporator. Some of the liquors used for the study of the effect of extractives on swelling were not skimmed. These black liquors were evaporated in a rotary vacuum evaporator under a 95 kPa vacuum in a water bath at 80°C.

Table 7 Kraft cooking conditions - loblolly pine

Sulfidity	25%	Time to temp.	90 min
Eff. alkali	16%	Time at temp.	94 min
Liquor/wood	4	Cooking temp.	173°C
H-factor	2000		
Results			
Yield	45.7%		
Kappa no.	25.7	BL solids	16.5%

Black liquor was evaporated in the rotary vacuum evaporator until a solids content of approximately 65% had been reached. Samples between 73 and 96% solids were obtained by placing black liquor at 65% solids in an oven under a 95 kPa vacuum at 90°C. Samples were taken out periodically so that a range of moisture contents were obtained. A 100% dry solids black liquor was obtained by allowing the liquor to dry overnight.

Loblolly pine was extracted according to TAPPI Standard T264 om-82. The first extraction lasted 8 hours and consisted of a 1:2 volume basis of 95% ethyl alcohol and benzene. Next, the wood was extracted with 95% ethyl alcohol for four hours. Finally, the chips were placed in boiling distilled water for one hour.

The first extractives were concentrated to about 60% in a rotary vacuum evaporator at 95 kPa vacuum at 60°C. This solution was mixed with black liquor. The solvent mixture (alcohol-benzene) was found to have no effect on the swelling of black liquor.

Measurement of Black Liquor Char Volume

An indirect measurement of particle volume was sought in order to gain a better understanding of the kraft black liquor swelling. The analysis of photographs with a planimeter was used initially and found to be acceptable. A planimeter was used to measure the projected area of a particle obtained from a photograph. A spherical volume was calculated by assuming that the area represented a circle. The volume calculated was used for the black liquor char volume. A photograph of a ball bearing in the reactor was used for calibration purposes. This method was compared to a direct measurement technique developed earlier (7). The two methods agreed with each other by approximately $\pm 5\%$ for a number of char particles tested which varied in size and shape.

Preparation of the Components of Black Liquor

A loblolly pine kraft black liquor at approximately 17% solids was heated on a hot plate to approximately 30% solids. Any soap formed during the evaporation was skimmed off. The black liquor solution was then diluted with distilled water to approximately 15% solids. The pH was gradually lowered to pH 2.5 with 1N H₂SO₄. The solution was centrifuged for an hour at 2000 rpm. The precipitated kraft lignin was washed and centrifuged two times.

The remaining filtrate was concentrated (almost to dryness) in a rotary vacuum evaporator at 95 kPa and 80°C. Acetic acid corresponding to double the volume of the sugar acid solution was added and allowed to stand overnight. The precipitated inorganic material was removed. After vacuum evaporation a syrupy product was obtained. Distilled water was added to give about a 30% solution.

The solution was then passed through a column of Dowex 50-X8 (H⁺) ion exchange resin (100 cm³ of resin to 250 cm³ solution). The solution was then mixed with Dowex 3 (OH⁻) for approximately 10 minutes (50 cm³ of resin to 250 cm³ of solution). The solution was next passed through a column filled with adsorbent resin (Amberlite XAD-8, 250 cm³ resin to 50 cm³ solution). The solution was then placed in a beaker with Amerlite XAD-2 and allowed to stand overnight. This solution was then evaporated in a rotary vacuum evaporator to approximately 30% solids. The procedure basically follows that given by Alen and Sjoström (11,12) yielding what was termed the "crude" hydroxy or sugar acid fraction.

The ultrafiltration of the isolated kraft lignin was performed at the University of Maine at Orono. The sample of kraft lignin was made alkaline (pH 13) by the addition of 1N NaOH and diluted to a 1% solids solution. The lignin solution at 60°C was put through the filtration process for a few minutes.

The concentrate retained on the 50,000 MWCO membrane represented the high molecular weight fraction. The medium molecular weight fraction consisted of those lignins which passed through the 50,000 MWCO membrane but were retained by the 20,000 MWCO membrane. The lignin which passed through the 20,000 MWCO membrane was used for the low molecular weight fraction.

When the materials were concentrated to a higher solids content (> 20%), none of the samples swelled to a large extent. Upon concentration the caustic levels (inorganics) were too high for swelling to occur. The samples were acidified, washed and then brought back up to a pH of 12. This produced samples which swelled upon pyrolysis.

SULFUR RELEASE AND RETENTION DURING COMBUSTION OF KRAFT BLACK LIQUOR

James G. Cantrell and David T. Clay

ABSTRACT

Single droplets of black liquor were burned under a variety of conditions to study sulfur release and retention. The significant influencing variables, in decreasing order, were droplet size, solids content, and the oxygen content of the surrounding gas. In general, the sulfur release and the reaction rate decreased with larger droplets, higher solids, and higher oxygen levels.

INTRODUCTION

Black liquor is a substance produced from the kraft pulping process. It contains the dissolved lignin, various organic by-products and the spent cooking chemicals, including sodium sulfide, sodium carbonate, sodium sulfate, sodium hydroxide and various sodium organic compounds. It is concentrated to 65-75% solids before being sprayed into the recovery boiler. In the recovery furnace, the organics are combusted, with the resulting energy release used for steam generation. More importantly, the cooking chemicals, sodium sulfide and sodium carbonate, are recovered as smelt from the furnace.

The kraft process is unique because it uses sodium sulfide, which produces greater fiber strength and results in a higher yield. Although the use of sodium sulfide has great advantages, the introduction of sulfur into the pulp mill causes potentially odorous emissions from the recovery boiler. Strict EPA guidelines on total reduced sulfur gas release and the high cost of makeup cooking chemicals makes the recovery of sulfur an absolute necessity. Other problems associated with high levels of sulfur gas emission are corrosion of boiler tubes and harder to remove tube deposits. Although most of the sulfur can be recovered as sodium sulfate in electrostatic precipitators or in sulfur dioxide scrubbers, the preferred and more economical way of maximizing the recovery of sulfur is to control it at the source, which is the burning particle.

Most of the studies on sulfur gas release have been mill studies on recovery boilers (1,2). These studies have indicated that spray coarseness and solids content have a significant effect on sulfur gas release. Coarser sprays and higher solids content reduce sulfur gas release. Only recently has the combustion of black liquor been studied on single particles (3-5). From these

studies, various stages of combustion were identified as follows: (I) drying, (II) pyrolysis and combustion of volatiles, (III) char burning and (IV) inorganic reactions.

The present study uses the single particle burning technique to observe the effect of the important process variables including particle size, solids content, added sulfur (either as sodium sulfate or emulsified), and oxygen content of the gas stream. The purpose of this work was to gain a better understanding of the kinetic release of sulfur gas in the recovery boiler in order to minimize sulfur losses from the recovery boiler furnace cavity.

APPROACH

The radiant single particle reactor used for this study is shown in figure 1. The description and major details of the apparatus, procedure, black liquor synthesis and data analysis are given in the appendix. A black liquor particle was placed within the reactor. As the burning proceeded, air, nitrogen or a mixture of the two, entered the gas inlet and carried the combustion gases through the outlet. The major mode of heat transfer to the particle was by radiation. The furnace temperature was maintained at about 1090 deg C for all experiments. Combustion gases leaving the gas outlet proceeded to a sulfur dioxide analyzer, which measured sulfur dioxide concentration as a function of time. A computer in conjunction with an analog/digital interface was used for data acquisition.

The major process variables studied were particle size, solids content, added sulfur and gas stream oxygen content. Particle size and solids content were varied at four different levels with each combination being studied. The

RADIANT SINGLE PARTICLE REACTOR

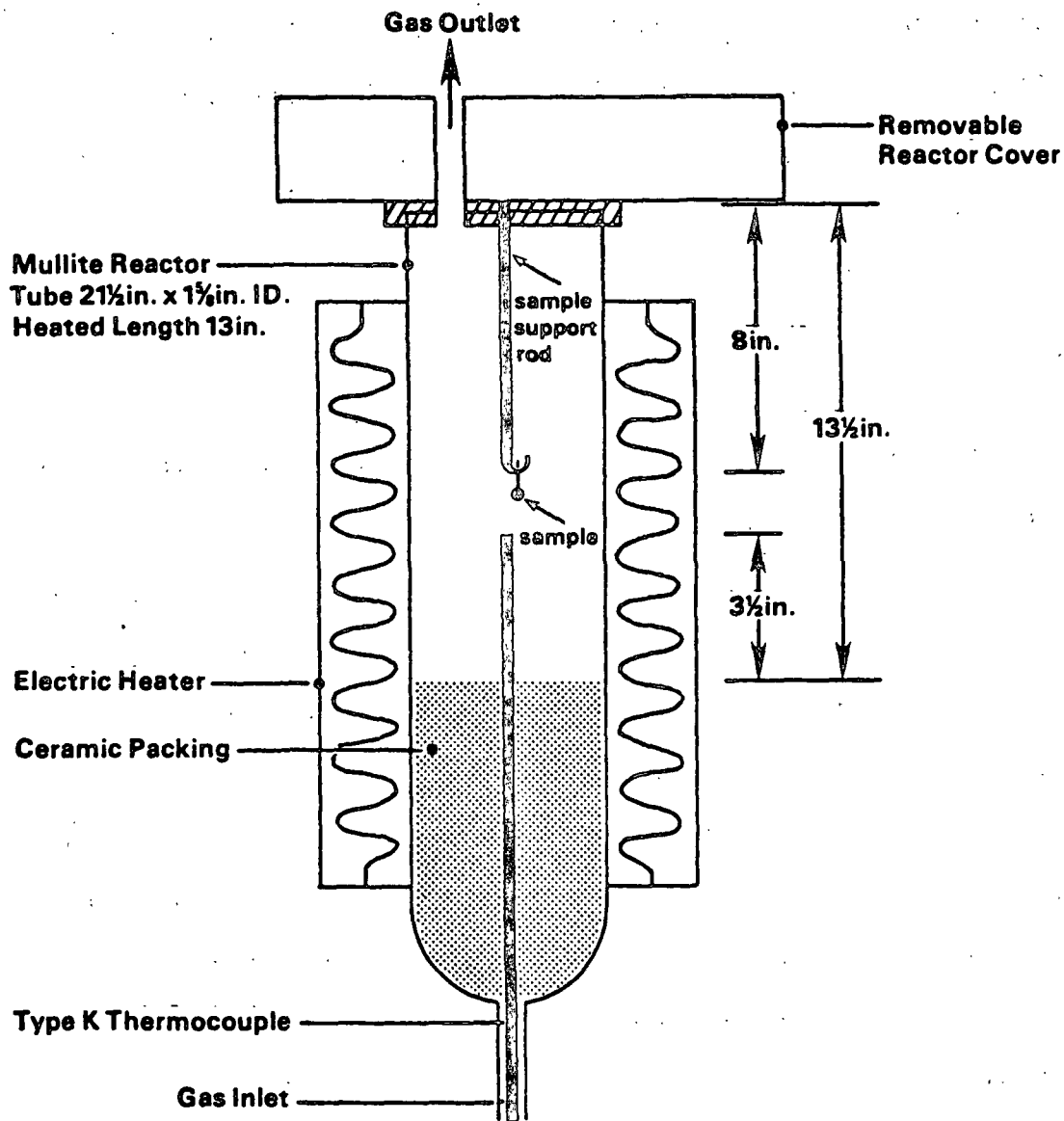


Figure 1. Radiant Single Particle Reactor

particle size and solids content that maximized sulfur release were used in the added sulfur and gas stream oxygen content experiments. All conditions used in the experimental runs are given in table 1.

RESULTS

Particle size had the greatest effect on sulfur gas release. From figure 2, one can see that as particle size is increased the total sulfur released decreases in an exponential fashion approaching some constant value. Also, as particle size is increased, the rate constant decreases as seen in figure 3.

Solids content had only a moderate effect on sulfur release. As solids content increases, the total sulfur released decreases. This effect becomes much less noticeable as particle size increases. For large particles, it appears that the particle size effect is controlling as can be seen in figure 4. The rate constant decreases as solids content increases until it reaches a minimum at about 85% solids. Then the rate constant begins to increase rather sharply as dry solids content is approached as shown in figure 5.

Although the oxygen content of the gas stream did not affect the normalized rate of sulfur release, it had a significant effect on the total sulfur released. At about 13% oxygen the percent total sulfur released reaches a maximum of about 75% for this particular system. This can be seen in figure 6.

Table 1. Particle Burn Conditions

Experiment	Diameter (mm)	% Solids	% Sulfur (E or S)	% Oxygen
Size + % Solids	1.0	63.3	3.34	21.0
"	2.0	"	"	"
"	3.0	"	"	"
"	4.0	"	"	"
"	1.0	71.9	"	"
"	2.0	"	"	"
"	3.0	"	"	"
"	4.0	"	"	"
"	1.0	83.3	"	"
"	2.0	"	"	"
"	3.0	"	"	"
"	4.0	"	"	"
"	1.0	98.9	"	"
"	2.0	"	"	"
"	3.0	"	"	"
"	4.0	"	"	"
Added Sulfur	2.0	63.3	"	"
"	"	64.4	4.29 E	"
"	"	66.1	5.26 E	"
"	"	63.9	5.59 S	"
"	"	68.0	6.17 E	"
% Oxygen	"	63.3	3.34	21.0
"	"	"	"	15.4
"	"	"	"	10.5
"	"	"	"	5.6
"	"	"	"	0.0

E = added as emulsified sulfur

S = added as sodium sulfate

Furnace temperature = 1090 deg C

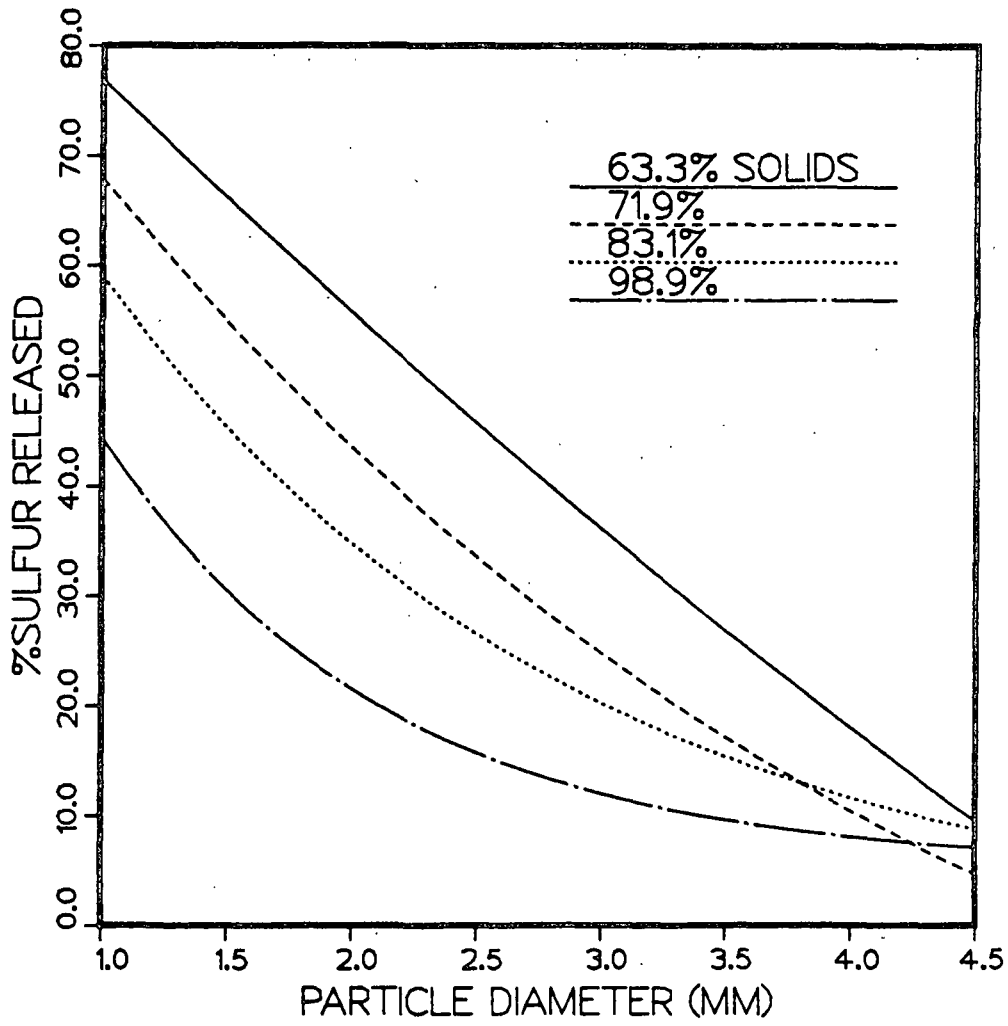


Figure 2. % Initial Sulfur Released vs. Particle Diameter

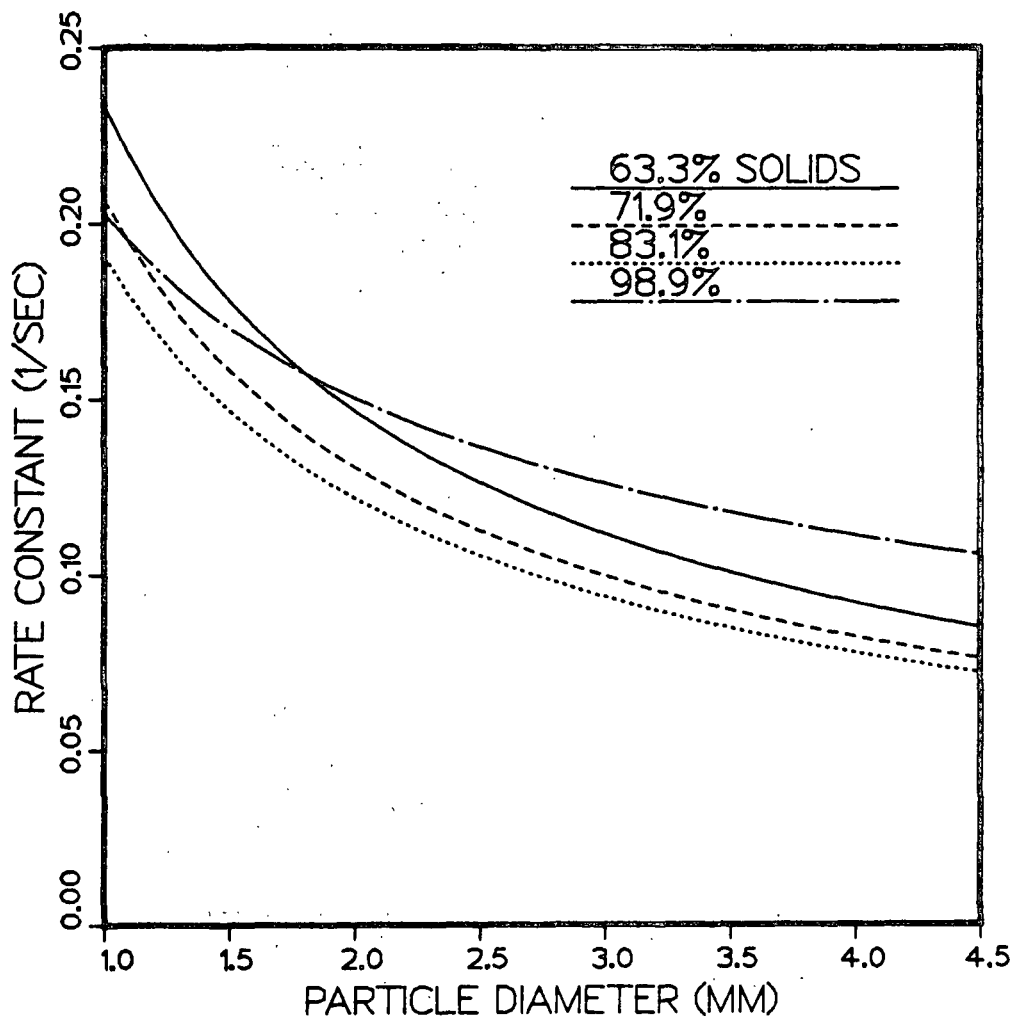


Figure 3. Rate Constant vs. Particle Diameter

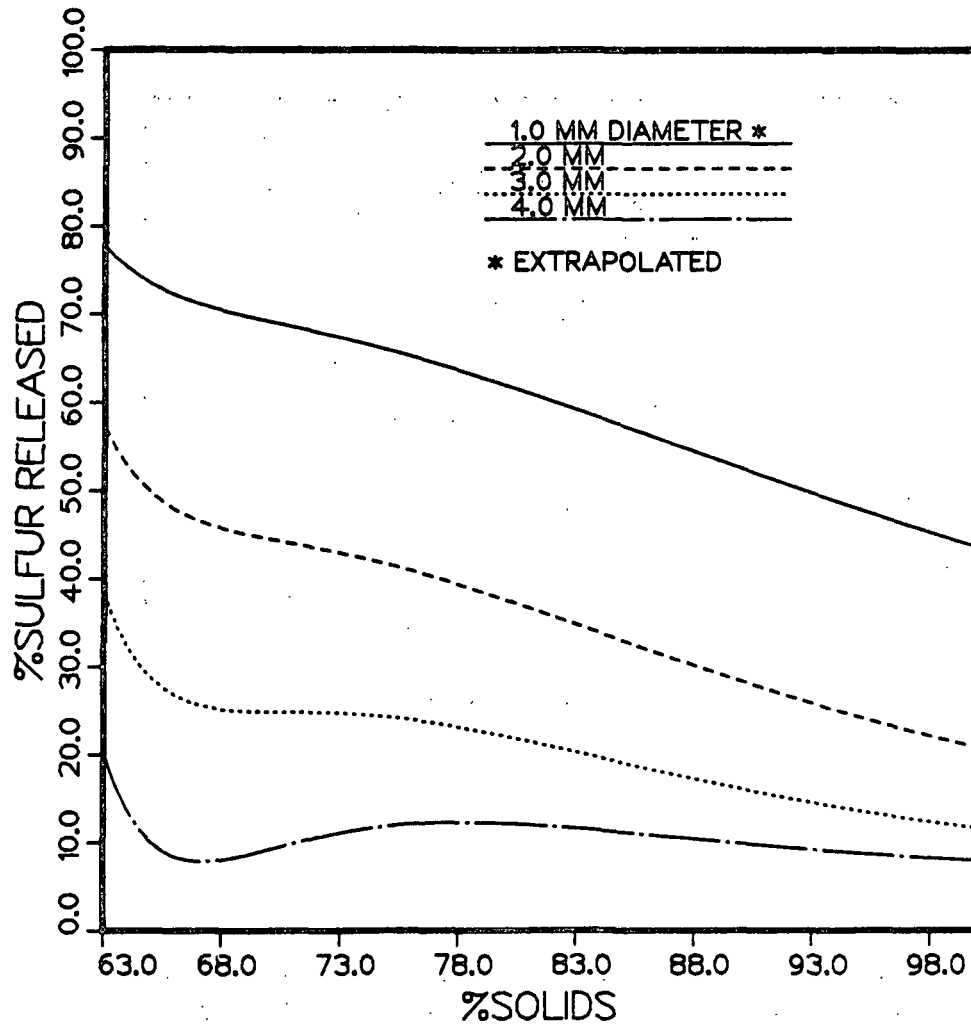


Figure 4. % Initial Sulfur Released vs. Solids Content

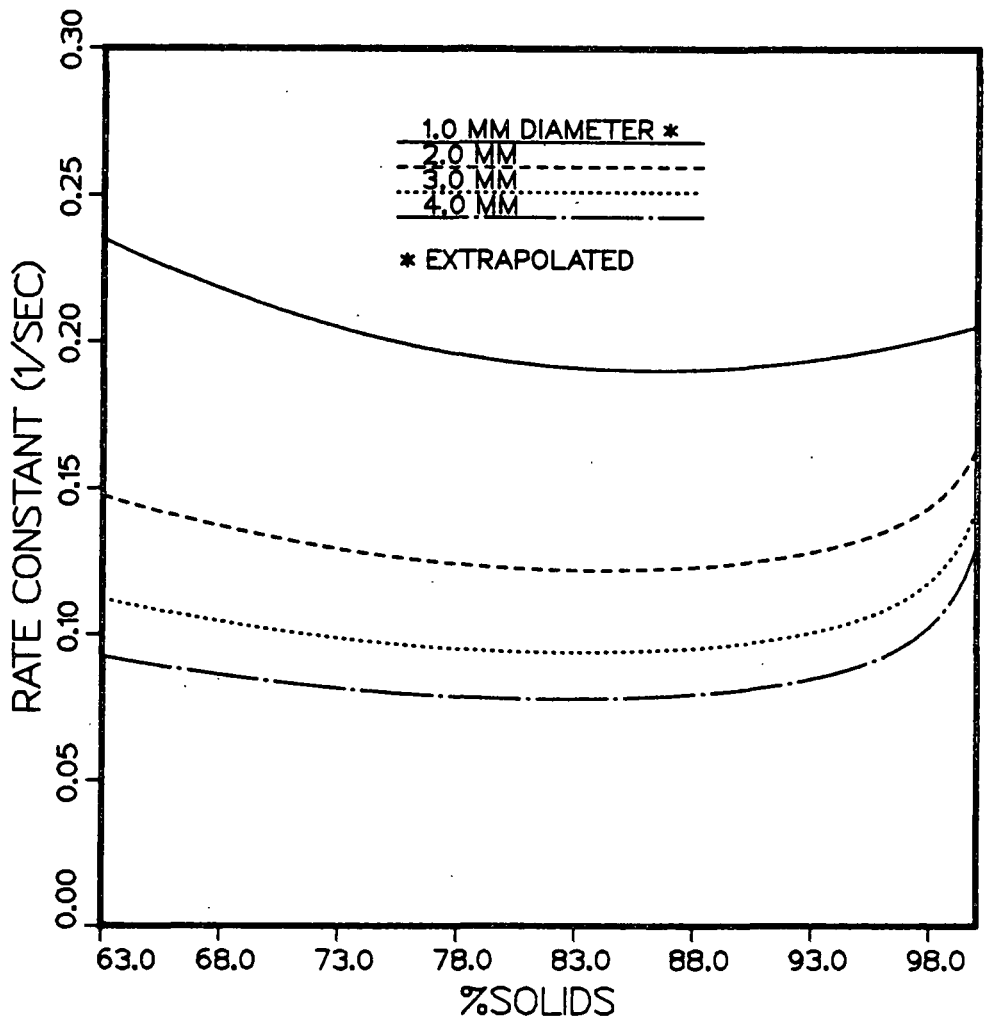


Figure 5. Rate Constant vs. Solids Content

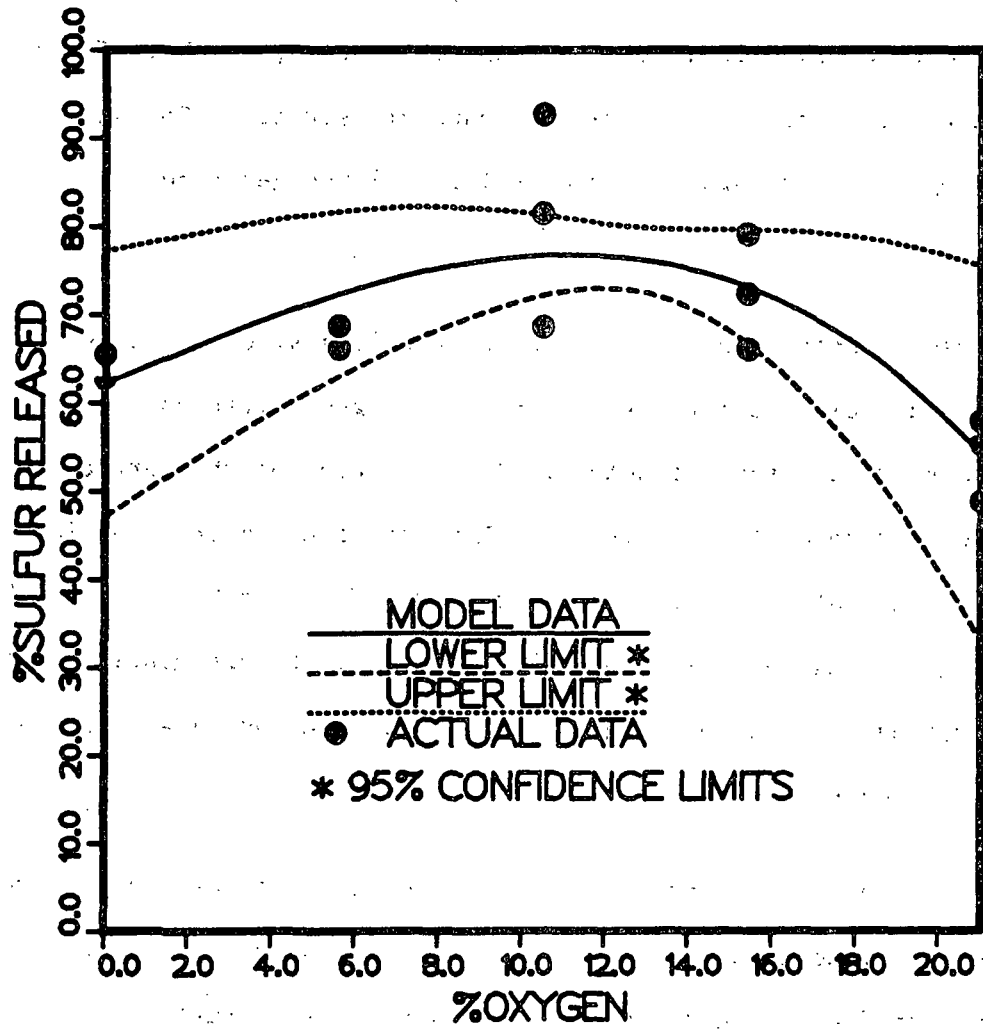


Figure 6. % Initial Sulfur Released vs. Gas Stream Oxygen Content

DISCUSSION

Four different phases of combustion occur during the combustion of black liquor particles, which are (I) drying, (II) pyrolysis and combustion of volatiles, (III) char burning and, (IV) the inorganic reactions (3). Most of the sulfur gas is released during the pyrolysis stage, which occurs between 250-750 deg C (6). These gases consist mostly of hydrogen sulfide, which is further combusted to sulfur dioxide as it leaves the particle surface. Sodium carbonate is produced during the char burning stage as the sodium-organic compounds combust.

From the present data, one can see that as particle size increases, the percent total sulfur released decreases. For the larger particles there is more of a temperature gradient from the outer to inner portion of the particle during the initial stages of combustion. Figure 7 shows temperature profiles for various particle sizes after two seconds of exposure for an 80% solids black liquor. The larger particles have a vastly greater temperature gradient, which allows for the various combustion stages to occur simultaneously at different radial positions throughout the particle.

The general scenario for larger particles leading to reduced percent sulfur released can be described based on a sodium carbonate capture mechanism. The large temperature gradient within the particle causes the combustion processes to proceed faster in the outer particle. After ignition takes place, a smelt shell abundant in sodium carbonate rapidly forms in the outer particle. At the same time, pyrolysis is occurring in the inner particle because of lower temperatures (500 deg C). Pyrolysis produces gases including various reduced sulfur compounds, predominantly hydrogen sulfide, which drives the swelling

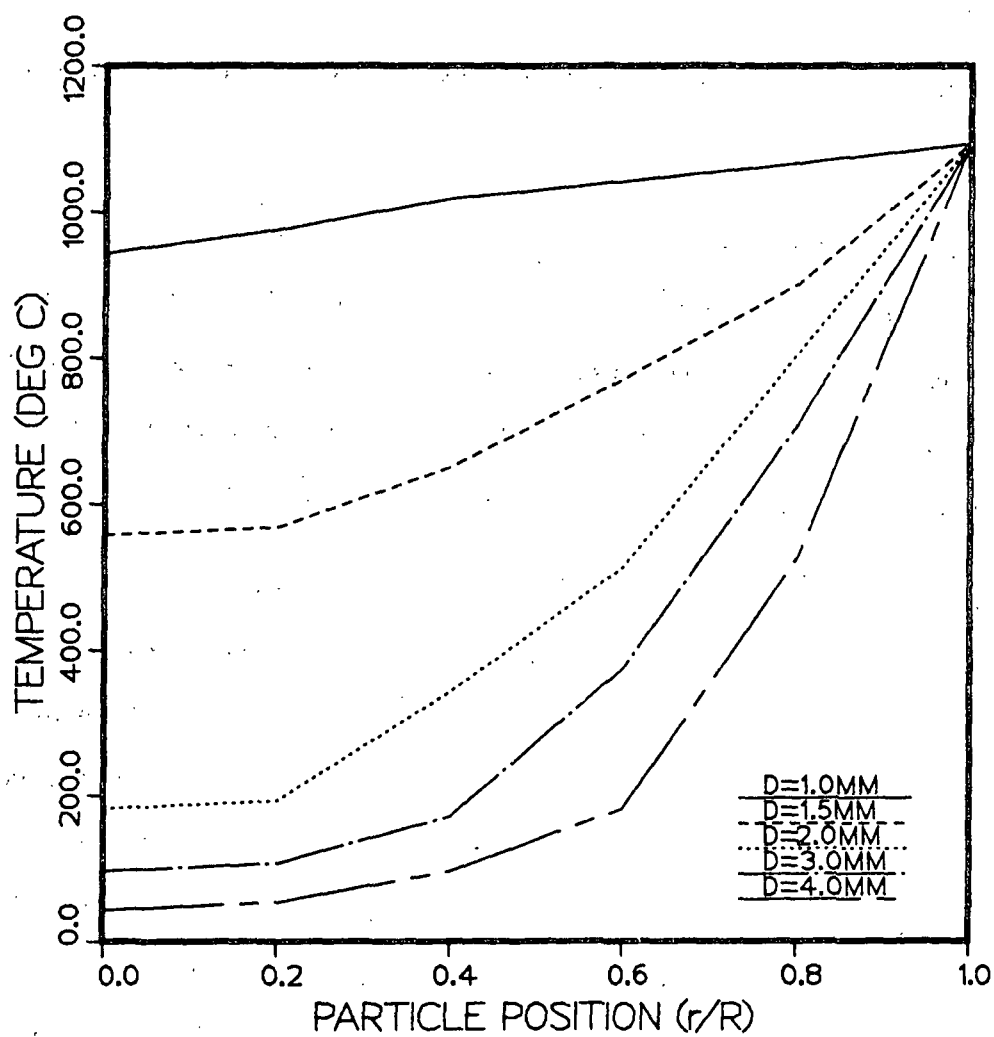
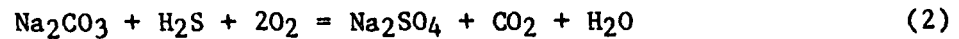
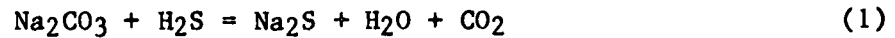


Figure 7. Conductive Temperature Profiles

*Source: Welty, Wicks and Wilson, Fundamentals of Momentum, Heat and Mass Transfer, Wiley, New York, 2nd ed., 724-725 (1976).
Thermal property data for black liquor from reference (7).

process. As these gases transfer through the outer particle, the sulfur gas is captured by sodium carbonate in the smelt as follows (8):



This action causes an overall decrease in the percent total sulfur released as particle size increases.

Smaller particles have much less of a temperature gradient, so the combustion stages occur discretely and uniformly throughout the particle. Any sulfur gas released during the pyrolysis stage is not captured because no smelt exists yet in the outer layer of the particle. This gas is further combusted to sulfur dioxide at the particle surface before leaving the furnace.

As can be seen from figure 4, an increase in solids causes a decrease in sulfur release, but the effect is not as great as the particle size effect. In addition, as particle size increases the solids content has less of an effect. Thermal conductivity and heat capacity decrease while density increases, causing an overall decrease in the thermal diffusivity as solids content increases. This has the net effect of decreasing the release of sulfur and the normalized release rate. Particles of higher solids content are larger than particles of lower solids content for a given particle size after the moisture has been removed. This also decreases the sulfur gas release and normalized release rate for the higher solids content particles.

Added sulfur had no effect on either the total sulfur release or the rate. Sulfur added as sodium sulfate was expected to have no effect, since sulfate is

already in a high oxidation state and is unreactive. Sulfur added as emulsified sulfur apparently reacted with sodium carbonate in the smelt phase to form sodium sulfide and sulfate.

Although oxygen had no effect on the normalized sulfur release rate, there was an observed maximum at around 13% oxygen for the percent total sulfur released. The value of 64% total sulfur released as sulfur dioxide for 0% oxygen is questionable, since it does not take much oxygen to completely combust the TRS compounds to sulfur dioxide. Therefore, it is possible that there may have been air leakage into the system during the experimental runs. At any rate, the observed maximum is probably due to two controlling factors. First, as gas stream oxygen content is initially decreased the combustion temperature and resulting temperature gradient are decreased, allowing more sulfur gas to escape during pyrolysis. Second, as oxygen content is decreased further, there is insufficient oxygen to completely combust all TRS compounds to sulfur dioxide before leaving the furnace. The net result is an observed maximum sulfur dioxide release at 13% oxygen for this system.

CONCLUSIONS

Of all the process variables studied, particle size had the greatest effect on sulfur gas release. As particle size increases, sulfur release decreases. Solids content and gas stream oxygen content had moderate effects. An increase in solids content caused a decrease in sulfur release. This effect becomes less prevalent as particle size increases. Sulfur dioxide release reaches a maximum at around 13% gas stream oxygen content. Added sulfur had no effect on the release of sulfur gas during black liquor burning at 1090 deg C in air.

The temperature profile generated in larger particles enable them to retain more sulfur by the sodium carbonate capture mechanism. Higher solids changes the physical and thermal properties of the black liquor, resulting in sulfur retention similar to large particles, but to a lesser extent. Decreased oxygen content in the gas stream decreases the temperature gradient generated, allowing more sulfur to be released. Sulfur added as emulsified sulfur is apparently captured by sodium carbonate in the smelt phase, resulting in no effect on sulfur release for air at 1090 deg C.

ACKNOWLEDGMENTS

Portions of this work were used by J. Cantrell in partial fulfillment of the Master of Science in Chemical Engineering degree from Georgia Tech. The author would like to acknowledge support from both The Institute of Paper Chemistry and the School of Chemical Engineering at Georgia Tech. The sulfur dioxide analyzer was provided by the Department of Energy, Office of Industrial Programs.

LITERATURE CITED

- (1) Borg, A., et al., Tappi, 57, (1), 126-129, (1974).
- (2) Thoen, G. N., et al., Tappi, 51, (8), 329-333, (1968).
- (3) Hupa, M. and Solin, P., TAPPI International Recovery Conference, Book 3, 445-559, (1985).
- (4) Moreland, B. A. and Clay, D. T., "The Influence of Water on Black Liquor Combustion," The Institute of Paper Chemistry, (1985).
- (5) Clay, D. T. and Ragland, K. W., "Kraft Black Liquor Combustion: Sensitivity to Key Process Variables," AIChE meeting, San Francisco, (1984).
- (6) Brink, D. L., Thomas, J. F., and Jones, K. H., Tappi, 53, (5), 837, (1970).
- (7) Harvin, R. L., A Study of the Thermal and Physical Properties and Heat Transfer Coefficients of Sulphate Paper Mill Black Liquor, Ph.D. Thesis, University of Michigan, (1955).
- (8) Bauer, T. W. and Dorland, R. M., Can. J. Technol., 32, 91-101, (1954).

APPENDIXAPPARATUS

The radiant single particle reactor is shown in figure 1. A mullite reactor surrounded by an electric heater was used to heat the particle. A flow-rate of 240 cc/min was used to minimize convective heat transfer. Ceramic packing was used to maintain a uniform flow of gas to the particle and to aid in heating the incoming gas. A thermocouple coming up through the gas inlet to the locality of the particle was used to measure the furnace temperature, which was kept constant at 1090 deg C. The particle was formed on a wire hook, which rested on the sample support rod during the burn.

The analytical equipment used consisted of a Teledyne series 600 UV photometric sulfur dioxide analyzer. The analyzer continuously measured the concentration of sulfur dioxide in the flue gas stream by measuring the amount of ultraviolet radiation that was absorbed by the gas at a specific frequency characteristic of only sulfur dioxide. The analog signal from the sulfur dioxide analyzer was converted to a digital signal and stored on a floppy disk by a data acquisition system.

All of the experimental runs were carried out in the following manner:

- (1) forming a black liquor particle of specific size on the end of an inch-long Nichrome wire hook, (2) attaching the sample at the bottom of the sample support rod, (3) activating the data acquisition system to receive data, (4) beginning the burning process by placing the reactor cover in place, (5) removing the cover after about two minutes when the run was over, (6) purging the gas line from the reactor to the analyzer with nitrogen in preparation for the next run,

(7) periodic calibration of the sulfur dioxide analyzer. The time at which the sulfur dioxide concentration began to rise was defined as time zero.

BLACK LIQUOR SYNTHESIS

The black liquor samples were made from a weak black liquor which was obtained from a standard kraft cook of loblolly pine wood chips in a laboratory digester. The cooking conditions are given in table 2.

Table 2. Laboratory Black Liquor Cooking Conditions

Dry Wood = 3600 g
Sodium Sulfide = 345.1 g
Sodium Hydroxide = 637.1 g
Water = 10,947.7 g
Moisture Content = 46.2%
Effective Alkali = 16%
Sulfidity = 25%
H-factor = 1876
Liquor/Wood = 4
Black Liquor Yield = 8 liters

The black liquor was then placed in a rotary evaporator under a vacuum of 90 kPa, in a water bath at approximately 60-70 deg C. When the sample reached 25% solids, the soap residue was removed from the sample by filtering it through a sponge and then the sample was concentrated to about 50% solids. At 50% solids, the sample was placed in an oven at approximately 140 deg C in a nitrogen atmosphere under a vacuum of about 75 kPa. Fifteen gram portions were taken as the black liquor solids reached about 65, 75, 85, and 95% solids. The sulfur

was always added to the 50% solids liquor for the added sulfur samples before continuing the evaporation process.

METHOD OF ANALYSIS

A sample data curve is shown in figure 8 along with the fitted curve. Assuming first order overall release of sulfur along with first order system dynamics the following equation was fit to the data to obtain k, the rate constant:

$$(dS/dt)_{rec} = (e^{-kt} - e^{-t/\tau})K\Delta S/(1-k\tau) \quad (3)$$

Where dS/dt = % initial sulfur/second, τ = time constant, t = time and ΔS = % total sulfur released. Correlation coefficients for the above equation averaged around 0.8. Delta S was obtained through direct numerical integration of the data curve. After delta S and k were obtained for all the experimental runs, they were fitted to empirical equations for curve representation.

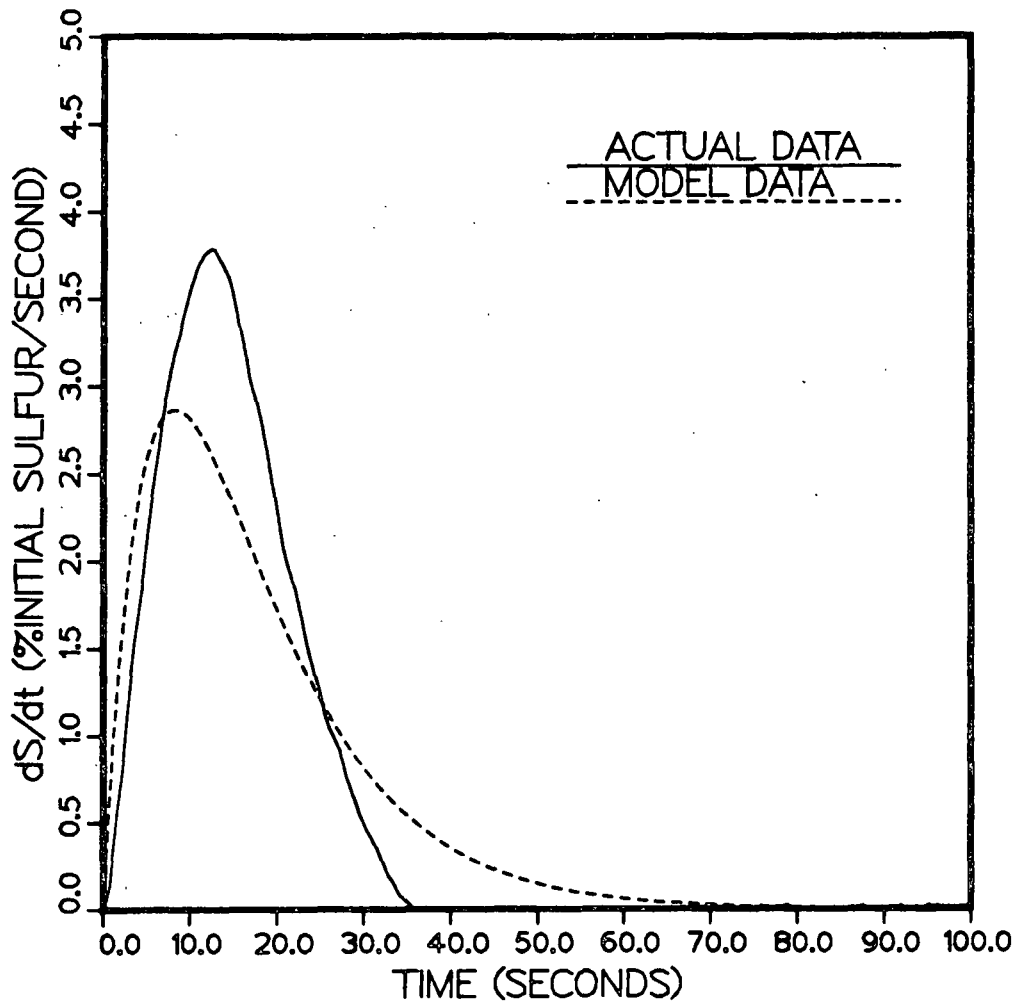


Figure 8. Sample Data Curve (63.3% solids, 2.0 mm dia.)

Status Report

FUNDAMENTAL PROCESSES IN ALKALI RECOVERY FURNACES

Implementation of Black Liquor Combustion Knowledge

An extensive research effort now underway is increasing our knowledge of the black liquor combustion process. This work is targeted to continue for approximately two years. The ultimate payoff of this research has to be improved recovery boiler performance. The basic question is how to make use of the growing process knowledge to improve recovery boiler performance. This report addresses that question and presents a plan of attack.

We proceed in three steps:

1. Identify and list all methods for improving recovery performance.
2. Select from this list those items which can benefit from improved process knowledge and which are important improvements. These are then used to develop suitable technical targets.
3. Develop a strategy to use the fundamental process knowledge to achieve these target opportunities.

IMPROVED PERFORMANCE

1. Reduce the capital cost of recovery systems
 - a. Increase design loadings to permit greater throughput of liquor solids in a given physical size unit
 - b. Increase throughput in existing recovery boilers

- i. Provide for higher firing rates without increasing boiler plugging
 - ii. Develop more effective clean-up techniques to permit "living with" high carryover rates
 - iii. Provide capability to fire liquors from higher yield pulping processes
 - c. Provide means for obtaining incremental production capacity for an incremental investment in a low cost recovery technique
 - d. Decrease erected equipment cost
 - i. Reduce the amount of field labor (modular units)
 - ii. Use lower cost materials
 - iii. Standardize engineering
 - e. Develop a cheaper particulate collection system that will meet emission standards
 - f. Increase the amount of NaOH in the smelt so as to reduce subsequent causticizing requirements
2. Reduce recovery boiler operating and maintenance costs
 - a. Decrease amount of operating labor required
 - i. Automatic process control systems
 - ii. Automated liquor firing system
 - iii. Automated cleaning of ports, etc.
 - b. Reduce scheduled and unscheduled outages
 - i. Eliminate trouble-prone furnace elements
 - ii. Make system "immune" to smelt-water explosions
 - iii. Decrease shutdown and turnaround times
 - c. Eliminate corrosion problems and/or allow the use of cheaper metallurgy without corrosion

- i. Reduce metal temperatures
 - ii. More benign atmospheres in furnace
 - iii. More effective protective coatings
 3. Improve energy generation effectiveness
 - a. Increase thermal efficiency of the unit
 - i. Complete combustion with minimum excess air
 - ii. Decrease water input
 - iii. Decrease flue gas discharge temperature.
 - iv. Minimize sootblowing steam and other steam usage.
 - b. Improve power/thermal balance
 - i. Higher steam pressures and temperatures
 - ii. Use reheat cycles
 - c. Increase capability to operate as a swing unit
 4. Reduce risk and improve insurability
 - a. Eliminate or reduce the likelihood of serious smelt-water explosions
 - i. Automatic leak detection systems
 - ii. Reduce smelt inventory
 - iii. Eliminate large slag falls
 - b. Eliminate black liquor pyrolysis gas explosions
 - i. Improve black liquor firing (spray) system
 - ii. Improve air supply to minimize gas pockets
 - iii. Easy cutoff and restart of black liquor firing
 - c. Minimize overheat failures
 - i. Good level control and low-water cutout systems -
integration with firing practice
 - ii. More positive boiler water circulation

- d. Present technology should be adequate to prevent auxiliary fuel explosions
5. Reduce environmental impacts
- a. Eliminate TRS emissions
 - b. Eliminate SO₂ emissions
 - c. Reduce dust loading to ESP
 - i. Decrease fume production
 - ii. Increase agglomeration before ESP
 - d. Provide waste handling capability
 - i. Waste gas incineration
 - ii. Liquid waste incineration
 - e. Elimination of toxic trace hydrocarbon emissions
6. Improve operability
- a. Make the correct way to operate the "easiest" way
 - b. Provide for a self-stabilizing system
 - c. Develop instrumentation to provide reliable real-time measurement of important furnace parameters
 - d. Develop strategies that will sustain peak performance over a wide load range.
 - e. Automatic process control systems
 - f. Develop predictive capability of how liquor composition affects performance and what operating changes are needed to cope

TARGET SELECTION

The listed items for improving recovery boiler performance do not all have equal priority, and some of them do not depend on a better understanding of black liquor combustion. The next step is to select from the list those items

which are important and which could benefit from improved process knowledge.

The selected performance items and the associated technical needs are summarized below in order of decreasing priority.

Performance Item	Technical Need
Increase design loadings	Reduce upper furnace plugging
Increase throughput in existing units	Reduce upper furnace plugging
Increase thermal efficiency	Complete combustion with minimum XS air
Decrease corrosion rates	Reduce metal temperature
	Minimize sulfur release
Reduce causticizing requirements	Increase NaOH in smelt
Reduce explosion risk and emergency turnaround time	Reduce smelt and bed inventory

From this listing of technical needs, the following implementation targets can be defined.

1. Reduce plugging of the upper furnace
 - a. Develop a firing technique (air and liquor supply systems) that will allow higher firing rates without significant carryover of smelt or unburned char
 - b. Develop criteria for the conditions in the gas stream leaving the furnace cavity and the state of suspended material that quantify the extent of the plugging problem
 - c. Develop means to minimize peak temperature of gas leaving the furnace cavity
 - i. Maximize heat transfer to the furnace waterwalls
 - ii. Eliminate gas flow patterns causing nonuniform temperature distributions

- iii. Provide for combustion to be completed in the lower part of the furnace
 - d. Develop means to avoid sticky ash
 - i. Keep SO_2 and O_2 in flue gas low
 - ii. Minimize enrichment of deposits with K and Cl
2. Optimize combustion and chemical processes
- a. Obtain complete combustion with minimal excess air by achieving effective mixing of air and combustibles in the furnace
 - b. Achieve complete burnout of carbon in the furnace
 - i. Eliminate carryover combustion
 - ii. Minimize carbon in smelt stream
 - c. Retain sulfur with inorganic
 - i. Prevent sulfur release during pyrolysis
 - ii. Maximize SO_2 recombination in lower furnace
 - d. Optimize product smelt composition
 - i. Maintain reduction efficiency $> 95\%$
 - ii. Increase NaOH or Na_2O content in smelt.
 - iii. Minimize $\text{Na}_2\text{S}_2\text{O}_3$ in smelt.
3. Maximize heat transfer to waterwalls without causing excessive metal temperatures.
- a. Use the upper furnace as a flue gas cooler.
 - i. Enhance radiant heat transfer to waterwalls
 - ii. Minimize inhomogeneities in wall heat fluxes
 - iii. Manipulate particulate loads and sizes and gas composition to optimize heat transfer
 - b. Control lower furnace processes to maximize combustion rates without excessive metal temperature

- i. Control location of combustion heat release
 - ii. Define critical areas where refractory might be needed
 - c. Maintain a protective frozen smelt layer on the wall
4. Optimize bed conditions
- a. Determine influence of bed shape on in-flight processes
 - b. Develop self-stabilizing bed configurations of optimal size/shape

IMPLEMENTATION STRATEGY

The top priority item is to develop a firing technique (both air and liquor injection systems) that will allow higher firing rates without significant carryover of smelt or unburned char. This requires two coupled programs to be carried out simultaneously.

1. A black liquor spray nozzle characterization and development program
2. Development and use of a mathematical model of the furnace to derive specifications for liquor sprays and air inputs.

The spray nozzle program would be experimentally based and would take place in three stages.

1. Characterization (droplet size and vector velocity distribution) of existing nozzles as functions of major variables.
2. Assessment of various mechanical techniques that could influence spray characteristics.
3. Development of specific liquor gun designs to meet predefined spray characteristics which would give optimum performance.

The modeling effort will develop a 3-dimensional mathematical model of the fireside of the furnace. Sensitivity studies on the model will determine the variables having the greatest effect on carryover. From numerical experiments on the model and its component submodels we would expect to get

1. Desired spray patterns for various existing air supply configurations, and
2. Desired spray patterns for optimal air supply configurations.

The second priority item is to develop criteria to quantify the plugging rate as a function of boiler geometry and conditions in the gas stream leaving the furnace cavity. The approach to be taken will be to develop a mathematical model of the plugging process, with subsequent verification in the DOE reactor and by furnace testing.

Many of the remaining items can be approached through direct use of the fundamental data or by exercising the furnace model.

At this time, neither funds nor manpower is available for a program on firing techniques. Also, expertise outside that of the current recovery group will be needed to direct the effort. We are currently considering various alternatives that will allow us to proceed in an expeditious manner.

THE INSTITUTE OF PAPER CHEMISTRY



Thomas M. Grace
Group Leader, Recovery
Pulping Sciences
Chemical Sciences Division

THE INSTITUTE OF PAPER CHEMISTRY

Appleton, Wisconsin

Status Report

to the

PULPING PROCESSES

PROJECT ADVISORY COMMITTEE

Project 3473-6

FUNDAMENTAL STUDIES OF BLACK LIQUOR COMBUSTION

(DOE FUNDED PROJECT)

September 4, 1986

PROJECT SUMMARY FORM

DATE: September 4, 1986

PROJECT NO. 3473-6: FUNDAMENTAL STUDIES OF BLACK LIQUOR COMBUSTION
(DOE FUNDED PROJECT)

PROJECT LEADER: D. T. Clay

IPC GOAL:

Develop fundamental data on black liquor combustion which can be used to enhance energy efficiency and productivity of recovery boilers.

OBJECTIVES:

The three main objectives are

- a) To develop laboratory scale flow reactor systems which will enable the study of both state-of-the-art and advanced recovery systems
- b) To study gas phase and char bed mechanistic processes under realistic and controlled environments with advanced optical and spectroscopic techniques
- c) To develop a data base which will bridge the gap between ongoing fundamental research and commercial application of the resultant findings, culminating in increased thermal efficiency, productivity, and capital effectiveness

CURRENT FISCAL YEAR BUDGET (Dec. 30, 1985 through Dec. 31, 1986):

\$300,000 (Contract with DOE, OIP) (\$125,000 of this will be a subcontract to the National Bureau of Standards, NBS)

SUMMARY OF RESULTS SINCE LAST REPORT:

The first progress report to DOE issued December 1985. This covered the first year and a quarter of work at both IPC and NBS on Phase 1, in-flight chemical and thermal processes. The second progress report, which will conclude the Phase 1 work, will issue during the first half of 1987. Intermediate progress reviews have been held with DOE in July 1985 at the University of Maine, Orono, and at the University of Florida, Gainesville, in conjunction with other DOE funded black liquor projects. The project reviews were attended by industrial and academic individuals involved in various aspects of kraft chemical recovery. A third DOE black liquor program review is scheduled October 1-3 at IPC. The results of equipment and process testing are summarized below.

The IPC flow reactor system successfully operates during continuous operation. Uniform black liquor droplets (nominal 2 mm diameter) are injected at a flow rate of nominally 15 grams/min (1.3 lb solids/hr). The upward gas flow is nominally at 1.5 m/sec (5 ft/s). The average upper gas temperature limit is nominally 1670°F (910°C) when only limited heat is liberated via particle combustion. The gas treatment package (incinerator, quench, scrubber, ID fan) enables the flow reactor to operate for long continuous time periods.

The initial module of the NBS dilute-phase flow reactor (DPFR) was expanded for detailed study of the early in-flight processes. Sample observation sections (SOS) were added at the top and bottom of the quartz glass section. Black liquor droplets (1.3 to 2.0 mm diameter) are injected one drop at a time. The upward gas flow rates range up to 12.8 ft/s (3.9 m/s). The gas temperature reached 1814°F (990°C). The work on this short version has been successfully completed. The equipment has now been reassembled into the full-height DPFR. The complete Phase 1 DPFR system is now undergoing checkout.

The results from these two systems provide a continuously updated data base on the in-flight processes. Significant characterization has been done of the droplet formation processes and the temperature profiles within the reactors. Droplet expansion and its influence on the velocity and trajectory has been measured at NBS via high speed movies during the initial portion of the droplet flight. Calculated velocities compare favorably with those measured. During the early in-flight processes, essentially the drying stage, significant volumetric expansion occurred.

Expansion during the initial char formation phases and the subsequent chemical and physical property changes have been studied at IPC. Sulfur loss from the particle occurs prior to complete carbon fixation. There is significant early decomposition of $\text{Na}_2\text{S}_2\text{O}_3$ to form Na_2S , Na_2SO_4 and release gaseous S. The black liquor injection temperature significantly influences the total amount of sulfur released during these early phases. The gas phase oxygen content had only minor influences on char chemistry. There was a significant influence of gas phase oxygen content on char bulk density. There were a number of other significant chemical interrelationships.

PLANNED ACTIVITY THROUGH FISCAL YEAR 1987:

Complete Phase 1 work. Issue Progress Report Number 2. Put into operation the IPC Phase 2 bed burning furnace. Achieve design black liquor flow rates (10 lb/hr of black liquor solids). Put into operation the full-height NBS DPFR.

FUTURE ACTIVITY:

Develop a conceptual approach for studying fuming in the IPC flow reactor system. Initiate work on Laser Doppler Velocimetry measurements and gas phase species analysis at NBS.

THE INSTITUTE OF PAPER CHEMISTRY

Appleton, Wisconsin

Status Report

to the

PULPING PROCESSES

PROJECT ADVISORY COMMITTEE

Project 3474

IMPROVED PROCESS FOR BLEACHED PULP

Low-Lignin Pulps

Nonchlorine Bleaching

September 11, 1986

PROJECT SUMMARY FORM

DATE: September 11, 1986

PROJECT NO. 3474: IMPROVED PROCESS FOR BLEACHED PULP

PROJECT LEADERS: T. J. McDonough

IPC GOAL:

Improved process for bleached chemical pulp.

OBJECTIVE:

Define pulping and bleaching technology that will decrease the number and size of the required process stages, including reduced needs for effluent treatment.

CURRENT FISCAL YEAR BUDGET: \$35,000

SUMMARY OF RESULTS SINCE LAST REPORT:

With increased emphasis on high yield pulping, only modest effort has been expended on this project since the last report appeared. Research conducted by a special student, Mr. A. Eagle, was directed toward the objectives of this project and resulted in models summarizing the kinetics of delignification in sulfite-anthraquinone systems, including estimates of the relevant activation energies. A substantial quantity of kinetics data has been obtained and awaits analysis. Ph.D. thesis research in the area of sulfite-anthraquinone kinetics will probably be initiated in the near future.

We have begun research aimed at enhancing the rate of lignin removal in oxygen bleaching relative to that of carbohydrate degradation. Pretreatment with nitrogen dioxide has been studied as a first step. Selectivity improvements were only partially attributable to enhanced delignification rates; a major component of the observed effect was carbohydrate protection. Implication of this observation for developing improved pretreatments will form the basis of future experiments.

PLANNED ACTIVITY THROUGH FISCAL YEAR 1986/1987:

Existing data on the kinetics of sulfite anthraquinone pulping will be analyzed, summarized and reported as time allows. Opportunities for mill experimentation with kraft pulping to low lignin contents will be sought.

Experiments based on the concept of lignin derived radicals participating or intervening in carbohydrate degradation reactions will be performed.

FUTURE ACTIVITY:

Emphasis will continue on understanding the kinetics of lignin and carbohydrate reactions in both pulping and bleaching, with a view to improved selectivity and control of residual lignin structure.

STUDENT RESEARCH:

M. Burazin, Ph.D.-1985; S. Pugliese, Ph.D.-1987; E. Arrington, M.S.-1985;
R. Barkhau, M.S.-1985; J. Bastian, M.S.-1985; S. Dibbs, M.S.-1985; R. Kirk,
M.S.-1985; B. Burns, M.S.-1986, Ph.D.-1988; M. Breining, M.S.-1986; J. Fisker,
M.S.-1986; J. Rogers, M.S.-1986; K. Sime, M.S.-1986, Ph.D., 1988;
D. Boyle, M.S.-1987; T. Stroh, M.S. 1987.

Status Report

IMPROVED PROCESS FOR BLEACHED PULP

PART 1. LOW-LIGNIN PULPS

The status of this part of the project has undergone relatively little change since the last report, owing to unavailability of professional manpower. A substantial amount of kinetic data has been accumulated and awaits analysis. Analysis of one body of data has been completed as part of a research project conducted with A. Eagle of Amcor, Ltd., during his stay at the Institute. The results are summarized in the attached manuscript, which will be published in Appita.

A Ph.D. thesis in this area is being actively considered and will probably begin within the next two months. A likely subject is the kinetics of sulfite-anthraquinone pulping.

Status Report

IMPROVED PROCESS FOR BLEACHED PULP

PART 2. NONCHLORINE BLEACHING

NITROGEN OXIDES AS PRETREATING AGENTS
BEFORE OXYGEN BLEACHING

We have recently proposed to convert the lignin of kraft pulp into a cellulose protecting agent before oxygen bleaching, in view of the unacceptable performance of other added protecting agents.¹ Of several possibilities, that of altering lignin aromaticity by suitable substitution was deemed the most likely of immediate success. Our early experiments in this direction showed that a gaseous nitrogen oxide mixture applied to pulp at room temperature before oxygen bleaching did protect cellulose from degradation during oxygen bleaching.

These initial experiments were run with nitrogen dioxide that contained small amounts of "impurities." The impurities, mainly N_2O_3 , are mixed oxides of nitrogen produced from trace amounts of water present in the nitrogen dioxide storage cylinder.

The present report describes further evaluation of these pretreated pulps and gives results obtained with pure, dry, gaseous nitrogen dioxide. All data have not yet been accumulated or evaluated. Rationalizations for the action of nitrogen oxides as pretreating agents before oxygen bleaching are presented as are generalizations for future experimentation.

Pure and impure nitrogen dioxide act similarly as pretreating agents before oxygen bleaching. Neither removes lignin by itself, and neither appreciably affects the removal of lignin when 4 or 6% caustic is used during oxygen bleaching (Fig. 1). The extent of lignin removal is more dependent upon the

alkalinity of the oxygen bleach. When 2% NaOH is used during the bleach, a moderately beneficial trend toward lignin removal is observed as the quantity of applied nitrogen dioxide is increased. Nitric acid pretreatment has no effect on the extent of delignification.

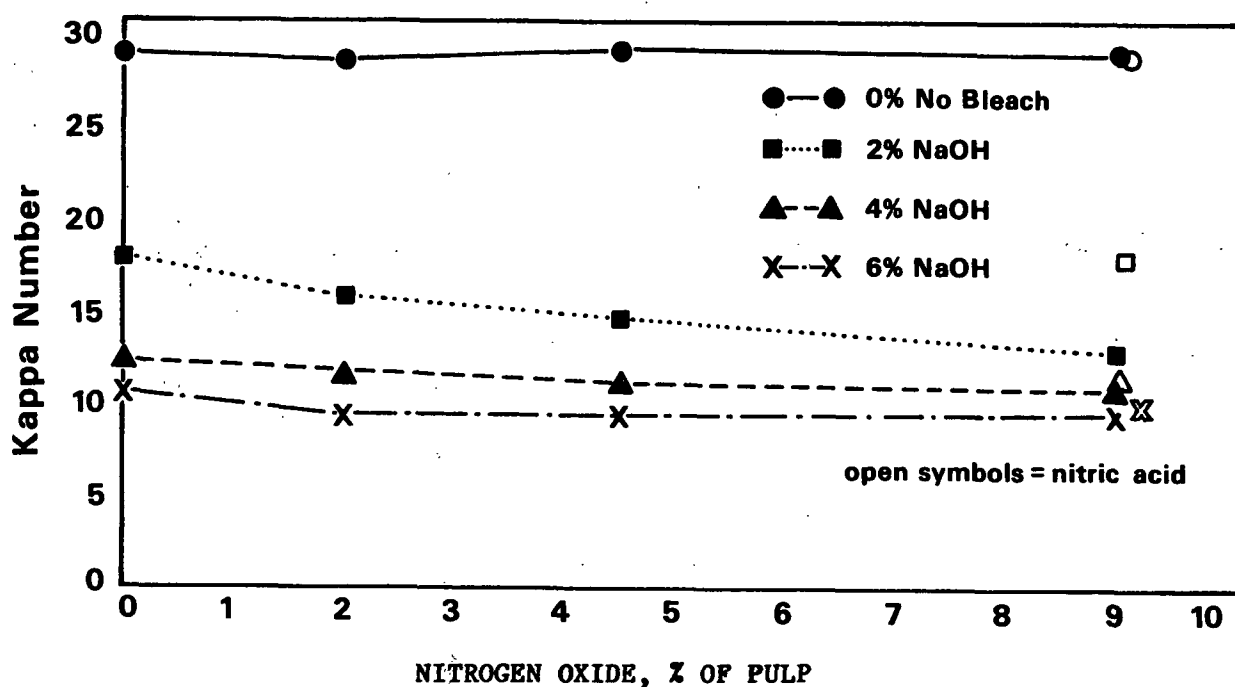


Figure 1. Oxygen bleaching of S. pine kraft pulp. Pretreatment with impure nitrogen dioxide.

There is no significant difference in stabilizing action on cellulose between pure and impure nitrogen dioxide pretreatments. Both partially stabilize cellulose similarly against degradation during oxygen bleaching. The data in Fig. 2 show that nitrogen dioxide (without oxygen bleaching) is more harmful in this regard than is nitric acid. The situation is reversed after bleaching. It is speculated that radicals derived from lignin during oxygen bleaching attack cellulose. The lesser degradation during oxygen bleaching of pulps pretreated with nitrogen dioxide (compared to nitric acid pretreated pulps)

suggests that lignins reacted with nitrogen oxides do not form as many reactive radicals during the bleach that are capable of degrading cellulose. Hardwoods such as eucalyptus behave in a similar manner.

So far it is not possible to eliminate all cellulose degradation by oxygen by pretreatment with nitrogen dioxide. It was postulated that this is due to the oxidation of cellulose to carbonyl and carboxyl rich derivatives during the pretreatment stage. Research by Nevell² shows that nitrogen dioxide does not specifically oxidize C-6 but also attacks C-2 and C-3. Nitration (and subsequent radical decomposition) may also occur. The failure of an attempt to stabilize cellulose by reducing pretreated pulp with sodium borohydride before bleaching demonstrates that carbonyl groups are not the source of the degradation. The alternative possibility of a radical degradation derived from the decomposition of nitro or nitroso groups in cellulose is currently being considered as is the stability of uronic acids to oxygen and alkali.

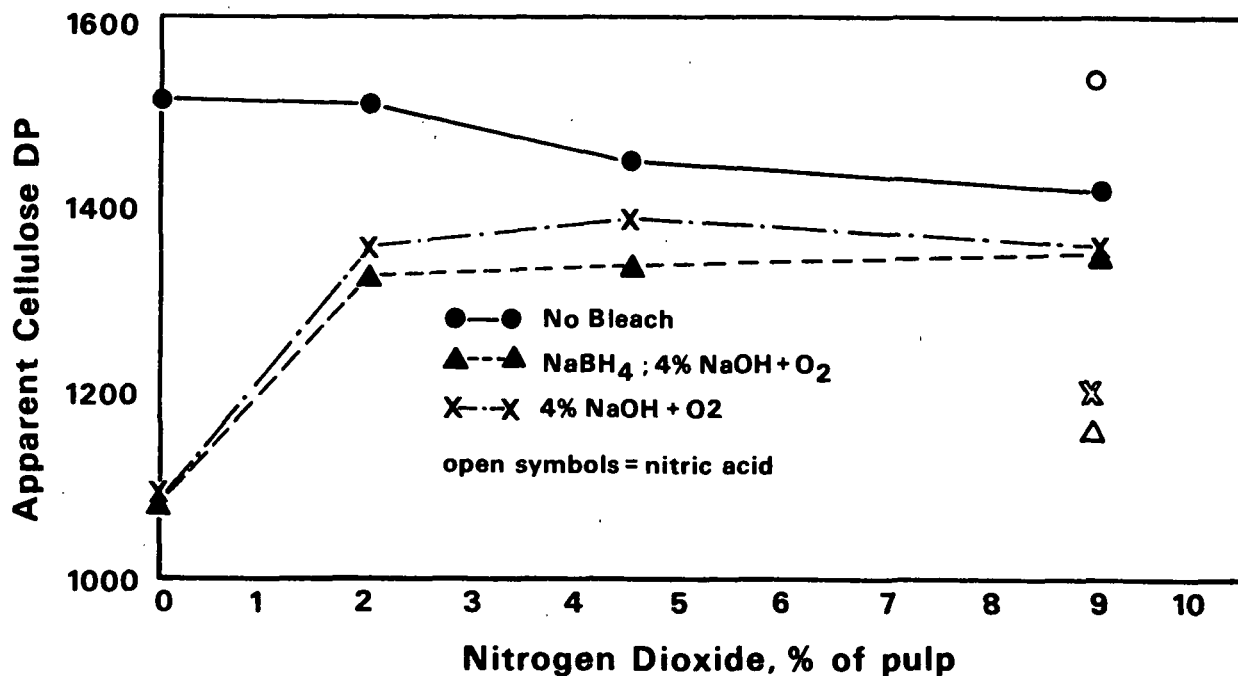


Figure 2. Oxygen bleaching of S. pine kraft. Pretreatment with pure nitrogen dioxide and stabilization with borohydride.

The zero-span tensile strengths of pulps bleached after pretreatment with impure nitrogen oxides have been measured. The results show that zero-span is increased by pretreating with nitrogen oxides, as shown in Fig. 3. The pulps pretreated with nitric acid have lower zero-span strengths. Higher applications of nitrogen oxides and alkali lead to better zero-span strengths.

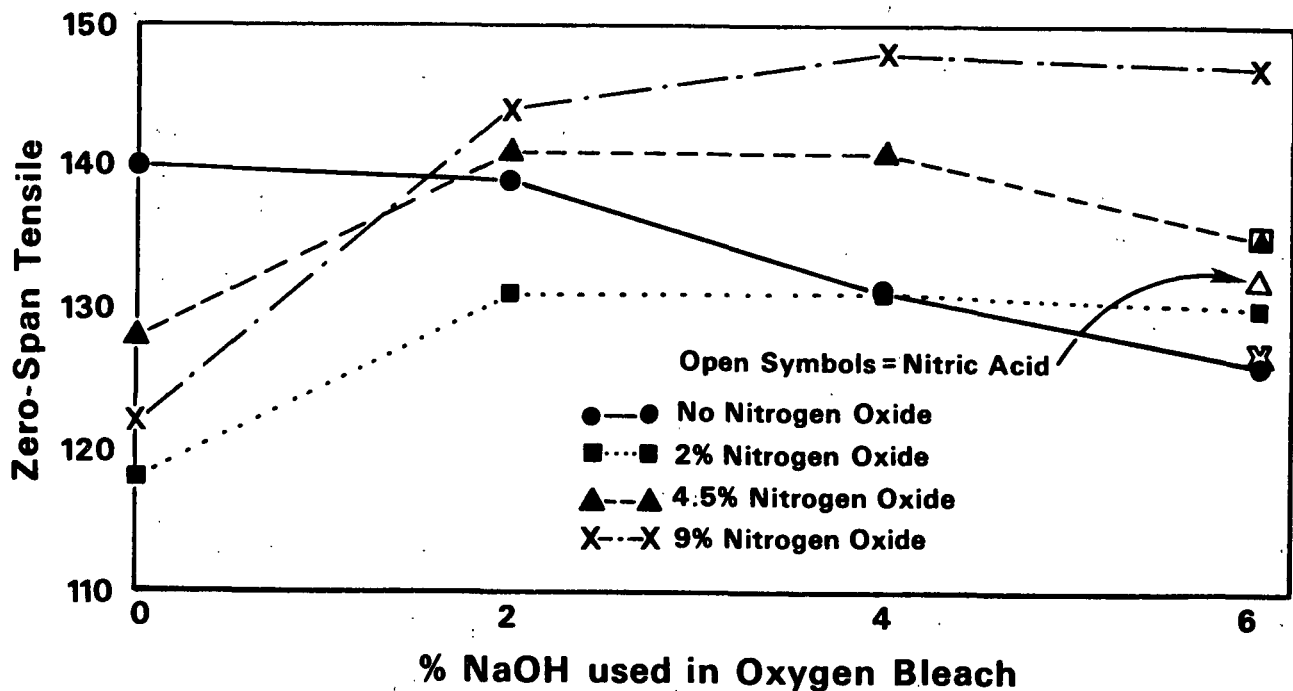


Figure 3. Effect of alkali charge as zero-span tensile strength after oxygen bleaching and pretreatment with various amounts of nitrogen oxide.

There is no obvious relationship between viscosity (DP) and zero-span strength because the oxygen bleaches did not reduce the viscosity to where it is likely to have been the major factor in determining strength. Consequently other physical factors such as internal flexibility, compressibility, ability to be hydrated, and other properties such as brittleness probably make major contributions.

Pulps pretreated with nitrogen oxides before oxygen bleaching are darker after the oxygen stage than the controls that have not been pretreated. Other researchers have found that nitrogen dioxide pretreated pulps are more difficult to bleach to the same degree as controls. We have observed that a borohydride posttreatment after the nitrogen oxide stage does lighten the pulp considerably but that no improvement is observed after the oxygen stage. On the other hand, sodium dithionite reduction bleaches pretreated pulp and preserves brightness after oxygen bleaching. Quantitative confirmation of these observations is in progress. Whether these advantages of strength with maintained brightness can be preserved after terminal bleaching stages using chlorine dioxide, etc. remains to be seen.

In summary, pretreatment of the lignin of kraft pulp (hardwood or softwood) before oxygen bleaching with nitrogen oxides enhances lignin removal only slightly under the conditions used here. Cellulose viscosity (DP) can, however, be improved by such pretreatments. The zero-span strengths of the pretreated pulps are improved in a manner that does not reflect significant dependence upon the viscosity. Sodium dithionite is a useful bleach for improving the brightness of these pulps. Directions for optimization of these treatments and brightness and strength limitations will become more apparent as additional data is accumulated.

ACKNOWLEDGMENT

Dr. N. S. Thompson played a major role in the planning and reporting of the work described in this report. Mr. H. M. Corbett was responsible for skillful execution of the experiments.

REFERENCES

1. Thompson, N. S., Executive's Conference, May (1985).
2. Nevell, T. P., J. Textile Inst. 42:T91-T129(1951).

THE INSTITUTE OF PAPER CHEMISTRY



Thomas J. McDonough
Group Leader, Pulping/Bleaching
Pulping Sciences
Chemical Sciences Division

Appita Preprint - Not for Publication

A KINETIC STUDY OF HIGH YIELD AQ-SULPHITE
PULPING OF LOBLOLLY PINEA.J. EAGLE^{*}, T.J. McDONOUGH^{**}

* Technical Manager - Pulp, Australian Paper Manufacturers,
Maryvale Mill, P.O. Box 37, Morwell, Victoria.

** Professor of Engineering, Institute of Paper Chemistry,
Appleton, Wisconsin.

SUMMARY

Delignification of Loblolly pine by sulphite-anthraquinone pulping at 160°C to 180°C and pH 10 was studied. Pulping rate was increased by an order of magnitude relative to sulphite in isolation. A parallel reaction model gave the best fit to data with an activation energy of 37.0 kcal/gmole for AQ associated reactions. Mass transfer was limiting for chips greater than 1mm thick.

INTRODUCTION

The objective of this study was to determine the apparent activation energy for sulphite-anthraquinone pulping of Loblolly pine at yields above 50% OD/OD, by fitting a general "n"th order reaction expression to experimental data.

Published data (1,2) on Canadian and Scandinavian softwood species have shown that sulphite-anthraquinone processes in the neutral and alkaline pH range show potential for substantial gains in yield and bleachability, relative to the kraft process. Studies at the Institute of Paper Chemistry (15,16) have extended these findings to include Loblolly Pine.

In addition, Tay et al (6,9) have shown improved pulp strengths and pulping rate when anthraquinone (AQ) or its soluble disodium salt (SAQ) is used in the production of high yield sulphite pulps from both jack pine and black spruce.

Lignin removal in pulping processes is usually divided into three phases, termed initial, bulk and residual delignification. Heitner et al (5) have studied sulphonation of black spruce at temperatures up to 140°C and pH 7 and have strongly implicated quinone methide reactions as significant under these conditions. The activation energy for the sulphonation of lignin under these conditions was estimated by Heitner as 14.95 kcal/gmole. Mortimer (3) in his study of coniferyl alcohol production in alkaline systems has demonstrated the importance of free phenolic hydroxyl units at temperatures below 150°C. In this case the production of quinone methide intermediates was associated with coniferyl alcohol formation via β aryl ether cleavage.

The above studies indicate that reactions of free phenolic hydroxyl units, which typify the initial phase, could be expected at the 10 pH chosen for this study. Such reactions would however be complete before temperatures of 160°C were achieved. Thus different kinetic expressions would be involved above and below 160°C. For this study it was therefore decided to concentrate on reactions occurring at temperatures of 160°C or higher, and to equate this with the bulk delignification phase.

For bulk delignification a number of estimates have been made of the activation energy for NSSC pulping of hardwoods (11-13). The reported values range from 24.6 kcal/gmole to 27.98 kcal/gmole.

PRELIMINARY STUDIES

In order to study the reaction kinetics of the sulphite-AQ / Loblolly Pine system it was first necessary to establish that the system was not mass transfer limited. This aspect has not received widespread study but experience with commercial manufacture of Pinus radiata pulps in Australia had indicated that it may be significant (10). Tay et al (6,9) have also reported the dissolution of wood constituents for sulphite-AQ pulping of both black spruce and jack pine chips to be influenced by chip size.

To verify this, chips varying in thickness from 5mm to 0.5mm were prepared by hand and pulped under otherwise identical conditions. A very strong mass transfer limitation was observed, as can be seen from Table 1

The results show that chip thicknesses less than 1mm are required to achieve a reaction limited system. This could explain shive problems encountered in some commercial trials.

Take in Table 1

When the cooked 5mm chips were split open there were two zones visible. Centres were white suggesting that sulphite was present to limit chromophore formation, while the outer portion was best described as a translucent yellow. The outer zone was approximately 0.5 - 1mm thick along the radial and tangential directions, and 4 - 5mm in extent along the grain. As a consequence it was decided to use shavings for the remainder of the study. The use of wafers was considered, but rejected due to the possibility of the wafers adhering and creating a "thick chip".

The sensitivity of the process to AQ charge was also investigated. For meaningful results the AQ charge must be sufficient to ensure that AQ concentration does not become reaction limiting. Data of Amos et al (4) and others have indicated that there is an addition level of AQ above which there is no further beneficial effect. This effect was investigated by varying the AQ charge from 0% to 2.5% on OD wood at a liquor to wood ratio of 25:1. A similar temperature ramp to that used for the chip thickness study was applied, and the results presented in Table 2.

Take in Table 2

Clearly there is a minimum for both yield and hypo number at the 1% on wood addition level. The possible slight increase in values at the 2.5% level may be due to the presence of unreacted AQ influencing the yield and hypo number measurement. A yellow powder, thought to be AQ, was observed in the three highest addition samples. This effect was not investigated.

For subsequent studies an addition level of 1% on OD wood was used. It should be noted that although 1.0% on OD wood represents a very large dosage in terms of current commercial practise, the actual dissolved concentration is only slightly in excess of what would be encountered commercially at normal liquor to wood ratios.

RESULTS

Results are summarised in Tables 3 and 4:-

Take in Tables 3 and 4

Carbohydrate analyses of pulps cooked at 180°C were also undertaken and a summary of these is presented in Table 5.

Take in Table 5

ANALYSIS

The general "n"th order reaction expression can be written thus:-

$$\frac{-dL}{dt} = A \exp(-E/RT) L^n S^m \quad (1)$$

- Where
- L = lignin content on original OD wood
 - t = time (min)
 - E = energy of activation (cal/gmole of lignin)
 - R = gas constant = 1.9872 cal/K.mol
 - T = temperature °K
 - S = concentration of sulphite (g/L as Na₂O equiv.)
 - n = lignin exponent
 - m = sulphite exponent
 - A = constant

This equation was rearranged and numerically integrated, assuming values for E, n and m, to produce estimates of the changes in lignin content as a function of time. These could then be compared with the measured values and the degree of fit measured by linear regression. In practise all six series of cooks, (sets 3,4,5,6,7-5 to 7-8, and 8-5 to 8-8) at different temperatures and chemical concentrations, were used to determine the correlation coefficient. Also by using splining techniques to describe the temperature profiles of each cook it was not necessary to restrict the analysis to constant temperature values, so that

all data points taken at temperatures of 157°C or higher were used. Advantage was also taken of an observed linear correlation of sulphite concentration to lignin (Fig 1) to express the sulphite concentration in

Take in Fig. 1

terms of the lignin content, thus making the calculations more rigorous (and simpler). Values of E, n and m were then varied to obtain the optimum value of the correlation coefficient.

Results were also checked by assuming S and T in equation (1) to be constant and fitting an "n"th order rate expression to the constant temperature portion of the curves. The results are summarised in Table 6. They show that the exponent with respect to lignin appears to be varying. As one possible explanation for this is that mass transfer effects had not been completely eliminated at 180°C, the analysis was repeated excluding data taken after three minutes at 180°C.

Take in Table 6

It was also observed that there was a different relationship between unreacted sulphite and the amount of lignin remaining undissolved for the AQ free cooks (Fig.1). This trend extrapolates through the initial conditions (48 g/l sulphite as Na₂O and 32.3% total lignin on OD wood). However the curves for the cooks containing AQ suggest that 4.5-5.5% lignin was removed prior to any measurable reaction with sulphite.

Consequently the scope of the analysis was broadened to include a parallel reaction model of the form:-

$$\frac{-dL}{dt} = A_1 e^{(-E_1/RT)} L^{n_1} + A_2 e^{(-E_2/RT)} L^{n_2} \quad (2)$$

Symbols are as defined previously, with subscripts defining reactions one (no AQ) and two (AQ only). The effect of sulphite concentration was excluded from the model in order to limit the number of constants to be evaluated from the relatively small data base. The constants for the "no

AQ" reaction were derived from the comparative cooks done without AQ at 160°C and 180°C. Using these values the total equation was then fitted to the constant temperature portion of the AQ-sulphite cooks, (sets 3,4,5,6) again varying A2, E2, and n2 so as to minimise the sum of errors squared. Results of the analyses are presented in Table 7.

Take in Table 7

In order to compare the first two models with the third (which applies at only one chemical concentration) in some quantitative manner, a subset of the data was chosen for the error analysis. This data (sets 4, 5 and 6, Table 3) were all at the same initial chemical concentration, spanned the range of temperatures used and most closely approximated the programmed temperature profiles. The derived kinetic expressions were then integrated up the theoretical temperature profiles, from arbitrary starting points, and compared with the actual measured values. Starting points were varied for each model to give a good overall fit. This was necessary as the models do not apply for temperatures below 155°C, so that it is not possible to anchor the calculation on unreacted wood at time zero. Standard errors were defined as:-

$$\text{Standard Error} = \sqrt{\left(\sum_{n=1}^N (\text{actual} - \text{predicted})^2 \right) / (\text{number of points})}$$

DISCUSSION

All three expressions developed show that the lignin removal rate increases very rapidly with temperature, so that at 180°C the rate is approximately 13 times faster than measured for the AQ-free system, all else being equal. It is also clear that whatever expression is chosen, the activation energy associated with AQ is substantially greater than values reported for NSSC hardwood systems. It is also greater than the usually accepted value of 32.02 kcal/gmole for Kraft pulping.

When this is taken in conjunction with the lower usage of sulphite (approximately 35% less in cooking to 12% lignin on original wood) there is evidence that AQ is not a catalyst for the normal sulphite reactions, but instead reacts with or catalyses reactions with species not normally attacked by the sulphite in isolation. Thus of the models developed, the

parallel reaction model would appear most consistent with the observations, and this is supported by it having the best degree of fit as defined by the standard error (Table 7).

Take in Fig. 2

However the expressions do not apply to the initial phase and as approximately 34% of the original lignin is removed by the time that the cooks reached 160°C, compared with only 21% for the AQ-free system, further study of the initial phase would appear worthwhile.

Another interesting observation is that over the range of 5 - 22% lignin on original wood, there is a very strong linear correlation between yield and lignin content. The correlation relation is:-

$$\text{Yield (\% OD/OD)} = 47.35 + 1.5889 \times \text{Lignin (\% on wood)} \quad (3)$$

$$\text{Correlation coefficient} = 0.999$$

$$\text{Number of data points} = 23$$

$$\text{Mean square of errors} = 0.127$$

This implies that lignin and carbohydrate are removed in the mass ratio of 1.7:1, independent of temperature. As it is unlikely that there are two independent reactions occurring with the same activation energies, this could suggest the possibility of a lignin carbohydrate complex or a reaction mechanism involving both species. The carbohydrate analysis indicates that it is the dominant hemicellulose, glucomannan, that is linearly related to the lignin content.

Finally, the sulphite-AQ system has a significant yield advantage at a lignin content relative to the sulphite system alone. In the range 14-23% lignin on original wood, the pulps produced using AQ had a yield advantage of 8-9% at the same lignin content.

CONCLUSIONS

The sulphite AQ pulping process when applied to Loblolly Pine exhibits the following features:-

- 1) An apparent energy of activation greater than values previously reported for sulphite or kraft pulping.
- 2) A lignin removal rate an order of magnitude greater than sulphite alone at 180°C.
- 3) A linear relationship between lignin removal and carbohydrate dissolution in the range of 5-22% of lignin on original wood.
- 4) A significantly decreased demand for sulphite relative to the AQ free system (35% difference to achieve 12% lignin on wood)
- 5) A limit to the amount of AQ for which an effect is observed. This is approximately 1% on OD wood under the conditions used.
- 6) A significant mass transfer limitation when chip thickness is in excess of 1mm.

The bulk of the evidence supports the propositions that the AQ-sulphite system at pH 10 is mass transfer limited under normal commercial practise and that the action of AQ in the sulphite system is not that of a catalyst for sulphite reactions, but enables reaction with lignin species that are relatively inert in the absence of AQ.

EXPERIMENTAL

Preparation of wood

For all studies, three logs of Loblolly Pine were divided and composited. The logs were from the Southern US and kept in cold storage until use. Sections of the logs were split and shavings produced by passing through an industrial planer. The shavings were then screened, air dried to 6% moisture, and rescreened retaining the + $\frac{1}{4}$ inch fraction. The thickness distribution was assessed by measuring the maximum thickness of shavings from a sample of approximately 200. Mean thickness was 0.37mm and 95% of chips were thinner than 0.70mm.

Preparation of cooking liquid

The sulphite liquor was prepared by dissolving 99.54g of analytical grade sodium sulphite and 20.52g of analytical grade sodium carbonate per litre of deionised water. This corresponds to a nominal sulphite concentration

of 48g/L as Na_2O equivalent. The pH was adjusted to 10.0 before addition to the chips, by bubbling carbon dioxide through the liquor. Where the sulphite concentration was varied from the nominal 48 g/L as Na_2O (to 40 g/L), analytical grade sodium sulphate was added to maintain the same ionic concentrations in solution. AR grade AQ was added as a 97% pure powder to the bombs before addition of other components.

Treatment of chips

Following addition of AQ to the 500ml bombs, approx. 16.0g of OD shavings were added to the bombs, followed by 400mls of cooking liquor. The bombs were then evacuated twice and left to soak overnight before cooking.

The bombs were placed in a rotating cradle in an oil bath and heated to 90°C, held there for 30 min to allow some heating and mixing in the bombs, and then ramped at 2°C/min to the desired temperature. Up to four bomb internal temperatures could be measured whilst in the bath, by thermocouple. The average of all readings was used to describe the temperature profile for each batch of cooks. It should be noted that times are reported as elapsed minutes from the start of the ramp for the oil bath, whereas actual bomb temperatures, which are quoted, lagged approximately 8 minutes behind the bath temperature. Thermocouple indication was to the nearest 1°C, and calibration was checked at the end of each run by immersion in the oil bath, and comparing with a mercury bulb thermometer.

For the preliminary studies on chip size and AQ charge, the bath temperature profile chosen was 2°C/min rise to 180°C and 3 minutes at 180°C. Liquor to wood ratio was 20:1 (increased to 25:1 in following studies) in order to minimise liquor concentration variations and AQ charge was 1% on OD wood. The remaining sets of cooks were conducted at 160°C, 170°C and 180°C. Limited cooks were also conducted without AQ present and with reduced sulphite.

After removal from the bath the bombs were quenched by immersion in cold water. The shavings were washed twice to remove associated liquor then soaked for 6-10 hours in deionised water to allow diffusion from the chips.

This process was repeated three times before air drying and weighing the shavings. Checks of filtrate showed that conductivities were less than 50 mhos after the second soaking and there was no visible color present.

Analysis of spent liquor

Cooking liquors were analysed for sulphite and pH. The method of Palmrose (14) was initially used for sulphite determination. However errors due to SO₂ emission from solution necessitated a slight modification to the standard procedure.

Analysis of lignin content of pulps

The extent of reaction was followed using the lignin content of pulps, corrected to an original OD wood basis. This was determined from the "Hypo Number" of the unscreened pulps in accordance with Tappi Standard Method T 253 om-81, using the expression:-

$$\text{Total lignin on pulp} = 1.062 \times \text{Pulp Hypo No.} - 0.345 \quad (4)$$

$$\text{Coefficient of correlation} = + 0.9966$$

$$\text{Mean square of errors} = 0.272$$

The relation was established by analysis of some samples to determine Klason lignin and soluble lignin using the method of Effland (7). Soluble lignin was determined at 205nm, although results were only approximate due to lack of an absorbance peak.

The only result excluded from this correlation was that for the wood itself. This was substantially different and it is thought that the presence of resinous extractives in the wood prevented wetting and interfered with the chlorine consumption. Observed wetting characteristics were different to all other samples.

Carbohydrate analysis was also conducted, for those samples where Klason lignin was determined, using the method of Borchardt and Piper (8).

REFERENCE LIST

1. KETTUNEN J., VIRKOLA N., AND YRJALA I.
The effect of anthraquinone on neutral sulphite and alkaline sulphite cooking of pine.
Paperi ju Puu 61 (11) : 685 (1979)
2. INGRUBER O.V., STRADAL M., AND HISTED J.A.
Alkaline sulphite-anthraquinone pulping of eastern Canadian woods.
Pulp Paper Canada 83 (12) : T342 (1982)
3. MORTIMER R.D.
The formation of coniferyl alcohol during alkaline delignification with anthraquinone.
Canadian Wood Chemistry Symposium Niagara Falls 1982
4. AMOS L.W. AND ECKERT R.C.
The influence of methylation on the solubility and efficiency of anthraquinone in soda pulping.
Canadian Wood Chemistry Symposium Niagara Falls 1982
5. HEITNER C., BEATSON R.P. AND ATACK D.
Factors affecting sulphonation of Eastern black spruce wood chips.
Journal of Wood Chemistry and Technology, 2(2) : 169 (1982)
6. TAY C.H., FAIRCHILD R.S. AND MANCHESTER D.F.
Sulphite/quinone pulping for production of chemimechanical pulp from Jack pine.
Journal of Pulp and Paper Science September 1984

7. EFFLAND M.J.
Modified procedure to determine acid-insoluble lignin
in wood and pulp.
Tappi 60 (10) : 143-144 (Oct. '77)
8. BORCHARDT L.G. AND PIPER C.V.
A gas chromatographic method for carbohydrates as
alditol acetates.
Tappi 53 (2) : 257-261 (Feb. '70)
9. APM Ltd, Internal Report.
11. CHARI N.C.S.
Kinetic study of neutral sulphite pulping of aspen chips.
Ind.Eng.Chem., Process Des.Develop. 7 (3) : 372 (Jul. '68)
12. BASU S., KRAUSE Th., AND SCHURZ J.
Delignification kinetic studies of NSSC pulping and its
correlation with H-factor for pulp scheduling.
Holzforschung 28 (4) : 121-130 (1974)
13. SINGH S.V., PANT RAJESH, AND GUHA S.R.D.
Kinetics of delignification in NSSC pulping of Eucalyptus
spp. and validity of H-factor.
Ippta 14 (2) : 103-110 (April-June '77)
14. PALMROSE C.G.
Tech. Assn. Papers 18 : 309 (1935)

15. McDONOUGH, VAN DRUNEN AND PAULSON

J. Pulp Paper Sci 11(6) : J167 (Nov.,1985)

16. McDONOUGH AND PAULSON

Preprints of the 1985 Tappi Pulping Conference

Hollywood, Florida, November 1985

Table 1
Effect of chip Thickness

Chip Thickness (mm)	Pulp Yield (% OD/OD)	Hypo No. of Pulp (unscreened)
0.5	66.1	15.1
1.0	66.8	15.4
2.0	67.8	16.3
3.0	70.6	17.8
4.0	74.1	19.1
5.0	74.4	20.1

Table 2
Effect of AQ addition Level

AQ Charge % on OD wood	Pulp Yield % OD/OD	Hypo No. of Pulp
0	75.0	26.8
0.10	68.5	21.3
0.20	67.5	20.0
0.49	66.7	18.6
1.01	66.4	17.6
1.49	66.6	17.5
2.49	67.6	17.9

Table 3
SULPHITE / AQ COOKING OF LOBLOLLY PINE

ID No	Minutes from 90°C	Temp. °C	Yield OD/OD %	Total Lignin (OD wood)	Residual Sulphite	Residual pH
3-1	43.25	160	81.2	21.2		9.71
3-2	48.25	169	75.6	17.7		9.70
3-3	56	181	67.5	12.5		9.70
3-4	60	181	63.7	10.3		9.70
3-5	66	179	60.6	8.4		9.69
3-6	75	176	58.4	6.9		9.69
4-1	42	157	82.6	21.9		9.70
4-2	48	169	76.8	18.4		9.70
4-3	55	180	67.4	12.3		9.70
4-4	61	180	63.8	10.1		9.69
4-5	75	180	57.6	6.5		9.68
4-6	80	180	56.2	5.7		9.67
5-1	34	141	87.5	24.4	47.4	9.78
5-2	39	150	84.7	23.5	47.0	9.77
5-3	51	170	74.4	17.2	45.7	9.78
5-4	57	170	70.0	14.0	45.2	9.77
5-5	83	170	60.5	8.5	44.2	9.74
5-6	106	171	57.1	6.4	43.5	9.72
6-1	30	131	91.0	26.3	47.6	9.82
6-2	45	160	80.0	21.2	46.7	9.73
6-3	61	161	72.7	16.1	45.6	9.74
6-4	85	161	66.8	12.4	45.1	9.74
6-5	125	161	62.0	9.1	44.0	9.73
6-6	170	161	58.5	7.0	43.5	9.72
6-7	221	161	56.9	5.9	43.4	9.71

All cooks at initial sulphite concentration of 48gpl

Table 4

SULPHITE / AQ COOKING OF SOUTHERN PINE COMPARISON DATA

REDUCED SULPHITE CONCENTRATION - 40gpl Na₂O

ID No	Minutes from 90°C	Temp. °C	Yield OD/OD %	Total Lignin (OD wood)	Residual Sulphite	Residual pH
7-5	55	180	64.7	11.9	36.5	9.75
7-6	67	180	58.3	7.7	35.5	9.74
7-7	76	180	56.6	6.6	34.8	9.73
7-8	93	180	53.1	4.7	34.5	9.72
8-5	45	160	78.5	20.2	38.2	9.76
8-6	63	160	71.5	15.5	37.4	9.75
8-7	107	160	64.1	10.7	36.5	9.75
8-8	235	160	56.6	6.1	35.2	9.75

NO AQ COMPARISON RUN

ID No	Minutes from 90°C	Temp. °C	Yield OD/OD %	Total Lignin (OD wood)	Residual Sulphite	Residual pH
7-1	55	180	73.9	22.4	45.7	9.69
7-2	62	180	71.2	21.1	44.8	9.68
7-3	93	180	64.3	16.8	44.4	9.65
7-4	121	180	60.4	14.4	43.7	9.65
8-1	45	160	83.6	25.4	46.6	9.76
8-2	105	160	74.4	22.3	45.3	9.68
8-3	206	160	67.1	17.9	44.5	9.66
8-4	345	160	62.6	15.3	43.8	9.66

Table 5

PULP ANALYSES - PERCENT ON OD WOOD

Sample Desig.	Yield % OD/OD	Cellulose %	Lignin %	Hemicellulose %	Total Cols 3-5
3-0	100.0	38.4	32.3	24.6	95.3
4-1	82.6	35.1	21.6	19.5	76.2
3-1	81.2	37.6	21.6	19.6	78.8
4-2	76.8	36.1	19.1	18.8	74.0
3-2	75.6	36.4	17.1	17.8	71.3
3-3	67.5	36.4	12.3	14.5	63.2
4-3	67.4	34.2	12.1	14.4	60.7
4-4	63.8	34.8	10.1	14.8	59.7
3-4	63.7	36.6	10.5	15.7	62.8
3-5	60.6	36.3	-	14.1	-
3-6	58.4	34.7	7.2	14.0	55.9
4-5	57.6	34.0	6.3	13.4	53.7
4-6	56.2	33.0	5.6	12.2	50.8

CARBOHYDRATE AND LIGNIN ANALYSES - PERCENT ON OD PULP

Sample	Araban	Xylan	Mannan	Galactan	Glucan	Klason Lignin	Soluble Lignin
3-0	1.5	7.7	10.0	2.1	41.7	31.7	0.6
4-1	1.5	8.2	8.9	2.1	45.4	25.0	1.2
3-1	1.5	8.8	8.9	2.1	49.3	25.1	1.5
4-2	1.6	8.8	8.8	2.2	50.1	23.4	1.4
3-2	1.4	8.9	8.4	2.2	51.0	21.4	1.3
3-3	1.6	9.3	7.3	0.9	56.4	16.6	1.7
4-3	1.7	9.2	7.4	0.4	53.3	16.3	1.6
4-4	1.6	8.6	8.2	1.9	57.3	14.2	1.6
3-4	1.5	9.2	9.1	2.0	60.5	14.7	1.7
3-5	1.4	8.9	8.4	1.8	62.6	-	1.8
3-6	1.4	8.7	8.7	2.2	62.4	10.0	2.4
4-5	1.5	8.8	8.5	1.7	61.9	9.4	1.6
4-6	1.3	8.1	7.8	1.7	61.3	8.2	1.7

Table 6
Initial Lignin Exponent Estimation

Cook ID Nos	Temperature (°C)	Data Range (% lignin)	No. of Data Points	Lignin Exponent	Correlation Coefficient
6-2 to 6-7	160	21.2-5.9	6	2.4	0.9994
8-5 to 8-8	160	20.2-6.1	4	2.4	0.9999
5-3 to 5-6	170	17.2-6.4	4	2.2	0.9999
4-3 to 4-6	180	12.3-5.7	4	1.4	0.9999
7-5 to 7-8	180	11.9-4.7	4	2.0	0.9978

Table 7

	General "n"th Order Reaction Model	Parallel Reaction Model*
	**Using all data over 155°C	**Using only data at 48gpl chemical conc.
	**All data except that below 155°C and at 180°C.	
Activation Energy		
kcal/gmole	34.25	35.25
		29.15 (1) 37.00 (2)
Reaction Constant	1.249×10^{13}	2.511×10^{13}
		1.389×10^{10} (1) 1.102×10^{15} (2)
Lignin Exponent	2.2	2.4
		2.4 (1) 2.4 (2)
Sulphite Exponent	0.5	0.5
		N/A
Standard Error- Selected Data**	0.49	0.39
		0.35

* (1) denotes sulphite only reaction, (2) denotes AQ reactions

** Refer analysis section for details.

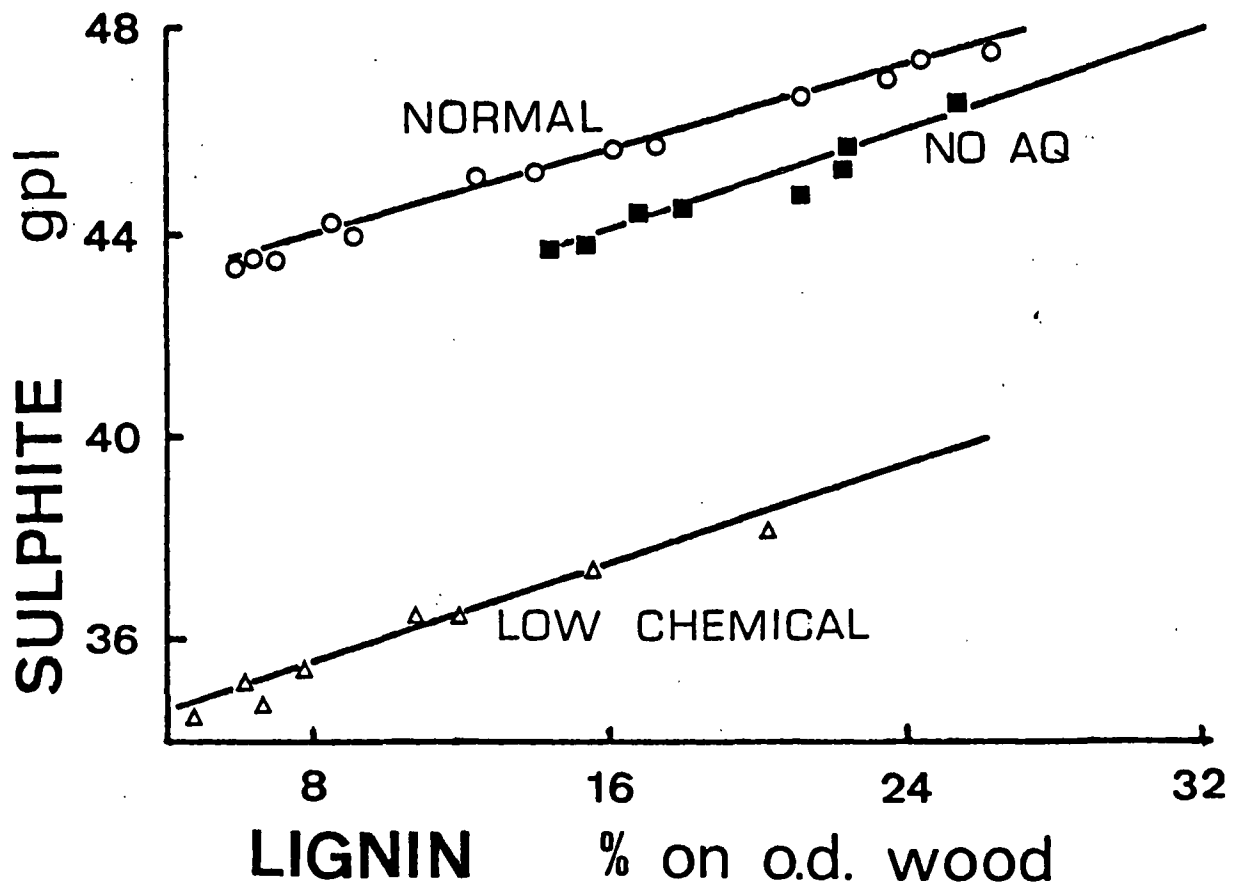


FIG. 1 RESIDUAL CHEMICAL

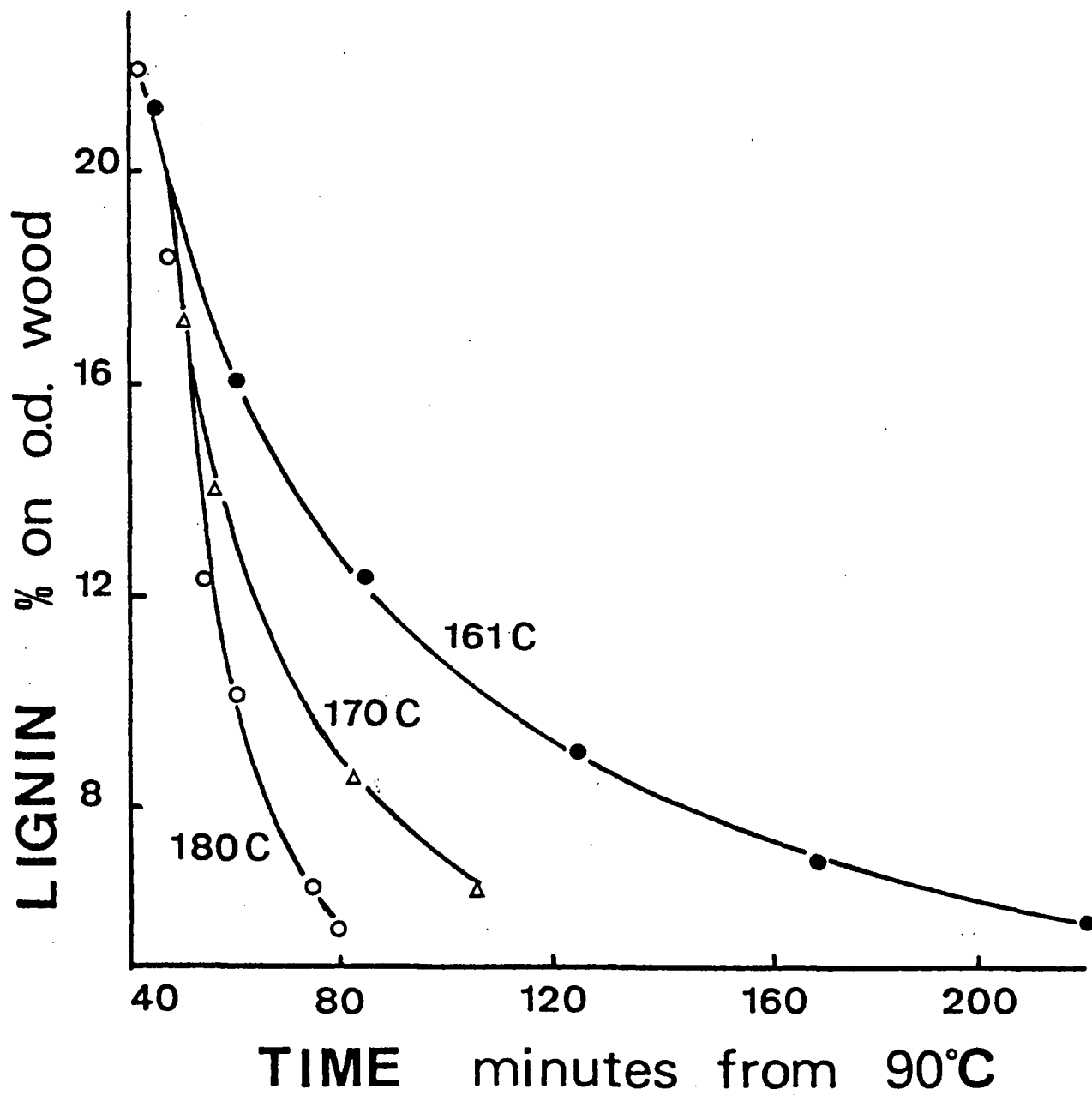


FIG. 2 PARALLEL REACTION MODEL

THE INSTITUTE OF PAPER CHEMISTRY

Appleton, Wisconsin

Status Report

to the

PULPING PROCESSES

PROJECT ADVISORY COMMITTEE

Project 3475

FUNDAMENTALS OF SELECTIVITY IN PULPING AND BLEACHING

Delignification Reactions

Carbohydrate Reactions

September 9, 1986

PROJECT SUMMARY FORM

DATE: September 9, 1986

PROJECT NO. 3475: FUNDAMENTALS OF SELECTIVITY IN PULPING AND BLEACHING

PROJECT LEADER: D. R. Dimmel

IPC GOAL:

Improved process for bleached chemical pulps

OBJECTIVE:

Provide a fundamental understanding of the chemical and physical reactions that control both:

- (1) the rate of lignin removal, hemicellulose dissolution, and cellulose degradation, and
- (2) the structures of the lignin, hemicelluloses and cellulose that remain in the pulp after pulping and bleaching.

CURRENT FISCAL YEAR BUDGET: \$150,000

SUMMARY OF RESULTS SINCE LAST REPORT:

Lignin Reactions

The chemistry of anthraquinone pulping has been singled out for study because of the high selectivities of this process. Studies into the detailed chemistry of anthrahydroquinone-model lignin interactions indicate the possible existence of unique, single electron transfer (SET) reactions.

Further studies in the last year add more support to arguments for SET reactions. Lignin models containing β -methoxy groups should be more difficult to fragment (a reaction analogous to delignification) than the typical β -aryl ether groups found in lignin and usual lignin models. Indeed, this was observed. By slowing the β -ether cleavage reactions, we then observed the types of reactions which may normally precede the cleavage reactions. The existence of reduction products suggested that SET reactions had occurred between anthraquinone (AHQ) and the β -methoxy models.

Related student research (D. Smith) has shown that α -pentenyl groups cyclize to the C_{α} -quinonemethide carbon (generating 5-membered rings) in the presence of AHQ and glucose at 135°C in alkali. The observed C_{α} - C_{γ} cyclization provides proof that radicals were formed at C_{α} -sites and, consequently, SET reactions had occurred. The student's model had built-in steric effects which probably prevented AHQ and glucose from bonding to the C_{α} -QM carbon and thus favored SET reactions. Attempts to synthesize lignin models which are analogous to Smith's "electron-detector" compound but have β -aryl ether groups have been unsuccessful. Correspondingly, models with one less carbon in the side chain were synthesized, tested, and found to be inappropriate.

Extensive studies have been carried out on a set of models containing β -propyl substituents, in which the terminal carbon of the propyl group is an olefin, alcohol, or O-trityl group. The propyl alcohol compound, but not the others, shows a large reactivity difference when using kraft or soda/AQ conditions. The results support an SET mechanism in the AQ case. Supporting data for this conclusion will come from the Ph.D. research of Gregg Reed, in which data on the relative nucleophilicities of hydroxide, hydrosulfide and AHQ ions will help distinguish simple ionic reactions from SET reactions.

Experiments aimed at understanding the cleavage reactions of vinyl ether compounds have been completed and have proved informative. The Ph.D. thesis research of P. Apfeld has produced an insoluble lignin model compound; tests have been conducted recently by us to determine the suitability of the model for lignin studies. Preliminary data suggest that the point of attachment of the lignin subunit to the polystyrene matrix is not stable to kraft pulping conditions.

A second generation high temperature electrochemical cell has been constructed, and testing is now underway.

Carbohydrate Reactions

Previous work has indicated the AQ has the potential to accelerate random chain cleavage reactions and thus cause pulp viscosity losses. Amylose is extensively cleaved by AQ, while crystalline cellulose is not. Recent degradations of two water soluble carbohydrate models, one representative of amylose and one of cellulose, gave approximately the same incremental increase rate of cleavage for both models. This result indicates that the stereochemistry of the carbohydrate linkages (amylose is α -1,4 and cellulose is β -1,4), does not play a major role in AQ-induced chain cleavage. Rather, the physical structure of the carbohydrate appears to be an important factor.

Recent efforts have been directed toward understanding the effect of anthraquinone on the viscosity and molecular weight distribution of amorphous cellulose degraded in 1M NaOH. To put the emphasis on chain cleavage rather than peeling, the amorphous cellulose has been reduced with sodium borohydride to stop primary peeling. The amorphous nature of the cellulose should not protect the cellulose from the potential harmful effects of anthraquinone. Preliminary results indicate that the anthraquinone can accelerate chain cleavage in the amorphous cellulose, suggesting that cellulose's usual partially crystalline nature protects it from adverse chain cleavage reactions with anthraquinone. The observed effects were small, but the levels of AQ were also small. Attempts to correlate chain cleavage levels with AQ levels have been foiled by our recent inability to prepare a high viscosity amorphous cellulose sample. Recent research has been concerned with generating amorphous cellulose samples from an SO₂/DEA/DMSO solvent system and examining better methods of derivatizing cellulose samples prior to molecular weight determinations.

PLANNED ACTIVITY THROUGH FISCAL YEAR 1987:

Testing of our most recent electrochemical cell will be continued. We need to show that the cell works well at both low and high temperatures. Initially,

simple substrates will be examined; eventually, we would like to attempt detection of quinonemethides at 130°C. Studies will be continued in an attempt to show the value of insoluble lignin model compounds for providing mechanistic information on pulping and bleaching reactions.

Work will continue on developing convenient, consistent procedures for generating high viscosity amorphous cellulose and for derivatizing cellulose samples. The improved procedures will be used to further verify the effects which AQ has on cellulose chain cleavage reactions. The synthesis of an alkali insoluble model will be completed; evaluation of its utility for defining cellulose chain cleavage reactions will be initiated.

FUTURE ACTIVITY:

The high temperature electrochemical studies will be expanded into evaluating methods to monitor pulping and promoting (probably indirectly) beneficial pulping reactions. As new information on SET reactions becomes available, we will examine novel ways to promote these reactions in an economical manner.

Methods which have been developed for determining cellulose molecular weight distribution will be applied to assess the effect of carbohydrate physical structure (crystalline vs. amorphous) on the extent of chain cleavage reactions. The methods will also be used to systematically study how changes in pulping and bleaching conditions affect carbohydrate chain cleavage reactions. For example, studies of cellulose chain cleavage in alkaline pulping indicate that increased ionic strength accelerates the cleavage reaction. Thus, the effect of "dead load" (increased ionic strength) on cellulose chain cleavage during pulping could be examined. Possible further applications of insoluble cellulose models will be explored.

STUDENT RESEARCH:

D. Geddes, Ph.D.-1987; M. Bovee, Ph.D.-1987; G. Reed, Ph.D.-1987; W. Molinarolo, Ph.D.-1987; J. Leege, M.S.-1987; P. Sands, M.S.-1987; P. Medvecz, M.S.-1987; R. Barkhau, Ph.D.-1988; J. Wozniak, Ph.D.-1988.

Status Report

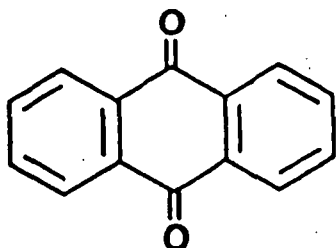
FUNDAMENTALS OF SELECTIVITY IN PULPING AND BLEACHING

Carbohydrate Reactions

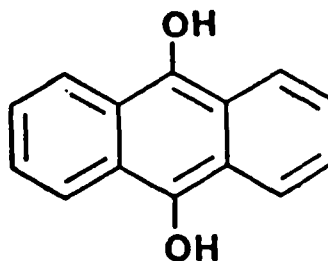
OBJECTIVE

The goal of chemical pulping is to liberate cellulosic fibers from wood through delignification without degrading or removing the wood polysaccharides. Unfortunately, alkaline pulping processes are not very selective for delignification. For example, in kraft pulping the loss of carbohydrate material may be comparable to, or even exceed, the lignin removal.¹⁻² In addition, reduction of the polysaccharide chain length, leading to decreased pulp viscosity and product strength, also occurs.¹⁻³

The objective of this project is to elucidate the mechanisms of carbohydrate and lignin degradation reactions which occur during pulping and bleaching. A better understanding of the chemistry involved will ultimately facilitate better control of pulping and bleaching selectivities. The fact that anthraquinone (AQ) increases pulping selectivity has stimulated interest in its chemistry. An immediate goal is to understand what role anthraquinone (AQ) plays in random glycosidic bond cleavage of wood polysaccharides and what role anthrahydroquinone (AHQ) plays in the rate of delignification of wood during pulping.



AQ



AHQ

LIGNIN REACTIONS

How do pulping chemicals, such as NaOH, NaSH, Na₂SO₃, AQ, etc., cause the lignin in wood to dissolve in pulping liquors? Most wood chemists would answer that all pulping chemicals act in a similar ionic fashion, adding to reactive lignin subunits known as quinonemethides (QMs) and then generally assisting in the cleavage of ether linkages which hold lignin units together.

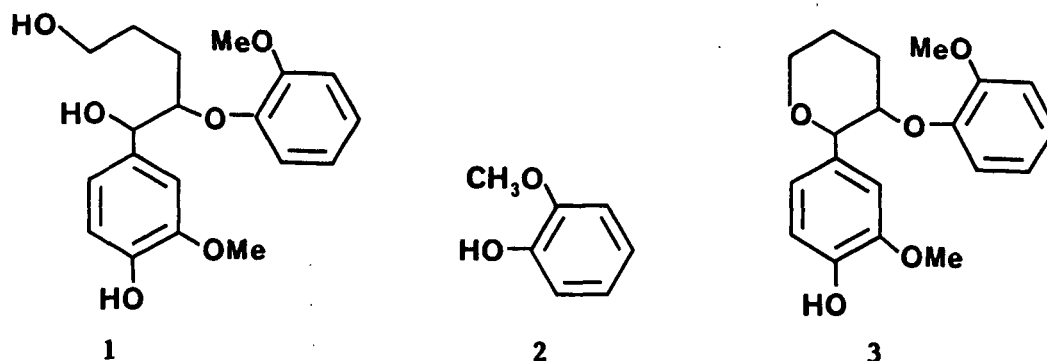
While this view may be correct for many pulping reagents, we feel that it is probably not accurate for explaining the rapid delignification associated with AQ pulping. We have been attempting to show in the last several years that single electron transfer (SET) mechanisms⁴ account for the effectiveness of AHQ, the reduced form of AQ, as a delignification aid.

Differentiation between pure ionic and SET mechanisms has not been easy. Often the results of carefully planned experiments have provided ambiguous answers.⁵ The results have been compatible with the SET mechanism and, in at least two cases, an electrochemical study⁶ and the thesis work of IPC student Dean Smith,⁷ have left no doubt that such reactions occur between AHQ and QMs. The question remains as to whether the SET reactions of AHQ dominate over possible pure ionic reactions of AHQ. We have tried in the last year to answer this and other basic questions about pulping mechanisms.

REACTIONS OF A β -PROPANOL LIGNIN MODEL

Compound 1 shown below has been synthesized and reacted at 135-150°C in aq. alkali with NaSH, glucose, and glucose/AQ (\equiv AHQ). Two principal products were observed: guaiacol (2), a fragmentation product (indicative of a delignification reaction) and the cyclized compound 3. The yields of 2 and 3 as a

function of time with the various reagents are shown in Fig. 1. [The yields with glucose are the same as that of the simple NaOH experiment.]



The yields of guaiacol follow the order AHQ \gg NaSH \gg NaOH. We interpret that the superior efficiency of AHQ indicates that it operates by a mechanism (SET) which is superior to the standard ionic mechanisms assigned to NaSH and NaOH. Except for some follow-up data, as shown in Fig. 1, the discussion of the data and results can be found in IPC Technical Paper Series Number 179, June, 1986.

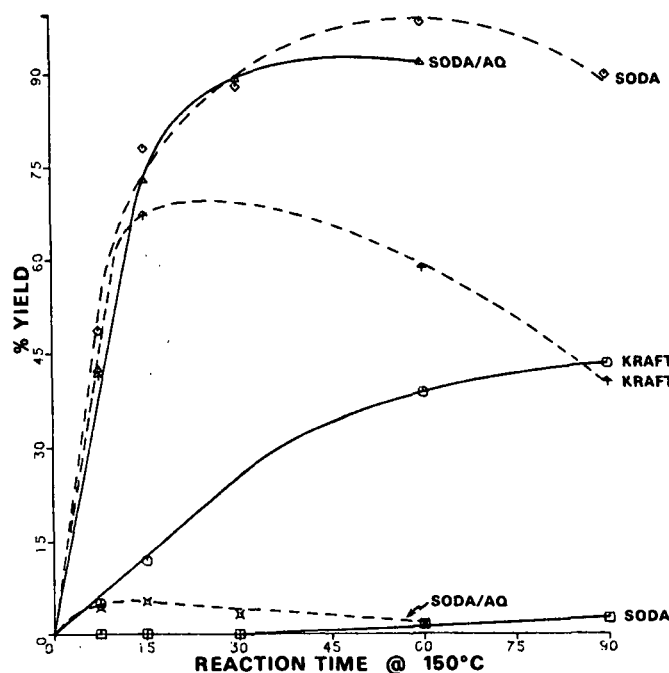
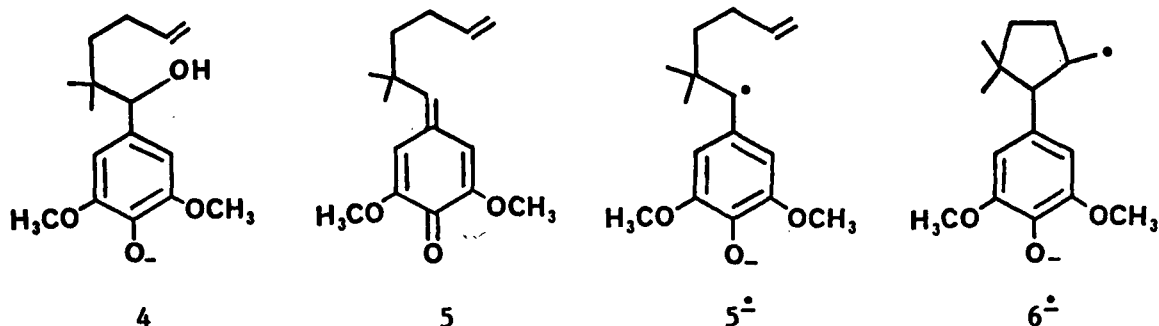


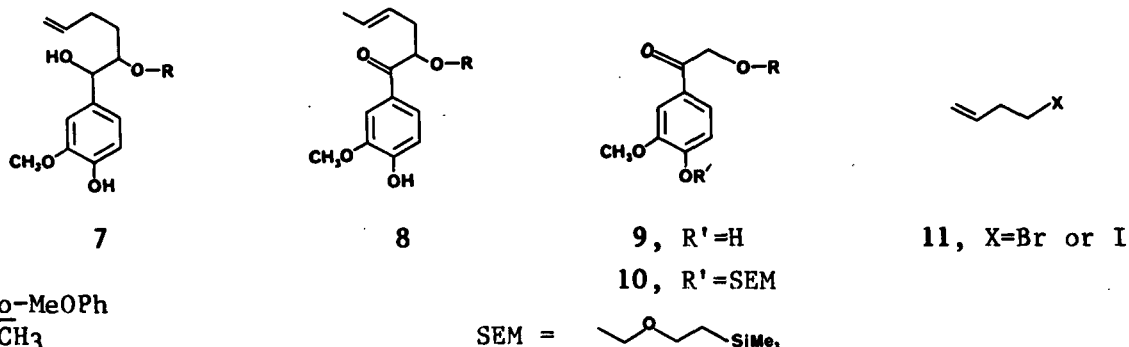
Figure 1. Yields of guaiacol (—) and cyclized compound 3 (---) as a function of time in the soda, kraft and AHQ degradations of model 1 at 150°C.

ATTEMPTED PREPARATION OF β -PROPENYL LIGNIN MODEL COMPOUNDS

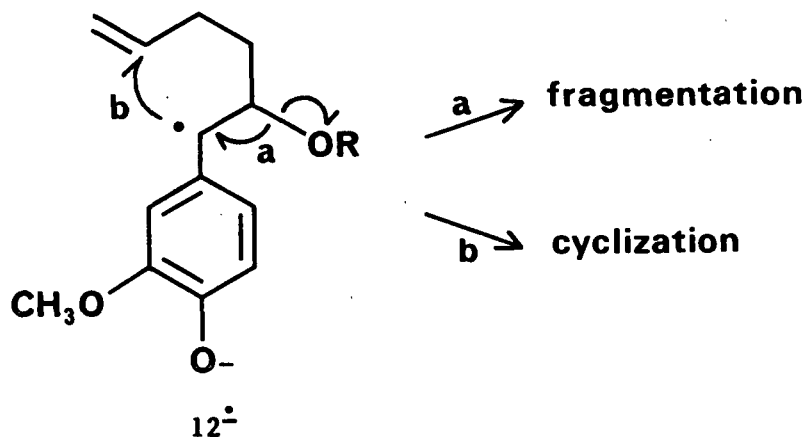
We have prepared, studied, and reported⁷ several reactions of compound 4. In alkali at elevated temperatures, this compound becomes ionized and interconverts with QM 5 and $^{\ominus}\text{OH}$. In the presence of electron donor compounds, QM 5 is converted to a radical anion $5^{\cdot-}$ which can cyclize to another radical anion $6^{\cdot-}$; various products of $6^{\cdot-}$ are observed. [Recently, we have been trying to isolate a sample of QM 5.]



The success of using compound 4 as an indicator of electron transfer reactions in pulping systems has led us to attempt to synthesize analogs 7A and 7B, having β -ether units. Unfortunately, we have been unsuccessful in preparing 7A and 7B by two different routes. One route involved attempted isomerizations of the alkene units in 8A and 8B; the other route involved attempted alkylations of 9A, 9B, and 10A (SEM is a phenol protecting group) with butenyl halides (11) under a wide variety of conditions.



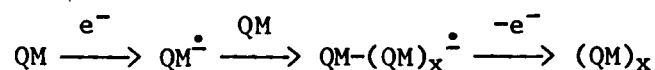
Our interest in 7 stemmed from the prospects that it would convert to a QM at elevated temperatures in aqueous alkali and that the QM 12 might accept an electron from an electron donor, such as AHQ⁻². The resulting QM 12^{•-} would be expected to fragment and/or cyclize. Since the rates of cyclizations of radicals to 5-membered rings are known, or can be determined,⁸ the rates of β -ether cleavage could be estimated.



ELECTROCHEMICAL STUDIES

Assuming that SET reactions are viable, important pathways for the destruction of lignin, how do we capitalize on this kind of chemistry? One way may be electrochemistry; here, electrons are supplied by an electrode. We have been working with Helena Chum at the Solar Energy Research Institute (SERI) to continue studies⁶ directed at understanding electron transfer reactions of QMs. We have been supplying SERI with compounds and helping to separate and characterize product mixtures.

Recent results indicate that electron transfer reactions in a solution which has a high concentration of QMs leads to polymers:



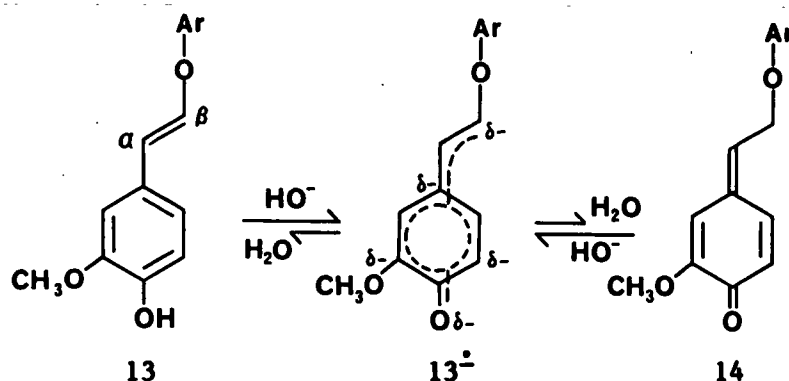
The polymeric material no longer has QM structural units, but can liberate QMs upon depolymerization.⁹

Of more immediate interest are the prospects of performing high temperature aqueous electrochemistry of solutions containing lignin model compounds or wood. Our first electrochemical cell provided us with some crude, insufficient results. Our second cell uses a different working electrode material (glassy carbon rather than platinum), an external reference electrode, and a different means of stirring. The cell was recently completed and preliminary results look encouraging.

We are anticipating that high temperature electrochemical studies will allow us to monitor the progress of pulping reactions and also provide a means to keep certain pulping catalysts, such as AQ, in their active forms. We are still waiting reply from the Department of Energy on our request for funding (\$800,000 over 3 years) on a joint proposal with SERI to pursue expanded research efforts in this area.

VINYL ETHER DEGRADATIONS

In degrading lignin models, and presumably during the pulping of wood, vinyl ether products are formed.⁵ Our previous work indicated that vinyl ethers, such as 13, slowly degraded in alkali.⁵ Because of interest expressed by PAC members and our own interest in the mechanism of vinyl ether degradations, we prepared, characterized, and studied the reactions of a vinyl ether model compound, 13, where Ar = 2-methoxy-4-methylphenyl.



The mechanism which we previously proposed⁵ was supported by our recent work. That is, in alkali 13 interconverts with QM 14; the latter can be attacked by good pulping additives, such as AHQ⁻² and SH⁻, and be fragmented. Attack of 14 by OH⁻ usually leads to regeneration of a vinyl ether but occasionally gives fragmentation. The observed fragmentation efficiencies were: AHQ⁻² \approx SH⁻ \gg OH⁻. The reversibility of the reactions, $13 \rightleftharpoons 14$, was demonstrated by running the degradation of 13 in D₂O/OD⁻ and observing the incorporation of deuterium in the C _{β} -position.

It should be mentioned that the extent of fragmentation of 13, even by a good catalyst (AHQ), was only about 25% after 2 hours. This low degree of fragmentation indicates a poor efficiency for the conversion of 13 to QM 14. In other words, reprotonation of 13⁻ is either unfavorable at 150° in aq. alkali or prefers a site other than the β -position. The work of Gratzl and coworkers¹⁰ provides additional support of these results and conclusions.

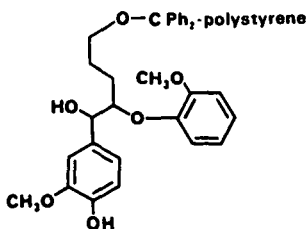
The significance of these findings is that processes such as soda pulping which produce many vinyl ether by-products will be slow at dissolving lignin. Our best processes will be those which capture or divert the quinone-methides before deprotonation to vinyl ethers occurs; the captured or diverted quinonemethides must be prone to fragment.

INSOLUBLE LIGNIN MODELS

The recently completed Ph.D. thesis of P. Apfeld concerned the synthesis, characterization, and preliminary reactions of a polymeric insoluble lignin model compound. Our interest in this model stems from the realization that pulping chemistry involves the degradation of **insoluble** lignin to soluble lignin particles. Studies involving degradation of **soluble** lignin model compounds may not accurately describe the true nature of the chemistry. Yet, soluble studies are the best we can presently do; detailed studies of actual lignin reactions are very complex due to the structural complexities of lignin.

Apfeld's thesis left many unanswered questions concerning the usefulness of his insoluble lignin model. We have taken up studying his model, since an understanding of the applicability of models of this type is needed to define the scope of other student thesis work and will guide us in future research directions.

Our recent work has involved synthesizing more of Apfeld's model 15 and demonstrating that the model-to-polymer tritylether linkage is not as stable as we had hoped. Kraft degradations of the model give the cyclized compound 3, mentioned earlier, along with guaiacol (a fragmentation product). However, much or all of the guaiacol appears to have come from degradation of the liberated cyclized compound and not the intact polymer model. Work is continuing toward finding a more stable model-to-polymer linkage.



FUTURE WORK

Continued testing of our present high temperature electrochemical cell will be a top priority activity. If this cell has deficiencies, we will build another. The information which could come out of these studies warrants a thorough investigation. The pace of the research has, however, been slower than expected due to our inability to rapidly get specialized pieces, such as glassy carbon, silver epoxy, etc., and our own inexperience. Therefore, additional research in other areas has been, and probably will continue to be, necessary as a supplement to our electrochemical activities.

We plan to continue studies directed at establishing the value of insoluble lignin model compounds for providing mechanistic information on pulping and bleaching reactions.

CARBOHYDRATE REACTIONS

INTRODUCTION

This part of the project work has been under the direction of Dr. L. R. Schroeder for as many years as the project has existed. However, with Leo's departure in April came a change in project leadership to one which is less experienced in carbohydrate chemistry. We have encountered a large number of problems lately which may reflect our inexperience or may be attributable to the nature of reactions; we like to think it is the latter. The problems have caused us to reexamine the basic procedures which have been applied in this research area.

REVIEW

Previous IPC student thesis work established that AQ (at a 5% level) caused a loss in the degree of polymerization (DP) of amylose for soda/AQ

experiments performed at 100°C.¹¹ Subsequently, the effects of AQ on DP loss in cellulose have been studied by two research groups; both used cotton linters as their substrate.

The Institute study² compared kraft to kraft/AQ and soda to soda/AQ at 170°C and a 0.5% addition level of AQ. The AQ experiments gave higher carbohydrate yields and, based on Cuene viscosity and DP_w analysis by gel phase chromatography (GPC) after sample derivatization, no apparent significant decrease in DP loss as compared to the cooks without AQ.

An Australian research team¹² examined three levels of AQ: 0, 0.1, and 5.0%. Within the probable errors of the experiments, there were no real differences in yields, Cuene viscosities, DP_w , and carboxyl groups per molecule for the 0 and 0.1% AQ cooks. In contrast the 5% AQ cooks showed higher yields and carboxyl groups per molecule and lower viscosities and DP_w 's than the corresponding no additive cooks.

In attempting to use realistic levels of AQ, both research groups may have underestimated the proper amounts of AQ to use. Typically, AQ is used at around a 0.1% level during pulping and, because of redox reactions, its concentration remains near this level during at least the first hour of reaction. The cotton linter experiments lack components necessary for sustaining an AQ/AHQ redox cycle. It is well known that AQ is converted to AHQ by reactions with carbohydrate reducing end groups (a reaction which increases carbohydrate retention). Both research groups have shown that AHQ has no effect on yield preservation or DP loss. Therefore, at low levels, AQ may be primarily consumed in yield preservation reactions and little remains to promote DP losses. Only at a 5% level does the DP loss become apparent.

In some elegant work, Schroeder and Lingnowski demonstrated that AQ causes roughly the same amount of glycosidic bond cleavage (analogous to a DP loss reaction) for carbohydrate models having either α -linkages (analogous to amylose) or β -linkages (analogous to cellulose).¹³ The AQ effect was rather small, again because a low level was used, along with nonredox cycle conditions. These results led Schroeder to conclude that the difference in reactivity between amylose and cellulose, when exposed to AQ, was physical rather than chemical.

With this as the premise, the project work was directed at examining the effects of AQ on DP losses of amorphous cellulose. The latter should be more physically accessible to reaction than highly crystalline cellulose, such as exists in cotton linters. A stabilized amorphous cellulose was produced by dissolving cotton linters in paraformaldehyde/DSMO, regenerating by addition to methanol/sodium methoxide, washing, treating with aq. NaBH_4 and drying (Fig. 2).¹⁴ The sodium borohydride step is necessary to reduce aldehyde end groups, thereby preventing primary "peeling," and placing the emphasis on chain cleavage reactions.

Some of the data which were generated and presented at the April 1986 PAC meeting are shown in Fig. 3 to 5. Clearly, the DP_w and Cuene viscosity analyses for one amorphous cellulose degradation agree (Fig. 3 and 4) and indicate greater chain cleavage in the presence of AQ. A second degradation of another amorphous cellulose gave similar viscosity trends (Fig. 5). The difference between no additive and AQ runs was small, but the levels of AQ employed were also small.

RECENT RESULTS

If a small amount of AQ causes a small drop in carbohydrate DP, a large amount should cause a large drop. Therefore, we set out to establish a relationship

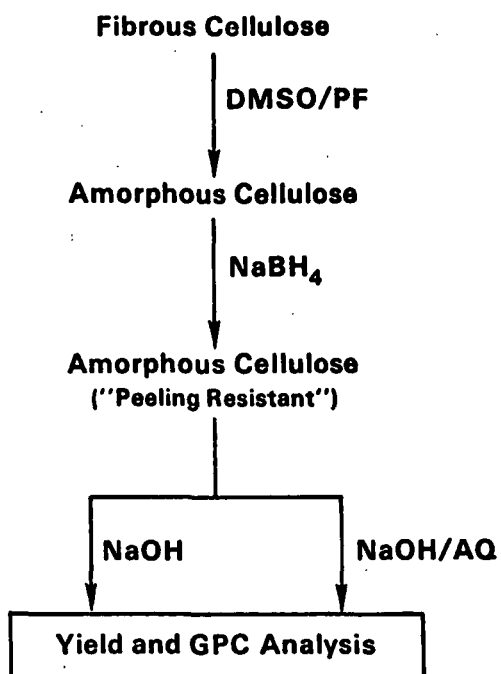


Figure 2. Amorphous cellulose preparation and reaction scheme.

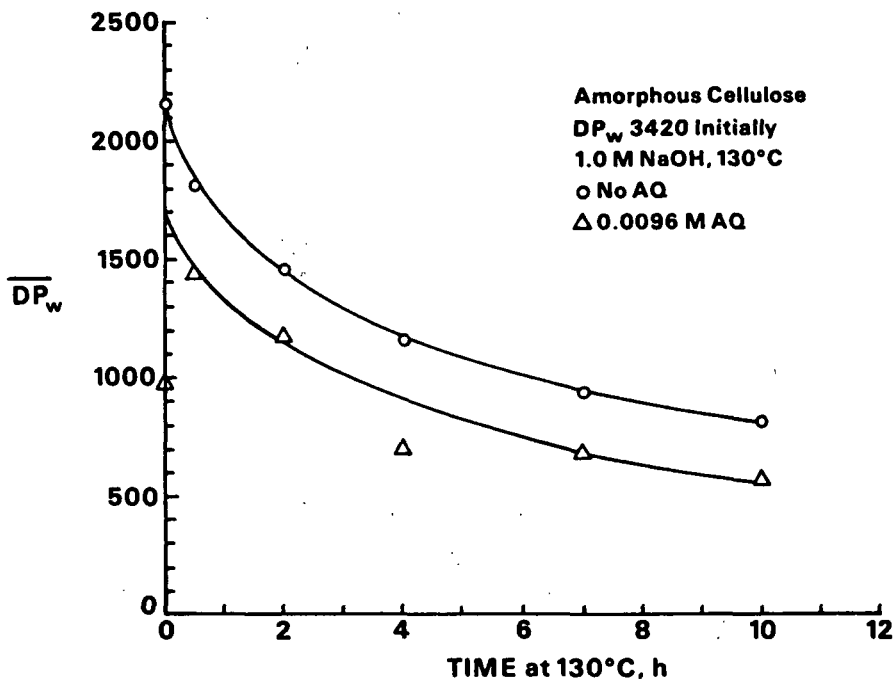


Figure 3. Changes in \overline{DP}_w with time for degradations of amorphous cellulose batch 21.

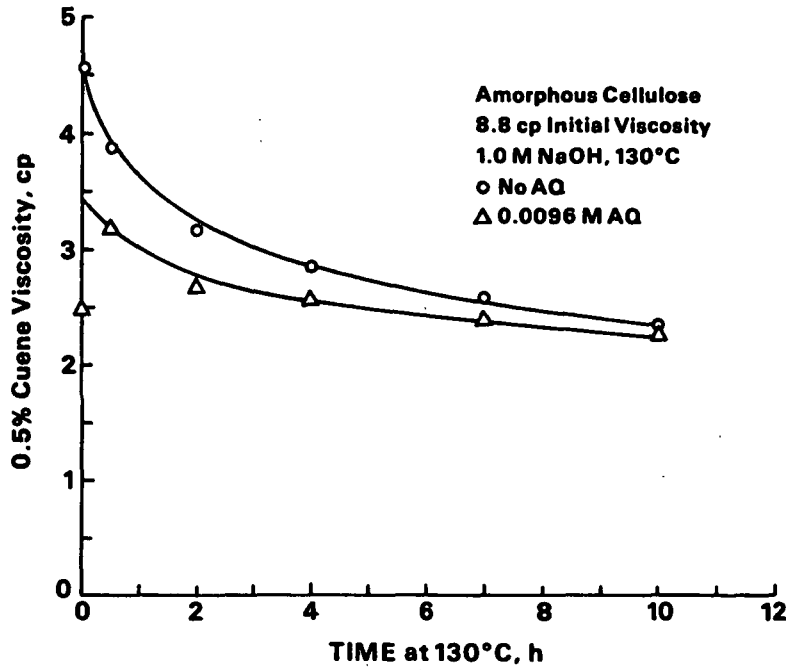


Figure 4. Changes in 0.5% Cuene viscosities with degradations of amorphous cellulose batch 21.

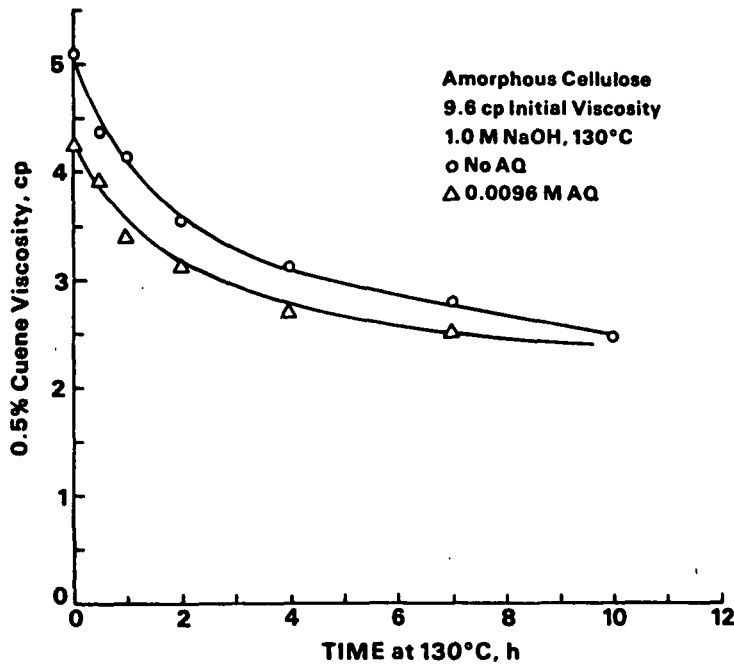


Figure 5. Changes in 0.5% Cuene viscosities with degradation of amorphous cellulose batch 9.

between AQ level and DP loss by varying the AQ concentration and/or providing for an AQ/AHQ redox cycle. Another approach taken was to lower the temperature of the reactions as a means to better accentuate the additive's effect.

Degradations done at 110°C provided data similar to those in Fig. 3 to 5, except differences between no additive and additive were smaller and the scatter in the data was greater. The viscosities of the various batches of amorphous cellulose and of the degraded sample were becoming too low. Cooks with various levels of AQ and with low levels of AQ, supplemented with lignin models, produced roughly the same low viscosity cellulose.

Our trouble in preparing a reasonably high viscosity amorphous cellulose and the time involved to do so by the paraformaldehyde/DMSO method led us to search for a better procedure. We found that we could, in general, prepare significantly higher viscosity amorphous cellulose samples in much less time using SO₂/diethylamine (DEA)/DMSO as a cellulose solvent.¹⁵ Further research showed that the magnitude of the amorphous cellulose viscosity depended on the method of precipitation of the soluble cellulose from the DMSO solution.

The SO₂/DEA/DMSO is an excellent solvent system for derivatizing cellulose;¹⁵ we have briefly explored other uses of this solvent. For example, we found that amorphous cellulose does not dissolve in this solvent system. It may, however, be possible to reduce cellulose with NaBH₄ in this solvent and to benzoylate cellulose in a closely related solvent mixture, namely SO₂/triethylamine/DMSO.

We have also been exploring better ways to carbanilate amorphous cellulose samples, prior to GPC analysis. The procedure which has most often been used in this project work involves employing phenyl isocyanate in pyridine;

derivatization yields have been quite variable. Preliminary work with the same system, except replacing the pyridine with DMSO and varying the work-up procedure, appears to be a promising way to obtain high derivatization yields.

SUMMARY

We are searching to understand the factors which contribute to the generation of a high viscosity, high DP amorphous cellulose sample and the efficient derivatization of cellulose samples. The improved procedure will be used to study the effects of AQ on cellulose DP losses.

FUTURE STUDIES

Our immediate goals are to develop convenient, consistent procedures for generating high DP amorphous cellulose and for derivatizing cellulose samples. Next, we will use these procedures to assess the importance of carbohydrate physical structure on the extent of chain cleavage reactions and to systematically study how changes in pulping and bleaching conditions affect carbohydrate chain cleavage reactions.

One of our Ph.D. students, Matt Bovee, is in the finishing stages on a project involving the synthesis of an alkali insoluble cellulose model. With his guidance, we will be synthesizing additional quantities of his model and then will proceed to test its value for defining cellulose chain cleavage reaction mechanisms.

STUDENT RESEARCH

There is considerable student research activity in the wood chemistry area related to this project work. Briefly listed below are the students and their research topics.

MS STUDENTS

Leege, Joseph C.

A characterization of the thermodynamic functions of activation for 1,5-anhydromaltitol under alkaline conditions.

Sands, Peggy D.

The role of the 1,2-hydride shift mechanism in base-catalyzed aldose-ketose isomerizations.

Medvecz, Patrick J.

o-Quinone formation in hardwood and softwood TMP.

Ph.D. STUDENTS

Reed, Gregg A.

The role of sulfur species in pulping reactions.

Molinarolo, Wm. E.

High temperature alkaline degradation of phenyl beta-D-glucopyranoside.

Barkhau, Robert A.

Anthraquinone inhibited lignin condensation.

Wozniak, John. C.

Preparation and reactions of Diels-Alder adducts of lignin-derived quinones.

Bovee, M.

The synthesis and evaluation of an alkali insoluble cellulose model.

REFERENCES

1. Matthews, C. H., Svensk Papperstid. 77:629(1974).
2. Schroeder, L. R., Project 3284 Interim Report to the Program Committee, March 17, 1986.
3. Schroeder, L. R.; Wabers, B. A., Project 3475-1 Interim Report to the Program Committee, Sept. 10, 1982.

4. Dimmel, D. R., J. Wood Chem. Technol. 5:1(1985).
5. Dimmel, D. R.; Schuller, L. F., IPC Technical Paper Series Number 159, 160, and 165; J. Wood Chem. Technol., accepted for publication.
6. Dimmel, D. R.; Perry, L. F.; Chum, H. L.; Palasz, P. D., J. Wood Chem. Technol. 5:15(1985).
7. Smith, D. A.; Dimmel, D. R., Internat. Symp. on Wood and Pulping Chem., Vancouver, B.C., Canada, August 28, 1985; Project 3475-2 Interim Report Sept. 5, 1985; Ph.D. Thesis, June, 1986.
8. Beckwith, A. L. J.; Easton, C. J.; Lawrence, T.; Serelis, A. K., Aust. J. Chem. 36:545(1983).
9. Manuscript in preparation.
10. Araki, H.; Hawes, D. H.; Schroeter, M. C., Chen, C. L.; Gratzl, J. S., Canadian Wood Chem. Symp., Harrison Hot Springs, B.C., Canada, Sept., 1979.
11. Arbin, F. L. A.; Schroeder, L. R.; Thompson, N. S.; Malcolm, E. W., Tappi 63(4):152(1980); *ibid.*, Cellulose Chem. Technol. 15:523(1981).
12. Wallis, A. F. A.; Wearne, R. H., Internat. Symp. on Wood and Pulping Chem., Vancouver, B.C., Canada, August 1985, p. 89 of the abstracts; Evans, R., Wallis, A. F. A., and Wearne, R. H., personal communication.
13. Schroeder, L. R.; Lingnowski, H. J., Project 3475-1 Interim Report, Sept. 5, 1985.
14. Schroeder, L. R.; Gentile, V. M.; Atalla, R. H., J. Wood Chem. Technol. 6:1(1986).
15. Isogai, A.; Ishizu, A.; Nakano, J., J. Appl. Polym. Sci. 29:2097(1984).

THE INSTITUTE OF PAPER CHEMISTRY



Donald R. Dimmel
Senior Research Associate
Wood Sciences
Chemical Sciences Division

Lois F. Schuller
Research Assistant

Holly J. Lingnowski
Research Assistant

THE INSTITUTE OF PAPER CHEMISTRY

Appleton, Wisconsin

Status Report

to the

PULPING PROCESSES

PROJECT ADVISORY COMMITTEE

Project 3477

DEVELOPMENT AND APPLICATION OF ANALYTICAL TECHNIQUES

Determination of Lignin in Wood Pulp by Diffuse Reflectance
Fourier Transform Infrared Spectrometry

Analysis of Pulp and Bleaching Liquors by Ion Chromatography

Pyrolysis Gas Chromatography

September 3, 1986

PROJECT SUMMARY FORM

DATE: September 3, 1986

PROJECT NO. 3477: DEVELOPMENT AND APPLICATION OF ANALYTICAL TECHNIQUES

PROJECT LEADER: D. B. Easty

IPC GOAL: N/A

OBJECTIVE:

Evaluate and/or develop analytical techniques which are required to meet demands of both Institute and member company activity.

CURRENT FISCAL YEAR BUDGET: \$60,000

SUMMARY OF RESULTS SINCE LAST REPORT:

Determination of Lignin in Wood Pulp by Diffuse Reflectance
Fourier Transform Infrared Spectrometry

Linear relationships were found to exist between the area of the 1510 cm^{-1} infrared band, measured by diffuse reflectance FTIR, and kappa number and Klason lignin. The relationships are affected little by species and hardwood-softwood differences, and they apply to kraft and ASAQ pulps prepared over a wide yield range (1-20% lignin, 10-120 kappa).

Infrared band areas in the midrange of the data from this study may be used to estimate kappa number within about ± 4 kappa and Klason lignin within about $\pm 0.5\%$. Klason lignin can be predicted almost as accurately from IR band area as from kappa number.

Techniques developed in this study can be used to measure FTIR lignin band areas on pulp samples as small as 0.5 mg. These findings complete the work planned for this investigation.

Analysis of Pulping and Bleaching Liquors by Ion Chromatography

Results of our earlier studies on analysis of bleaching liquors by ion chromatography were published in May [Easty, Johnson, and Webb, Paperi Puu 68(5):415 (1986)]. That work showed that the ion chromatograph was capable of determining chlorine-containing anions, chlorine dioxide (as chlorite), and chlorine (as hypochlorite) in bleach liquors.

Scheduled for presentation at a symposium in September are our findings regarding ion chromatographic determination of sulfide and sulfate. Our studies documented the value of the UV detector for sulfide and also showed that sulfate could be determined in green liquor if it is diluted with deoxygenated water and immediately injected into the ion chromatograph.

A revision of TAPPI Test Method T699, Analysis of Bleaching and Pulping Liquors by Ion Chromatography, was written during the summer. The first draft, containing many of the findings from this project, was sent to a few ion chromatographers in the industry for their comments. A second draft incorporating their suggested revisions is being prepared for submission to TAPPI in September.

Recent laboratory work has been directed at identifying and correcting potential errors in the ion chromatographic analysis of pulping liquors. Techniques have been suggested for withdrawing and diluting samples of black liquor. Errors due to chromatography may be reduced by frequent running of standards and monitoring of peak shapes and baselines.

Pyrolysis Gas Chromatography

The investigation of pyrolysis gas chromatography (PGC) was undertaken to develop that technique as a complement to FTIR for the identification of polymeric unknowns in our laboratory. After pyrolysis and GC conditions had been tentatively adopted, "unknown" samples from industry, previously identified by FTIR, were analyzed. Ease of interpretation of a pyrogram was found to depend on the polymer itself as well as on accompanying interferences.

PLANNED ACTIVITY THROUGH FISCAL YEAR 1987:

We will follow closely the progress of the revised TAPPI Test Method on ion chromatography as it is reviewed in TAPPI's Process and Product Quality Division. Responses to negative votes will be developed as needed.

Limited studies of errors in the ion chromatographic analysis of pulping liquors will be continued. Liquor instability and problems in withdrawing representative samples will be considered further.

The objectives of continued work on pyrolysis gas chromatography will be to expand our library of pyrograms, reduce the complexity of pyrograms, and improve techniques for complex pyrogram interpretation.

A headspace gas concentrator will be interfaced with the gas chromatograph/mass spectrometer. Its use for analysis of mill air samples and paper samples having odors will be investigated.

FUTURE ACTIVITY:

Future work will involve continued studies of pulp and liquors by chromatographic and spectrometric techniques. Likely topics are improved material balance in unbleached pulp analysis and use of Raman spectrometry for determination of sulfur-containing inorganics in kraft pulping liquors.

Status Report

DEVELOPMENT AND APPLICATION OF ANALYTICAL TECHNIQUES

Determination of Lignin in Wood Pulp by Diffuse Reflectance
Fourier Transform Infrared Spectrometry

INTRODUCTION

Methods most often used for quantitative determination of lignin in wood and pulp are time consuming wet chemical procedures. The Klason lignin determination¹ requires about three days. This time may be reduced somewhat by using a small-scale variation of the method.² Kappa number measurements³ require about 15 minutes, provided the required reagents have previously been prepared. The relationship of kappa number to Klason lignin varies with wood species and pulping process.^{4,5}

Infrared (IR) spectrometry has been employed for the study of lignin in wood and pulp for over 20 years.⁶⁻⁹ Differential IR spectra were obtained with a KBr pellet containing wood meal or pulp in the sample beam and holocellulose in the reference beam. A characteristic of these differential spectra was the extreme care necessary to prepare matched pellets and to balance the energy levels of the sample and reference beams. In many cases the spectra suffered from poor resolution associated with low energy levels characteristic of dispersive IR spectrometers. Using the differential method, about 10% lignin was the lower limit for pulp samples which would permit the recording of spectra.⁷

Determination of lignin by infrared was significantly improved by use of the multiple internal reflection (MIR) technique.¹⁰ Pulp samples were made into handsheets and clamped in contact with the MIR prism in the IR spectrometer. The transmittance difference between the 1510 cm^{-1} lignin peak and the 1310 cm^{-1}

carbohydrate peak was found to correlate with lignin content and kappa number. This correlation was enhanced when the 1310 cm^{-1} peak was set at $45 \pm 0.5\%$ T by adjustment of the clamping pressure.

Infrared spectrometry has been revolutionized by the advent of Fourier transform infrared (FTIR) spectrometers. The heart of the instrument is an interferometer, which permits the FTIR system to measure a complete IR spectrum in the same time it takes a dispersive spectrometer to measure one resolution element. A computer is used to run the instrument, collect the raw data (interferogram), and calculate the Fourier transform to give the absorbance or transmittance spectrum. A single FTIR scan can be performed in less than a second. Thus, signal averaging of multiple FTIR scans can be used to obtain a useful spectrum with little noise from measurements involving low levels of infrared energy. The FTIR has no energy-limiting slits and allows more energy (than dispersive IR) to reach the sample and subsequently the detector. This yields higher analytical sensitivity.

A consequence of the great sensitivity of FTIR is its ability to generate useful spectra from the surface of ground or powdered samples by diffuse reflectance. This technique has recently been used by Schultz et al. to characterize hardwood chips which had been pretreated by a rapid steam hydrolysis (RASH) process.¹¹ The pretreated samples were air dried, ground with KCl, and their diffuse reflectance FTIR spectra were obtained. Manipulation of the absorbances of 18 peaks yielded predicted lignin, glucose, and xylose contents which correlated with the measured amounts of these components in the samples.

Over four years ago, exploratory work was initiated in this laboratory to examine the possibility of determining lignin in unbleached pulps by diffuse

reflectance FTIR. It was hypothesized that if the diffuse reflectance spectrum of an unbleached pulp is obtained and a carbohydrate spectrum is subtracted from it, a lignin spectrum should result. The intensity of the lignin spectrum should be proportional to the lignin content of the pulp. Such spectra would provide the basis for a method of lignin determination which is rapid and requires minimal sample preparation. The method would be validated by correlation with Klason lignin and/or kappa number.

Initial results revealed a linear relationship between IR absorbance at 1500-1510 cm^{-1} and kappa numbers of pulps from one wood cooked to varying degrees. Despite the limited basis for this relationship, other investigators at the Institute began requesting "FTIR lignin" on pulps that they were studying. Thus the need for this method was demonstrated.

Recent efforts have been directed at learning whether the correlation between IR absorbance and lignin content varies with wood species and pulping processes. The utility of the method for analysis of small samples and those with low lignin content has also been studied. This investigation has documented the validity of the FTIR lignin method and has demonstrated its ease and simplicity.

INSTRUMENTATION AND PROCEDURES

Spectra were collected on a Nicolet 7199 FTIR spectrometer equipped with a liquid nitrogen-cooled MCT detector and a Harrick Praying Mantis diffuse reflectance attachment. Maximum spectral resolution was 2 cm^{-1} . Five hundred scans for each sample were accumulated in approximately nine minutes.

Pulp fiber clumps were placed in the diffuse reflectance attachment where the IR beam was focused for maximum signal output. Infrared spectra were

recorded for various pulps and cotton linters. Each spectrum was ratioed against a background of potassium chloride before baseline correction. The reference cotton linters was subtracted from each pulp sample by manually obtaining the best baseline subtraction in the aliphatic C-H stretch region (2800-3000 cm^{-1}). To determine the best subtraction factor, the spectrum of the cotton linters was overlaid on the pulp spectrum on the computer screen. The area of the lignin band at 1510 cm^{-1} was integrated and recorded for data analysis.

Typical IR spectra are shown in Fig. 1 to 3: an unbleached pulp, the reference cotton linters, and a subtraction spectrum showing clearly the 1510 cm^{-1} peak.

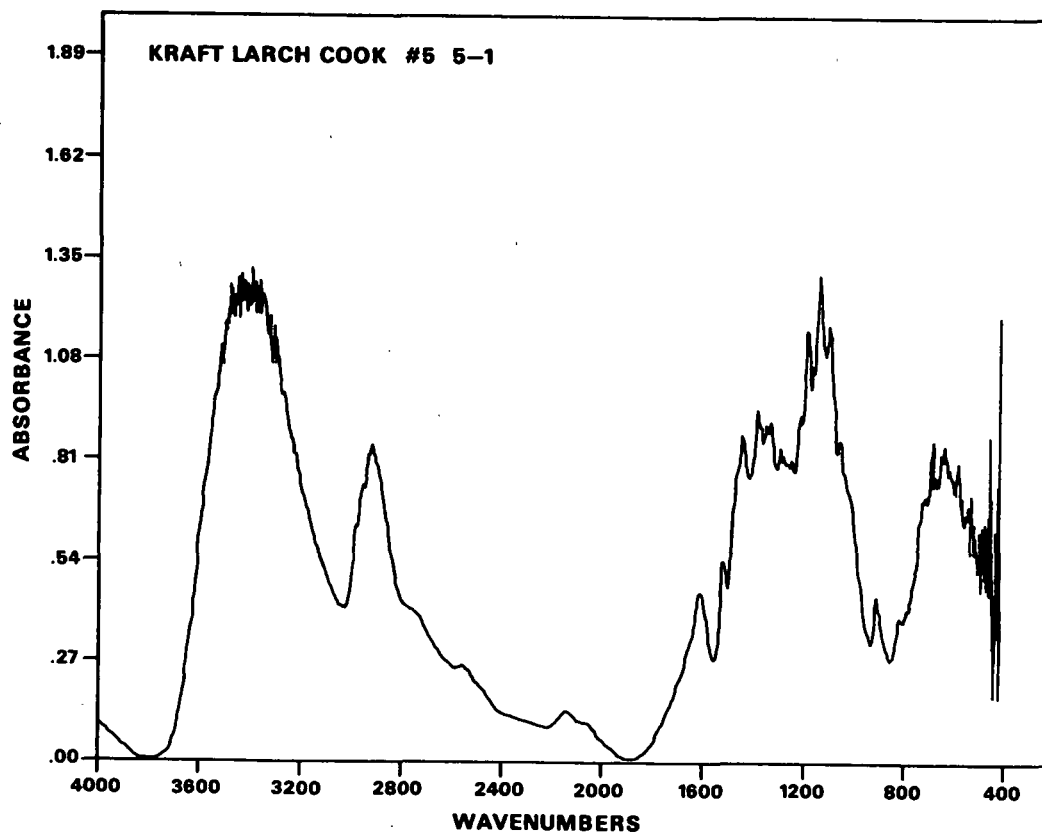


Figure 1. Diffuse reflectance FTIR spectrum of an unbleached pulp.

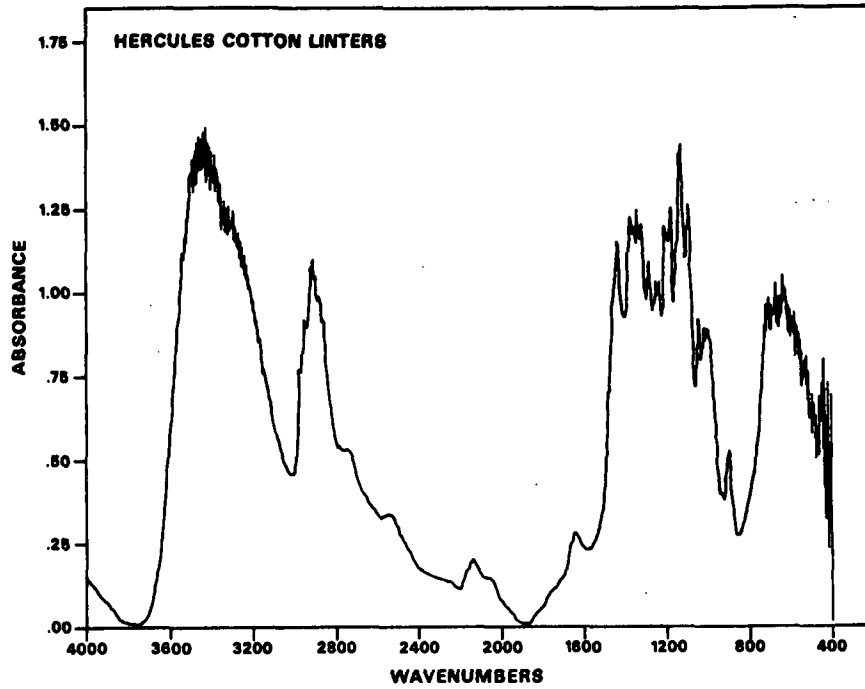


Figure 2. Diffuse reflectance FTIR spectrum of cotton linters.

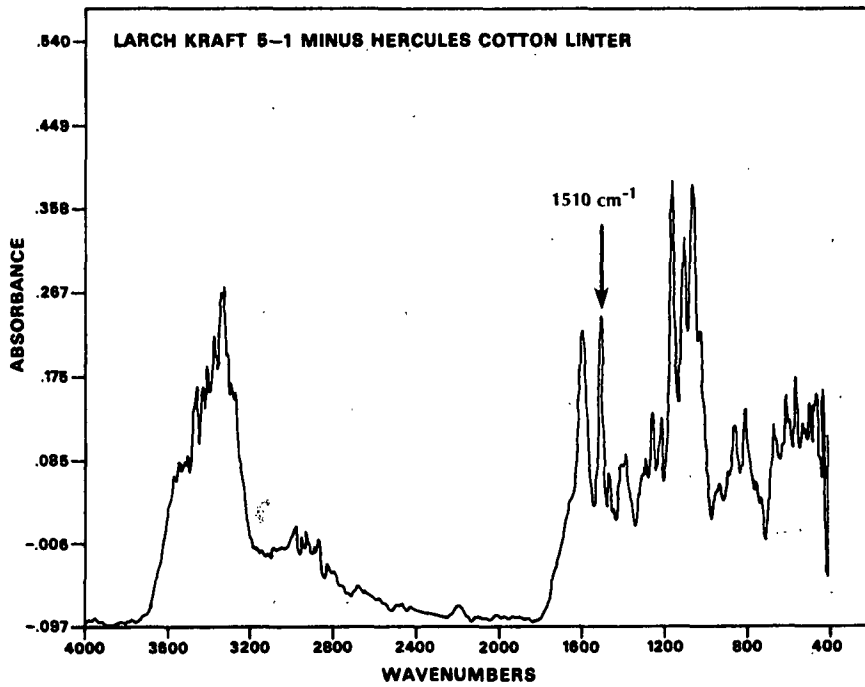


Figure 3. Subtraction spectrum. Unbleached pulp minus cotton linters.

Diffuse reflectance FTIR spectra do not provide an independent measurement of lignin in pulps. Infrared band areas must first be shown to correlate with lignin contents determined by other methods such as kappa numbers and Klason lignin values. Regression lines may then be regarded as representing functional relationships between band areas and lignin contents, and they will assume the role of calibration curves. The final step in measuring "FTIR lignin" must involve referring the sample's IR band area to a calibration curve to determine the lignin content of the pulp.

RESULTS AND DISCUSSION

CORRELATIONS WITH KAPPA NUMBER AND KLASON LIGNIN

Plots of infrared band area vs. kappa number and Klason lignin are shown in Fig. 4 to 9. Band areas are in arbitrary units. Data were obtained on kraft pulps prepared over a wide yield range from three hardwoods and two softwood species. Also included are data on several loblolly pine alkaline sulfite anthraquinone (ASAQ) pulps; for these pulps the plotted "Klason lignin" values are actually Klason plus acid-soluble lignin. Solid lines on the figures are calculated regression lines. Dashed lines represent 95% confidence contours. Correlation coefficients are shown as r-values.

The figures reveal, in general, the existence of linear relations between IR band area and lignin content expressed as kappa number and Klason lignin. Correlation coefficients range from 0.97 to 0.99. Although the lines would be expected to go through the origin, all have finite intercepts. Use of the lines below about 1% lignin and a kappa number of 10 is therefore not recommended.

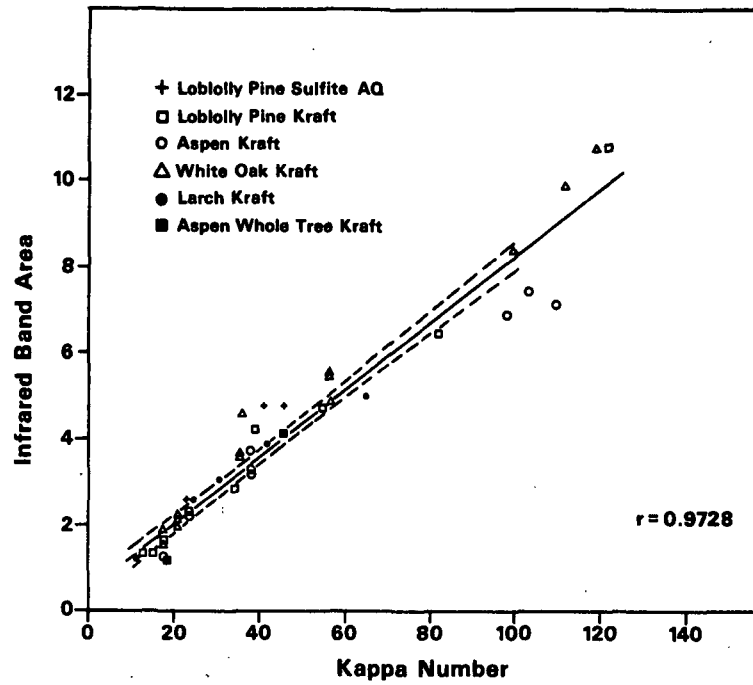


Figure 4. IR band area vs. kappa number. All species.

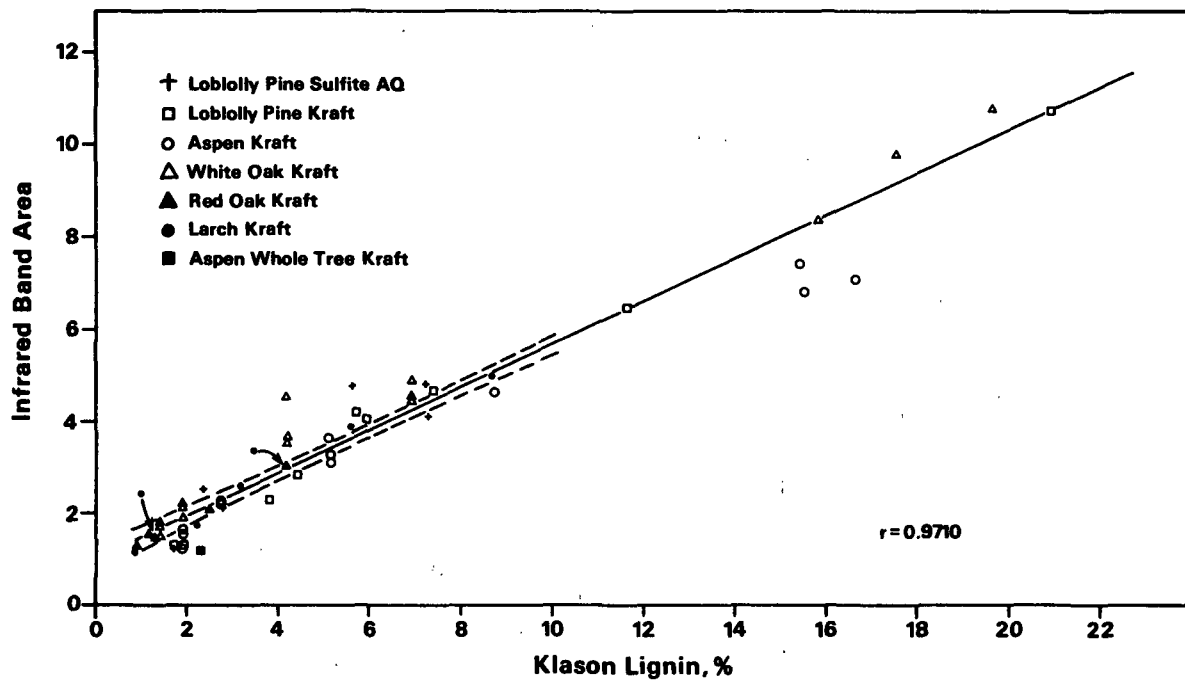


Figure 5. IR band area vs. Klason lignin, %. All species.

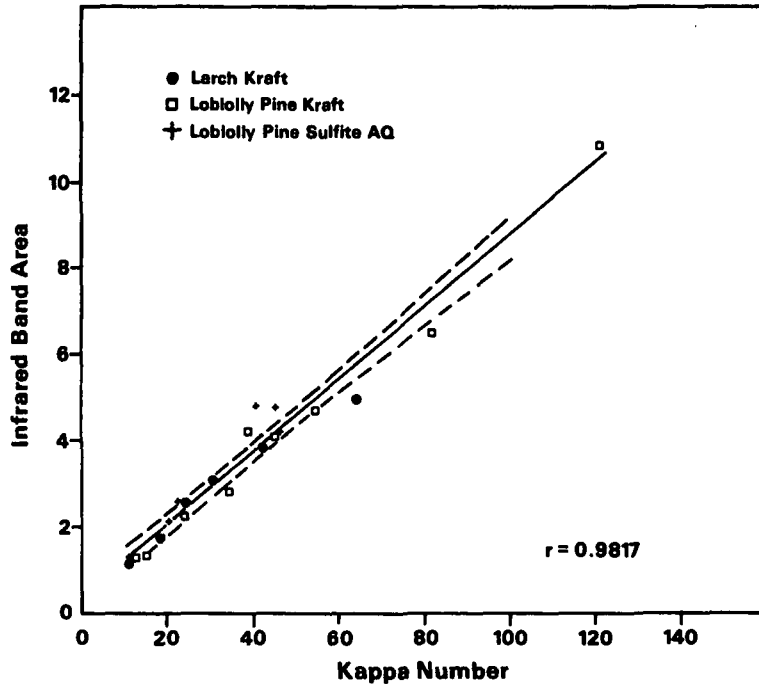


Figure 6. IR band area vs. kappa number. Softwood.

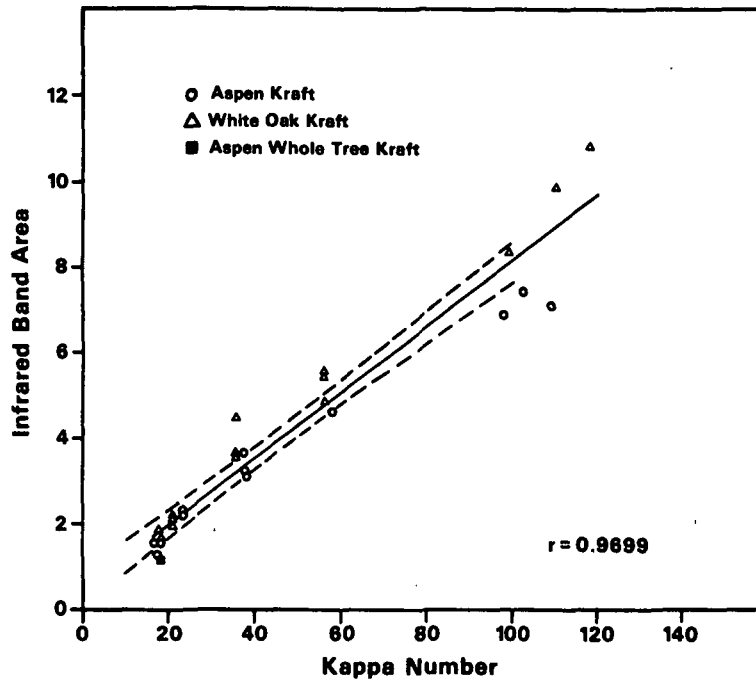


Figure 7. IR band area vs. kappa number. Hardwood.

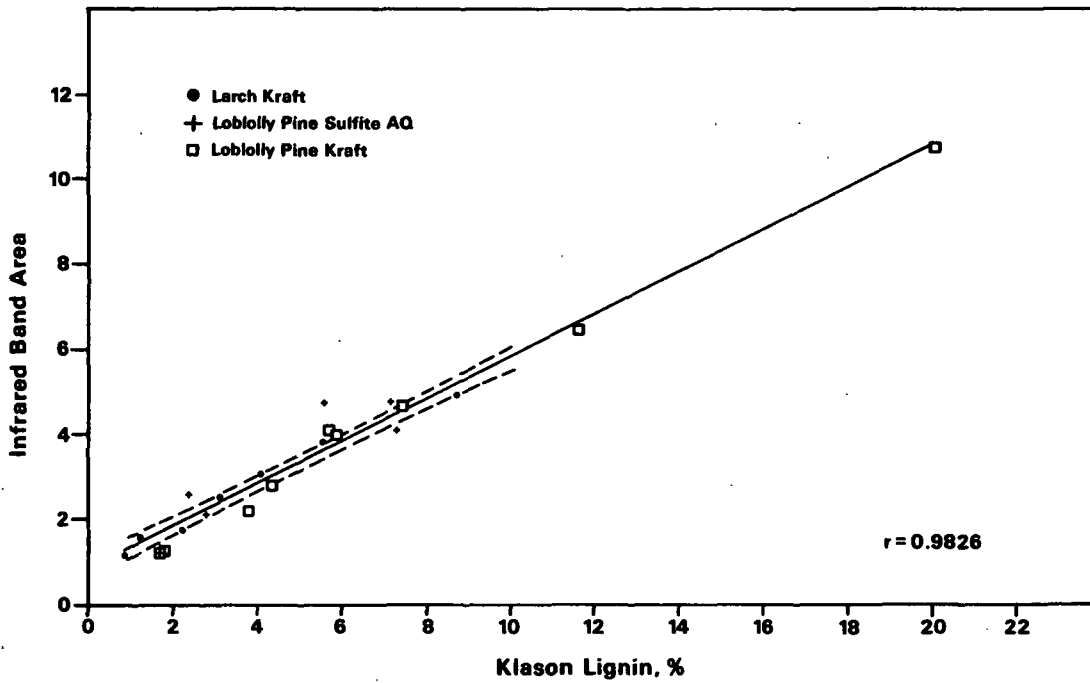


Figure 8. IR band area vs. Klason lignin, %. Softwood.

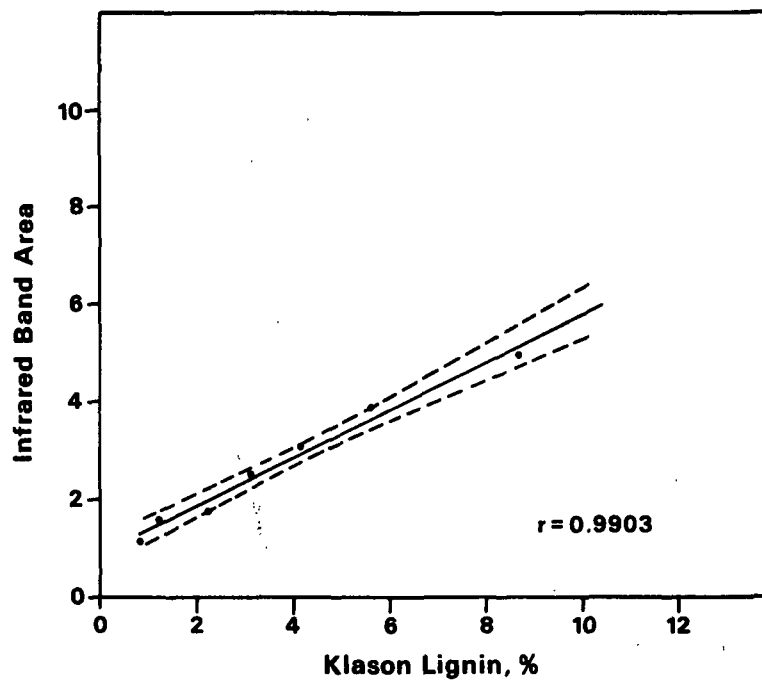


Figure 9. IR band area vs. Klason lignin, %. Larch kraft.

Figures 4 and 5 contain all of the data from this investigation. Points for hardwood pulps with high lignin contents tend to be farthest from the regression lines. These high-yield pulps had undergone very little delignification, and they perhaps were not homogeneous. Diffuse reflectance FTIR is a surface measurement, while kappa number and Klason lignin should indicate the lignin content of the whole sample.

Infrared band areas are not strongly affected by generic differences between hardwoods and softwoods. Figure 6, which contains softwood data, and Fig. 7, for hardwoods, have very similar slopes (0.083 and 0.077, respectively).

The 95% confidence contours can be used to indicate how closely kappa number and Klason lignin values could be estimated from IR band areas.¹² From Fig. 6 and 7, kappa number may be estimated within about ± 4 kappa (95% confidence limits). Figures 8 and 9 show that Klason lignin may be estimated within about $\pm 0.5\%$. Note that the confidence limits become larger above and below the mean of the IR band areas.

Figure 10 is a plot of the kappa number and Klason lignin data obtained in this study. Substantial scatter about the regression line is evident. It seems likely that Klason lignin could be predicted almost as accurately from IR band area as from kappa number.

COMPARISONS WITH OTHER WORK

Most of the data used to develop correlations between diffuse reflectance FTIR lignin band areas and lignin contents in this work were collected below kappa number 60 and 10% Klason lignin. Differential IR spectra measured on KBr pellets using dispersive IR spectrometers were insensitive below 10%

lignin in pulp.⁷ Thus, FTIR instrumentation provides enhanced sensitivity in lignin measurements by infrared.

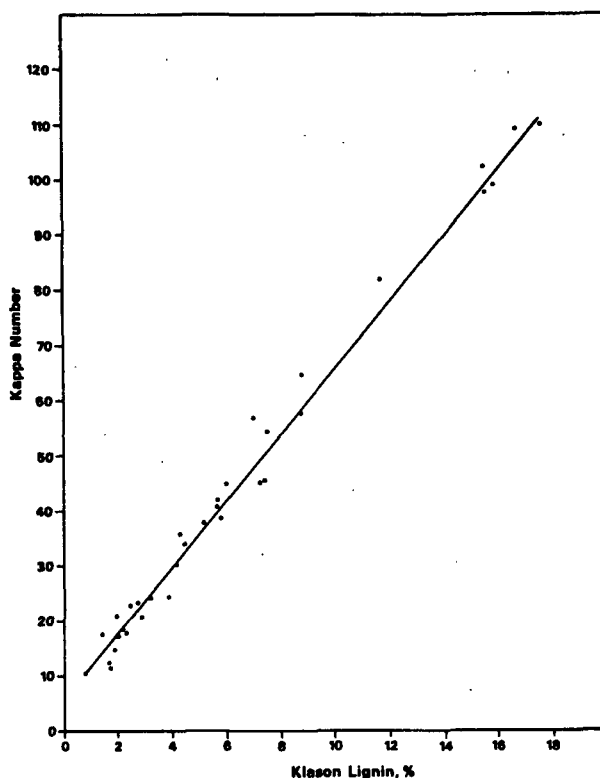


Figure 10. Kappa number vs. Klason lignin.

Multiple internal reflection IR measurements of lignin were sensitive to lignin contents as low as 2%, even in a dispersive spectrometer.¹⁰ However, pulps first had to be formed into handsheets, dried, and clamped against the reflection plate with a pressure necessary to set the 1310 cm^{-1} peak at 45% T. For diffuse reflectance FTIR, the pulps, as a small bundle of loose fibers, needed only to be dry.

Work recently performed elsewhere has shown the value of diffuse reflectance FTIR for predicting lignin, glucose, and xylose in hardwoods treated by the RASH process.¹¹ Most lignin data were obtained on RASH process products which contained 25-40% lignin. Thus these were not conventional wood pulps.

Samples were ground with KCl before analysis, and the data treatment employed the absorbances of 18 peaks. In contrast, the current investigation required essentially no sample preparation, and use of a single IR band area as the basis for lignin determination was simple and quick. Additionally, the current study has demonstrated the versatility of diffuse reflectance FTIR for analysis of a range of hardwood and softwood pulps from high-yield and conventional kraft processes and from the alkaline sulfite anthraquinone process.

The ability of diffuse reflectance FTIR to record lignin spectra of small pulp samples has not previously been evaluated. Stepwise reduction of sample size and recording of spectra has revealed that a lignin spectrum can be obtained on a sample of pulp as small as 0.5 mg. This technique would therefore be of value in small scale, sample-limited experiments such as those performed on isolated fiber wall fragments.

ALTERNATE METHODS OF MEASURING FTIR LIGNIN

Kubelka-Munk Spectra

A general theory for diffuse reflectance from layers within a sample capable of scattering radiation was developed by Kubelka and Munk.¹³⁻¹⁴ This theory has been applied to diffuse reflectance FTIR measurements by Fuller and Griffiths.¹⁵⁻¹⁶ The reflectance of a sample (relative to a good diffuse reflector such as ground KCl), of sufficient depth that any further increase does not alter the spectrum, is termed R_{∞} . For the IR analysis of weakly absorbing samples, "sufficient depth" is about 3 mm; for strongly absorbing samples it is less than 1 mm. Quantitatively, R_{∞} is related to the concentration of an absorbing sample in a nonabsorbing matrix by the Kubelka-Munk relationship:

$$f(R_{\infty}) = (1 - R_{\infty})^2 / 2 R_{\infty} = 2.303 \epsilon c / s$$

where ϵ is the absorptivity, c is the concentration, and s is the scattering coefficient. The scattering coefficient is held as constant as possible in a diffuse reflectance FTIR experiment. For IR bands of low absorptivity, a plot of $f(R_{\infty})$ vs. wave number may be used for qualitative and semiquantitative analysis. Such plots are termed Kubelka-Munk (K-M) spectra; they often appear similar to absorbance spectra of samples ground and pressed into KBr pellets.

Kubelka-Munk spectra were prepared from ground wood samples early in the current investigation. Subtraction of a cotton linters K-M spectrum was performed to yield a spectrum of lignin. Reversal of strong bands occurred when the wood was not mixed with KCl; dilution with KCl has been reported to be essential for subtraction of complete spectra.¹⁵ However, subtraction of small regions of spectra appeared feasible without dilution.

Diffuse reflectance FTIR spectra of three white oak pulps with kappa numbers ranging from 10.8 to 19.7 were obtained without KCl dilution. A linters spectrum was subtracted from the 1510 cm^{-1} band expressed as absorbance and as K-M values. The integrated absorbance values correlated with kappa number; the integrated K-M values did not. Consequently, absorbances rather than K-M values were used in subsequent correlation studies. Reasons for the choice were that the process was successful and that sample preparation (no KCl) and data manipulation were simplified.

The K-M theory applies most rigorously to dilute samples in nonabsorbing matrices such as KCl. Apparently, lignin in a cellulose matrix does not meet that requirement.

Alternate Cellulose Reference Materials

The 1510 cm^{-1} band used as a measure of lignin was obtained by subtracting a cellulose spectrum from the spectra of unbleached pulps. Hercules P-500 cotton linters has been most often used here as the reference cellulose. Two other types of linters were studied, a bulk linters and an acetate grade. All three types of linters were used in preparing plots of IR band area vs. kappa number for aspen and white oak kraft pulps. Regression lines of the data based upon use of the three different linters were practically superimposable. Thus the linters chosen as reference cellulose is not critical.

A chlorite holocellulose made from the pulp being investigated has also been evaluated as reference cellulose. The holocellulose exhibited a small 1510 cm^{-1} band, possibly due to residual lignin. Although the holocellulose was an adequate reference, its use was not worth the additional effort needed to correct for the residual lignin.

CONCLUSIONS AND FUTURE WORK

Linear relationships exist between the area of the 1510 cm^{-1} infrared band, measured by diffuse reflectance FTIR, and kappa number and Klason lignin. Species differences and generic differences between hardwoods and softwoods have little effect on these relationships. This finding applies to kraft and ASAQ pulps prepared over a wide yield range (1-20% lignin, 10-120 kappa).

Infrared band areas in the midrange of the data from this study may be used to estimate kappa number within about ± 4 kappa and Klason lignin within about $\pm 0.5\%$. Klason lignin can be predicted almost as accurately from IR band area as from kappa number.

Techniques developed in this study can be used to measure FTIR lignin band areas on pulp samples as small as 0.5 mg.

Diffuse reflectance FTIR might be applicable for on-line lignin determinations in dry samples. Virtually no sample preparation is required. This method probably senses surface lignin rather than total lignin; this may be an advantage in some applications.

Further studies in this funded project are not planned. We anticipate additional work in a cooperative project on on-line lignin sensors.

LITERATURE CITED

1. TAPPI Test Method T222 om-83.
2. Effland, M. J., Tappi 60(10):143(1977).
3. TAPPI Test Method T236 hm-85.
4. Berzins, V.; Tasman, J. E., Pulp Paper Mag. Can. 58(10):154(1957).
5. Tasman, J. E., Pulp Paper Mag. Can. 60(Convention No.):231(1959).
6. Kolboe, S.; Ellefsen, O., Tappi 45:163(1962).
7. Bolker, H. I.; Somerville, N. G., Pulp Paper Mag. Can. 64:T187(1963).
8. Vander Linden, N. G.; Nicholls, G. A., Tappi 59(11):110(1976).
9. Saad, S. M.; Issa, R. M.; Fahmy, M. S., Holzforschung 34:218(1980).
10. Marton, J.; Sparks, H. E., Tappi 50(7):363(1967).
11. Schultz, T. P.; Templeton, M. C.; McGinnis, G. D., Anal. Chem. 57(14):2867 (1985).
12. Caulcutt, R.; Boddy, R. Statistics for analytical chemists. New York, Chapman and Hall, 1983:83.
13. Kubelka, P.; Munk, F., Z. Tech. Phys. 12:593(1931).
14. Kubelka, P., J. Opt. Soc. Am. 38:448(1948).

15. Fuller, M. P.; Griffiths, P. R., Anal. Chem. 50(13):1906(1978).
16. Fuller, M. P.; Griffiths, P. R., American Lab. 10(10):69(1968).

THE INSTITUTE OF PAPER CHEMISTRY

Sally A. Berben *W*

Sally A. Berben
Research Assistant
Analytical Sciences
Chemical Sciences Division

Dwight B. Easty

Dwight B. Easty
Group Leader
Analytical Sciences
Chemical Sciences Division

Status Report

DEVELOPMENT AND APPLICATION OF ANALYTICAL TECHNIQUES

Analysis of Pulping and Bleaching Liquors by Ion Chromatography

INTRODUCTION

Earlier work in this project has documented the validity of ion chromatography (IC) for the analysis of pulping liquors¹ and bleaching liquors.² TAPPI Test Method T699 pm-83 provided the focus for our investigation. Although the test method described essential equipment and reagents, the analysis procedure appeared to be based upon limited experience with pulping and bleaching liquors. Consequently, the approach taken in our studies involved evaluation of the procedures in T699, development of supplemental techniques when necessary, and validation of IC results by spike recovery studies and comparisons with other methods.

Planned as the next phase of this project was preparation of a revised TAPPI Test Method for ion chromatography. However, two questions had to be answered before the revised method could be written: a) Is the recently proposed ultraviolet detector an improvement over the amperometric detector for determining sulfide? b) Must green liquor be diluted with 0.1% HCl in order for sulfate to be determined accurately?³ Our subsequent studies documented the value of the UV detector for sulfide and also showed that sulfate could be determined in green liquor if it is diluted with deoxygenated water and immediately injected into the ion chromatograph. These findings were reported to the membership in May via IPC Technical Paper Series Number 170; they will be discussed in a symposium on ion chromatography in September.⁴

A revision of TAPPI Test Method T699 was written during the summer; the original method was divided into two separate procedures, one for pulping

liquors and one for bleaching liquors. The first draft of the revised methods was sent to a few selected ion chromatographers in the industry for their comments. A second draft incorporating their suggested revisions is being prepared for submission to TAPPI in September.

Analysis of kraft pulping liquors is the principal use of ion chromatography in our laboratory and very likely in other laboratories throughout the industry. Limited work under this project has therefore been continued, with the objective being improvements in the use of IC for pulping liquor analysis. We have found solutions to problems as they arose in our own analyses, and we have been examining the pulping liquor analysis procedure for potential sources of error. Recent findings are described below.

RESULTS AND DISCUSSION

REPEATABILITY VALUES

The need for an evaluation of sources of error in the IC analysis of pulping liquors was revealed in repeatability values developed for inclusion in the revised TAPPI Test Method. Values are shown in Table 1. TAPPI Test Method T1206 os-69, Precision Statement for Test Methods, defines, "Repeatability (within a laboratory) = 2.77 times the standard deviation of a test result." A test result in ion chromatography is a single determination. When repeatability is expressed as a percentage of the test result, relative standard deviation (or coefficient of variation) is used in the calculation. TAPPI's manual for test method preparation⁵ further describes repeatability as the maximum expected difference between two test results.

Table 1. Repeatability values for ion chromatographic analysis of pulping liquors.^a

	Carbonate	Sulfate	Chloride	Sulfite	Thiosulfate	Sulfide
Black liquor	20	12	50	30	16	NA ^b
Green liquor	5	4	40	25	3	NA

^aRepeatability expressed as percentage of mean.

^bNA = not available.

At the time Table 1 was prepared, insufficient data were available on white liquors for calculation of repeatabilities.

Several of the repeatability values in Table 1 appear to be excessive, especially for black liquor. The chloride repeatability is high, but it is not of great concern. It probably results from the low chloride content of a typical black liquor, about 0.2% of solids, which is used in the denominator of the calculation of relative standard deviation. This explanation should also apply to the high repeatability of sulfite. The repeatability of carbonate is rather high, and it is of concern. Sources of error in the carbonate determination have been studied, and they will be discussed below.

POTENTIAL SOURCES OF ERROR IN ION CHROMATOGRAPHIC ANALYSIS OF PULPING LIQUORS

Instability of Liquor Samples

A very limited study of white liquor stability has been performed and reported.¹ Bottles were completely filled and kept sealed at room temperature for varied storage times up to 120 hours. No consistent trends in sulfoxy anion (sulfite, sulfate, thiosulfate) contents were noted. Additional studies are needed; other ions and storage conditions should be included.

Homogeneity of Liquor and Representative Nature
of Sample Taken for Analysis

Weak (15%) and heavy (62%) black liquors from the same mill have been analyzed in our laboratory. Although concentrations of other ions, expressed as percentage of solids, were similar in both liquors, the carbonate content of the heavy liquor has been found to be consistently lower than that of the weak liquor. It seems unlikely that the total carbonate content of the liquor was reduced as it passed through the evaporators. However, something happened, perhaps precipitation, that has reduced the carbonate content of the diluted and filtered portion of the heavy liquor injected into the ion chromatograph. This problem, which has not been completely resolved, illustrates the difficulties in obtaining a representative sample from a bottle of heavy black liquor.

The following procedure for sampling heavy black liquors has been suggested for inclusion in the revised TAPPI test method.⁶ Because black liquor data are reported on a weight basis, the sample taken from the liquor must be weighed.

"Heat heavy black liquor to 70-80°C in a hot water bath. Withdraw about 10 mL of hot liquor into a glass tube connected to a syringe. Expel the liquor into a preweighed container of dilution water. Reweigh to obtain weight of liquor added."

In this technique a rather large amount of a hopefully homogeneous liquor is taken for analysis. It should represent an improvement over a smaller sample taken from a lower-temperature semisolid liquor.

Dilution Technique

Pulping liquors must be diluted from 1:250 to 1:5000 prior to ion chromatographic analysis. The extent of dilution depends on the liquor's solids

content, the concentration of the ion being determined, and the sensitivity of the ion chromatograph for that ion. Accurate dilution techniques are therefore essential.

We have found the Rainin "Pipetman" to be an accurate and rapid dilution device. However, it must be used with great care in performing the initial dilution of a white or green liquor.

One-milliliter samples of white liquor were being withdrawn with the "Pipetman" for dilution and determination of carbonate. Duplicate data differed by about 10% of the value, which was excessive. Careful observation revealed that small amounts of liquor were being retained in the pipet. Complete transfer of the liquor was found to result if the analyst pushed the plunger to the first stop very slowly, waited a moment, and then expelled the sample. Differences between duplicates were thereby reduced to a more acceptable 2% level.

Instability of Samples Diluted for Analysis

Work here and elsewhere has shown the instability of pulping liquors diluted sufficiently for ion chromatographic analysis.^{1,3,4} Sulfide and sulfate were found to change with time; sulfide decreased and sulfate increased, both due to oxidation. Changes in both ions are retarded by dilution with deoxygenated water. Ascorbic acid was found to be an effective antioxidant for sulfide.

To minimize errors due to instability, it is recommended that liquors be injected into the ion chromatograph immediately following dilution.

Chromatography

Ion chromatography would be greatly simplified if factors affecting separation and detection of ions did not vary with time. Unfortunately, these

factors do change, and we must account for their variability by the running of standards. If the standards are not run frequently enough, serious errors are incurred.

Carbonate standards of 5, 10, 15, and 20 ppm were run on each of six days. Peak heights rather than areas were measured, because carbonate peaks tail somewhat. Calibration lines of peak height vs. concentration were prepared. Linear correlation coefficients and slopes are shown in Table 2.

Table 2. Carbonate calibration lines.

Date	No. of Standards Run	Correlation Coefficient	Slope
8-01-86	6	0.9998	3.86
8-04-86	3	0.9998	4.90
8-11-86	4	0.9993	5.16
8-12-86	5	0.9996	5.30
8-18-86	5	0.9969	5.85
8-19-86	6	0.9967	5.32

Variations in slope of the carbonate calibration line from day to day demonstrate the need to run full calibration lines each day. This conclusion is supported by the day-to-day variation in individual peak heights; the height of the 15 ppm standard ranged from 61 to 103 mm.

Instances in Table 2 when 5 and 6 standards were run represent repeat injections to monitor variation in response within a day. The magnitude of errors that can result from undetected response variation is shown by the following example: Two green liquors were analyzed late in the day, but standards were run only in the morning. The analyst recognized that the carbonate

column was approaching the end of its useful life. Sodium carbonate contents measured in the green liquors were 40.6 and 39.4 g/L. Because the values appeared to be unrealistic, the analysis was repeated using a new column. Results of the repeat analysis were 92.7 and 128 g/L. Apparently the ion chromatograph's sensitivity had decreased between the calibration runs on the old column in the morning and the initial analysis of the green liquors in the afternoon. To detect within-day changes in carbonate response, a standard is now run after each sample. In addition, the analyst closely monitors the baseline and peak shapes to discern changes in column performance.

Within-day variations in results as a function of chromatograph performance were also tested in the determination of sulfoxy anions. Standards, 4 ppm sulfate and 10 ppm thiosulfate, were injected every 1-2 hours between analyses of liquors. This study was conducted on 8-11-86 when a steady baseline was observed and on 8-12-86 when the baseline was unstable. The first standard injected served as the basis for calculating the concentrations of subsequent injections, which were treated as unknowns.

On 8-11-86 the sulfate and thiosulfate repeatabilities were 3.3 and 5.5%, respectively. Repeatabilities increased to 42 and 46% on 8-12-86, presumably due to the unstable baseline. Possible causes of baseline instability are air bubbles in the system and an imbalance between eluent flow rate and the flow rate of regenerant through the fiber suppressor. It is evident that when baseline instability is observed, analysis of samples must be stopped until the problem is found and corrected.

CONCLUSIONS AND FUTURE WORK

Actions necessary to ensure correct results in the ion chromatographic analysis of pulping liquors include careful dilution of samples, prompt injection

following sample dilution, and the running of sufficient standards to correct for variations in ion separation and detection. When baseline instability occurs, sample analysis must stop. The analyst must be alert for problems in column and system performance in order to avert their devastating effect on analytical accuracy and precision. To paraphrase John Philpot Curran, "Eternal vigilance is the price of accuracy."

Problems in the storage of liquors and the securing of representative samples will be addressed in future work.

EXPERIMENTAL

Procedures used in this work are essentially those which are described in TAPPI Test Method T699 pm-83. Additional details are provided in the publications from this laboratory noted in Literature Cited.

ACKNOWLEDGMENT


The laboratory work for this report was performed by Connie Weber. Her efforts are greatly appreciated.

LITERATURE CITED

1. Easty, D. B.; Borchardt, M. L.; Webb, A. A., Paperi Puu 67(9):501(1985).
2. Easty, D. B.; Johnson, J. E.; Webb, A. A., Paperi Puu 68(5):415(1986).
3. Parigi, J. S., American Lab. 16(9):124(1984).
4. Easty, D. B.; Johnson, J. E. Recent progress in the ion chromatographic analysis of pulping liquors: determination of sulfide and sulfate. Proceedings, TAPPI 1986 International Conference on Process and Product Quality, Atlanta, Sept., 1986.

5. TAPPI. Guidelines for effective management, coordination, form and style for TAPPI Test Methods. Atlanta, 1984. p. 26.
6. Thurman, R. G. Union Camp Corporation, Personal communication, 1986.

THE INSTITUTE OF PAPER CHEMISTRY



Dwight B. Easty
Group Leader
Analytical Sciences
Chemical Sciences Division

Status Report.

DEVELOPMENT AND APPLICATION OF ANALYTICAL TECHNIQUES

Pyrolysis Gas Chromatography

INTRODUCTION

Pyrolysis gas chromatography (PGC) has established itself as an analytical method for the identification of polymers, resins, microorganisms, and biopolymers.¹ This project is directed toward developing a pyrolysis method to supplement the current Fourier transform infrared (FTIR) methodology. FTIR is our primary tool for polymer identification; however, it usually requires the polymer to be soluble in an organic solvent. One advantage of PGC is that it can analyze solid, liquid, and nonvolatile samples in appropriate mixtures to provide a "fingerprint" identification.² This technique could be used to verify FTIR results or perhaps identify samples that are not applicable to FTIR analysis.

As with many analyses involving complex materials, several techniques have developed for pyrolyzing samples. Using the CDS Pyroprobe 120, our initial study has been to try to identify previously analyzed polymers. PGC has recently been used as a rapid method for analyzing "sticky" contaminants in pulp and paper samples.³ However, a disadvantage of PGC for routine identification, whether for "sticky" or other polymers, is the requirement that each laboratory prepare a library of known compounds for "fingerprint" type identification. Despite this limitation, the "fingerprint" relationship is the most straightforward approach for identifying the less complex polymer samples.

PROCEDURE

Pyrolysis gas chromatography involves heating the sample, using controlled thermal degradation at the GC inlet. The CDS Pyroprobe 120 is the pyrolysis

system used in this study. It is sketched in Fig. 1. Samples, either solid or liquid (0.5-1.0 mg), are placed in a small quartz tube which is put into a platinum coil probe. This probe is then inserted into the GC inlet interface. Next, the probe temperature is increased to pyrolysis conditions (750°C).

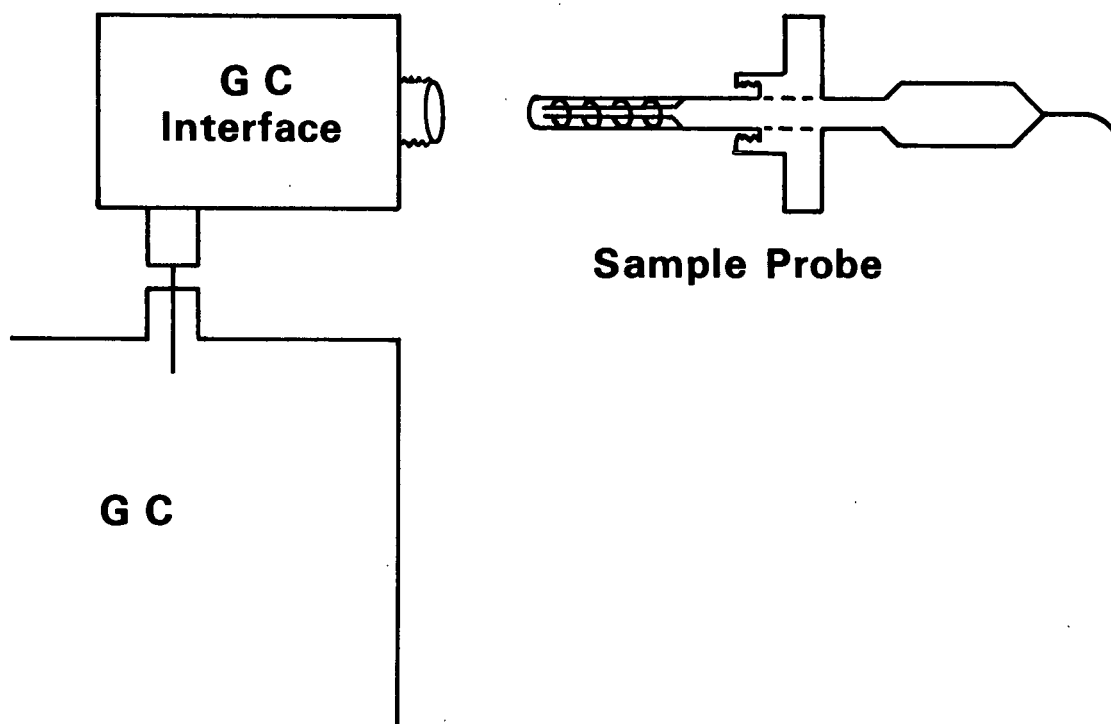


Figure 1. Pyrolysis gas chromatography.

Pyrolysis is done under dynamic conditions; as the products are formed, helium sweeps them into the GC (Hewlett Packard 5890). A packed GC column (Porapak Q or Carbo-pack B/SP1000) separates the pyrolysis components, which are monitored with a flame ionization detector and a HP 5988 data system. See Table 1 for PGC temperature and column conditions.

A method using the copolymer Kraton 1107 is used to calibrate the temperature and to assure the pyrolysis unit is working properly.

Table 1. Conditions for pyrolysis gas chromatography.

Instrumentation:

Hewlett Packard GC 5890A

Hewlett Packard Data System 3388A

CDS Pyroprobe 120 (Platinum Coil)

Probe Conditions:

Interface at 200°C

Pyrolysis temperature: 20°C/microsecond to 850°C (750°C actual)

Time: 20 seconds

Sample size: 0.5-1.0 mg

GC Conditions:

Detector 300°C. Injector 250°C

A - Porapak Super Q 100 to 200°C at 10°C/min

B - Carbopak B/3% SP1000 40 to 220°C at 8°C/min

Packed Glass Column - 2 mm x 6 ft

RESULTS AND DISCUSSION

An important concern when using the PGC "fingerprint" matching of pyrograms is the overall profile and its reproducibility. Pyrograms A and B in Fig. 2 illustrate the run-to-run reproducibility of polyisobutylene. Once the pyrolysis conditions were set to obtain repeatable results, we did not try to optimize temperature or column selection. An ether extract from a paper product previously identified as polyisobutylene using FTIR is shown in pyrogram C. Direct comparison of the ether extract produced an interference-free pyrogram that was easily matched to the known polyisobutylene pyrogram. To further check the pyrogram repeatability, a similar study was done using a Porapak Q column

instead of Carbopak B/SP1000 as in the above analyses. This column provided a less complex pyrogram which also resolved the major peaks to confirm the above results.

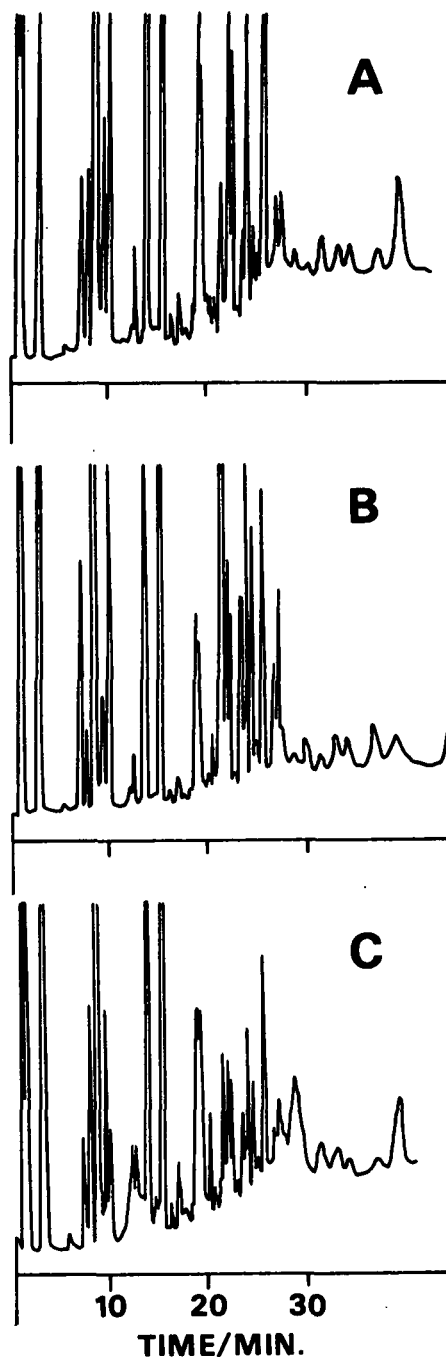


Figure 2. Pyrolysis gas chromatography of polyisobutylene.

In order to improve our ability to identify the material pyrolyzed, several known samples were evaluated for (fingerprint) library comparison. These include polyvinylacetate, ethylvinylacetate, high density polyethylene, polyethylacrylate, and a polyester.

This technique became more complex when samples were tried without solvent extraction clean up. Pyrogram D in Fig. 3 is a rewinder deposit which has been identified by FTIR as polyvinylacetate. However, when compared to the known Pyrogram E only a few early peaks match, making it difficult to establish an identification. Because of the above disadvantage, analysis of complex samples requires optimizing conditions or possible removal of interfering components. A few additional samples were tried without extraction; these pyrograms were also difficult to interpret.

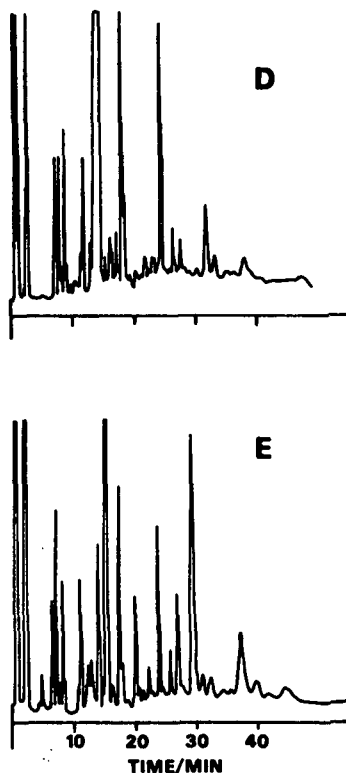


Figure 3. Pyrolysis gas chromatography of a rewinder deposit.

FUTURE WORK

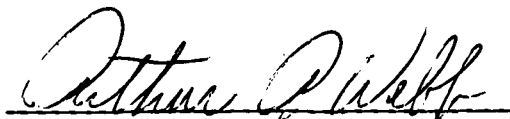
Future work will involve the analysis of additional polymers that have been identified using FTIR. This would also expand our library of polymer known compounds.

Techniques other than straightforward PGC may be needed for analysis of polymer mixtures and real deposits. For these analyses we may need to use pre-pyrolysis to separate the more volatile interferences followed by a higher temperature pyrolysis of the polymer of interest. In addition, the mass spectrometer might be used to identify characteristic peaks in the pyrogram.

LITERATURE CITED

1. Irwin, W. J. Analytical pyrolysis. A comprehensive guide. Chromatographic Science Series, Vol. 22, Marcel Dekker, Inc., New York and Basel (1982).
2. Liebman, S. A.; Wampler, T. P.; Levy, E. J., J. High Resolution and Chromatography Communications 7(4):178(1984).
3. Dunlop-Jones, N.; Allen, L. H. A rapid method for the qualitative analysis of "plastic" and "sticky" contaminants by pyrolysis-gas chromatography. Proceedings, TAPPI 1986 International Conference on Process and Product Quality, Atlanta, Sept., 1986.

THE INSTITUTE OF PAPER CHEMISTRY



Arthur A. Webb
Research Fellow
Analytical Sciences
Chemical Sciences Division

NOTE: The Analytical Sciences Group is hoping to acquire instrumentation for atomic spectrometry (ICP or DCP) in the near future. We would appreciate input from member company representatives on desirable features, experience with specific models, and the availability of instruments at modest cost (used or demonstrators).

THE INSTITUTE OF PAPER CHEMISTRY

Appleton, Wisconsin

Status Report

to the

PULPING PROCESSES

PROJECT ADVISORY COMMITTEE

Project 3524

FUNDAMENTALS OF BRIGHTNESS STABILITY

September 1, 1986

PROJECT SUMMARY FORM

DATE: September 1, 1986

PROJECT NO. 3524: FUNDAMENTALS OF BRIGHTNESS STABILITY

PROJECT LEADER: W. F. W. Lonsky

IPC GOAL:

A significant increase in yield of useful fibers.

OBJECTIVE:

Elucidate mechanism for brightness loss in high-yield pulps.

CURRENT FISCAL YEAR BUDGET: \$140,000

SUMMARY OF RESULTS SINCE LAST REPORT:

The major reaction sequences of the sheet-yellowing reaction have been defined. In a photochemical induction cycle, the absorbed energy of the UV radiation causes the excitation of an α -carbonyl group of the lignin, which in turn can abstract a hydrogen atom from a phenolic species of the lignin molecule. A phenoxy radical is formed. The resonance stabilized forms of this radical interact with oxygen of the air. The intermediate peroxy radical rearranges after hydrogen abstraction mainly to an o-quinonoid structure.

Experimental evidence is provided for all major steps of this reaction sequence. Singlet oxygen does not take part in the reaction sequence.

PLANNED ACTIVITY THROUGH FISCAL YEAR 1987:

A detailed study of the photoinduction cycle of the sheet-yellowing reaction by means of ESR techniques has been started in cooperation with the National Biomedical ESR Center at Milwaukee, WI. The effect of radical scavengers (polymeric thiocompounds) will be further explored to obtain brightness stability of the high-yield pulps.

FUTURE ACTIVITY:

At the time, specific future plans are in a state of flux. W. Lonsky, the project leader, has recently left IPC and we have just started the search for a replacement. Generally, future work will use the reaction mechanisms now defined as a basis for research aimed directly at finding ways of inhibiting photoinduced yellowing. The new concepts and experimental technique will be used initially to establish how hydrogen peroxide, sodium hydrosulfate, and other likely bleaching chemicals affect the yellowing sequence.

STUDENT RESEARCH:

A-490 Stuart S. Lebo:

A study of the quantum yield of the sheet-yellowing reaction; identification of the major chromophoric structures.

A-190 Christine L. Stoffler

Preparation of a UV radiation absorbing retention aid by polymer modification; application as brightness stabilizing agent.

A-190 Patrick J. Medvecz

A study on the formation of 3-methoxy-ortho-quinonoid structures during light yellowing of softwood and hardwood mechanical pulp sheets.

Status Report

FUNDAMENTALS OF BRIGHTNESS STABILITY

INTRODUCTORY REMARKS

One of the major drawbacks of high-yield pulp application for paper products is poor brightness stability; that is, the products turn yellow on exposure to daylight. If high-yield pulps are to have broad application in the future, the chemical mechanism of this phenomenon has to be understood to solve the problem. The objective of this research project is to elucidate the mechanism for brightness loss in high-yield pulps.

In the following a brief summary will be provided of the important facts contributing to the deduction of the sequence of events that takes place during light-induced color reversion.

GENERAL OBSERVATIONS AND INFORMATION

It was shown earlier (Status Report, Feb. 1, 1983) that the high lignin content of high-yield pulps is responsible for discoloration. Sheets prepared from cellulose or holocellulose did not lose brightness when exposed to artificial sunlight. In the presence of oxygen, UV radiation in the range 290 to 380 nm causes formation of quinonoid lignin structures in high-yield pulp sheets. This last sentence - which per se is correct - contains three questionable parameters which deserve clarification.

OXYGEN

There is a widespread opinion that singlet oxygen is the driving force of the yellowing reaction. It is assumed that it is formed in a photosensitized

reaction between an excited lignin carbonyl group and the normal triplet oxygen of the air. (Singlet oxygen is an oxygen molecule that has two single electrons with antiparallel spin orientation, whereas in triplet oxygen the two spins are parallel to each other.) Singlet oxygen differs from triplet oxygen in its higher energy content and presumably high reactivity as an oxidant. The absence or reaction of singlet oxygen is a key question for the sequence of occurrences during the photoyellowing process.

UV RADIATION

Within the given range UV radiation of any wavelength initiates the yellowing of high-yield pulps. However, knowing at which wavelength the maximum rate of yellowing is observed will help us understand the primary photoreaction.

QUINONES

Leary¹ postulated the formation of ortho-quinones based on the observed methanol formation. Other researchers, like Nimz,² consider the para-quinones as dominant chromophores. The knowledge that o-quinones are the major products will be important for the understanding of the different rates of yellowing of softwood and hardwood high-yield pulps.

Recently done ESR studies will demonstrate the radical nature of the reaction sequence. Finally, a logical mechanism, free of contradiction, will be developed.

THE MECHANISM OF THE LIGHT-INDUCED YELLOWING REACTION

SINGLET OXYGEN IS NOT INVOLVED IN THE MECHANISM OF THE LIGHT-INDUCED COLOR REVERSION

The effect of singlet oxygen on high-yield pulp sheets was studied to verify or disprove the claims of various researchers that this particular molecular

oxygen species is involved in the light-induced yellowing process. A study like this is of industrial importance as well as of academic interest for the chemical aspects. Singlet oxygen quenchers are produced for many product stabilizing purposes, especially for the plastics industry. It is conceivable to build quenchers into retention or drainage aids. Up to this point we had our doubts that singlet oxygen is an active intermediate in the photooxidation cycle at all.

The experimental apparatus and the flow system are shown in Fig. 1. (The experimental part of this work was done in cooperative research with Dr. E. Ogryzlo and Mr. A. Ali at the University of British Columbia, Vancouver, Canada.) Basically, singlet oxygen is generated from oxygen in an argon atmosphere in a microwave cavity. The partial pressures of Ar and O₂ through the discharge tube were 1.70 torr and 0.15 torr, respectively. The formation of oxygen atoms was quenched by the addition of a drop of mercury into the cavity. Their absence was confirmed by the absence of any visible afterglow when NO₂ was added. (For a detailed description see Appendix: Singlet Oxygen Generator and Detection System.)

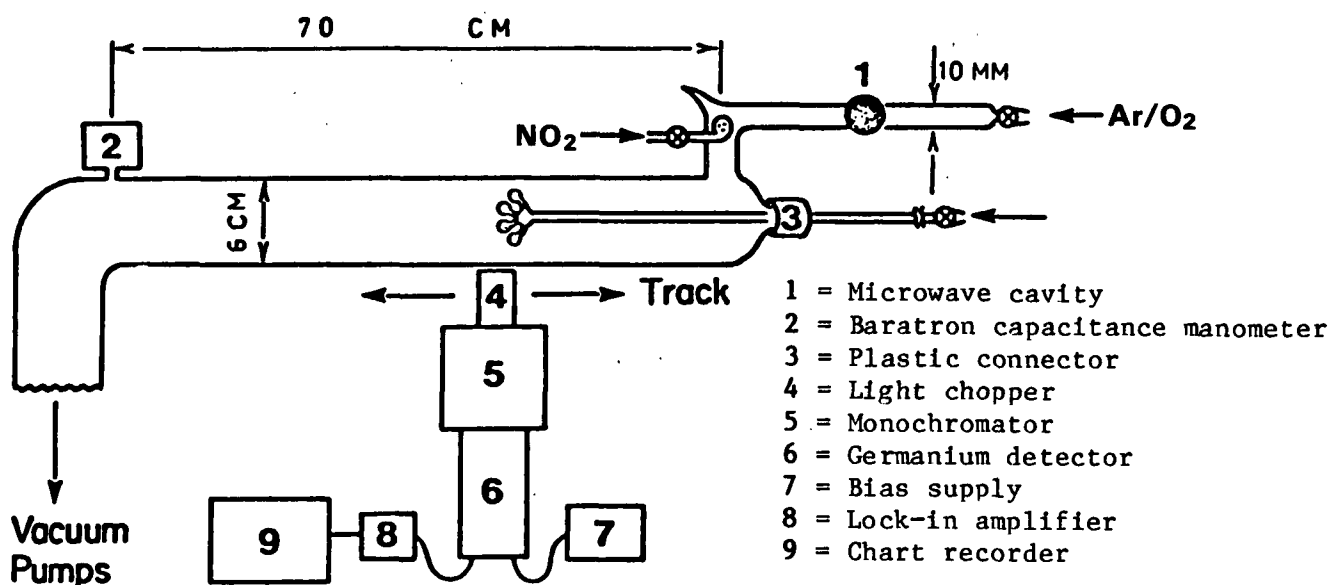


Figure 1. The singlet oxygen generator: the flow system and the detection system.

In the presence of high-yield pulp sheets, the presence of UV radiation (290 nm cut-off) showed no effect on the singlet oxygen concentration. The typical value of 1.4×10^{14} molecules per cm^{-3} was found with the UV source off and 1.3×10^{14} with the source on. This difference is considered to be insignificant. The presence of UV radiation caused a brightness loss of the sheets, and the typical quinone band appeared in the difference reflectance spectrum, whereas in the absence of UV radiation the brightness remained constant within the margin of error ($\pm 0.5\%$). This was true for bleached and unbleached pulp sheets, humidified or dry.

These results provide direct evidence that singlet oxygen is not involved in the sunlight (UV radiation) induced color reversion of high-yield pulps.

THE PRESENCE OF o-QUINONOID LIGNIN STRUCTURES IN SUNLIGHT-YELLOWED HIGH-YIELD PULP SHEETS

Leary¹ indicated the likelihood of quinones being responsible for the yellow appearance of newsprint after sunlight exposure. He did not discuss details of their formation or chemical nature. Probably initiated by the numerous reports on photochemical studies of phenolic compounds in solution, the hypothesis of p-quinone formation in pulp sheets as major contributors to the yellow appearance has been generally considered and accepted. Norrish type reactions (photochemical cleavage of a carbon chain in the immediate neighborhood of a carbonyl group) are reported to occur readily.³ The reaction product in the case of lignin would be 2-methoxy-p-benzoquinone (dominant product from softwood mechanical pulps) or 2,6-dimethoxy-p-benzoquinone (dominant product from hardwood mechanical pulps). We noticed during reflectance spectroscopy studies that 2-methoxy-p-benzoquinone sublimed off the sheet at room temperature in the dark

when it was absorbed on mechanical pulp sheets. This observation leads to the conclusion that any liberated p-benzoquinone that has been formed by sidechain cleavage would be volatile and leave the sheet. It will not contribute to its lasting discoloration. Only p-quinones which are chemically linked through the 5-position to the lignin could be retained permanently. However, this is not a major bond type in native lignin.

Evidence for the presence of o-quinonoid structures in unbleached mechanical pulps was obtained when the pulps were treated with two different methylating reagents, diazomethane (CH_2N_2) and DMS [dimethylsulfate (CH_3) $_2$ SO_4]. Both reagents methylate the phenolic hydroxyl groups, i.e., diazomethane and carboxylic acids. DMS treated pulp is not brighter after the treatment. Methylation with diazomethane increases the brightness strongly. Its bleaching action is understood as the reduction of o-quinones by the carbene intermediate ($:\text{CH}_2$; formed from diazomethane by loss of a nitrogen molecule, N_2) which is considered yielding methylenedioxy ether structures. p-Quinones do not undergo this reaction.

A thorough investigation of the nature of the major quinone products was done on the basis of the reducing action of trimethyl phosphite. o-Quinones are known to form a cyclic adduct.⁴ p-Quinones react too. However, the reaction product is a noncyclic ester. This class of compounds shows a distinct and easily identifiable P-31 NMR signal.⁵ The treatment of light-yellowed sheets with trimethyl phosphite in a dry methanolic solution under a nitrogen atmosphere brightened the sheets. The presence of water traces in the sheets leads to partial hydrolysis, forming the indicated end product (Fig. 2). This hydrolysis reaction has been shown by GC/MS analysis to proceed on a model quinone compound. The solid state P-31 NMR spectra of the treated sheets showed the presence of the expected structure (Fig. 2).

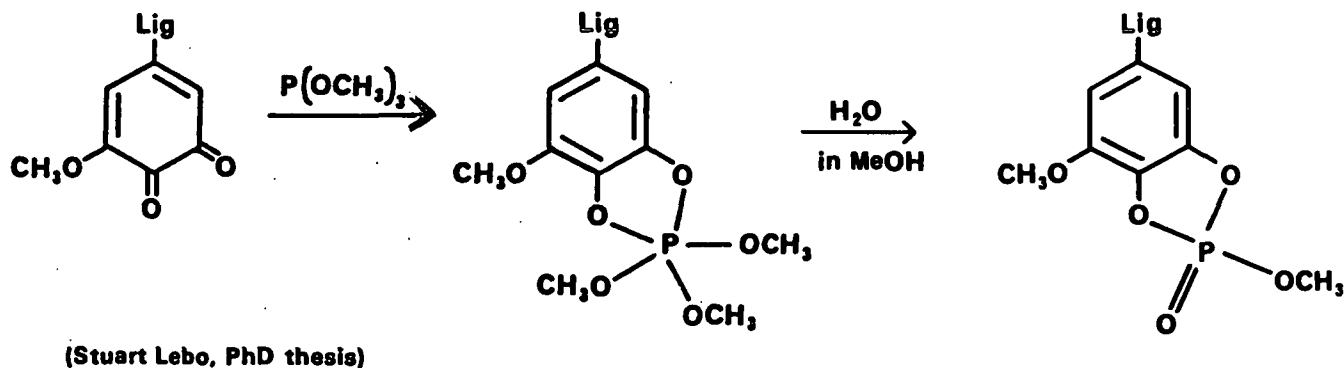


Figure 2. An "ortho-quinone specific" reagent.

The same result was obtained with tris-dimethylaminophosphine as reducing agent. Hydrolysis and methanolysis of the phosphorus substituents on the cyclic intermediate yielded the cyclic methoxyphosphoric ester of pyro-catechol.

Since any quinone is converted into the corresponding hydroquinone phosphoric ester upon exhaustive treatment with trimethoxyl phosphine, the phosphorus can be used as a quinone label. By cross sectioning the light-exposed and phosphine-treated sheet with the microtom, the relative phosphorus concentration in the various fiber layers can be determined with the energy dispersion spectroscopy technique. The distribution curve for phosphorus along the sheet caliper is shown in Fig. 3. It clearly demonstrates that yellowing by light occurs in the near-to-surface fiber layers. The curve levels off toward the inside of the sheet, indicating the natural quinone level of the pulp. A quantitative, colorimetric phosphorus analysis permits one to determine the total phosphorus content in the sheet. Thus, the quinone concentration can be calculated.

In this context the work of M. C. Neumann et al.⁶ is noteworthy. Based on the interpretation of the transient spectrum of a flash photolyzed deaerated dioxane lignin solution, the authors suggest that the initial photochemical process is the excitation of the α -carbonyl groups, followed by an abstraction of the phenolic hydrogen forming ketyl and phenoxy radicals. Recombination of the radicals yields the end products.

Although this investigation was carried out with soluble (low molecular weight) dioxane lignin in solution, the very same reaction sequence for the photo-induced reaction can be expected to occur in the sheet. The radical recombination is not expected to occur in the solid state because of the relative immobility of the lignin. A longer lifetime of the radical has to be expected, as verified by our ESR experiment.

Hon⁷ also reported in the meeting on ESR studies on photoirradiated lignin. Phenoxy radicals were reportedly formed. Unfortunately, neither the light source nor the wavelength region could be specified during the following discussion.

THE MECHANISM OF THE SUNLIGHT-INDUCED YELLOWING REACTION OF HIGH-YIELD PULPS

The photooxidation of lignin in MPs is a complex system consisting of two major parts. In a photochemical induction cycle, the absorbed energy of the UV radiation causes ($n-\pi^*$) or ($\pi-\pi^*$) excitation of an α -carbonyl group (see Fig. 4). The energy can be dissipated by release of thermal energy, whereby the molecule returns to its original groundstate; or radiation of longer wavelength can be emitted (fluorescence or phosphorescence) allowing the molecule to go back to the groundstate; or hydrogen abstraction from another part of the

molecule can lead to a photochemical reaction. The carbonyl group is then converted into a ketyl radical that can act as a hydrogen donor by transferring its hydrogen atom to a reactive acceptor group and reforming its original carbonyl group. The hydrogen abstraction occurs preferentially from a phenolic species, which gives the lignin its well-known antioxidant property. A phenoxy radical is formed.

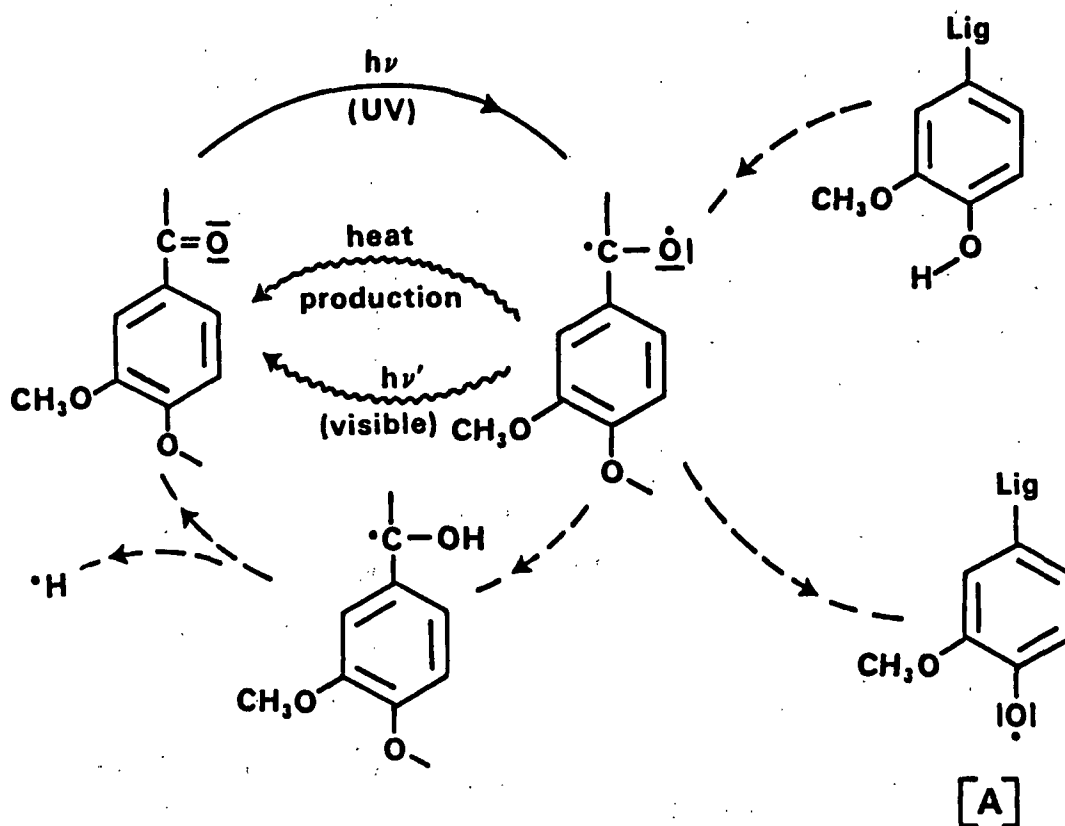


Figure 4. The photochemical induction cycle.

In a "dark reaction" sequence (Fig. 5), the resonance stabilized forms of the phenoxy radical can react then with oxygen of the air. The intermediately formed peroxy radical structure might accept a hydrogen atom from the ketyl radical to yield the cyclic hydroperoxy dienone (Fig. 5), which in turn rearranges to the o-quinone and water.

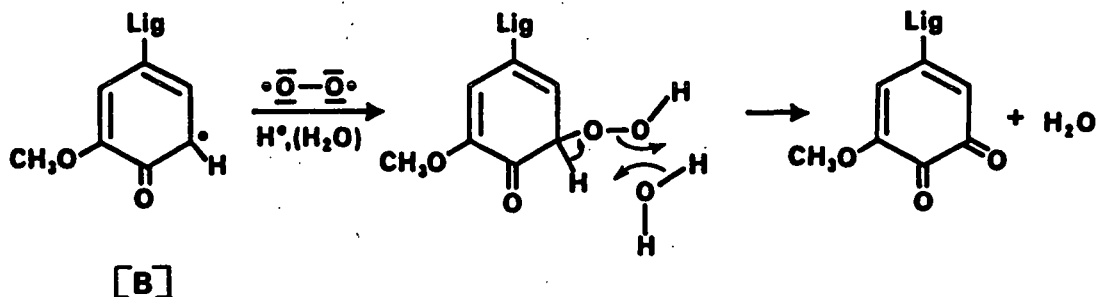


Figure 5. Humidity assisted rearrangement.

Which of the indicated three pathways leading to products (Fig. 6) will be the preferred one is dependent on the contribution to the resonance energy of the species [A] through [D]. Also, the steric effect of the substituent, where the oxygen attack occurs, is important. The order of decreasing reactivity will be $H > OCH_3 > \text{lig}$ (lignin sidechain). Thus, the preferred product will result from the resonating structure [B].

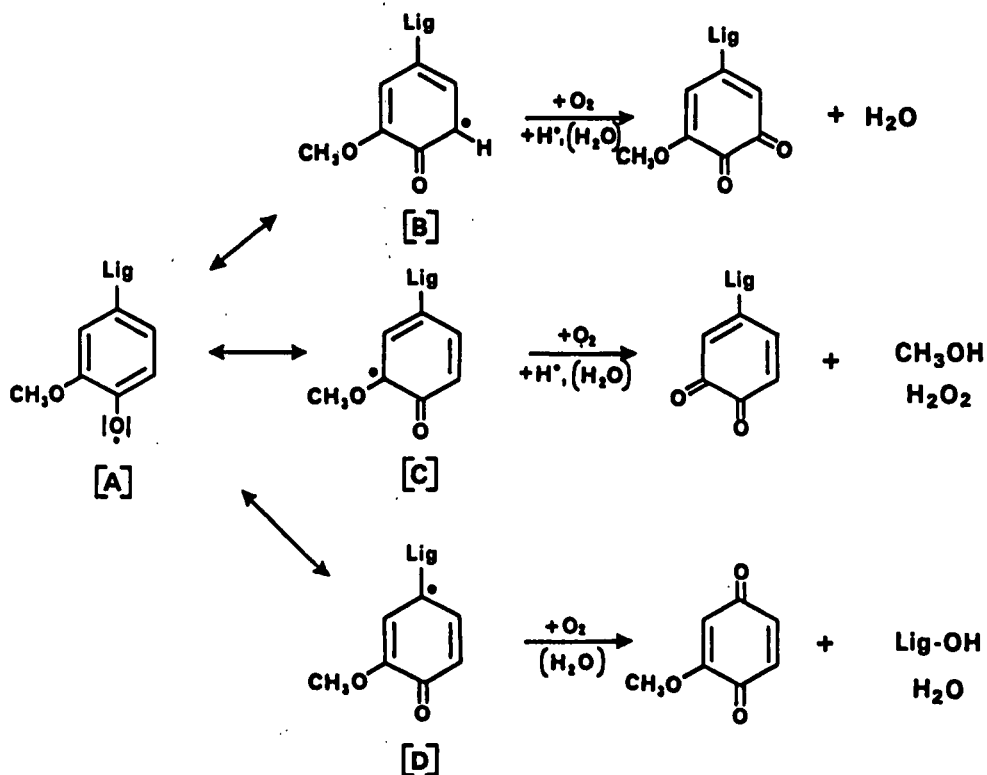


Figure 6. The various products formed in the "dark reactions."

In the dominant structures of hardwood lignins the hydrogen is replaced by a second methoxy group. Thus the reaction product will be the same for softwoods and hardwoods (see Fig. 7). However, since the methoxy group (in hardwoods) is much bulkier than the hydrogen (in softwoods), hardwood mechanical pulps will produce the same chromophore at a lower rate than softwood mechanical pulps.

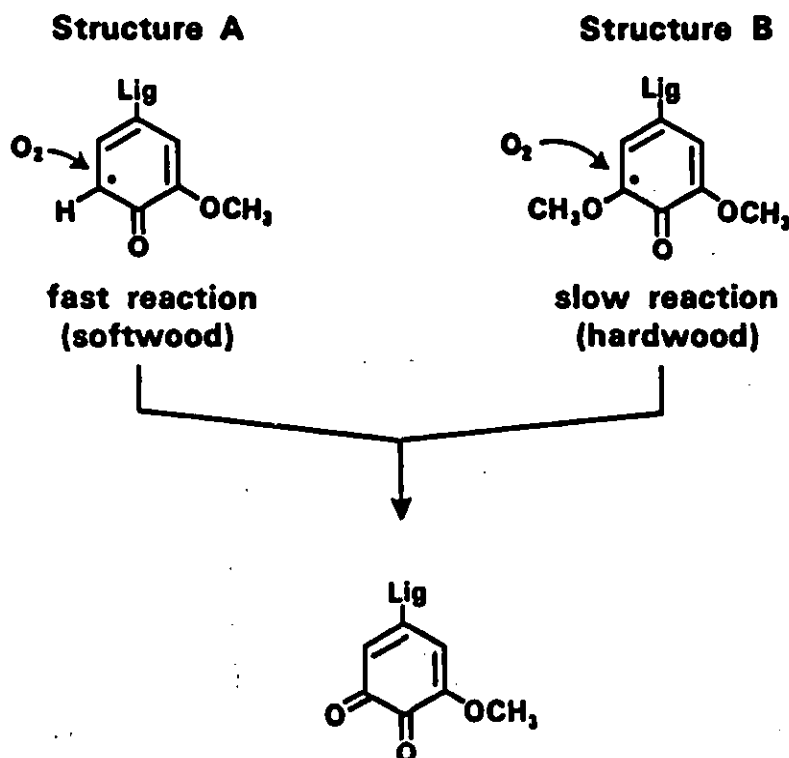


Figure 7. Softwoods and hardwoods generate the very same chromophore.

An enhancing effect has to be expected from the lignin concentration, which is generally higher in softwoods than in hardwoods. The higher lignin concentration means an increased probability for the formation of a phenoxy radical [A] in the photochemical induction cycle (Fig. 4). We found that at comparable brightness levels softwood mechanical pulps generally yellow faster than aspen mechanical pulp. A plot of K/S (absorption coeff./scattering coeff.) vs. the logarithm of time for a series of bleached and unbleached MPs demonstrates this.

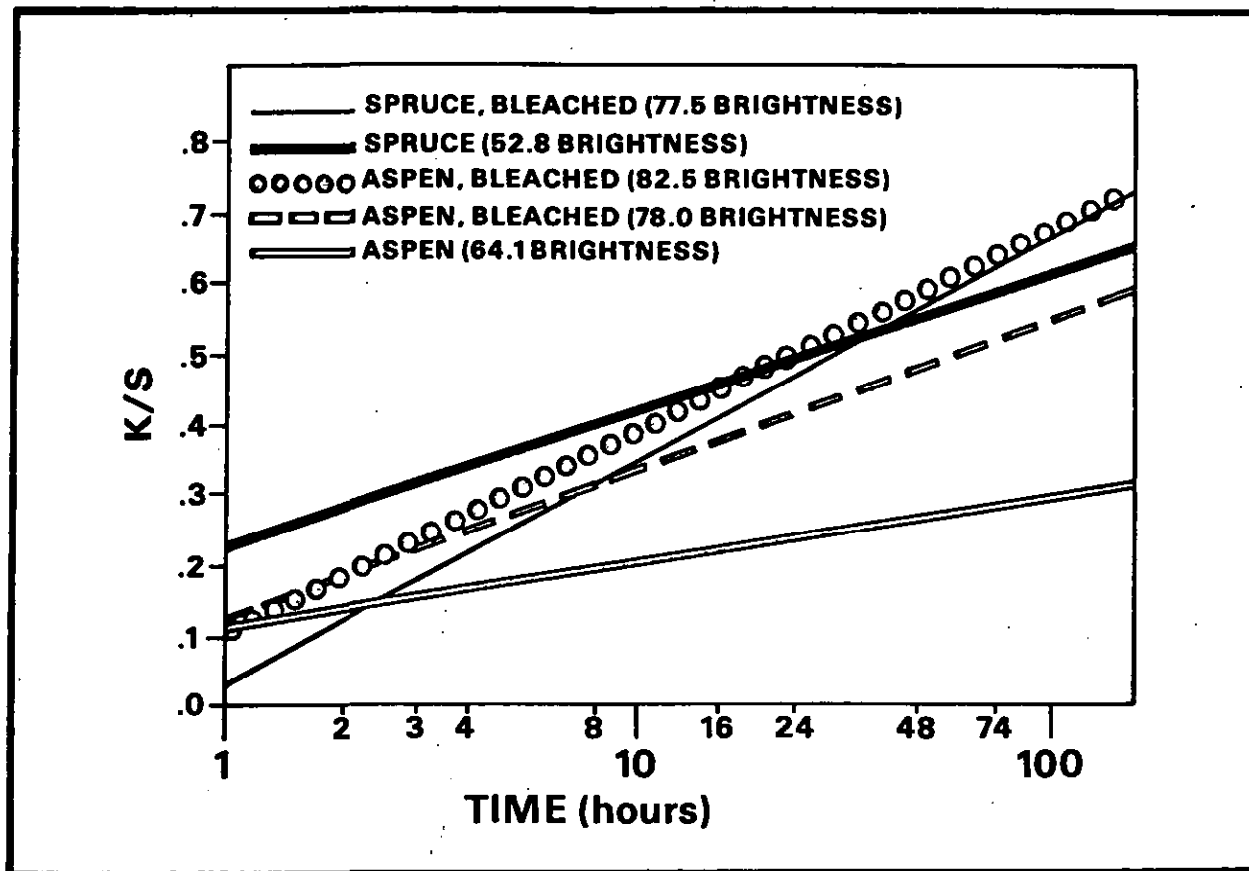


Figure 8. The kinetics of yellowing of unbleached and bleached softwood and hardwood mechanical pulps.

The wavelength of 310 nm has been identified as the most efficient UV wavelength for the yellowing reaction of high-yield pulps caused by quinone formation (Fig. 9). Lignin structures containing (alpha)-carbonyl groups have their absorption maximum at this particular wavelength. The width of this UV absorption band is unknown, but has to be considered to extend from the maximum absorbance wavelength to the sunlight's UV cut-off (290 nm) and to 330 to 350 nm.

CONCLUSIONS

In Fig. 10 the photoinduction cycle and the dark cycle are combined, so that the complex interaction of light with lignin, and lignin with oxygen becomes apparent.

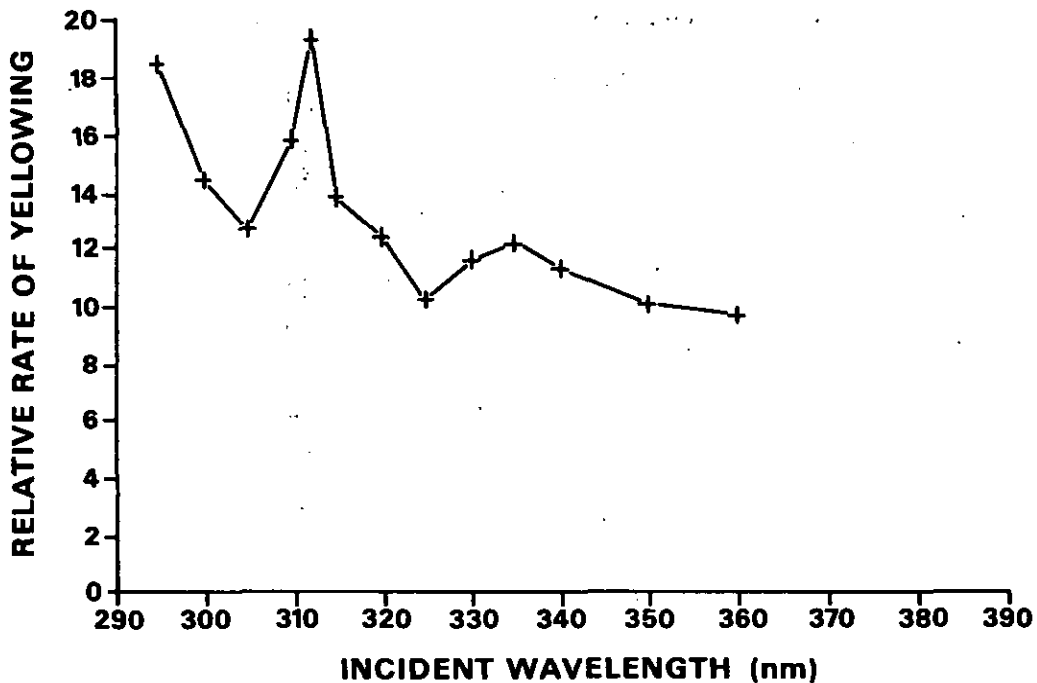


Figure 9. Dependence of relative rates of yellowing on the irradiating wavelength.

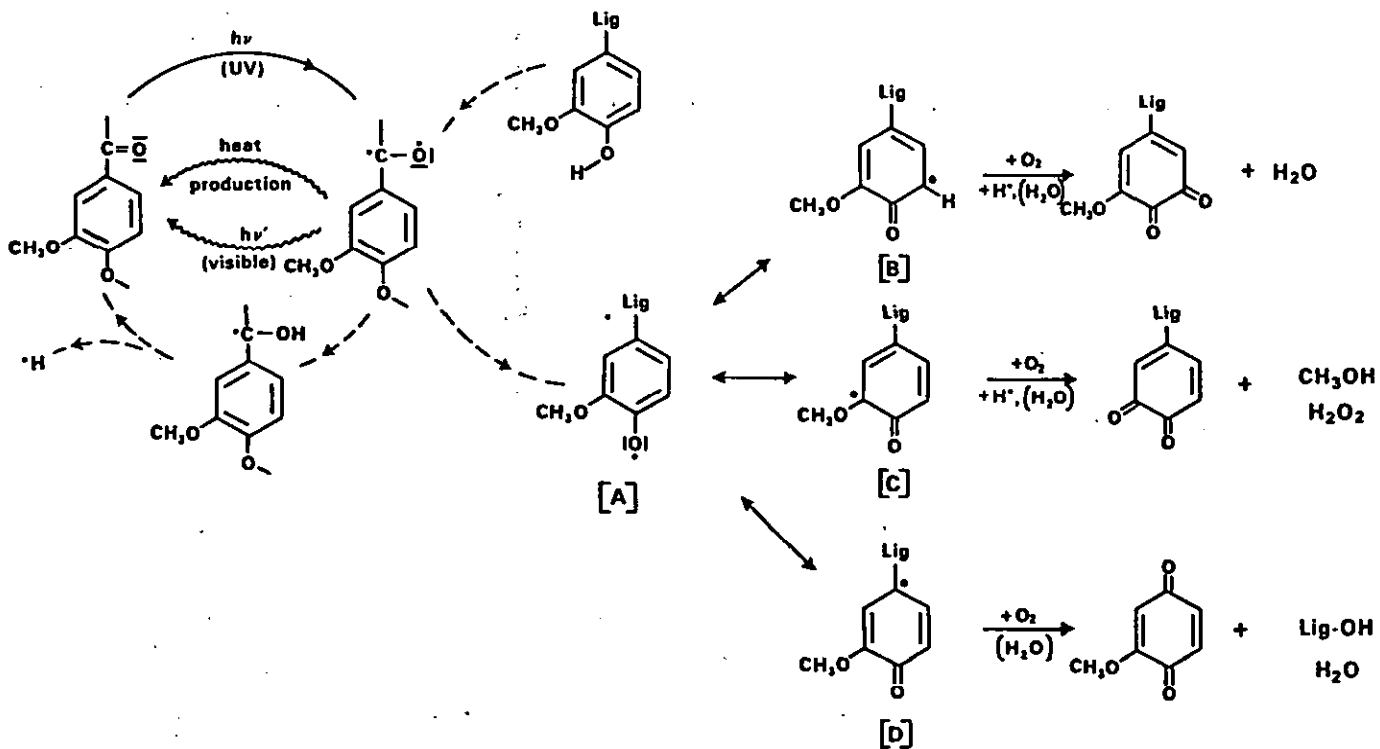


Figure 10. The mechanism of the light-induced yellowing reaction of high-yield pulps.

There are two obvious steps in the sequence, where there is a chance to intercept the yellowing reaction. The quenching of the UV radiation before it becomes absorbed by the carbonyl group is practiced by protecting the high-yield pulp either through coating or surrounding it in a sandwich type manner with fully bleached chemical pulp layers. The application of fluorescent dyes to convert the UV radiation into visible light, as proposed by us some time ago, could not be achieved yet. However, some new approaches are undertaken in a Master's Thesis.

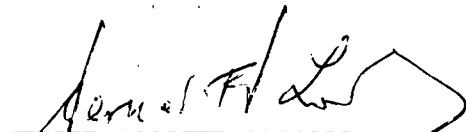
The use of antioxidants as radical scavengers (reduction of the phenoxy radical) has been explored and seems to be achievable. Restrictions are given through the relatively good antioxidant property of lignin itself that implies that only strong antioxidants can be effective. Organic hydrosulfide groups are promising compounds. In first experiments we used cystein - a naturally occurring amino acid - as reagent. Due to its zwitterionic nature it seems to be easily absorbed onto the fibers. A brightness stabilizing effect has been observed, but complete analytical data are not yet available.

LITERATURE CITED

1. Leary, G., Nature 217:672(1968).
2. Nimz, H. Proceedings of the 1982 TAPPI Research and Development Division Conference, p. 51ff.
3. Calvert, J. G.; Pitts, J. N., Jr. Photochemistry, John Wiley and Sons, Inc., 1967:382.
4. Schenck, G. O.; Pfundt, G. In: 1,4-cycloaddition reactions. J. Hamer, Ed., Academic Press, Inc. 1967:345.
5. Ramirez, Fausto, Accounts Chem. Res. 1(6):168-74(1968).
6. Neumann, M. C.; De Groote, R. A. M. C.; Machado, A. E. H. Book of Abstracts of the 190th ACS National Meeting, Chicago, CELL 32; Sept. 8-13, 1985.

7. Hon, D. N.-S. Book of Abstracts, CELL 31; 190th ACS National Meeting, Chicago, IL; Sept. 8-13, 1985.

THE INSTITUTE OF PAPER CHEMISTRY



Werner F. W. Lonsky
Research Associate
Wood Sciences
Chemical Sciences Division

APPENDIX

SINGLET OXYGEN GENERATOR AND DETECTION SYSTEM

In order to study the effect of O_2 and UV light on the paper samples the flow system and the detection system shown in Fig. 1 were used. O_2 and Ar were passed through the discharge tube, and this resulted in the formation of singlet oxygen and O-atoms. Dissociation energy was provided by microwaves as the gas flowed across the microwave cavity. An Electro Medical Supplies Microton 200 was used to generate microwaves.

The gases used in the experiments were obtained from Linde Specialty Gases. The listed minimum purity for Ar was 99.998%, and Linde's "dry" O_2 , had a listed minimum purity of 99.995%. The gases were used directly from "T-sized" cylinders. Prior to entry into the flow tube the pressures of the compressed gas was reduced by a regulator attached to the cylinder, and then a Nupro shut-off valve. Fine-control of the gas flow was obtained by using an Edwards needle valve immediately preceding entry of the gas into the flow tube.

DESCRIPTION OF THE DETECTION SYSTEM

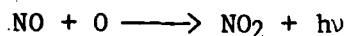
The detection system used to monitor the singlet oxygen emission is depicted in Fig. 1. It consisted of the following components:

- a) A combination light-chopper and 200 Hz oscillator assembly from American Time Products.
- b) A Bausch and Lomb model 33-06-03 grating monochromator.
This is operational between 700 and 1600 nm.
- c) A North Coast model EO-817 intrinsic germanium detector and bias supply unit.

- d) A Princeton Applied Research Corporation model 5101 lock-in amplifier.
- e) A BBC Goerz Metrawatt Servogor 120 dual sample chart recorder.

An extension at the front of the monochromator was used to limit its field of view to a 6 mm horizontal distance at the far wall of the flow tube. The calibration of this detection system to yield the absolute singlet oxygen concentration from observed peak heights is described in Avoub Ali's MSc thesis (University of British Columbia, May 1986).

For some experiments it was useful to monitor the relative [O] along the flow tube. The intensity of the NO₂ afterglow from the following reaction is proportional to [O] and [NO] (F. Kaufman, 1961, Prog. React. Kinetics, 1, 1).



However, there is no net change in [NO] along the length of the flow tube because of the following fast reaction:



Therefore, any change in the NO₂ emission intensity along the flow tube must result from changes in [O].

A Hamamatsu IP28 photomultiplier tube was used to monitor the greenish-yellow NO₂ afterglow. The photomultiplier was fastened to the singlet oxygen detection assembly; this allowed for the simultaneous measurement of the singlet oxygen emission and the NO₂ emission. An Ortec system consisting of a model 9349 log/lin ratemeter, a model 9301 fast preamplifier, and a model 9302 amplifier/discriminator was used in conjunction with the photomultiplier. A Hamner model

NV-19 high voltage power supply was used to provide power for the Ortec system. The absolute $[O]$ was determined using the NO_2 titration method. NO_2 was added until the yellowish-green NO_2 afterglow was extinguished. At this point the flow of O-atoms is equal to the flow of NO_2 added (F. Kaufman, 1961, Prog. React. Kinetics, 1, 1).

THE INSTITUTE OF PAPER CHEMISTRY
Appleton, Wisconsin

Status Report
to the
PULPING PROCESSES
PROJECT ADVISORY COMMITTEE

Project 3566
STRONG, INTACT, HIGH-YIELD FIBERS

September 10, 1986

PROJECT SUMMARY FORM

DATE: September 10, 1986

PROJECT NO. 3566: STRONG, INTACT, HIGH-YIELD FIBERS

PROJECT LEADERS: T. J. McDonough, S. Aziz

IPC Goal:

Significant increase in the yield of useful fibers.

OBJECTIVE:

Develop methods of wood fiber separation which will allow the production of separated fibers having the same physical strength and geometrical form possessed when bound in the original wood matrix.

CURRENT FISCAL YEAR BUDGET: \$175,000

SUMMARY OF RESULTS SINCE LAST REPORT:

Load-elongation testing of individual fibers sampled from spruce thermomechanical and thermochemimechanical pulps indicates that their fibers are substantially stronger than those of southern pine refiner pulps. The latter were, in turn, capable of carrying from 50 to 100% more load than the corresponding kraft-fibers.

Measurement of secondary wall fibril angle by direct microscopic observation of stained fibers has been attempted and has given promising results. Mechanical pretreatment to remove the primary wall was found to be required.

A study of the relationships between fiberization variables and fiber length and strength has been completed. The yields of fibers and fiber fragments have been interpreted in terms of effects of fiberizing conditions on the probability of success of any given impact event experienced by a wood particle. Both primary effects (on intercellular bond strength) and secondary effects (on stress transfer efficiency) have been observed. A steam explosion effect resulting in fiber fragmentation was also observed. Zero-span tensile strength measurements were generally more reflective of interfiber bond strength than fiber strength, although they did provide a definite indication that atmospheric fiberization of untreated wood at 80°C gives lower fiber strength than either fiberization of sulfonated wood at 80-160° or fiberization of untreated wood at 120-160°.

Properties of handsheets made from the coarse pulps produced under various conditions were also measured. The data were generally interpretable in terms of effects of lignin softening on fiber flexibility and fines generation. An exception was the unusually high tear strength obtained after sulfonation and subsequent fiberization at 120°C.

Work aimed at converting strong high-yield fibers into strong sheets has begun. Treatment of 90% yield fiber with ozone to increase specific bond strength has given sheets 80% as strong as kraft controls. Hot pressing of the same fiber without ozone treatment gave sheets 70% as strong as kraft.

PLANNED ACTIVITY THROUGH FISCAL YEAR 1987:

The basic assumptions underlying our approach will be further examined. Experiments directed at answering the question of whether existing high-yield pulping methods decrease fiber strength will be continued. Also the degree of fiber strength loss suffered during kraft pulping will be further characterized. Both questions will be addressed by determination of single fiber load-elongation characteristics.

Experiments will be done to demonstrate that strong high-yield fibers can be bonded to form sheets with strengths comparable to those of kraft sheets containing far fewer fibers.

Studies of the relationships between fiberization variables and fiber properties will be continued. These will include trials in which disk refiners, either pilot scale or full scale, are used to accomplish the fiber separation.

Procedures for determining secondary wall fibril angle will be established and the results used to assist in the interpretation of single fiber strength data.

FUTURE ACTIVITY:

Prediction of fiberization behavior from wood properties, alternative fiber separation methods and biological pretreatment of wood will be investigated.

STUDENT RESEARCH:

T. Heazel, Ph.D.-1986; E. Byers, Ph.D.-1986; C. Nordberg, Special Student-1985; T. Cornbower, M.S.-1987.

Status Report

STRONG, INTACT, HIGH-YIELD FIBERS

OBJECTIVES

The ultimate objective of this project is to develop methods of wood fiber separation that will allow the production of separated fibers having the same physical strength and geometrical form that they possessed as parts of the original wood matrix. The current short term goals are to identify the factors governing retention of fiber strength and integrity during fiber separation and to develop methods of controlling them.

INTRODUCTION

Pulps having a yield of 85-90% and the strength of kraft pulps will consist of fibers that have high values of four important attributes:

1. length
2. strength
3. conformability
4. active bonding surface

Existing processes that produce pulp in this yield range and that represent the state of the art have invariably been developed by changing process variables to simultaneously increase the first, third and fourth of these. Compromises have been a part of this empirical optimization process; for example, active bonding surface is often obtained at the expense of fiber length.

Project 3566 is based on the premise that it is better to focus effort on achieving the above attributes one at a time instead of all at once. Learning

how to separate high-yield fibers without significantly reducing their strength would move us one step closer to the goal of ultrastrong high-yield pulps if the following assumptions are justified:

1. Kraft pulps (the properties of which define the term "ultrastrong" as applied to high-yield pulps) are comprised of fibers that have undergone appreciable strength losses as a result of the manufacturing process.
2. Existing high-yield processes also cause appreciable fiber strength losses.
3. High-yield fibers separated without strength loss can subsequently be made to bond to one another to such a degree that fiber strength controls sheet strength.

Assumption 1 is necessary to justify any kind of research aimed at producing 90% yield pulps with kraft strength. Fiber strength is known to be an important factor in the strength of sheets made from beaten kraft pulp.¹ Doubling the pulp yield would result in the number of fibers in the sheet being halved at the same basis weight. This would in turn result in a 50% strength loss unless the fiber strength could simultaneously be increased. It seems likely that the only way to do this would be to prevent loss of native fiber strength.

There is evidence, both in the literature and in the results of our work, that justifies this assumption. Stone and Clayton,² for example, showed that the load-bearing ability of thin wood sections pulped in the kraft process decreased progressively as the degree of delignification was increased. In addition, we have measured the strengths of single fibers sampled from refiner

mechanical pulp, chemimechanical pulp and kraft pulps from southern pine. The results showed that the breaking load of fibers from both types of high-yield pulps were very similar and from 55 to 125% higher than those of the kraft pulps, depending on the source of the latter and whether or not they had been bleached.

The justification for assumption 2 is not as clear-cut. In fact, much of the data we have collected so far are consistent with the view that the separation of fibers at high yield levels does nothing to reduce fiber strength. Thus, fibers from high-yield spruce and pine pulps have been shown to have breaking lengths that are 50 to 60% higher than the average breaking lengths of the corresponding thin wood sections (Table 1). This apparently paradoxical result becomes less so when it is realized that the breaking length of thin wood sections having cross sections that consist of a thousand or more fibers is probably considerably smaller than the mean breaking length of all of the constituent fibers. Polydispersity of individual fiber breaking stresses and moduli, as well as the occurrence of stress concentrations, are responsible. (A first approximation to the relationship between wood section strength and mean fiber strength should be accessible by simple Monte Carlo simulation of wood section failure in tension. This will be further investigated.) In addition, the value of fiber strength obtained by averaging the strengths of individual fibers sampled from the pulp is subject to an upward bias. This occurs because only those fibers and fiber fragments whose length exceeds the minimum test span (representing roughly half the total weight of the pulp) are represented in the average. Fiber fragments may be weaker because initially strong fibers are weakened by the same events that break or cut them. In the latter case fiber strength loss would go undetected.

Table 1. Estimated average breaking lengths of pine and sprucewood and pulp fibers, km.

	Pine	Spruce
Wood ^a	26	39
Pulp ^b	40	60

^aAverage of earlywood and latewood zero-span breaking lengths, as determined on thin (2-4 fiber layers thick) wood sections.

^bAverage strength of single refiner mechanical pulp fibers converted to breaking lengths by assuming a wall density of 1.5 g/cm³.

In view of these complicating factors, the available data do not justify the conclusion that mechanical separation of high-yield fibers does not reduce their strength. The question of whether existing high-yield pulping methods decrease fiber strength deserves more attention. If the answer is in the negative, research emphasis should be shifted to another of the four desirable fiber attributes listed at the beginning of this report. If affirmative, significant gains may be expected by correlating fiber strength retention with the variables that characterize the refining process. Assuming the negative answer risks sacrificing these gains. We are approaching the question by obtaining more data on single fiber strength of high-yield pulps, including those obtained under conditions that maximize fiber length retention and therefore minimize data censoring of the type discussed above by looking for effects of fiberization variables on fiber strength, and by mathematical modelling of wood section failure.

Assumption 3 is necessary to justify an approach that involves first making long, strong, separated fibers without regard to their ability to bond to one another to form a strong sheet. We are currently examining it, as described later in this report.

Consideration of the objectives and assumptions outlined above leads to the following questions:

1. How long and strong are the fibers in wood?
2. How long and strong are the fibers in kraft pulp?
3. How long and strong are the fibers in high-yield pulp made under standard conditions?
4. How can high-yield pulping conditions be changed to minimize effects on fiber length and strength?
5. Can strong high-yield fibers be bonded together to form a sheet in which a fiber number disadvantage relative to kraft is largely or completely compensated for by their fiber strength advantage?
6. To what extent are the answers to the above questions dependent on species?
7. Can the strength of a wood fiber be increased beyond its native value?

The remainder of this report summarizes our status with respect to these questions.

FIBER LENGTH AND STRENGTH IN WOOD

A procedure was developed for obtaining information on the strength of fibers in wood by measuring the zero-span (ZS) tensile strength of thin wood sections. Sections taken from many locations within 2 pine trees and 2 spruce trees were tested.³ Spruce is stronger than pine, latewood stronger than earlywood. Individual pulp fibers of both species were stronger than expected on the

basis of the wood strengths, indicating that average fiber strength estimates based on wood measurements are low and/or those based on testable fiber measurements are high. It is likely that both are true. An effort will be made to relate the observed wood strength to the average fiber strength by means of a simple mathematical model.

The distribution of lengths of fibers taken from each annual ring of each of two spruce trees and two pine trees was measured and is available for comparison with pulp fiber length distributions.

FIBER LENGTH AND STRENGTH IN PULP

SINGLE FIBER TENSILE STRENGTH

Refiner pulps made from unsulfonated and presulfonated southern pine chips (RMP and SCMP) were found to contain 28 mesh fractions consisting of fibers having a strength of about 60 kg/mm^2 , which is about the same as reported by Hardacker⁴ for a commercial southern pine bleached kraft whole pulp (Table 2). The 48 mesh fractions were slightly weaker.³ The combined weight of these two fractions represented 40-55% of the total weight of the pulp. Hardacker's kraft fibers had the same breaking stress as the high-yield fibers, but only half the cross-sectional area (CSA) and therefore half the breaking load. To extend this we made some kraft pulp from the same wood that gave the RMP and SCMP and tested its fibers in the unbleached state. It had the same CSA as Hardacker's pulp, but a 40% higher breaking load. Taken together, these observations indicate that a high-yield fiber can carry 50 to 100% more load than a kraft fiber. The difference between the two results, although it could be attributable to bleaching, drying or other differences between the two samples,

suggests that additional experiments are necessary to quantify the strength losses accompanying kraft pulping.

Table 2. Pine single fiber properties and their standard errors.

Pulp	Load,	Area, μm^2	Stress, kg/mm^2	Modulus, kg/mm^2
RMP ^a	32 ± 2	580 ± 35	59 ± 4	1100 ± 135
CMP ^a	34 ± 2	590 ± 30	59 ± 2	1350 ± 80
BK ^b	15 ± 1	250 ± 20	62 ± 3	580 ± 30
UBK ^c	22 ± 3	250 ± 20	86 ± 9	1040 ± 140

^aLaboratory refiner mechanical (RMP) or chemimechanical (CMP) pulps from southern pine.³

^bCommercial bleached kraft.⁴

^cUnbleached kraft made in laboratory from southern pine.

Sulfonation was shown not to affect the strength of thin wood sections, an observation that is consistent with the similarity between the properties of fibers from pine RMP and SCMP. The latter observation does not preclude the possibility that more extensive sulfonation and lignin softening than was used in this experiment lessens fiber damage during fiberization and thereby increases pulp fiber strength.

Testing of spruce fibers has given data which are at present difficult to interpret. Single fibers sampled from different fractions of classified pulps gave the data shown in Table 3. In this case the pulps were very coarse ones prepared in an Asplund mill to just separate the fibers and minimize any subsequent mechanical action which might weaken the fiber. A thermomechanical pulp (TMP) gave fractions in which the slenderness of the fibers increased with increasing screen mesh number, and fiber breaking load decreased proportionately. As a result, the breaking stress was about the same for all fractions and about

50% higher than for pine RMP fibers. The latter difference is consistent with the earlier observation that thin wood sections from spruce are about 50% stronger than those from pine. Thermochemimechanical pulp (TCMP) of 74% yield gave fractions in which the fibers had breaking loads about the same as, or marginally lower than those of the TMP fibers. However, the TCMP fibers exhibited larger CSA values, with the result that the breaking stress was lower.

Table 3. Spruce single fiber properties and their standard errors.

Pulp	Mesh Size	Load, g	Cross-sectional area, μm^2	Stress, kg/mm^2	Modulus, kg/mm^2
TMP ^a	14	14 ± 2	165 ± 15	100 ± 15	1930 ± 340
	28	12 ± 1	170 ± 10	90 ± 15	1690 ± 230
	48	10 ± 1	150 ± 15	90 ± 20	2040 ± 425
TCMP ^b	14	12 ± 1	200 ± 10	60 ± 4	850 ± 60
	28	13 ± 2	195 ± 15	65 ± 5	640 ± 50
	48	9 ± 1	180 ± 10	55 ± 5	610 ± 50

^aLaboratory thermomechanical pulp.

^bLaboratory thermochemimechanical pulp.

Why the CSA of the TCMP should be so much greater than that of the TMP under the testing conditions (50% RH and 73°F) is not clear. Fibers sampled from the whole pulps displayed the opposite trend, as shown in Table 4, raising questions about the validity of the measurements of the CSA of the spruce fibers. Breaking load measurements were more consistent, all but the 48-mesh fractions giving values in the range 12-14 g.

Additional experiments are planned to compare fiber cross-sectional areas and breaking loads for mechanical, chemimechanical and kraft pulps from

both spruce and pine. This aspect of the work has been proceeding slowly because of limited availability of the test instrument. That problem has now been resolved, and the pace of the single fiber testing will accelerate.

Table 4. Spruce single fiber properties and their standard errors: anomalous fractionation effects.

Pulp	Fraction	Load, g	Area, μm^2	Stress, kg/mm^2	Modulus, kg/mm^2
TMP ^a	Whole	12 ± 1	240 ± 20	72 ± 13	1410 ± 230
	14 Mesh	14 ± 2	165 ± 15	100 ± 14	1930 ± 340
TCMP ^a	Whole	14 ± 1	155 ± 10	91 ± 6	1270 ± 130
	14 Mesh	12 ± 1	200 ± 10	58 ± 4	850 ± 60

^aLaboratory thermomechanical pulp.

MEASUREMENT OF FIBRIL ANGLE

The work of Page and others has demonstrated the existence of a correlation of fiber tensile strength with the angle that the helical winding of cellulose microfibrils in the middle (S₂) layer of the secondary wall makes with the fiber axis. Although this correlation is not of central interest in the present work, accurate estimation of the fibril angle would provide an extremely useful covariable to facilitate the interpretation of fiber strength data. If it could be measured for each fiber subjected to tensile testing, it would allow the effect of fibril angle to be separated from the observed variation, making it easier to detect and estimate the effects of interest. For this reason, a part of our effort has been directed toward finding a rapid, routine method for measuring fibril angle.

The methods described in the literature employ polarized light, phase contrast, X-ray diffraction and deposition of crystals. Polarized light microscopy

is perhaps the most popular. It requires light to be passed through a single cell wall, so this must be arranged by sectioning the fiber longitudinally or by some other means.⁵ Page's modification of the polarized light technique⁶ requires that the fiber lumen be filled with mercury to reflect the illuminating light beam and prevent it from passing through both walls. Leney⁷ macerated the fiber sample, which produced the single walled fragments necessary. This method, however, may change the angle being measured. The phase contrast, near ultraviolet method⁸ is direct and accurate, but is time-consuming and requires painstaking technique, and the S2 angles are often hard to differentiate from S1 and S3 angles. X-ray diffraction is a relatively quick and uncomplicated method but is indirect and the diffractograms are subject to varying interpretation.⁹

The method of Bailey¹⁰ relies on visualization of the fibril angle by deposition of iodine crystals in the fiber wall. They tend to nucleate in cracks and, since the structure of the wall normally results in cracks being parallel to the fibrils, reveal the fibril angle. The method has recently been reinvestigated by Senft and Bendtsen,¹¹ who modified it with respect to the manner of inducing cracks in the cell wall. Since it appeared to be rapid and direct we experimentally evaluated its applicability to the fibers of a 74% yield pulp made by fiberizing sulfonated wood chips in an Asplund mill at 120 degrees C. We tried several methods of inducing wall cracking, including repeated oven drying and repeated immersion in liquid nitrogen, and several combinations of iodine-potassium iodide stain concentration and exposure time. The results were unsatisfactory, regardless of conditions. Many relatively large, randomly oriented crystals were formed on the fibers, making any angle difficult to discern. Only about 20% of the fibers tested clearly revealed their fibril angles after staining and crystal deposition.

As an alternative to the iodine crystal deposition method, direct visualization by staining with safranin was tried. Earlier data had indicated that direct observation of the fibril angle would be facilitated by removal of the primary wall, so these experiments were carried out after mechanical pretreatments of varying severity. The resulting fibers were classified by assigning them descriptive codes according to the following scheme:

- A) fibril angle not discernible
- B) few fibrils apparent, but angle clearly discernible at various points along the fiber
- C) many fibrils apparent but only on parts of the fiber
- D) many fibrils apparent along entire length of fiber
- E) fibrils apparent by virtue of fiber damage

The latter 4 categories are exemplified by the photomicrographs in Fig. 1 through 4.

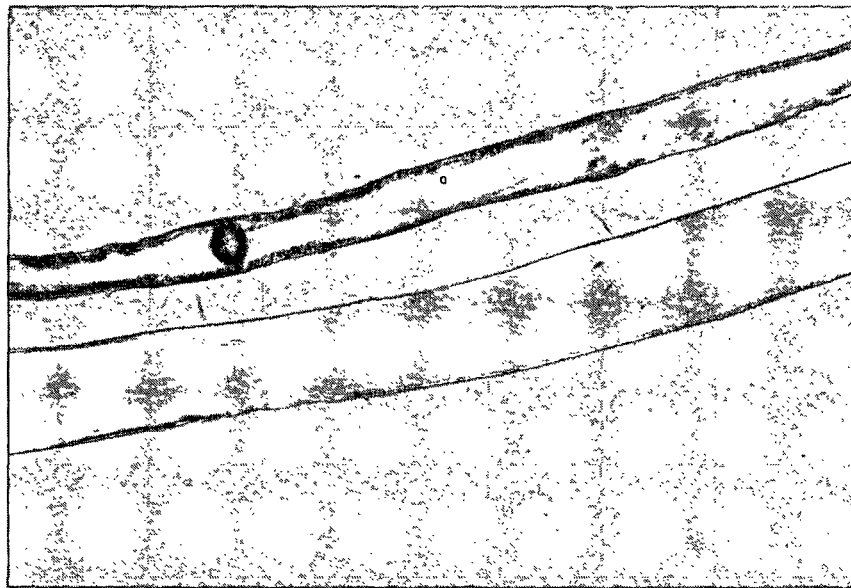


Figure 1. Safranin stained spruce TCMP fiber - category B.

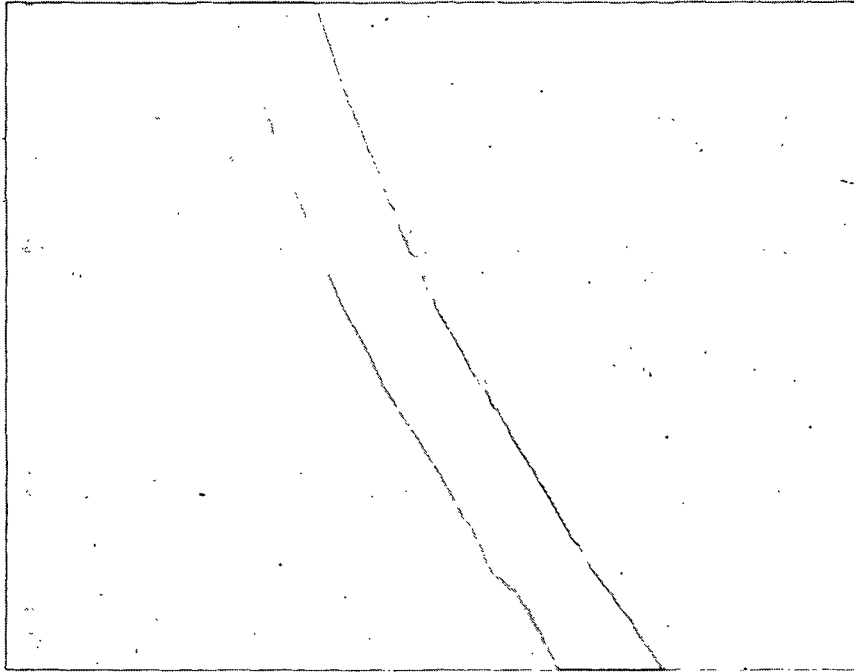


Figure 2. Safranin stained spruce TCMP fiber - category C.

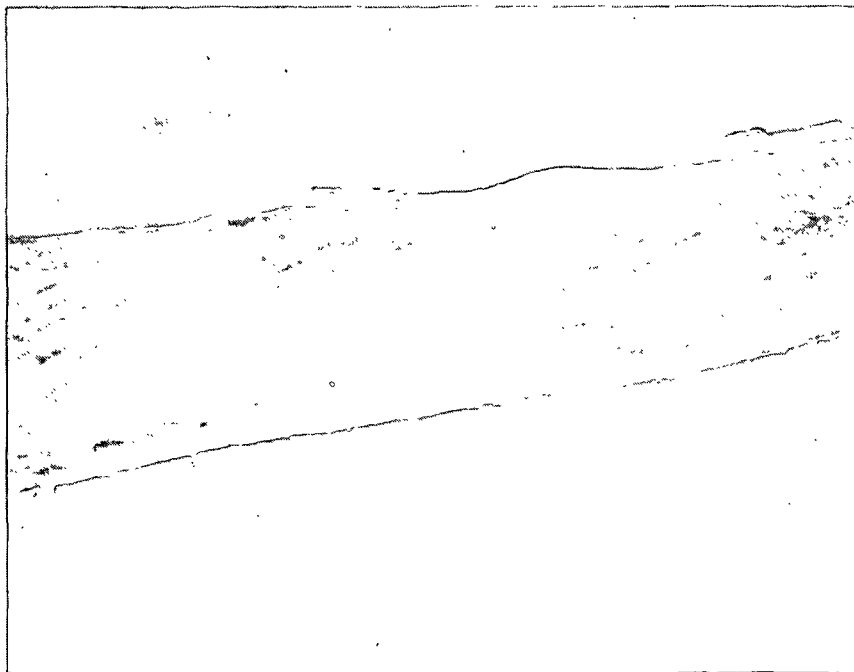


Figure 3. Safranin stained spruce TCMP fiber - category D.

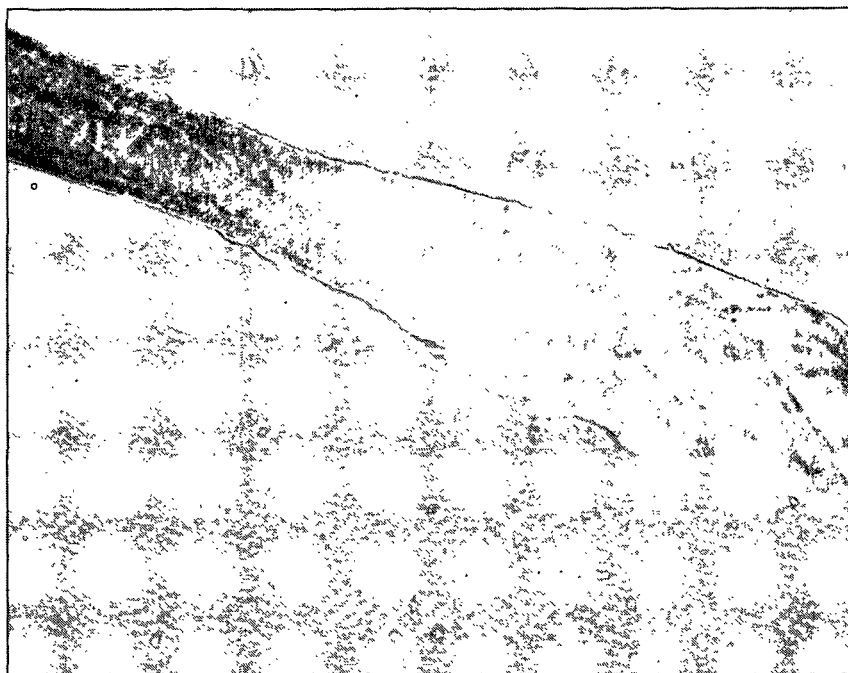


Figure 4. Safranin stained spruce TCMP fiber - category E.

Table 5 shows the percentage of the observed fibers that fell into each category as a function of the degree of mechanical action applied to a sample of approximately 1 gram of fibers before staining. This mechanical action consisted of magnetically stirring the sample at 900 rpm in 20 mL of deionized water to which 50 glass beads (4 mm in diameter) had been added. In a sample stained without any prior stirring, 46% of the fibers displayed no measureable fibril angle. After one hour of stirring this was reduced to 15%, but 34% of the fibers were sufficiently damaged that there was some doubt as to whether the measured angle was meaningful.

Table 6 gives the results of another experiment similar to the first in all respects except that the number of glass beads was reduced from 50 to 10, and the stirring time was extended. After 8 hours of stirring, the number of fibers with invisible fibril angles was reduced to 24% of the total, and only 5% were extensively damaged - a 71% success rate.

Table 5. Effect of stirring time on fibril visibility (% fibers in indicated category).^a

Fiber Category	Stirring Time, min				
	0	15	30	45	60
A	46.12	32.71	27.59	16.99	15.04
B	40.78	41.59	43.84	30.10	23.89
C	7.77	8.41	5.91	8.74	6.19
D	4.85	10.75	10.84	19.42	20.35
E	0.49	6.54	11.82	24.76	34.51

^a1 g fiber, 50 glass beads in 20 mL deionized water.

Table 6. Effect of stirring time on fibril visibility (% fibers in indicated category).^a

Fiber Category	Stirring Time, hour				
	0	6	7	8	9
A	46.12	31.53	27.73	24.55	27.19
B	40.78	35.47	35.00	39.29	38.71
C	7.77	9.36	7.73	4.02	3.69
D	4.85	18.72	26.82	27.23	22.58
E	0.49	4.93	2.73	4.91	7.83

^a1 g fiber, 10 glass beads in 20 mL deionized water.

Table 7 compares average measurements on fibers in each category after varying degrees of mechanical action. The most notable feature is the difference between the average angles for fibers in which only a few fibrils were visible and those in which many fibrils were visible in a localized area. It is not yet known whether the two categories represent different fiber types with different angles or the observed difference is an artifact. No consistent effect of the severity of mechanical action on the measured angle was apparent.

Table 7. Averages of fibril angle measurements on the same fiber (degrees) with standard deviations.

Stirring Time, min	No. of Glass Beads	Fiber Category ^a			
		B	C	D	E
45	50	12.4 \pm 1.2			
		16.5 \pm 1.7			
45	100		28.3 \pm 4.8	20.9 \pm 1.6	
60	100			20.4 \pm 2.1	22.3 \pm 2.5
					17.7 \pm 2.1
540	10	14.8 \pm 1.8		18.9 \pm 1.6	
960	10		22.7 \pm 0.5	20.4 \pm 1.9	

^aCategory B - few fibrils apparent.

C - fibrils locally apparent.

D - many fibrils apparent.

E - fibrils apparent by virtue of damage

See also page 287.

Insufficient experiments have been done with chemical pulp fibers to allow conclusions to be drawn about the applicability of this method at low yields.

EFFECTS OF PULPING CONDITIONS ON FIBER PROPERTIES

To achieve the goal of producing separated fibers that have the same length and strength they possessed before separation, it will be necessary to develop a body of knowledge on the effects of changes in fiberization conditions on fiber length and strength retention. Ideally, this should take the form of a theory of the fiberization mechanism that can both summarize existing information and allow extrapolation to new conditions. In any case, it will be necessary to experimentally determine these effects under a variety of conditions.

Our first step in this direction has been to carry out a designed experiment to evaluate the effects of temperature, retention time and chip sulfonation on the length and strength of fibers liberated in an Asplund mill, a batch machine. This equipment was used in the absence of a pressurized disk refiner at IPC and in the belief that it will serve as a useful model system for disk refiners, at least at the early stages of our work in this area. The justification for this belief is the likelihood that in the process of wood particle size reduction (as opposed to refining or development of surface area), the dominant forces are applied in shear, whether it be in a disk refiner or in an Asplund mill. Since, at least for the present, we wish to study fiber separation and not surface development, the results of the application of shear force to wood are of interest, regardless of the type of equipment used to apply it.

The above arguments notwithstanding, it will be necessary to demonstrate that the fiberizing behavior of the Asplund mill is similar to that of the disk refiner, as has been pointed out by the Pulping Processes Project Advisory Committee. Pilot plant runs for this purpose will be started in early September, with the cooperation of Mead Corporation. Fiberization trials will be run in a pilot scale disk refiner system at their Chillicothe, Ohio laboratories. The results will confirm the data obtained at IPC or clarify the need to do all further trials in disk refiners at outside laboratories, pending our acquisition of suitable equipment.

The purpose of the Asplund mill experiments was primarily to determine the response of fiber length and strength to changes in temperature and duration of fiberization for both untreated and extensively sulfonated wood. To capitalize on the opportunity of obtaining data on the effects of the same variables on bonding-related properties, handsheet properties were also measured. Fiber

length distributions were measured by the Kajaani instrument and Bauer-McNett classification. Fiber strength was to be estimated both by zero-span tensile strength measurements and by single fiber tensile testing; the latter measurements have not yet been made, owing to unavailability of the test instrument.

The intent of the experiments was to study the effects accompanying fiber separation, apart from those of subsequent mechanical action. Consequently, conditions were chosen to produce very coarse, unrefined pulps. These were screened on a 0.006-inch slotted flat screen to remove unfiberized wood and large shives. Nevertheless, it turned out to be impossible to make acceptable sheets from the screen accepts for determination of zero-span tensile and other sheet properties, without some additional refining. This was accomplished by agitation of the pulps in a TAPPI disintegrator, a method chosen for the mildness of its action, to minimize the likelihood of fiber damage. Each pulp was evaluated after agitation for 0, 1, 2 and 3 hours to enable determination of the maximum value of each property, as well as its response to refining.

FIBERIZATION DEGREE AND MECHANISMS

Table 8 contains the results of flat screening of the 18 pulps produced, as accepts percentages, together with the results of Bauer-McNett classification and Kajaani fiber length distribution analysis of the accepts. The accepts ratio of fiber from untreated chips varied with temperature and retention time as shown in Fig. 5. Surprisingly, it decreased with increasing temperature, except at the shortest retention time. To further investigate this effect, each accepts figure was divided into two parts on the basis of the Bauer-McNett data. One part consisted of the fractions retained by 14, 28, and 48 mesh screens and was termed the "fibrous fraction." The other consisted of the fractions that passed through the 48 mesh screen and was termed "fragments." Figure

6 shows that the yield of fibrous fraction increased with increasing temperature, except at the long retention time, where it decreased slightly. The increase is attributed to the effect of lignin softening on intercellular bond strength, which results in a greater proportion of the refining bar-wood impacts and wood-wood impacts being successful in fracturing the wood between fiber walls. Because the average particle size decreases with increasing retention time, and the occurrence of such an impact depends on a particle or aggregate of particles spanning the fixed gap between "refining" surfaces, the number of impacts per unit time decreases at a rate proportional to the fiberization rate. As a result, the effect of lignin softening is greater at shorter retention times. At very long retention times, a secondary effect becomes dominant. It is hypothesized that this secondary effect is either a reduced coefficient of friction of the particle surfaces or reduced shear modulus, either of which would reduce the efficiency of shear stress transfer to a potential failure site.

As in the case of fiber liberation, the generation of fragments also depends on temperature in a way that suggests the existence of more than one kind of effect. As shown in Fig. 7, the yield of fragments decreases continuously with increasing temperature, except at the shortest retention time. This can be attributed to a combination of the effects of lignin softening on intercellular bond strength and fiber wall brittleness. A given impact is more likely to separate, rather than break, a bound fiber if it is less strongly anchored and if its wall is less brittle. Similarly, an already separated fiber caught in an impact zone will be less likely to break if its wall has been softened. The increase in fines generation observed upon increasing the temperature from 80 to 120 degrees at short retention times is probably associated with the production of "primary fines" - particles predisposed to separate from the fibers. A further temperature increase reduces their tendency to separate

by virtue of the lignin softening effect, which dominates at higher temperatures. Lignin flow or tackiness can "heal" cracks in and between cell walls that would otherwise result in the generation of primary fines.

The behavior of chips in which the lignin has been sulfonated and partially removed differs considerably from that of unsulfonated chips, as shown in Fig. 8. The general level of accepts ratio is much higher, and it decreases with increasing temperature for all retention times. Decomposing the accepts data as described above gives the data plotted in Fig. 9 and 10. These figures can be interpreted in terms of the same effects observed in the case of the unsulfonated chips. Sulfonation is known to decrease the softening temperature of lignin to values below 100 degrees centigrade; this would explain the lack of any increase in the yield of fibers with increasing temperature. The lignin is already sufficiently soft at the lowest temperature that increasing the temperature does not significantly increase the likelihood of fiber separation. What was before a secondary effect, the negative dependence of stress transfer efficiency on temperature, now becomes dominant. As a result, the accepts ratio decreases with increasing temperature for all retention times.

Table 8. Effects of sulfonation and fiberization time and temperature on particle size distribution in white spruce fiber.

Run No.	Treatment	Temp., C	Time, min	Accepts, %	% Retained on Screen Mesh Size				Through 100, by difference	Wt. Av. Fiber Length, mm	% of Pulp Particles of Length < 0.4 mm
					14	28	48	100			
1	None	80	1	38.9	26.2	36.4	17.4	8.9	11.1	1.19	17
2	None	80	2	59.2	15.1	35.9	18.2	9.2	21.6	1.11	21.1
3	None	80	4	71.5	14.8	34.7	18.9	9.5	22.1	1.26	15.6
4	None	120	1	42.1	23.7	32.9	17.8	7.1	18.5	1.43	13.9
5	None	120	2	55.2	22.4	32.7	18.1	7.1	19.7	1.65	9.1
6	None	120	4	63.4	24.4	32.6	18.3	7.9	16.8	1.61	9.5
7	None	160	1	48.0	26.1	37.4	15.8	5.9	14.8	1.60	10.8
8	None	160	2	51.7	29.3	36.9	16.4	5.4	12.0	1.72	8.4
9	None	160	4	57.7	27.4	37.3	15.7	4.9	14.7	1.80	7.3
10	Sulfonated	80	1	63.5	44.2	32.8	12.3	4.5	6.2	1.99	5.0
11 ^c	Sulfonated	80	2	80.1	45.6	32.1	12.4	4.6	5.2	n.d.	n.d.
12	Sulfonated	80	4	81.4	56.4	32.6	13.5	4.8	2.7	1.73	8.6
13	Sulfonated	120	1	60.4	37.5	32.7	14.1	4.1	11.6	1.81	7.0
14	Sulfonated	120	2	75.2	37.6	34.9	13.0	4.6	9.9	n.d.	n.d.
15	Sulfonated	120	4	76.7	36.1	33.9	15.4	5.0	9.6	1.81	6.8
16	Sulfonated	160	1	51.5	46.8	30.1	15.1	4.1	3.9	1.92	5.5
17 ^d	Sulfonated	160	2	56.4	45.3	32.2	13.8	3.8	4.9	n.d.	n.d.
18	Sulfonated	160	4	62.8	46.6	33.2	12.3	3.4	4.5	1.97	5.7

^aFiberization conducted as a batch process in the Asplund mill after preheating the chips for 2 minutes at the fiberization temperature.

^bTwo batches of sulfonated chips (yields 74 and 78%) were used.

^cAverage of data from 2 experiments, one with 74% yield chips, one with 78% yield chips.

^dAverage of data from 3 experiments, one with 74% yield chips, two with 78% yield chips.

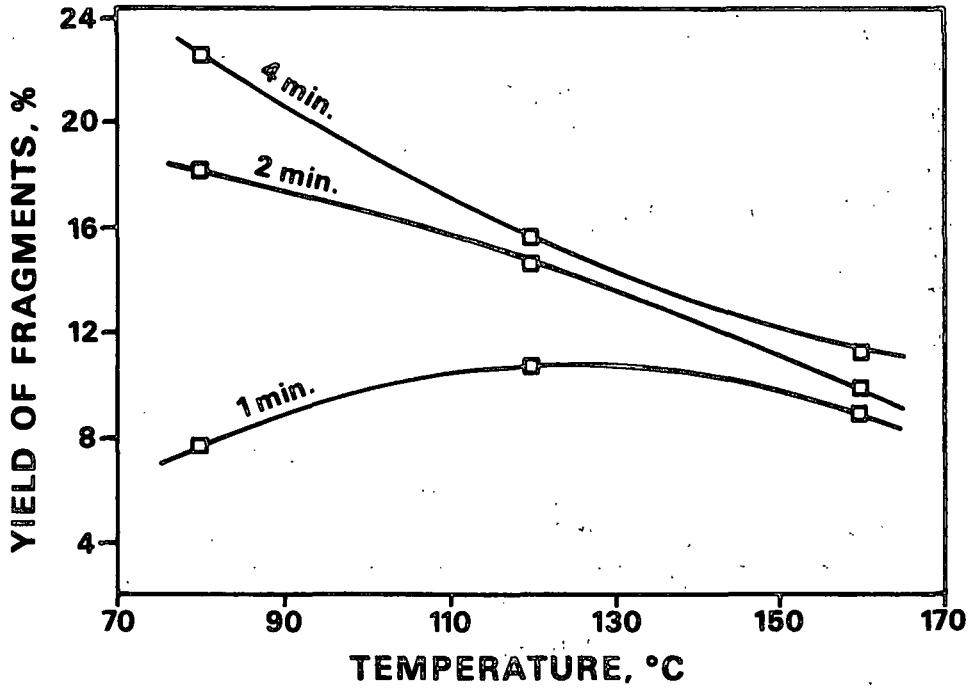


Figure 7. Effect of fiberization temperature on yield of fiber fragments (including fines) from untreated chips at various retention times.

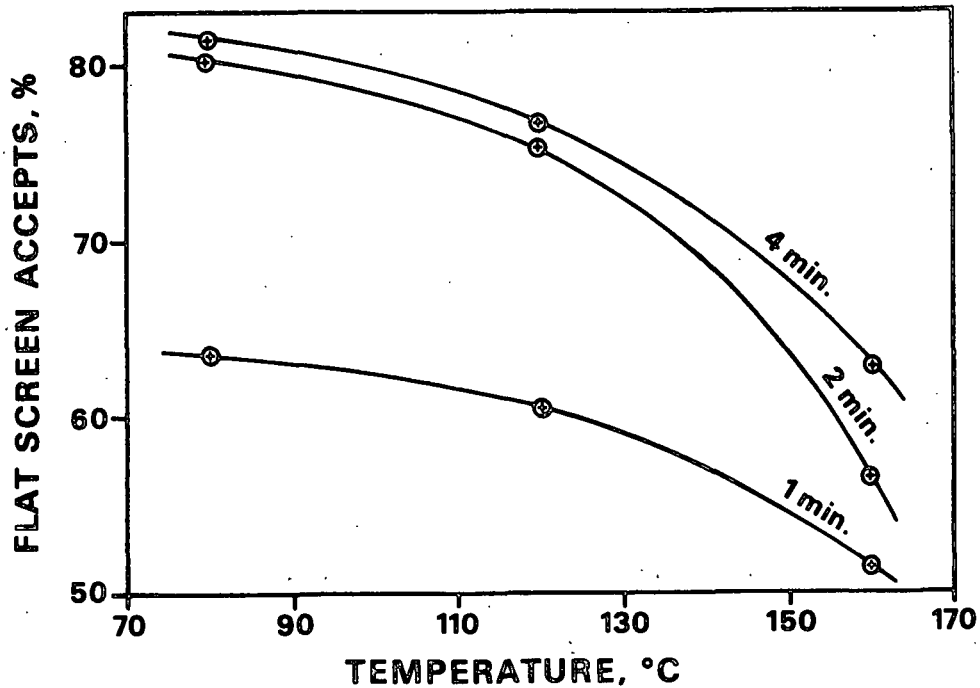


Figure 8. Effect of fiberization temperature on screen accepts ratio of fiber produced from 74% yield sulfonated chips at various retention times.

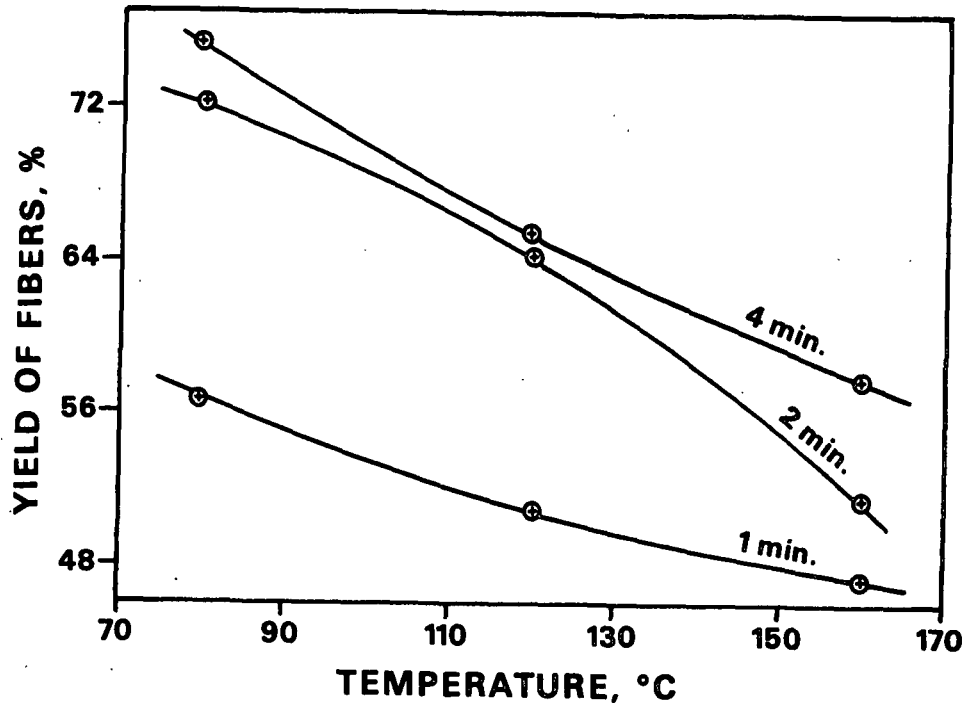


Figure 9. Effect of fiberization temperature on yield of fibers from 74% yield sulfonated chips at various retention times.

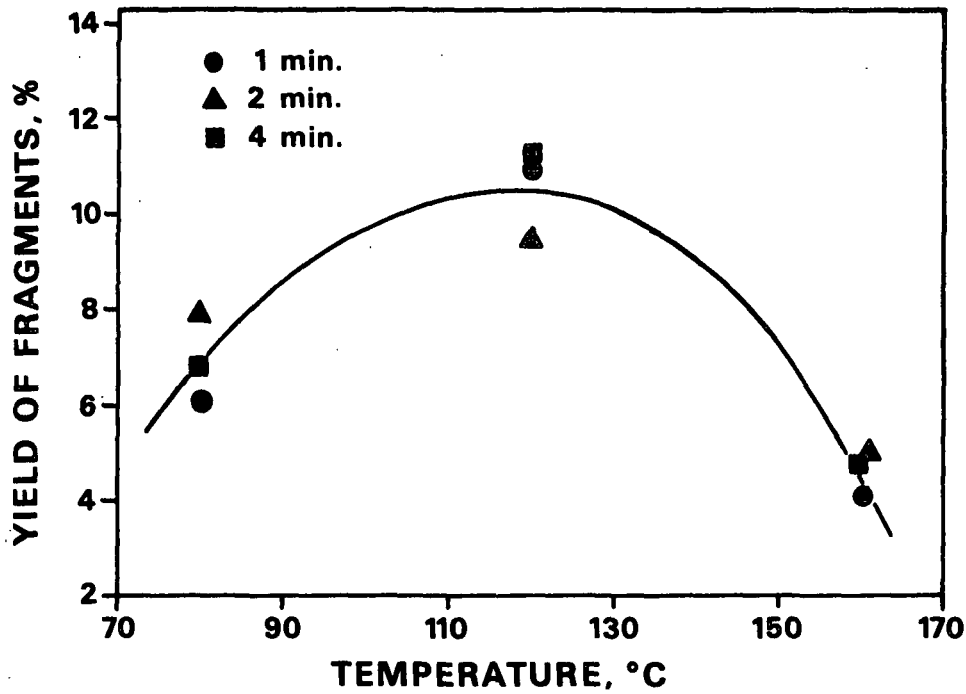


Figure 10. Effect of fiberization temperature on yield of fiber fragments (including fines) from untreated chips at various retention times.

The yield of fiber fragments (Fig. 10), unlike that from the untreated chips, does not increase with increasing retention time, suggesting that the fiber fragments and fines produced are "primary" in nature; they consist of fragments predisposed to separate from their parent fibers or of naturally short morphological elements such as ray cells. Increasing the temperature from 80 to 120 degrees increases the formation of these primary fragments just as it did in the case of unsulfonated chips. The reason for this may be the occurrence of an additional separation mechanism at the higher temperature - steam explosion - which can occur when the mill's wood charge is blown to atmospheric pressure.

FIBER STRENGTH

Pending determinations of the strength of single fibers produced under the various fiberization conditions studied, an attempt was made to draw inferences concerning fiber strength from measurements of zero-span tensile strength of handsheets. As already noted, it was necessary to mildly refine the fibers by agitation in the TAPPI disintegrator before acceptable handsheets could be made.

Zero-span tensile strength was observed to increase with increasing agitation time, presumably as a result of improved sheet formation and/or better interfiber bonding. To assess the effects of the experimental variables, regressions of zero-span on agitation time were performed for each fiberization condition. In each case, the slope was noted, and the value calculated by substituting a time of 3 hours into the regression equation was taken as the best estimate of zero-span tensile strength.

Agitation in the TAPPI disintegrator also increased handsheet density, making it necessary to apply a similar regression procedure to the density data

of $1.8 \pm 1.2 \text{ g/cm}^3$. The rate of density increase showed no statistically significant dependence on the experimental variables.

Figure 11 shows that zero-span was positively correlated with density, implying that bonding in these sheets was not sufficiently good to render negligible the small "residual span" that always exists in a zero-span test. As a result, it can be inferred that the test results obtained are more reflective of the degree of interfiber bonding than of fiber strength. In spite of this disappointing result, the data suggest that one fiberization condition gives lower fiber strength than all of the rest. Thus, at a given density (and therefore presumably at a given residual span) the fibers prepared from unsulfonated chips at the lowest temperature, 80°C , gave sheets with lower zero-span tensile strength than the value predicted by the regression line for sulfonated chips at any temperature and for unsulfonated chips at temperatures of 120 and 160°C .

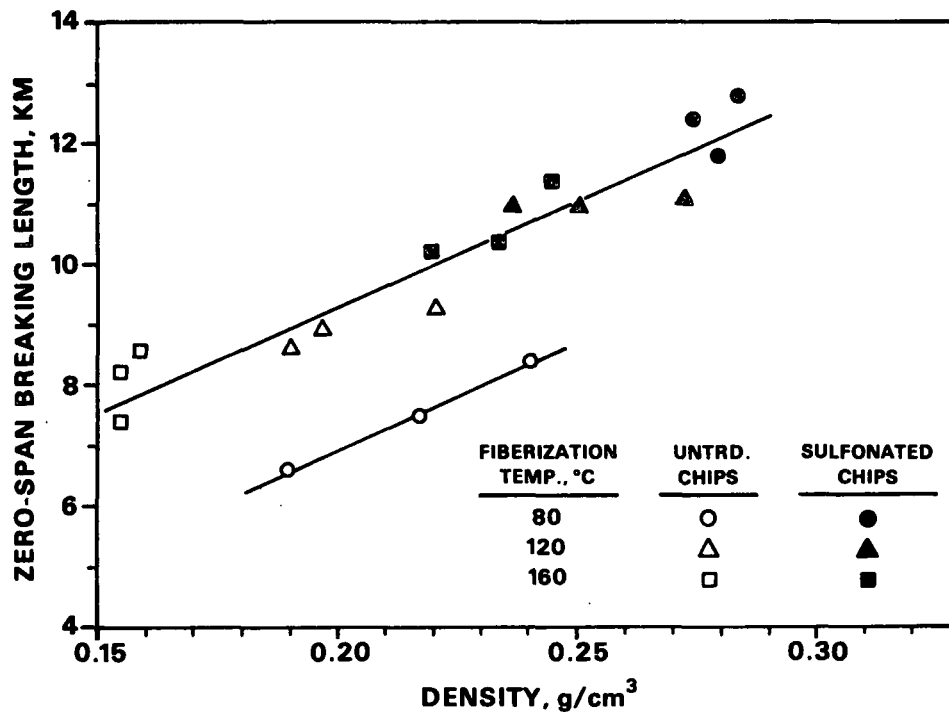


Figure 11. Zero-span tensile strength of handsheets made from fibers separated under various conditions.

SHEET PROPERTIES

Interpolation of regression equations to 3 hours agitation time and subsequent correlation with fiberization conditions or interpolated density gave the results shown in Fig. 12 to 15. Analysis of variance of the density data showed that it was affected by chip pretreatment and by fiberization temperature but not by fiberization retention time. Densities averaged over the three retention times are plotted against temperature in Fig. 12. The higher densities of pulps from sulfonated chips can be attributed to improved fiber flexibility, as is well known. Similarly, the decreased density of pulps produced at higher temperatures can be attributed to poorer surface development.

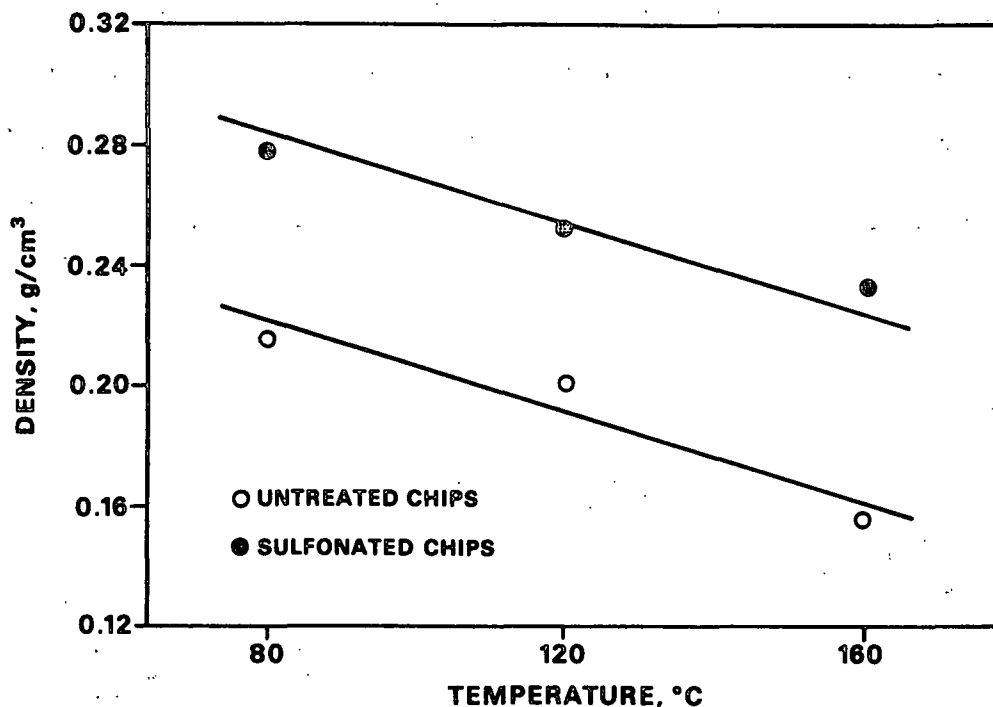


Figure 12. Density of handsheets made from fibers separated under various conditions.

Figure 13 shows that tensile index was determined by sheet density, with no significant effect of the experimental variables at a given density.

The scattering coefficient, on the other hand, was affected by chip pretreatment as well as sheet density, the pulps from sulfonated chips having lower light scattering power at any given density as shown in Fig. 14. This may be assumed to be due to the greater fines contents of the pulps from unsulfonated chips.

Tearing resistance also departed from an otherwise simple positive correlation with density inasmuch as the 3 pulps produced from sulfonated chips at 120 degrees C all had tearing resistances much higher than predicted on the basis of the correlation with density established by all of the other pulps (Fig. 15). The reason for this departure is not known; it was unexpected on the basis of the tensile strength, zero-span and fiber length data. It is possible that the relatively large amount and distinctive nature of the fines in this pulp (cf. Fig. 10 and related discussion) were in some way responsible.

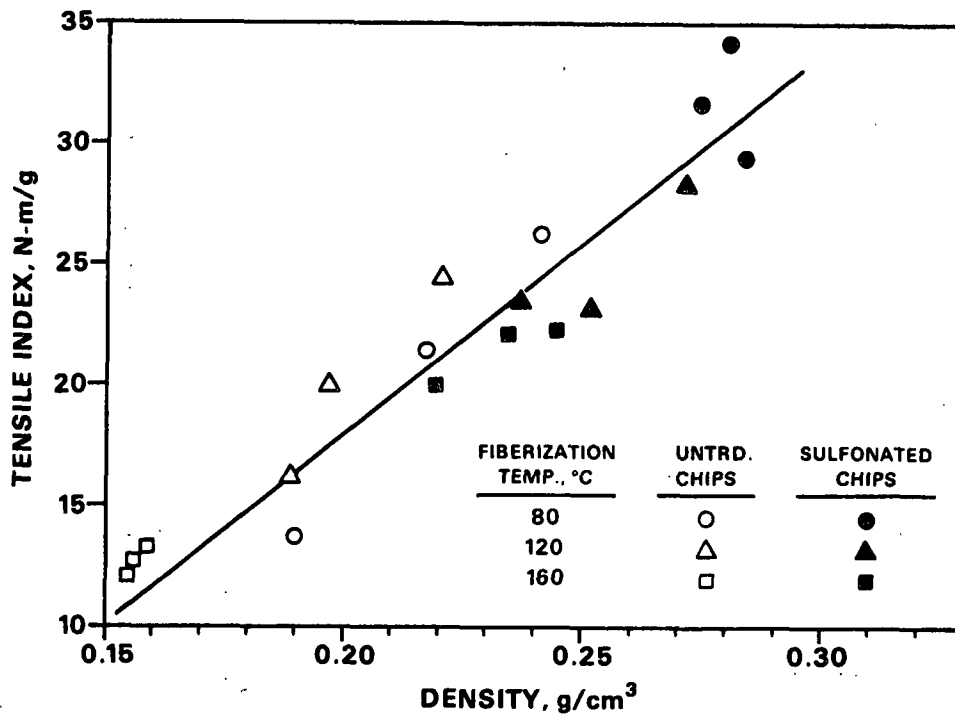


Figure 13. Tensile strength density-relationships for handsheets made from fibers separated under various conditions.

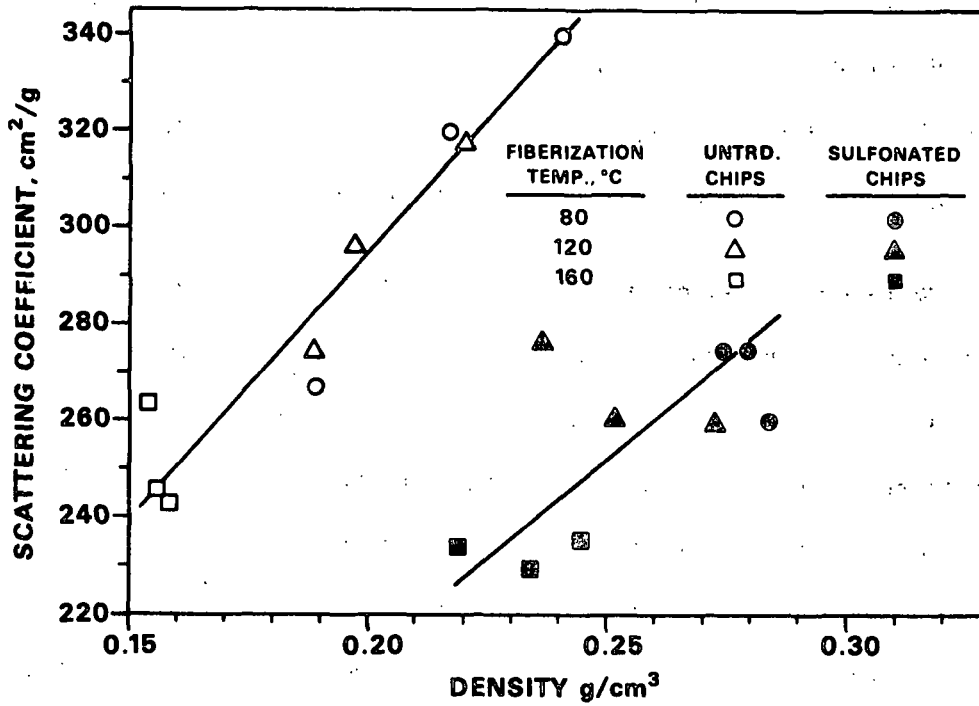


Figure 14. Scattering coefficient-density relationships for handsheets made from fibers separated under various conditions.

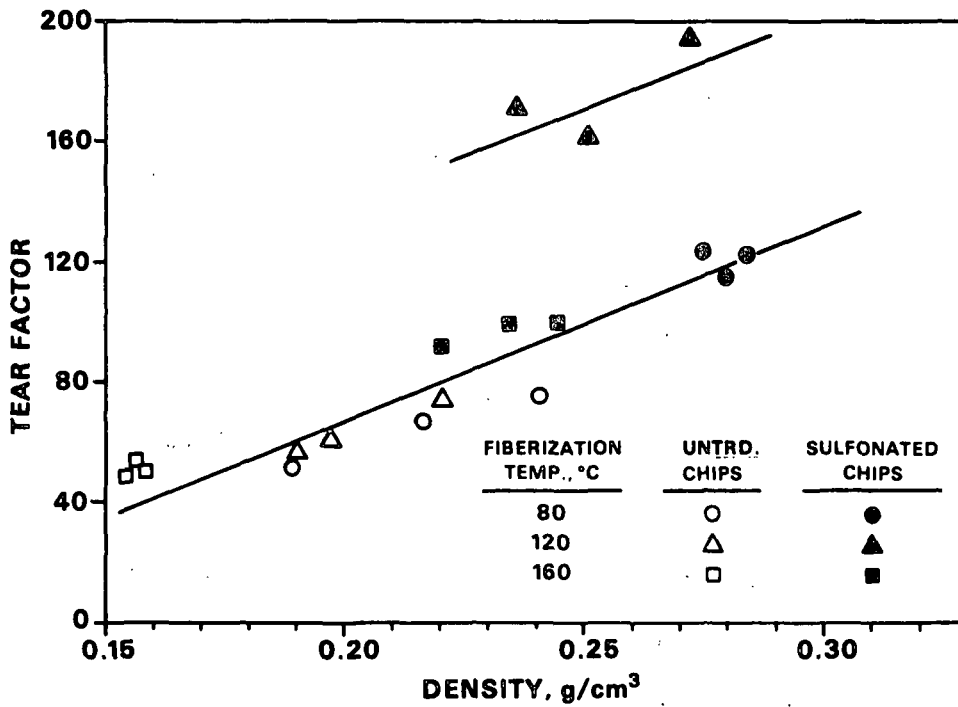


Figure 15. Tear factor-density relationships for handsheets made from fibers separated under various conditions.

BONDING STRONG, HIGH-YIELD FIBERS

As noted earlier, our approach assumes that fibers separated by means designed only to retain maximum fiber length and strength can subsequently be made to bond to form a sheet that realizes the full potential represented by the strength of the fibers. In earlier work, we have shown that single high-yield fibers have average breaking lengths ranging from 40 to 60 km. If our current efforts to understand and control fiberization are successful, we will know how to make high-yield pulps in which all the fibers are this strong and which should give sheets having zero-span breaking lengths of $3/8 \times 60 = 23$ km. If subsequent work on bonding these fibers effectively is also successful, we will have reached the goal of kraft strength at a yield twice as high as that of kraft.

For several reasons, it is of interest to find out how close we can come to this goal with what we know now - specifically, to make well bonded sheets from fibers produced at the 90% yield level. Positive results (very strong sheets) would (a) demonstrate the value of continuing research on fiberization, (b) provide a method of making well bonded sheets for meaningful zero-span tensile strength measurements, and (c) allow a test of the hypothesis that fiber strength controls the strength of sheets we can now make at this yield level. Accordingly, we have begun a series of experiments to determine the extent to which fibers separated from a 93% yield white spruce pulp can be converted to sheets with strengths similar to that of the corresponding kraft pulp. To date, we have prepared a large quantity (several kg) of fiber and have partially evaluated its physical properties after refining, with and without ozone pretreatment. Experiments in progress will explore the effects of sequential chlorine dioxide-alkali treatment, wet pressing, hot pressing, fines addition, and addition of chitosan and other bonding additives.

Duplicate chip sulfonations in 4 L/kg liquor containing 120 g/L Na_2SO_3 and 5 g/L NaOH for 30 min at 140 degrees C gave yields of 93.1 and 94.7%. The sulfonated chips were combined and fiberized in the Asplund mill in 100 g batches (2 min preheat and 2 min fiberization at 120 degrees C). Screening of the combined coarse pulps on a 0.008-inch cut flat screen gave 82.6% accepts. In a Bauer-McNett classification of a sample of the accepts 91% was retained on 100-mesh or coarser screens. Screening of the entire accepts on a 50-mesh Sweco screen gave a retained fraction of 92%. Classification of a sample of the retained fraction resulted in 99.1% being retained on 100-mesh or coarser screens.

Sixty gram samples were treated with 2.3% ozone at 34% consistency and pH 3.8 to give ozonated fiber in 98.7% yield. Samples were subjected to secondary refining in the PFI mill and the physical properties of the resulting pulps were compared with those of untreated and refined fiber. Figure 16 relates the tensile strength to density for both types of fiber, and Fig. 17 is the corresponding plot for tearing resistance.

As is apparent from the plots, the tensile and tear strengths of the untreated fiber after refining compare well with those of the best chemimechanical pulps. Ozone treatment effects a substantial improvement, albeit not nearly to a level that is typical of kraft pulps. Nevertheless, these results are encouraging inasmuch as these fibers represent a yield level of well over 90%, even after taking into account the yield loss upon ozonation, and keeping in mind that ozone is known to have a greater effect on specific bond strength than on fiber conformability. Methods chosen to have the maximum effect on both characteristics should produce substantially higher sheet strengths.

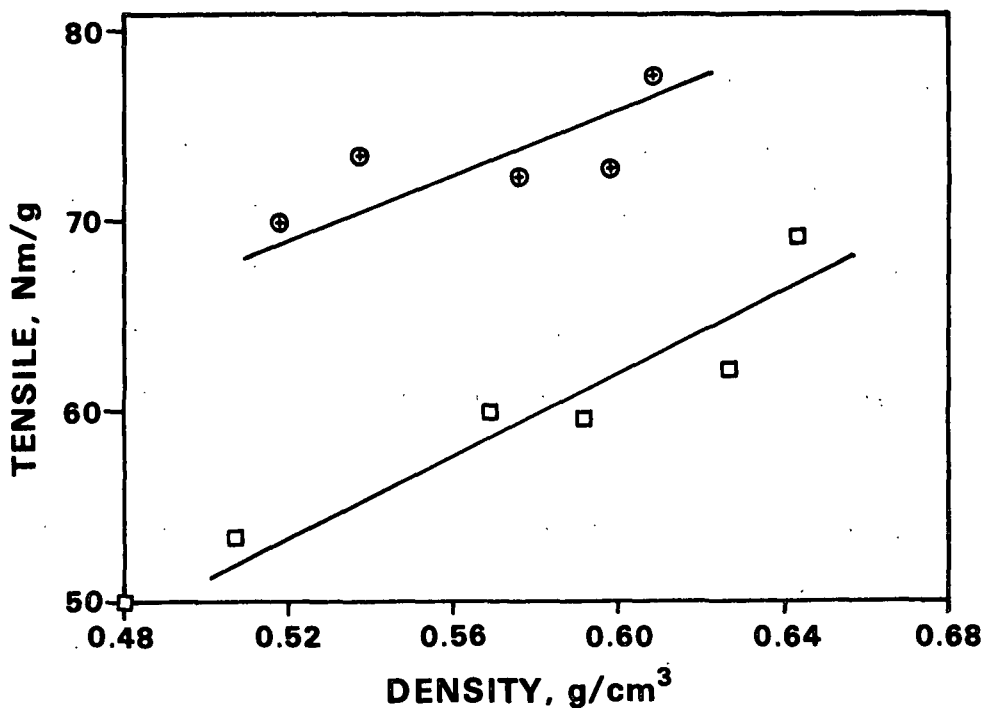


Figure 16. Tensile strength-density relationships for untreated (squares) and 2% ozone treated (circles) spruce fibers from sulfonated chips.

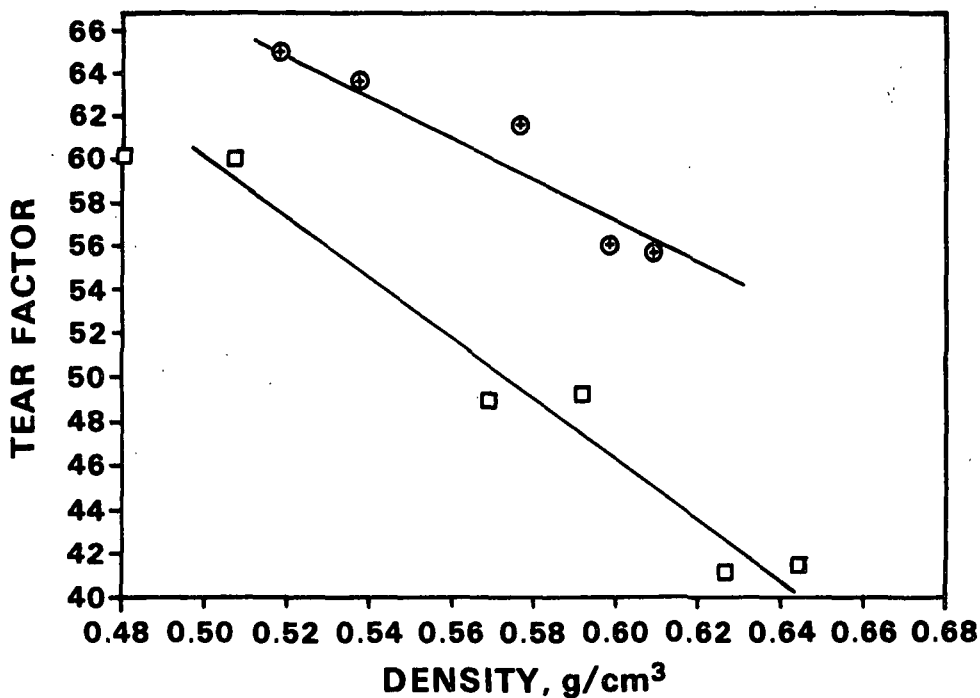


Figure 17. Tear factor-density relationships for untreated (squares) and 2% ozone treated (circles) spruce fibers from sulfonated chips.

In related experiments, we have explored in a preliminary way the effects of heat and pressure on the properties of sheets made from high-yield fibers separated after sulfonation of the wood. Hot pressing might be expected to have beneficial effects on interfiber bonding in such sheets by virtue of two different mechanisms: (a) increased bonded area as a result of fiber wall softening and subsequent fiber collapse under the applied pressure, and (b) enhancement of bond strength per unit of bonded area through flow and cohesion of lignin on adjacent fiber surfaces. The experiments have been conducted by prolonged application of pressure at modestly elevated surface temperature and also by the application of short pressure pulses at higher surface temperature (impulse drying). The latter represents an element of an "integrated process" approach to high-yield, high-performance products. This approach assumes that the optimum route to such products will involve changes not only in the pulping area, to provide new raw material for the converting operation, but also in the converting operation itself.

Table 9 contains the results of hot pressing experiments on fibers separated from sulfonated pulps at two yield levels. Substantial strength increases were achieved, the highest tensile index being about 70% of that of a kraft sheet at the same density. Combinations of hot pressing with other treatments designed to promote bonding may be expected to improve this ratio.

Table 9. Effects of hot pressing on handsheet properties of high yield fibers^a from sulfonated chips.

Yield, % o.d. wood	Pressure, psig	Temp., °C	Time, min	Sheet Density, g/cm ³	Tensile Index, Nm/g	Burst Index, kPa m ² /g	Zero-span Breaking Length, km
74	1000	19	5	0.185	7.2	0.40	9.4
	1000	177	10	0.530	56.9	3.76	12.5
	1000	177	20	0.530	56.2	3.76	12.0
	6000	177	10	0.598	63.5	5.03	11.4
87	1000	19	5	0.138	5.7	0.37	8.8
	1000	177	10	0.522	58.0	3.56	12.0
	1000	177	20	0.526	56.7	3.66	11.1
	6000	177	10	0.611	68.4	4.15	11.5
48 ^b				0.608	101	6.78	22.4
				0.748	126	9.75	20.4

^aCombined on-14 and on-28 mesh fractions of white spruce pulps.

^bWhite spruce kraft whole pulp, conventionally pressed and dried.

ACKNOWLEDGMENTS

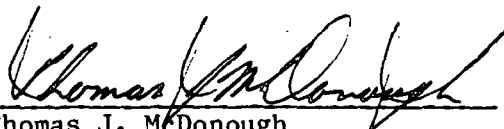
The experimental work described here was skillfully performed by Harry Grady, Amy Malcolm and Kristie Rankin. Amy Malcolm contributed much of the section on fibril angle measurement, and Dr. Terry Connors offered much advice and assistance.

REFERENCES

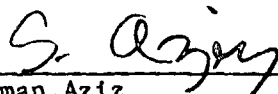
1. Van den Akker, J. A., Tappi 41(8):416(1958).
2. Stone, J. E.; Clayton, D. W., Pulp Paper Mag. Can. 61:T475(1960).
3. Status Report, Project 3566, September 6, 1985.
4. Hardacker, K. W.; Brezinski, J. P., Tappi 56(4):154(1973).

5. Preston, R. D., Phil. Trans. Roy. Soc. B224:131(1934).
6. Page, D. H., Microscopy 90(2):137(1969).
7. Leney, L., Wood Fiber Sci. 13(1)13(1981).
8. Crosby, C.; Mark, R., Svensk Papperstidn. 17:636(1977).
9. Meylan, B. A., For. Prod. J. 17(5):51(1967).
10. Bailey, I. W.; Vestal, M., J. Arnold Arboretum 18(3):185(1937).
11. Senft, J. F.; Bendsten, B. A., Wood and Fiber Sci. 17(4):564(1985).

THE INSTITUTE OF PAPER CHEMISTRY



Thomas J. McDonough
Group Leader, Pulping/Bleaching
Pulping Sciences
Chemical Sciences Division



Salman Aziz
Supervisor, Pulp Laboratory
Pulping Sciences
Chemical Sciences Division

THE INSTITUTE OF PAPER CHEMISTRY

Appleton, Wisconsin

Status Report

to the

PULPING PROCESSES

PROJECT ADVISORY COMMITTEE

Project 3605

COMPUTER MODEL OF RECOVERY FURNACE

August 27, 1986

PROJECT SUMMARY FORM

DATE: August 27, 1986

PROJECT NO. 3605: COMPUTER MODEL OF RECOVERY FURNACE

PROJECT LEADERS: T. M. Grace

IPC GOAL:

Increase the capacity potential of processes.

OBJECTIVE:

Develop a comprehensive mathematical model of fireside processes in a recovery furnace. The model would be based on first principles and would incorporate and integrate the results of ongoing fundamental studies of black liquor combustion.

CURRENT FISCAL YEAR BUDGET: \$20,000

SUMMARY OF RESULTS SINCE LAST REPORT:

This is a new project.

PLANNED ACTIVITY THROUGH FISCAL YEAR 1987:

The modeling effort will be carried out as three concurrent Ph.D. theses. The effort is divided into three parts.

1. Char bed model
2. Model of liquor supply and in-flight behavior
3. Overall model integrating these two along with air/flue gas flow patterns and heat transfer.

Two of these theses were initiated in early September and the third should be initiated by late October.

FUTURE ACTIVITY:

The complete model should be ready by the end of calendar year 1988.

STUDENT RESEARCH

Modelling:

A. Jones	- Overall Furnace Model	- Finish Summer 1988
A. Walsh	- Inflight Model	- Finish Summer 1988
D. Sumnicht	- Char Bed Model	- Finish Fall 1988

IPST HASELTON LIBRARY



5 0602 01064775 0